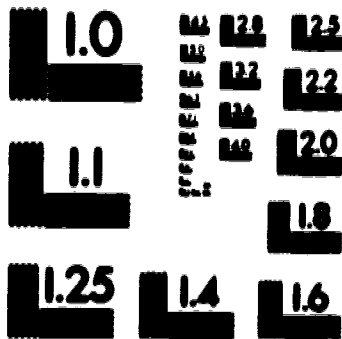


1

PM-1 3 1/2"x4" PHOTOGRAPHIC MICROCOPY TARGET
NBS 1910a ANSI/ISO #2 EQUIVALENT



PRECISION™ RESOLUTION TARGETS



National Library
of Canada

Bibliothèque nationale
du Canada

Acquisitions and
Bibliographic Services Branch

Direction des acquisitions et
des services bibliographiques

385 Wellington Street
Ottawa, Ontario
K1A 0N4

385, rue Wellington
Ottawa (Ontario)
K1A 0N4

Your No. / Votre référence

Our No. / Notre référence

NOTICE

The quality of this microform is heavily dependent upon the quality of the original thesis submitted for microfilming. Every effort has been made to ensure the highest quality of reproduction possible.

If pages are missing, contact the university which granted the degree.

Some pages may have indistinct print especially if the original pages were typed with a poor typewriter ribbon or if the university sent us an inferior photocopy.

Reproduction in full or in part of this microform is governed by the Canadian Copyright Act, R.S.C. 1970, c. C-30, and subsequent amendments.

AVIS

La qualité de cette microforme dépend grandement de la qualité de la thèse soumise au microfilmage. Nous avons tout fait pour assurer une qualité supérieure de reproduction.

S'il manque des pages, veuillez communiquer avec l'université qui a conféré le grade.

La qualité d'impression de certaines pages peut laisser à désirer, surtout si les pages originales ont été dactylographiées à l'aide d'un ruban usé ou si l'université nous a fait parvenir une photocopie de qualité inférieure.

La reproduction, même partielle, de cette microforme est soumise à la Loi canadienne sur le droit d'auteur, SRC 1970, c. C-30, et ses amendements subséquents.

UNIVERSITY OF ALBERTA

Mechanics of Porous Media

by



Craig J. Hickey

**A thesis submitted to the Faculty of Graduate Studies and Research in partial fulfillment of
the requirements for the degree of Doctor of Philosophy.**

IN

GEOPHYSICS

DEPARTMENT OF PHYSICS

EDMONTON, ALBERTA

Spring, 1994



National Library
of Canada

Acquisitions and
Bibliographic Services Branch

395 Wellington Street
Ottawa, Ontario
K1A 0N4

Bibliothèque nationale
du Canada

Direction des acquisitions et
des services bibliographiques

395, rue Wellington
Ottawa (Ontario)
K1A 0N4

Author:

Author:

The author has granted an irrevocable non-exclusive licence allowing the National Library of Canada to reproduce, loan, distribute or sell copies of his/her thesis by any means and in any form or format, making this thesis available to interested persons.

L'auteur a accordé une licence irrévocable et non exclusive permettant à la Bibliothèque nationale du Canada de reproduire, prêter, distribuer ou vendre des copies de sa thèse de quelque manière et sous quelque forme que ce soit pour mettre des exemplaires de cette thèse à la disposition des personnes intéressées.

The author retains ownership of the copyright in his/her thesis. Neither the thesis nor substantial extracts from it may be printed or otherwise reproduced without his/her permission.

L'auteur conserve la propriété du droit d'auteur qui protège sa thèse. Ni la thèse ni des extraits substantiels de celle-ci ne doivent être imprimés ou autrement reproduits sans son autorisation.

ISBN 0-612-11233-0

Canada

UNIVERSITY OF ALBERTA

RELEASE FORM

NAME OF AUTHOR: Craig J. Hickey


TITLE OF THESIS: Mechanics of Porous Media

DEGREE: Doctor of Philosophy

YEAR THIS DEGREE GRANTED: 1994

Permission is hereby granted to the University of Alberta Library to reproduce single copies of this thesis and to lend or sell such copies for private, scholarly or scientific research purposes only.

The author reserves all other publication and other rights in association with the copyright in the thesis, and except as hereinbefore provided neither the thesis nor any substantial portion thereof may be printed or otherwise reproduced in any material form whatever without the author's prior written permission.


RR#1 Nash Creek, Logan
New Brunswick
BOB 120

Date: January 27, 1994


UNIVERSITY OF ALBERTA

FACULTY OF GRADUATE STUDIES AND RESEARCH


The undersigned certify that they have read, and recommend to the Faculty of Graduate Studies and Research for acceptance, a thesis entitled **Mechanics of Porous Media** in partial fulfillment of the requirements for the degree of **Doctor of Philosophy in Geophysics**.




Dr. T. J. T. Spanos (Supervisor)
Department of Physics



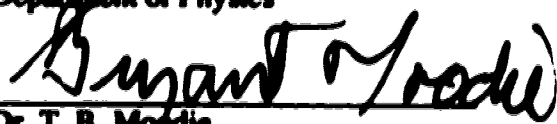
Dr. E. R. Kansewich
Chairman of the Department of Physics



Dr. D. R. Schmitt
Department of Physics



Dr. J. R. Beamish
Department of Physics



Dr. T. B. Moodie
Department of Mathematics



Dr. R. J. Knight
Department of Geological Sciences
University of British Columbia

Date: January 7, 1994

ABSTRACT

A study of infinitesimal, reversible deformations of porous media is presented. The volume averaging technique is used to provide the framework of the macroscopic descriptions. The primary advantage of such an approach is that there is a connection with the well established continuum descriptions at the pore scale (e.g. elasticity, single continuum thermodynamics).

Macroscopic relations for equilibrium thermodynamics of porous media are reviewed. The internal energy for a porous medium is discussed in the context of a system consisting of two superposed continua. The consequences of a unique energy potential for such a system is studied from a thermodynamic viewpoint.

A description of quasi-static deformations of a porous material consisting of a solid frame completely saturated by a single fluid is presented. The initial purpose was to utilize parameter values obtained in quasi-static experiments as estimates for the associated parameters in the wave propagation theory. The results obtained from the quasi-static description; however, have many points in contact with those found in the literature on poroelasticity.

The system of equations which form the basis of the description of low frequency wave propagation are based on the work of de la Cruz & Spanos (1985, 1989b). The system of equations, for the fully saturated case, used here differ in two respects. Firstly, the fluid bulk viscosity is now included. Secondly, macroscopic shear modulus and heat conductivities are introduced as phenomenological parameters. Numerical examples illustrate the changes in the phase velocity, attenuation and/or quality factor due to these modifications.

A description of low frequency wave propagation through a porous medium saturated by two fluids is presented. Firstly, an approximation is obtained by using the equations for single fluid saturated porous media and the assumption that the two fluids form a composite or effective fluid. Secondly, the governing equations are derived for the general case.

ACKNOWLEDGEMENTS

A special acknowledgement must go to my fiancée Rose, for the love, continuous support, and reassurance she provided during the term of my graduate studies. I thank her for being understanding and never (almost never!) questioning my decisions.

I am very grateful to my supervisor, Dr. T. J. B. Spence for his assistance and continuous guidance which enabled the completion of this work.

I am grateful to Dr. E. R. Kanasewich, Dr. R. J. Knight, Dr. T. B. Moodie, Dr. J. R. Beamish, and Dr. D. R. Schmitt for their comprehensive review of this work. Sincere thanks to Dr. N. Udey for proofreading this thesis and his many constructive suggestions. I thank Dr. V. de la Cruz for the assistance and discussions regarding the research contained in this thesis.

The financial support provided by the Alberta Oil Sands Technology and Research Authority, the Canadian Society of Exploration Geophysicists, and the Department of Physics is greatly appreciated.

I would like to thank my colleagues Dr. J. E. Eastwood, Dr. D. F. K. Shim, D. S. Yang, and A. Kebaili for their discussions and suggestions pertaining to this thesis. The support of my family and friends is gratefully acknowledged.

TABLE OF CONTENTS

CHAPTER	PAGE
1 INTRODUCTION	1
1.1 Introduction	1
1.2 Quasi-Static Deformations	1
1.3 Wave Propagation	4
1.4 Experimental Data	12
1.5 Outline of Thesis	14
2 THERMODYNAMICS OF DEFORMATION	16
2.1 Introduction	16
2.2 Volume Averaging	17
2.3 Review of Single Continuum Thermodynamics	20
2.4 Macroscopic Thermodynamics	24
2.5 Internal Energy for Porous Media	34
2.6 Conclusions	38
3 QUASI-STATIC DEFORMATIONS OF POROUS MEDIA	40
3.1 Introduction	40
3.2 Equations for Static Compression	41
3.3 Drained Compressional Deformations	43
3.4 Undrained Compressional Deformations	51
3.5 Shear Deformations	57
3.6 A Continuous Family of Compressibilities	59
3.7 Induced Pore Pressure Coefficient	63
3.8 Coefficient of Effective Stress	64
3.9 Conclusions	66

4	WAVE PROPAGATION IN FULLY SATURATED POROUS MEDIA	70
4.1	Introduction	70
4.2	Formal Equations of de la Cruz & Spanos (1989b)	72
4.3	Discussion of Fluid Bulk Viscosity	77
4.4	Generalized Macroscopic Shear Deformations	78
4.5	Generalized Macroscopic Heat Conduction	79
4.6	Evaluation of the Area Integrals $I_i^{(1)}$ and $I_i^{(3)}$	81
4.7	Evaluation of the Area Integrals $I^{(6)}$ and $I^{(8)}$	87
4.8	Solid Compliance Factor (δ_s) and Fluid Compliance Factor (δ_f)	89
4.9	Generalized Equations for Wave Propagation in a Porous Medium Saturated by One Fluid	91
4.10	Numerical Examples	96
4.11	Conclusions	138
5	SEISMIC WAVE PROPAGATION FOR PERMEABLE MEDIA CONTAINING TWO FLUID PHASES	141
5.1	Introduction	141
5.2	Composite Fluid Model	147
5.3	Derivation of Governing Equations for Wave Propagation Through a Porous Medium Containing Two Fluid Phases	153
5.3.1	Introduction	153
5.3.2	Volume Averaging of Pore scale Equations	154
5.3.3	Evaluation of Area Integrals	159
5.3.4	Conclusions	169
5.4	General Equations for Wave Propagation in a Porous Medium Saturated by Two Fluids	170
5.5	Special Limiting Cases of General Equations	172
5.6	Conclusions	177
6	CONCLUSIONS	179
	REFERENCES	185

LIST OF TABLES

TABLE	PAGE	
3.1	Various quasi-static tests and associated poroelastic parameters as derived in this chapter.	68
3.2	Relations among various quasi-static poroelastic parameters. The * indicates that the relation is only valid if $C(1)=C_1$.	69
4.1	Relationship in notation of variables and some parameters between the Biot theory and this work. The expression in parenthesis is with comparison to the Biot high frequency theory.	93
4.2	Comparison of coefficients for the Biot theory and the work presented here.	93
4.3	Elastic coefficients for the Biot theory in terms of quantities measurable in quasi-static experiments as derived by Biot & Willis (1957).	95
4.4	Elastic coefficients for the Biot theory in terms of quantities measurable in quasi-static experiments described in chapter 3.	95
4.5	Elastic coefficients for the Biot theory in terms of quantities measurable in quasi-static experiments under the condition that $C_{unj}=C_1$. For such a condition the expressions obtained from this work and the work of Biot & Willis (1957) are the same.	96
4.6	Physical properties for Berea sandstone. The constituent properties are assumed to be those of quartz and the values of the macroscopic properties are similar to those of a consolidated Berea sandstone.	99
4.7	Physical properties for water and the properties of the porous medium which are dependent on the pore fluid.	100
4.8	Physical properties for air and the properties of the porous medium which are dependent on the pore fluid.	101
4.9	Physical properties for bitumen and the properties of the porous medium which are dependent on the pore fluid.	102
4.10	Phase velocities of the various seismic waves propagating through a porous medium saturated with the specified fluid. If the mode is significantly dispersive, the numbers in parenthesis are the range of phase velocities for a frequency range of 1-1000 Hz.	103

4.11	Phase velocities for the various seismic P waves propagating through a porous medium saturated with the specified fluid when thermomechanical coupling is included. If the mode is significantly dispersive, the numbers in parenthesis are the range of phase velocities for a frequency range of 1-1000 Hz.	110
5.1	Relationships between area integrals as a consequence of the no-slip boundary condition at the pore scale interfaces.	161
5.2	Relationships between area integrals as a consequence of the continuity of stress boundary condition at the pore scale interfaces. The conditions at the fluid 1 - fluid 2 interface are valid only if the fluids are miscible.	167

LIST OF FIGURES

FIGURE	PAGE
2.1	Dependence of average on averaging volume. 18
3.1	Schematic of experimental set up for static compressibility measurements of porous materials. The impermeable jacket around the sample enables the pore-pressure and confining pressure to be controlled independently. 45
3.2	The deformation of a block of porous medium with a square cross section of width L , on which the faces normal the x -axis is subject to a constant uniform compressive stress $\tau_{xx} = -p$ and the pore fluid is allowed to flow out of the sample, $p_f = p_o$. The change in dimension of the sample is measured in the direction of applied stress (x -direction) and in one direction perpendicular to the direction of applied stress (y -direction). 51
3.3	The deformation of a block of porous medium with a square cross-section of width L subject to a constant uniform shearing stress $\tau_{xy} = \tau_{yx} = \tau$. The volume of the block is unchanged to first order. 58
4.1	Development of the theory. 74
4.2	Illustration of different possible thermal regimes of a porous medium during a seismic disturbance. 88
4.3	Schematic for numerical procedure used to calculate attenuation and phase velocity of various modes. 97
4.4	Phase velocity versus frequency for the 2nd P wave. Both the non-thermal and thermal (with thermomechanical coupling) exhibit similar frequency dependence. The saturating fluid is water. 104
4.5	Attenuation and inverse Q versus frequency for the 1st P wave. Inverse Q exhibits an approximate linear relationship versus frequency. The saturating fluid is water. 104
4.6	Attenuation and inverse Q versus frequency for the 1st P wave. Inverse Q exhibits an approximate linear relationship versus frequency. The saturating fluid is bitumen. 105
4.7	Attenuation and inverse Q versus frequency for the 1st P wave. Inverse Q exhibits an approximate linear relationship versus frequency. The saturating fluid is air. 105
4.8	Attenuation and inverse Q versus frequency for the 1st S wave. Inverse Q exhibits an approximate linear relationship versus frequency and is about an order of magnitude larger than the 1st P wave. The saturating fluid is water. 107

- 4.9 Attenuation and inverse Q versus frequency for the 1st S wave. Inverse Q exhibits an approximate linear relationship versus frequency and is the same order of magnitude as the 1st P wave. The saturating fluid is bitumen. 107**
- 4.10 Attenuation and inverse Q versus frequency for the 1st S wave. Inverse Q exhibits an approximate linear relationship versus frequency and is the same order of magnitude as the first P wave. The saturating fluid is air. 108**
- 4.11 Attenuation and inverse Q versus frequency for the 2nd P wave. Inverse Q exhibits an approximate linear relationship versus frequency. The saturating fluid is bitumen. 108**
- 4.12 Attenuation and inverse Q versus frequency for the 2nd P wave. Attenuation increases with frequency as is expected, however, inverse Q remains approximately constant with increasing frequency. The saturating fluid is water. 109**
- 4.13 Attenuation and inverse Q versus frequency for the 2nd P wave. Inverse Q exhibits a linear relationship versus frequency. The saturating fluid is air. 109**
- 4.14 Attenuation versus frequency for the 1st P wave for several ratios of bulk viscosity to shear viscosity. Water has a measured viscosity ratio of 2.3. 111**
- 4.15 Attenuation versus frequency for the 1st P wave for several ratios of bulk viscosity to shear viscosity. The effect of bulk viscosity is much larger than for the water case. Bitumen has a measured ratio of 5 but is strongly temperature dependent. 112**
- 4.16 Normalized 1st P wave attenuation versus ratio of bulk viscosity to shear viscosity for three different permeabilities. Bulk viscosity effects become important at very low permeabilities. Frequency is 100 Hz and the saturating fluid is water. 112**
- 4.17 Normalized 1st P wave attenuation versus ratio of bulk viscosity to shear viscosity for three different values of drained bulk modulus, K_{bc} . Changes in attenuation due to bulk viscosity are greater in materials with small values of K_{bc} . Frequency is 100 Hz and the saturating fluid is water. 113**
- 4.18 Phase velocity and attenuation of the 1st P wave versus a normalized material shear modulus. Saturating fluid is water and the frequency is 100 Hz. 115**
- 4.19 Phase velocity and attenuation of the 1st S wave versus a normalized material shear modulus. Saturating fluid is water and the frequency is 100 Hz. 115**
- 4.20 Phase velocity and attenuation of the 2nd P wave versus normalized material shear modulus. The saturating fluid is water and the frequency is 100 Hz. 116**

4.21	Attenuation of the 1st S wave versus frequency for three different values to material shear modulus, μ_M. The saturating fluid is water.	116
4.22	Inverse Q of the 1st S wave versus frequency for three different values to material shear modulus, μ_M. Inverse Q exhibits an approximate linear relationship versus frequency and is independent of the values of μ_M. The saturating fluid is water.	117
4.23	Phase velocity and attenuation of the 1st P wave versus a normalized material shear modulus. Phase velocity increases and the attenuation decreases as the frame becomes more rigid. Saturating fluid is bitumen and frequency is 100 Hz.	117
4.24	Phase velocity and attenuation of the 1st S wave versus a normalized material shear modulus. Phase velocity increases and the attenuation tends to zero as the frame becomes more rigid. Saturating fluid is bitumen and the frequency is 100 Hz.	118
4.25	Phase velocity and attenuation of the 1st P wave versus a normalized drained bulk modulus. Phase velocity increases (~linear) as a function of drained bulk modulus. The attenuation has a minimum in the compressible regime. Saturating fluid is water and the frequency is 100 Hz.	119
4.26	Phase velocity and attenuation of the 2nd P wave versus a normalized drained bulk modulus for a frequency of 100 Hz. Saturating fluid is water and the frequency is 100 Hz.	120
4.27	Attenuation versus frequency for the 1st P wave for several values of drained bulk modulus. The largest increase in attenuation corresponds to the largest value of drained bulk modulus. The saturating fluid is water.	120
4.28	Phase velocity and attenuation of the 1st P wave versus a normalized drained bulk modulus. Phase velocity increases (~linear) and the attenuation decreases as the frame becomes less compressible. Saturating fluid is bitumen and the frequency is 100 Hz.	121
4.29	Phase velocity and attenuation of the 1st P wave versus normalized unjacketed bulk modulus. The saturating fluid is water and frequency is 100 Hz.	123
4.30	Phase velocity and attenuation of the 2nd P wave versus normalized unjacketed bulk modulus. The saturating fluid is water and frequency is 100 Hz.	123
4.31	Phase velocity and attenuation of the 1st P wave versus normalized unjacketed bulk modulus. The saturating fluid is bitumen and frequency is 100 Hz.	124

4.32	Phase velocity and attenuation of the 1st P wave versus permeability. The saturating fluid is water and the frequency is 100 Hz.	126
4.33	Phase velocity and attenuation of the 1st S wave versus permeability. The saturating fluid is water and the frequency is 100 Hz.	126
4.34	Phase velocity and attenuation of the 2nd P wave versus permeability. The saturating fluid is water and the frequency is 100 Hz.	128
4.35	1st P wave phase velocity versus frequency for three values of permeability. Increasing the permeability moves the abrupt but small change in velocity to higher frequency. Water is the saturating fluid.	129
4.36	1st P wave attenuation versus frequency for three values of permeability. Increasing the permeability moves the change in attenuation to higher frequency. Water is the saturating fluid.	129
4.37	Phase velocity and attenuation of the 1st P wave versus permeability. The saturating fluid is air and the frequency is 100 Hz.	130
4.38	Phase velocity and attenuation of the 1st S wave versus permeability. The saturating fluid is air and the frequency is 100 Hz.	130
4.39	1st P wave phase velocity versus frequency for three values of induced mass coefficient. Phase velocity increases with increasing frequency reaching a maximum which is larger for smaller ρ_{12} (magnitude). Water is the saturating fluid.	132
4.40	1st P wave attenuation versus frequency for three values of induced mass coefficient. Decreasing the magnitude of the induced mass coefficient causes a much larger increase in attenuation at higher frequency. Water is the saturating fluid.	132
4.41	1st S wave phase velocity versus frequency for three values of induced mass coefficient. Phase velocity increases with increasing frequency reaching a maximum which is larger for smaller ρ_{12} (magnitude). Water is the saturating fluid.	133
4.42	1st S wave attenuation versus frequency for three values of induced mass coefficient. Decreasing the magnitude of the induced mass coefficient causes a much larger increase in attenuation at higher frequency. Water is the saturating fluid.	133
4.43	2nd P wave phase velocity versus frequency for three values of induced mass coefficient. Phase velocity increases with increasing frequency reaching a maximum which is larger for smaller ρ_{12} (magnitude). Water is the saturating fluid.	134

- 4.44** 2nd P wave attenuation versus frequency for three values of induced mass coefficient. Decreasing the magnitude of the induced mass coefficient causes a slightly larger increase in attenuation at higher frequency. Water is the saturating fluid. 134
- 4.45** Normalized phase velocity and attenuation of the 1st P wave versus the coefficient of heat transfer. Normalization was performed by dividing by respective non-thermal quantities. The saturating fluid is bitumen and the frequency is 100 Hz. 135
- 4.46** Normalized phase velocity and attenuation of the 1st P wave versus fluid thermal expansion. Normalization was performed by dividing by respective non-thermal quantities. The saturating fluid is bitumen and the frequency is 100 Hz. 136
- 4.47** Normalized phase velocity and attenuation of the 1st P wave versus solid thermal expansion. Normalization was performed by dividing by respective non-thermal quantities. The saturating fluid is bitumen and the frequency is 100 Hz. 137

CHAPTER I

INTRODUCTION

1.1 Introduction

The study of the deformation of rocks is a multi-disciplinary subject. It is of fundamental importance in a variety of fields such as geophysics, engineering and hydrogeology (cf. review by Kumpel, 1991). By the nature through which rocks are formed and the subsequent deformation and erosion, most rocks contain pores or cracks of varying texture. Texture is a qualitative classification based upon sizes, shapes, arrangements and distribution of the pores and cracks. These pores and cracks are filled with fluids such as air, water, oil, various gases and even molten rock. In the study of these rocks (which we will call porous rocks or porous media) the primary additional complexity is in the description of the interaction between the various pore fluids and the materials which form the porous skeleton (primarily aggregates of various minerals). Several processes occurring within porous rocks are studied in all fields but with regard to different applications.

1.2 Quasi-Static Deformations

Quasi-static loading is of importance, for example, to glacial rebound studies, land subsidence, variation in aquifer capacity due to compaction, and strength of materials. Parameters derived in the description of quasi-static loading are also used to estimate macroscopic parameters required in wave propagation theories. However, there is concern of whether or not statically determined values for parameters may be applied to dynamic situations (Kumpel, 1991). The mechanical behavior of porous media has many added complexities. For example, the fluid pressure within the pores affects the deformation. The first to recognize the importance of pore pressure was Terzaghi (1923). Others recognized the apparent correlation of earthquakes with injection of fluids in deep wells (Healy *et al.*, 1968; Bell & Nur, 1978; Rajendran & Talwani, 1992) and the possible association of pre and post earthquake phenomena with pore pressure (Nur, 1972; Nur & Booker, 1972; Schwarzschild, 1993). In Terzaghi's (1923) formulation, the concept of

effective stress was proposed as

$$\tau_{ik}^{eff} = \tau_{ik} + \chi p_f \delta_{ik} \quad (1.1)$$

where τ_{ik} denotes the applied stress (positive in tension), p_f is the pore pressure (positive in compression), δ_{ik} is the Kronecker delta and χ is the effective stress coefficient. The interest in effective stress is that it should enable one to predict the values of density, seismic velocity, porosity, etc., for any combination of confining and pore pressure after making only a series of measurements without pore pressure (Robin, 1973). There is a considerable amount of work published on the determination of the coefficient of effective stress (Biot & Willis, 1957; Nur & Byerlee, 1971; Carroll, 1979; Carroll & Katsube, 1983; Zimmerman *et al.*, 1986; Zimmerman, 1991; Berryman, 1992). However, there appears to be no unique law of effective stress, and such a law may not be very useful except in the case where $\chi = 1$ (Robin, 1973).

The deformation of porous media subjected to mechanical stresses involves the deformation of solid and fluid components as well as the interaction between these components. Such interactions require additional material parameters for an adequate description. Furthermore, because of the pore fluid's ability to flow, an additional degree of freedom is introduced. Some experiments may be conducted so that the pore fluid is allowed to flow freely out of the sample; these are usually called "drained" experiments. They are used to determine various types of drained compressibilities, Young's moduli and Poisson's ratios. If the fluid is restricted to remain within the sample then the experiments are classified as "undrained." The characteristic parameters obtained from such experiments have been studied for numerous years (Gassmann, 1951a; Biot & Willis, 1957; Geertma, 1957; Zimmerman, 1991) and measurements of various bulk moduli, and derivations of relationships between them have been reported for decades and are still of current interest (see Zimmerman, 1991, for a comprehensive exposition).

Biot (1941) developed one of the first complete sets of constitutive equations for porous media. Biot's (1941) work is independent of any micro-model and assumes infinitesimal, reversible and isothermal deformations of an isotropic porous medium with an incompressible pore fluid. The flow of the fluid through the porous skeleton is assumed to obey Darcy's law. The model was later generalized to include an anisotropic solid and a

compressible fluid (Biot, 1955, 1956a). The stress-strain relationships are introduced in analogy with the theory of elasticity combined with phenomenological arguments as to the effects of the pore fluid. The initial relationships contain five distinct physical constants. Under the assumption of a unique energy potential for the porous media, the number of physical constants is reduced to four. Other works which can be reconciled with Biot (1941, 1955) are Gassmann (1951a), Geertsma (1957), Morland (1972), Brown & Korringa (1975), Rice & Cleary (1976), Thomsen (1985), and Zimmerman *et al.* (1986) among others.

The relationship between stress and strain in solids containing cracks has been modelled quite differently. The approach here is to obtain a description of the fluid flow process of one crack (e.g. Dvorkin *et al.*, 1992; Palmer & Traviolia, 1980; Mavko & Nur, 1979) and then obtain a macroscopic description through a self consistent approximation (Rouleau, personal communication). The method of smoothing (Keller, 1964) has also been applied to the determination of elastic properties of materials with cracks (Hudson & Knopoff, 1989). The resulting equations usually depend on the aspect ratio, crack number density, as well as the distribution of cracks. These types of descriptions have also been addressed by Eshelby (1957), Walsh (1965a, 1965b), O'Connell & Budiansky (1974; 1977), Budiansky & O'Connell (1976), Chatterjee *et al.* (1978), and Hudson (1980; 1990a). The two modes of solid-fluid interaction, described independently through a macroscopic approach and the other using the microscopic method, must be intimately interconnected via fluid mass balance (Dvorkin & Nur, 1993).

The study of material properties also has technological implications. These studies are mostly conducted from an applied mechanics and engineering science point of view as surveyed by Hashin (1983). The material is usually referred to as a composite material and is defined as consisting of two or more materials that form regions large enough to be regarded as continua which are usually firmly bonded at the interface (Hashin, 1983). These include natural materials such as porous and cracked rocks, polycrystalline aggregates (metals), wood, as well as artificial materials. This research is oriented towards the fabrication of composite materials and measuring of its properties i.e. elasticity, thermal expansion, conductivities, etc. The measurements are obtained through destructive (breaking, burning) as well as non-destructive (ultrasonic, electrical, thermal) testing.

Analytic studies in this area are primarily oriented towards the prediction of material properties. These studies usually lead to the determination of bounds of "effective" elastic coefficients (Paul, 1961; Walpole, 1966; Thomsen, 1972; Berryman, 1979; Willis, 1981; also see Watt *et al.*, 1976 and Hashin, 1983, for comprehensive surveys). The most useful bounds available depend on the relative amounts and the elastic properties of the components. The first such bounds were presented in the work of Voigt (1910) and Reuss (1929). Hill (1952, 1963) has shown that the Voigt and Reuss expressions are upper and lower bounds respectively for the elastic moduli of a composite. Hashin & Shtrickman (1961a, 1961b, 1962a, 1962b, 1963) developed new variational principles that led to considerably tighter bounds. Experimental investigation of the Hashin-Shtrickman bounds was carried out by Watt & O'Connell (1980) on two phase aggregates. A narrow range of moduli estimates results only if the shear modulus of both phases are fairly closely matched. For samples where the shear moduli of the component phases varied by a factor of 5 the uncertainty in theoretical prediction can be 10 times larger than the experimental uncertainty. More restrictive bounds are available (Milton & Phan-Thien, 1982) but require additional information about the composite not readily available or imposition of specific assumptions about the geometry of the components in the aggregate.

1.3 Wave Propagation

Wave propagation must be understood if seismic data are to be utilized efficiently for imaging the interior of the earth, monitoring reservoir conditions (Dunlop *et al.*, 1991a, 1991b), subsurface site evaluation and possibly mapping contaminated groundwater aquifers. The usual observables for wave propagation are the phase velocity, reflection/transmission coefficients and attenuation, of rotational (S) and dilatational (P) waves.

In general, the displacement, velocity or a stress component of a wave travelling in the positive x -direction is given by an expression of the form

$$g = g(x-ct) \quad (1.2)$$

where the argument $(x-ct)$ is called the phase of the wave function. If the time is increased

by Δt and x is increased by $c\Delta t$ such that the value of $g(x-ct)$ does not change then the velocity c is termed the phase velocity. In the work considered here we will assume g to be a plane wave of the form

$$\mathbf{g} = A\mathbf{d}e^{i(\mathbf{k}\cdot\mathbf{p} - \omega t)} \quad (1.3)$$

where \mathbf{d} and \mathbf{p} are unit vectors defining the direction of motion and propagation respectively. If $\mathbf{p}\cdot\mathbf{d} = 0$ then the motion is transverse (rotational) and if $\mathbf{p}\cdot\mathbf{d} = 1$ the motion is longitudinal (dilatational). From the above expression the phase velocity in the direction of propagation, \mathbf{p} , is

$$c = \left(\frac{\omega}{k}\right) . \quad (1.4)$$

When a travelling wave strikes the interface between two media of different material properties part of the disturbance is reflected and part is transmitted across the interface. The reflection and transmission coefficients describe the partitioning of energy at an interface between two different media. For elastic media, these coefficients are functions of the impedance (phase velocity \times density) of both media as well as the angle of incidence. These relations are sometimes known as Zoeppritz' equations. Theoretical expressions for reflection and transmission coefficients in viscoelastic materials (Lockett, 1962; Borchardt, 1973, 1986) as well as porous materials (Deresiewicz & Levy, 1967; Sabatier *et al.*, 1986; de la Cruz & Spanos, 1989a; Wu *et al.*, 1990; Caviglia *et al.*, 1992; de la Cruz *et al.*, 1992; Sharma & Vashish, 1993) have also been developed. These expressions are usually very complicated and can only be reconciled with the expressions obtained from elasticity in restrictive limiting cases.

This partitioning of energy, commonly referred to as amplitude versus offset in exploration seismology, is used in hydrocarbon exploration and in reservoir characterization to extract reservoir properties from seismic data (Ostrander, 1984; Shuey, 1985; Mazzotti, 1990). The association of "bright spots," areas of large amplitude reflections, with gas and/or oil filled reservoir rocks (Rosa *et al.*, 1985; Hwang & Lellis, 1988) was a primary incentive for a large amount of research into reflection/transmission coefficients (Domenico, 1974; Clark, 1992). Others (Pione, 1980; Pione *et al.*, 1990; Nagy *et al.*, 1990; Nagy & Adler, 1992) have used the energy partitioning insight to

develop laboratory experiments to measure an additional dilatational mode present in multicomponent media (which will be referred to later as the second P-wave). This latter work can not be explained by the Zoeppritz relations.

Wave attenuation in porous rocks consists of intrinsic attenuation and extrinsic or geometric attenuation. Intrinsic attenuation is the loss of energy which is converted to heat due to interactions between the porous rock and the wave. The extrinsic attenuation is due to spherical spreading of the wave and elastic scattering. The elastic scattering phenomena are dependent on the contrast in the material properties of the scatterers from that of the medium, their geometrical shape, and the size of the scatterer relative to the wavelength of the incident wave (Kaul, 1993).

Goldberg & Zinser (1989) obtain P-wave attenuation values from resonant bar experiments that were much smaller than in-situ attenuation values obtained from sonic waveform analysis. They argue that the in-situ values are larger due to scattering from fine laminations and vugs, and mode conversions to shear wave energy near the borehole wall. Toksöz *et al.* (1990) determine shear wave attenuation as a function of frequency and depth in the crust. They conclude, based on the frequency dependence of the attenuation, that scattering is the dominant mechanism responsible for attenuation for depths between 2 and 10 km in the crust. Xu & King (1990) measure the phase velocity and attenuation of the P-wave and two S waves (S_1 is polarized perpendicular to the cleavage of the slate and S_2 polarized parallel to cleavage) in a slate before and after the induction of cracks. The attenuation of all modes are significantly affected by the presences of cracks. Scattering is believed to dominate the attenuation only for the S_1 -wave at low confining pressures. Kuster & Toksöz (1974a, 1974b) measure phase velocity and attenuation of ultrasonic waves through a medium of solid spherical particles suspended in various fluids. Various solids and fluids as well as the concentration of particles were examined. They conclude that at lower frequencies the scattering effect diminishes and the total attenuation is controlled by the intrinsic properties of the matrix and inclusion materials.

Theories of elastic scattering (Waterman & Truell, 1961; Kuster & Toksöz, 1974a; Hudson; 1990b; Peacock & Hudson, 1990; Kerr, 1992) are usually developed within the Raleigh regime, i.e. assuming that the size of the scatterer, usually a crack, is much less than the wavelength of the wave. This assumption enables the introduction of the concept

of an equivalent material. Many of the theories also assume that the scattered fields do not interact; this is commonly known as single scattering theory. Recent theoretical developments (Hudson, 1990b) have shown that if interactions between scatterers is accounted for, and the calculations are carried out such that effective continua holds, then the attenuation due to scattering should be zero. However, the crack models of Hudson (1990b) are currently under question (Sayers, 1993).

An understanding of extrinsic attenuation (scattering) is required so that it can be estimated in a given attenuation measurement (discussed by Klimentos, 1991a) so that correct values of the intrinsic attenuation may be obtained. The intrinsic attenuation is of great importance because it can give additional information about the petrophysical properties of rocks. Including intrinsic attenuation into the above plane wave expression (1.3), one has

$$g = A e^{-\alpha x} e^{i(kx - \omega t)} \quad (1.4)$$

so that the amplitude decays as it propagates in space. The coefficient α is the attenuation coefficient. An alternate way to describe the attenuation is to use the quality factor Q . The quality factor is defined as (Aki & Richards, 1980)

$$Q = \frac{2\pi E}{\Delta E} \quad (1.5)$$

where ΔE is the energy dissipated per wave cycle and E is the total elastic energy of a wave cycle. Assuming the above plane wave, one can rewrite (1.5) as

$$Q = \frac{\pi f}{\alpha c} \quad (1.6)$$

where α is the attenuation coefficient and c is the phase velocity at the frequency f .

There are several mechanisms through which mechanical energy may be converted to heat. First is the solid friction loss mechanism, which is concerned with the slippage of crack surfaces or grain contacts (Mindlin & Deresiewicz, 1953; Knopoff & McDonald, 1958; Walsh, 1966; Mavko, 1979; Palciauskas, 1992). This mechanism requires the

computed velocity and attenuation be dependent on the strain amplitude and is therefore a non-linear mechanism (Duffy & Mindlin, 1957), independent of frequency, and the low frequency stress-strain loops be cusped (Dutta, 1979). Supporting evidence for such a mechanism is that the attenuation does not vanish for dry rocks (Johnston *et al.*, 1979). The attenuation for low strains, $< 10^{-6}$, such as those associated with seismic waves, appears to be independent of strain amplitude (Gordon & Davies, 1968; Mason & Kuo, 1971; Winkler & Nur, 1982; Winkler, 1983; Stoll, 1979; Murphy, 1982; Bulau *et al.*, 1984; Murphy *et al.*, 1986). Furthermore, the mechanism is strongly inhibited by moderate confining pressures (Winkler *et al.*, 1979). Therefore, this mechanism may be of importance in large amplitude laboratory experiments, but it is probably not important for seismic losses in rocks in-situ.

Second is the viscous fluid-flow mechanism. It is associated with the relative motion of the viscous fluid with respect to the solid. The models developed for this mechanism can be grouped into two categories: (1) microscopic models and (2) macroscopic models. In the microscopic models (Walsh, 1968, 1969; Kuster & Toksöz, 1974a; O'Connell & Budiansky, 1974, 1977; Mavko & Nur, 1979; Toksöz *et al.*, 1979; Johnston *et al.*, 1979; Rouleau, 1993) the flow is "local" and takes place at the intergranular gaps which are to be distinguished from the pores. These microscopic models are developed for "cracked material" and contain parameters such as crack aspect ratio or crack number density.

The most popular macroscopic model for the viscous fluid-flow mechanism was developed by Biot (1956b, 1956c, 1962a, 1962b). This work is based on the previous model of Gassmann (1951a, 1951b) for the propagation of elastic waves through a packing of spheres. The stress-strain relations were previously obtained by Biot (1941a, 1955). The macroscopic "effective" parameters in Biot's wave propagation theory are related to static measurements in the work of Biot & Willis (1957), Fatt (1959), Yew & Jogi (1978) and Berryman & Milton (1991). The Biot model is semi-phenomenological in nature and is characterized by two coupled differential vector equations. The model predicts the existence of two P-waves and one S-wave. The model of Biot has been applied to acoustics of marine sediments in a series of works by Stoll (1989). Warner (1990), Johnson (1980), and Dutta (1980) among others have used the Biot work to interpret laboratory measurements performed on samples filled with liquid helium. Fang *et al.* (1993) used Biot's formulation to analyze in-situ pore pressure measurements in marine

sediments. Studies of the applicability of the Biot theory to low porosity materials (Ogushwitz, 1985a), suspensions (Ogushwitz, 1985b), marine sediments (Ogushwitz, 1985c) and sintered glass beads saturated with water (Berryman, 1980) indicate marginal success. None of these studies examine the consequences of the assumption of an energy potential as put forth by Biot.

Others have started with the equations governing each phase at the pore scale and have used various homogenization theories in order to obtain a macroscopic description. Burrige & Keller (1981) utilize the two space method of homogenization to derive a set of equations governing the mechanical behavior of a fluid filled porous elastic solid. When the dimensionless viscosity $\mu_f/\omega\rho_f H^2$ (where μ_f is the fluid viscosity, ρ_f is the fluid density, ω is the angular frequency and H is a macroscopic scale length) appropriate to the large scale is small, and the medium is macroscopically uniform, the results are of the form of Biot's (1962a). From comparison of their equations with those of Biot's they obtain expressions for Biot's coefficients (see Burrige & Keller, 1981: equations 43a-43h).

de la Cruz & Spanos (1985, 1989b) and Pride *et al.* (1992) construct the foundations for a macroscopic description through the use of volume averaging. Pride *et al.* (1992) make assumptions requiring the equations of motion to be similar to those of Biot (1956b) except for the definition of the added mass coefficient. Furthermore, their stress-strain relations are the same as Biot's (1956b) and the definitions of the effective elastic moduli are the same as given by Biot & Willis (1957). In the development of de la Cruz & Spanos (1989b) they demonstrate that the porosity is a variable which must be introduced at the outset. With the reminder that the porosity is kinematically independent of the average solid and fluid displacements they postulate a relationship between the dilation of the individual phases and the changes in relative proportions of the phases. The final system of equations can be written in the form of Biot's (1956b) subject to a compatibility condition (equation 37 of de la Cruz & Spanos, 1989b) which will be further discussed in chapter 4. A correspondence between the parameters is established (see de la Cruz & Spanos, 1989b: equation 46). The macroscopic material shear modulus in this model is simply the shear modulus of the solid component weighted by the volume fraction of solid. This model predicts the existence of two P-waves and two S-waves. The Biot model only predicts one S-wave. The second S-wave is the counterpart to Biot's P-wave of the second kind . It exists due to the solid-fluid interaction and is highly attenuated. However , if the

second S-wave does exist, it can be an additional energy loss mechanism operating in various wave phenomena. Other studies (Liu & Katsube, 1990; Katsube & Carroll, 1987a, 1987b; Crochet & Nagdhi, 1966) using the theory of mixtures (see Bedford & Drumheller, 1983 for a survey of the theory of mixtures) also support the notion of a second S-wave.

Bear & Corapcioglu (1989) obtain a description for wave propagation in a saturated compressible porous medium by starting with the macroscopic mass and momentum balance equations for the solid matrix and the pore fluid. They obtain as limiting cases: Darcy's Law, and the three-dimensional consolidation model of Biot (1941).

Other recent works based on various homogenization schemes are Walton & Digby (1987), Mei & Auriault (1989), Kowalski (1992), and Nigmatulin & Gubaidullin (1992). All above quoted macroscopic descriptions, including Biot's (1956b, 1956c), are formulated to describe wave propagation in the regime where the wavelength of disturbance is much larger than the average pore size.

Some recent efforts (Dvorkin & Nur, 1993) have been made to combine both the microscopic and macroscopic models for the viscous fluid flow mechanism. This work was carried out for P-waves only. The macroscopic model is that of Biot (1956b, 1956c). The microscopic model is based on the assumption that the solid skeleton of a rock deforms in a uniaxial mode parallel to the direction of wave propagation. The fluid which moves perpendicular to the direction of propagation, which they call "s squirt" flow, is the phenomenon which necessitates the microscopic model. The principle alteration from the Biot model is the effect of squirt flow on the fluid dynamic pressure. The only formal difference is in the coefficients of the fluid pressure equation. The coefficient is a constant in the Biot case, whereas in the combined model it becomes dependent on frequency and a characteristic squirt flow length.

A third mechanism is thermoelastic attenuation. This attenuation is due to the fact that mechanical disturbances associated with a propagating wave causes changes in temperature of the phases. The regions of compression experience an increase in temperature whereas the regions of dilation experience a decrease in temperature. Heat is then conducted away from the regions of compression towards the regions of dilation. Given the long

wavelength of the waves considered in this work the temperature gradients are usually very small and the amount of heat transferred during the period of a disturbance is usually very small. Therefore, the attenuation due to such heat conduction is usually negligible. Given the different physical properties of the pore fluid and matrix material, comprising a porous medium, they will also have different temperatures. The transfer of heat between constituents can be substantial because of the short distances (order of the pore size) and the large surface area of contact between the constituents. This transfer of heat may enhance the attenuation due to fluid flow by promoting motion of the fluid. Both types of heat transfer was theoretically modelled by de la Cruz & Spanos (1989b) using the volume averaging technique. Numerical studies by Hickey (1990) indicate that this mechanism will probably not be important except for some deep earth situations. Further numerical examples will be given in chapter 4.

Budiansky *et al.* (1983) derive an effective frequency dependent thermoelastic bulk modulus for an isotropic composite subject to an applied harmonic hydrostatic stress. Numerical results indicate that this mechanism could be of importance to regions such as the lower mantle. Vaisnys (1968) studied the propagation of acoustic waves through a system undergoing phase transformations. From the analysis he concluded that the attenuation due to phase transformation can be sufficiently large to contribute to seismic losses in the mantle.

An emergent consensus is that the seismic loss mechanisms associated with fluid flow are dominant for low strain amplitudes used for hydrocarbon prospecting (Dutta, 1979). The work presented here will be directed towards the modelling of the intrinsic attenuation due to the fluid f/w mechanism, for low frequency waves propagating through a fluid-filled porous solid.

Wave propagation through partially saturated samples or samples containing two fluid phases have also been studied. One approach is to utilize a theory for a fully saturated porous medium, such as the Biot (1956b, 1956c) theory, and account for the multiple fluid phases by replacing the original fluid parameters and some of the macroscopic parameters with "effective" parameters (Pride *et al.*, 1992; Smolders *et al.*, 1992; Berryman *et al.*, 1988; Berryman & Thigpen, 1985; Mochizuki, 1982; Dutta & Odé, 1979a, 1979b; Dutta & Seriff, 1979; White, 1975; Domenico, 1974). These effective parameters are constructed based upon specific assumptions about the interactions of the two fluid phases. More

general descriptions are obtained when the fluids are treated independently. The macroscopic descriptions are usually formulated through the use of some type of homogenization scheme (Hawkins & Bedford, 1992; Santos *et al.*, 1990a, 1990b; Garg & Nayfeh, 1986; Thigpen & Berryman, 1985). The governing system of equations in these general formulations contains numerous parameters which are not well understood and experimental procedures for their measurements are usually not presented.

1.4 Experimental Data

A considerable amount of experimental data exists concerning the phase velocity and attenuation of both compressional (P) and shear (S) waves. Experimental techniques employed are: (1) resonant bar (details can be found in Clark *et al.*, 1980), covering an approximate frequency range of 0.5 - 25 kHz, (2) pulse transmission technique (Kaarsberg, 1975; Sears & Bonner, 1981; Winkler & Piona, 1982), with a frequency range of about 0.1 - 50 MHz, and (3) others: forced torsional (Kampfmann & Berckheimer, 1985) and the shock tube technique (van der Grinten *et al.*, 1985, 1987) which measures strain and the pore pressure at one end of a sample due a step like pressure gradient at the other end. Experimental problems associated with the first two of these methods are discussed by Niblett & Wilks (1960), and Wyllie *et al.* (1962) as well as in numerous texts on acoustics.

Experiments are performed to study the dependence of attenuation (Q) and phase velocity on frequency (Bulau *et al.*, 1984; Winkler, 1986, 1985, 1983; Wang & Nur, 1990; Shankland *et al.*, 1993), temperature (Clark *et al.*, 1981; Jones & Nur, 1983; Kampfmann & Berckheimer, 1985; Wang & Nur, 1988; Vo-Thanh, 1992), pressure (Winkler & Piona, 1982; Jackson *et al.*, 1984; Christensen & Wang, 1985; O'Hara, 1985), and the properties of the constituent materials (Costley & Bedford, 1988; Vo-Thanh, 1990; Prasad & Meissner, 1992; Vernik & Nur, 1992).

Observation of the second P-wave (slow wave), predicted by Biot (1956b, 1956c) propagating through a sample of sintered glass beads (Piona, 1980), resin bonded glass beads and other synthetic samples (Piona *et al.*, 1990) have been noted at ultrasonic frequencies. Johnson & Piona (1982) conducted the experiment in fused and loose

(unconsolidated) glass bead samples. They did not observe the second P-wave in the loose glass beads sample. The search for the second P-wave has associated this mode to fourth sound in a porous "superleak" (Johnson, 1980; Johnson & Piona, 1982). Fourth sound is the acoustic mode of propagation through a superfluid entrained by a porous solid. For an account of studies of fourth sound see Warner (1990). Such studies of the 2nd P wave lends strong support for the Biot theory.

The experimental data are sometimes used to construct empirical relationships. The time average relationship of Wyllie *et al.* (1956) has been used to obtain porosities from acoustic velocities. Han *et al.* (1986) obtain relationships for P and S-wave velocity as functions of porosity and clay content by applying a least square fit to ultrasonic data. Klimentos (1991b) obtains a relation for the velocity of compressional waves with respect to porosity, permeability and clay content. Freund (1992) obtains velocity relationships as functions of porosity, clay content and confining pressure.

The influence of multiple (usually two) fluids saturating a porous medium on the character (velocity and attenuation) of sound waves have been investigated experimentally for quite some time. Changes in phase velocity and attenuation of sound waves, due to changes in saturation, are observed to be greatest at very low saturations or near complete saturation. Knight & Dvorkin (1992) studied the dependence of seismic and electrical properties of sandstones at very low saturations. They contend that although seismic and electrical properties vary with saturation through the entire range, the dependence at low saturation is distinctly different than at higher saturations. Furthermore, the phase velocities, for a water-air system, are larger when the sample is prepared through a drainage process as compared to values from a sample prepared by the imbibition process. For example, Knight & Nolen-Hoeksema (1990) investigated the variation in elastic wave velocities with saturation (water-air) during a continuous imbibition/drainage experiment. Measured P-wave velocities obtained during drainage are larger than those obtained during imbibition for saturations of 90 percent (maximum attained saturation) down to about 40 percent. Below 40 percent saturation the velocities are similar for both imbibition and drainage. The S-wave velocities exhibit a similar dependence on saturation and method of saturating as the P-wave velocities.

From the discussion above it is evident that rock and composite materials are extremely

complex systems and therefore some simplified models must be studied. These models will depend on the approach of the study (analytic, empirical, or numerical) as well as the process which one is interested in. In order for the resulting theory to be valid one must ensure that the physical assumptions used to construct the theoretical model describe the essential features of the physical system of interest. The poroelastic model considered here will consist of macroscopically homogeneous and isotropic porous rock saturated by one fluid and at most two fluids. The solid material will be assumed to obey Hooke's law and the fluid be Newtonian. The deformations will be reversible, infinitesimal and isothermal unless otherwise stated. Other assumptions used during the derivations of certain process will be noted at that time. The theoretical model will have an explicit dependence on the properties of the solid frame and pore fluids and their interaction. This model can therefore be used to optimize the extraction of information from say, high resolution seismic, sonic log, VSP, and laboratory core data.

1.5 Outline of Thesis

In chapter 1, a review of previous works dealing with quasi-static deformation of porous media and wave propagation through porous media is presented. Various processes occurring in permeable media are introduced and the various approaches used to quantify such processes are summarized.

In chapter 2, recently developed macroscopic relations for equilibrium thermodynamics are discussed. A brief review of single continuum thermodynamics is presented, followed by a development of macroscopic thermodynamic relations for the solid phase. The corresponding relations for the fluid component are then treated. Volume averaged equations are used to provide the linkage to pore scale thermodynamics. Finally, the internal energy for the porous medium is discussed in the context of a system consisting of two superposed continua. The consequences of a unique energy potential for such a system is studied from a thermodynamic viewpoint.

In chapter 3 a description of quasi-static deformations of a porous material consisting of a solid frame completely saturated by a single fluid is presented under the assumption of infinitesimal strains. The description is based on the quasi-static limit of the low-frequency

wave propagation work of de la Cruz & Spanos (1985; 1989b). Both drained and undrained compressibilities (bulk moduli) are considered. A continuous one-parameter family of compressibilities is introduced to permit greater flexibility in experimental set-ups. The problem of macroscopic shearing is analyzed. Formulas for "Young's modulus" and "Poisson's ratio" for porous media under drained and undrained conditions are derived. The results are compared to the work of Zimmerman (1986; 1991) and others. Expressions for the induced pore pressure coefficient and the coefficient of effective stress are also obtained.

In chapter 4 the system of equations which form the basis of the description of low frequency wave propagation is presented. Again these equations are based on the work of de la Cruz & Spanos (1985, 1989b), but are modified to include the fluid bulk viscosity and to accommodate phenomenological shear modulus and heat conductivities. The theoretical basis for the modification is given as well as numerical examples illustrating the changes in the phase velocity, attenuation and/or quality factor due to the modifications. In the work of de la Cruz & Spanos (1989b) porosity is an independent dynamic variable. They, however, introduce a relationship between porosity and the macroscopic displacement vectors involving two parameters, δ_r and δ_s . Expressions for δ_r and δ_s in terms of static compressibilities, determined in chapter 2, are used as initial estimates and numerical examples are presented showing the sensitivity on such parameters.

In chapter 5 a description of low frequency wave propagation through a porous medium saturated by two fluids is presented. First, an approximation is obtained by using the equations presented in chapter 4 and assuming that the two fluids form a composite or effective fluid. Suitable expressions for the effective parameters of the composite fluid are derived and the underlying assumptions clearly stated. Brief discussions about the effects on various macroscopic parameters are also presented. This analysis is based completely on descriptions obtained from volume averaging. Second, the governing equations are derived for the general case of wave propagation through a porous medium saturated by two fluids. Volume averaging is used to construct the basic equations and the approach parallels that of chapter 4 (see figure 4.1).

Chapter 6 contains a brief review of the results obtained in this dissertation as well as concluding remarks.

CHAPTER 2

THERMODYNAMICS OF DEFORMATION

2.1 Introduction

When viewed on a suitably large scale, a porous medium is often described in terms of two spatially superposed interacting media (e.g. Gassmann 1951a; Biot, 1941, 1956b, 1956c; Keller, 1977; Sanchez Palencia, 1980; Burrige & Keller, 1981; de la Cruz & Spanos, 1989b). The most widely applied work is that of Biot. In his initial work on poroelasticity, Biot (1941), "introduced the assumption of the existence of a potential energy of the soil" in order to obtain a relation between phenomenological parameters and thereby reducing the number of macroscopic parameters by one. The majority of his later work (Biot, 1956b, 1956c, 1962a, 1962b) commences with use of the energy potential for the porous medium. Therefore, it can be said that the Biot work is based on a "macroscopic thermodynamics" (de la Cruz *et al.*, 1993).

As mentioned in the introduction, other wave propagation theories (Burrige & Keller, 1981; de la Cruz & Spanos, 1989b) have been constructed in which the equations are of similar form to those of Biot (1956b). From comparison of their final equations with those of Biot they obtain expressions for Biot's coefficients subject to certain conditions. Of course, comparing formulas and/or definitions in two theories and equating corresponding symbols does not necessarily prove that they are identical. Given the foundations of the Biot theory it would be advantageous to obtain a description of such "macroscopic thermodynamics". The question then arises of how to express thermodynamic ideas using only quantities that are meaningful in the macroscopic description. Formulations of multiphase thermodynamics have appeared in the literature (Gurtin, 1988; Gurtin & Struher, 1990; Garcia-Colin & Uribe, 1991) and were developed primarily on the rigors of mathematics. The final solutions, however, are very complex and could possibly be simplified further on a physical basis. Other thermodynamic formulations (Scheidegger, 1974; Marie, 1982; Dallon, 1992) are derived with application to heat transfer or multiphase flow in undeformable porous media.

The aim of this chapter is to discuss recently developed (de la Cruz *et al.*, 1993) macroscopic relations for equilibrium thermodynamics of porous media. The approach uses volume averaged equations to provide the linkage to pore scale thermodynamics. The volume averaging procedure is therefore outlined. A brief review of single continuum thermodynamics is presented, followed by a development of macroscopic thermodynamic relations for the solid phase. The corresponding relations for the fluid phase are then treated. Finally, the macroscopic thermodynamics is used to construct an internal energy for a porous medium in the context of a system consisting of two superposed continua. Implications of Biot's use of an energy potential is then discussed.

2.2 Volume Averaging

The principle objective in reformulating the problem at a larger scale is to filter out the over abundance of physical detail at the pore scale in such a manner that no specific reference to pore scale motions remains. Following the work of de la Cruz & Spanos (1985, 1989b) an averaging procedure, called volume averaging, pioneered by Hubbard (1956), Whitaker (1966, 1969) and Slatery (1969) is utilized.

In the volume averaging procedure one constructs regions V in the porous medium of identical shapes, volumes, orientations. An average value for the physical quantities within the volume V is ascribed to a point x which uniquely defines V . For example, de la Cruz & Spanos (1983) assume V to be spheres and each V is specified uniquely by the centre of the sphere x . Also by choosing spheres the problem of orientation is avoided. If we assume $G_f(x)$ to be a physical quantity of the fluid and that $G_f(x)$ equals zero everywhere outside the fluid, then the volume average of G_f over any region V is defined as

$$\langle G_f \rangle = \frac{1}{V} \int_V G_f(x) dV \quad (2.1)$$

where $\langle G_f \rangle$ is a function of the center of the volume elements. If one assumes the center of the volume element is within the solid and plots $\langle G_f \rangle$ as a function of the volume V one might obtain a curve similar to figure 2.1 (Whitaker, 1969).

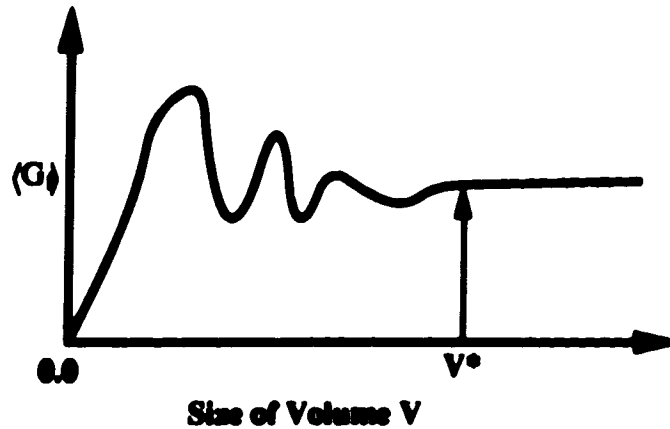


Figure 2.1 Dependence of average on averaging volume.

Since the center of the volume V was assumed to be in the solid component then $\langle G \rangle$ is zero at the origin. As one starts increasing the volume size, portions of the fluid are contained within the volume, and $\langle G \rangle$ increases from zero through fluctuations due to random distribution of the fluid at the pore scale. For values of V larger than say, V^* , the pore scale variations are smoothed out. Given that the dependence of the function $\langle G \rangle$ on volume element size is always continuous the critical volume, V^* , is the minimum volume element size where macroscopic variations completely dominate microscopic changes rather than a condition of continuity.

As one moves the volume element to different locations in the porous medium, $\langle G \rangle$ becomes a continuous function of x . However, for values of V larger than V^* the function $\langle G \rangle$ is independent of V . A precise value for V^* cannot be determined, but one can assume that it must be orders of magnitude larger than the pore scale. However, if there are structures much larger than the volume element, V^* , then appropriate macroscopic boundary conditions (de la Cruz & Spanos, 1989a) must be used.

A related quantity, the phasic average, \bar{G}_r is defined as

$$\bar{G}_r = \frac{1}{V_r} \int_V G_r(x) dV \quad (2.2)$$

where V_f is the volume of fluid in the volume V . This is related to $\langle G_f \rangle$ as follows

$$\bar{G}_f = \frac{1}{\eta} \langle G_f \rangle \quad (2.3)$$

where η is the volume fraction of that phase.

In the development of the average equations one will be dealing with gradients and time derivatives of such quantities. Slattery (1969) and Whitaker (1969) developed the following relationships between the averages of derivatives and the derivatives of averages:

$$\int_V \partial_i G_f dV = \partial_i \int_V G_f dV + \int_{A_{fs}} G_f n_i dA \quad (2.4)$$

and

$$\int_V \partial_t G_f dV = \partial_t \int_V G_f dV - \int_{A_{fs}} G_f v \cdot n dA \quad (2.5)$$

Here, A_{fs} refers to the area of the fluid-solid interfaces, n is the unit normal on those interfaces directed towards the solid, and v is the velocity of the fluid-solid interface element.

If one is to describe some process in the porous medium, say the propagation of a wave, then a lower bound on the scale at which deformations are described must be imposed. As the frequency of disturbance is increased the amount of pore scale detail in the macroscopic description must also be increased. However, for a "homogeneous" medium, provided one deals with wavelengths much larger than the pore scale, the equations are scale independent. Hence, application of this method is subject to the condition on the scale of deformation

$$d \ll L \ll \lambda \ll D \quad (2.6)$$

where d is a pore scale dimension, L is the volume element scale dimension, λ is the wavelength of disturbance, and D is a characteristic macroscale.

2.3 Review of single continuum thermodynamics

The first law of thermodynamics states that an infinitesimal change in the internal energy, \mathcal{U} , per unit volume of the undeformed body (most common in descriptions of solids), is equal to the difference between the heat dQ acquired by the unit volume considered and the work $d\mathcal{R}$ done by the internal stresses (Landau & Lifshitz, 1975a); i.e.,

$$d\mathcal{U} = dQ - d\mathcal{R} \quad (2.7)$$

If it is assumed that the process is thermodynamically reversible, then the second law states that the amount of heat is

$$dQ = T dS \quad (2.8)$$

where T is the temperature and S is the entropy. The work done is the product of the force and distance moved, the force being measured in the direction of the line along which it is acting. The force F is related to the internal stresses τ_{ik} by

$$F_i = \frac{\partial \tau_{ik}}{\partial u_k} \quad (2.9)$$

and therefore a small amount of work done $\delta\mathcal{R}$ by the internal stresses per unit volume can be written as

$$\delta\mathcal{R} = \frac{\partial \tau_{ik}}{\partial u_k} \delta u_i \quad (2.10)$$

where δu_i is a small change in the displacement vector. If the medium is of infinite extent and is not deformed at infinity then integrating over the entire body (performing an integration by parts) yields

$$\delta \mathcal{R} = -\tau_{ik} \delta u_{ik} \quad (2.11)$$

which is the work done $\delta \mathcal{R}$ per unit volume in terms of the strain tensor, u_{ik} . The strain tensor is simply related to the displacement vector (first order) as

$$u_{ik} = \frac{1}{2} \left(\frac{\partial u_i}{\partial x_k} + \frac{\partial u_k}{\partial x_i} \right) . \quad (2.12)$$

Substituting equation (2.8) and (2.12) into equation (2.7) we obtain a fundamental thermodynamic relation for deformed bodies (Landau & Lifshitz, 1975a) as

$$d\mathcal{U} = TdS + \tau_{ik} du_{ik} \quad (2.13)$$

Two other thermodynamic quantities (path independent) are, the Gibbs' free energy \mathcal{G} for isothermal changes at constant pressure and the Helmholtz free energy \mathcal{F} for isothermal changes at constant volume. These are defined as follows (Tabor, 1991):

$$\mathcal{F} = \mathcal{U} - TS \quad (2.14)$$

and

$$\mathcal{G} = \mathcal{U} - \tau_{ik} u_{ik} - TS . \quad (2.15)$$

These can be written in the form of equation (2.13) as

$$d\mathcal{F} = -SdT + \tau_{ik} du_{ik} \quad (2.16)$$

and

$$d\mathcal{G} = -SdT - u_{ik} d\tau_{ik} . \quad (2.17)$$

The components of the stress tensor may be obtained by differentiating the internal energy \mathcal{U} (equation 2.13) with respect to components of the strain tensor for constant entropy S

$$\tau_{ik} = \left(\frac{\partial u}{\partial u_{ik}} \right)_s \quad (2.18)$$

or differentiating the Helmholtz free energy \mathcal{F} (equation 2.16) at constant temperature T

$$\tau_{ik} = \left(\frac{\partial \mathcal{F}}{\partial u_{ik}} \right)_T . \quad (2.19)$$

Similarly, the components of the strain tensor can be obtained by differentiating Gibbs' free energy \mathcal{G} (equation 2.17) with respect to the components of the stress tensor, at constant temperature,

$$u_{ik} = - \left(\frac{\partial \mathcal{G}}{\partial \tau_{ik}} \right)_T . \quad (2.20)$$

To proceed, an expression for the free energy \mathcal{F} of the body in terms of the strains u_{ik} is required. Considering an elastic body undergoing small deformations, at constant temperature, the free energy is commonly written as (Landau & Lifshitz, 1975a)

$$\mathcal{F}_s = \mathcal{F}_s^0 + \mu_s \left(u_{ik}^2 - \frac{1}{3} u_{ii}^2 \delta_{ik} \right) + \frac{1}{2} K_s (u_{ii})^2 \quad (2.21)$$

where \mathcal{F}_s^0 is the free energy of the undeformed body, K_s is the isothermal bulk modulus and μ_s is the shear modulus. The notation used requires summation over repeated indices and therefore u_{ii} represents the solid dilation. If the body undergoes a change in temperature during deformation then additional terms must be added to the free energy to account for additional stresses caused by the change in temperature. The free energy is then written as

$$\mathcal{F}_s = \mathcal{F}_s^0 - K_s \alpha_s (T_s - T_0) u_{ii} + \mu_s \left(u_{ik}^2 - \frac{1}{3} u_{ii}^2 \delta_{ik} \right) + \frac{1}{2} K_s (u_{ii})^2 \quad (2.22)$$

where α_s is the thermal expansion coefficient of the body. Using equation (2.19) and the free energy (2.22) the stress tensor is

$$\tau_{ik}^e = -K_s \alpha_d (T_s - T_o) \delta_{ik} + 2\mu_d \left(u_{ik}^e - \frac{1}{3} u_{ll}^e \delta_{ik} \right) + K_s u_{ll}^e \delta_{ik} . \quad (2.23)$$

From equation (2.16) the entropy S can be calculate from the free energy \mathcal{F} as

$$S = - \frac{\partial \mathcal{F}}{\partial T} \quad (2.24)$$

so that, using equation (2.22), the entropy for an elastic solid, S_s , is

$$S_s = S_s^o(T_s) + K_s \alpha_d u_{ll}^e . \quad (2.25)$$

An alternate thermodynamic deformation, known as an adiabatic deformation, is performed such that no exchange of heat between the body and its surroundings takes place. Equation (2.8) requires that the entropy S be constant for such deformations. The stress tensor for an adiabatic deformation may be written as

$$\tau_{ik}^e = K_{ad}^s u_{ll}^e \delta_{ik} + 2\mu_d \left(u_{ik}^e - \frac{1}{3} u_{ll}^e \delta_{ik} \right) \quad (2.26)$$

where the adiabatic bulk modulus K_{ad}^s is related to the isothermal bulk modulus K_s by

$$\frac{1}{K_{ad}^s} = \frac{1}{K_s} - \frac{T_s \alpha_d^2}{C_p} \quad (2.27)$$

in which C_p is the specific heat per unit volume at constant pressure. Many processes by which elastic materials deform lie somewhere between the isothermal and adiabatic cases discussed above. However, the process dependent correction to the bulk modulus parameter, second term on right hand side of equation (2.27), is small for most elastic materials and therefore the error associated with the deviation in bulk modulus is usually small.

For fluids, the first law of thermodynamics (2.7) is commonly used as the basis for constructing an energy balance equation (Kundu, 1990). For a Newtonian fluid undergoing small deformations the energy balance equation is

$$\frac{\partial}{\partial t} \left(\frac{1}{2} \rho v^2 + e_f \right) + \nabla \cdot \left\{ v_f \left(\frac{1}{2} \rho v^2 + e_f \right) \right\} = -p_f \nabla \cdot v_f + \nabla \cdot (\kappa_f \nabla T_f) + \nabla \cdot (\tilde{\tau}_f \cdot v_f) \quad (2.28)$$

where e_f is the internal energy per unit volume and the viscosity stress tensor, $\tilde{\tau}_f$, is

$$\tilde{\tau}_f = \mu_f \left(\frac{\partial v_i}{\partial x_k} + \frac{\partial v_k}{\partial x_i} - \frac{2}{3} \frac{\partial v_l}{\partial x_l} \delta_{ik} \right) + \xi_f \frac{\partial v_i}{\partial x_i} \delta_{ik}. \quad (2.29)$$

The first term on the left hand side of equation (2.28) represents the change in total energy (both kinetic and internal energy), the second term represents the flux of total energy across the bounding surface. On the right hand side, the first term represents the rate of work done by the pressure, the second term represents the heat acquired due to heat conduction (it is assumed that the heat flux obeys Fourier's law), and the third term is the heating due to viscous dissipation.

The second law of thermodynamics (2.8) for a viscous fluid can be written as

$$\frac{\partial S_f}{\partial t} + \nabla \cdot (v_f S_f) = \frac{1}{T_f} \nabla \cdot (\kappa_f \nabla T_f) + \frac{1}{T_f} \nabla \cdot (\tilde{\tau}_f \cdot v_f) \quad (2.30)$$

where S_f is the fluid entropy per unit volume. The entropy production is due to heat conduction (first term on left hand side) and viscous generation of heat (second term on left hand side).

2.4 Macroscopic Thermodynamics

Turning now to the macroscopic description of the solid component, we shall be interested (as in the ordinary theory of elasticity) only in small deformations from a uniform, "unperturbed" state. Given that the free energy for the solid, equation (2.22), at the small scale is a second order equation, then applying volume averaging directly would not easily yield the required macroscopic free energy to second order. Thus, proceeding on the macroscopic level, de la Cruz *et al.* (1993) postulate that the work done δW_s , by a macroscopic solid stress $\hat{\sigma}_k$, through a small deformation is of the form

$$\delta R_s = - \int (\epsilon_{ik} \delta \bar{u}_{ik}^s - a \epsilon_{ii} \delta \phi) d^3x \quad (2.31)$$

where a is a dimensionless constant, ϕ is the volume fraction of solid, and \bar{u}_{ik}^s is the average solid strain which is related to the average solid displacement as

$$\bar{u}_{ik}^s = \frac{1}{2} (\bar{u}_{i,k}^s + \bar{u}_{k,i}^s) \quad (2.32)$$

Hence, when a deformation takes place, the volume fraction of solid (which related to porosity) as well as the (macroscopic) displacement \bar{u}_s are changed. The validity of equation (2.31) will be shown through the use of volume averaged relations shortly.

According to equation (2.31) a fundamental macroscopic relation for deformed porous media (in a similar form as equation (2.13) for the elastic case above) is

$$d U_s = \epsilon_{ik} d \bar{u}_{ik}^s + \bar{T}_s d S_s \quad (2.33)$$

where U_s and S_s denote the macroscopic internal energy and the entropy of the solid component, referring to the fixed amount of matter enclosed in a unit volume of the unperturbed medium and

$$\bar{u}_{ik}^s = \bar{u}_{ik}^s - a(\phi - \phi_0) \delta_{ik} \quad (2.34)$$

with $\phi_0 = 1 - \eta_0$ being the unperturbed value. The macroscopic solid free energy enters through

$$F_s = U_s - \bar{T}_s S_s \quad (2.35)$$

so that

$$d F_s = \epsilon_{ik} d \bar{u}_{ik}^s - S_s d \bar{T}_s \quad (2.36)$$

and therefore

$$\bar{d}_{ik} = \frac{\partial F_s(\bar{T}_s, \bar{u}_{ik})}{\partial \bar{u}_{ik}} . \quad (2.37)$$

By hypothesis, when $\bar{T}_s - T_o = 0$, $\phi - \phi_o = 0$, and $\bar{u}_{ik} = 0$, there is no stress

$$\left. \left(\frac{\partial F_s(\bar{T}_s, \bar{u}_{ik})}{\partial \bar{u}_{ik}} \right) \right|_{\bar{T}_s = T_o, \bar{u}_{ik} = 0} = 0 . \quad (2.38)$$

The most general scalar function F_s , satisfying equation (2.38) that can be constructed out of $\bar{T}_s - T_o$ and the symmetric \bar{u}_{ik} is, to second order, of the form

$$F_s(\bar{T}_s, \bar{u}_{ik}) = \phi_o \mathcal{F}_s^o(\bar{T}_s) + a_1(\bar{T}_s - T_o) \bar{u}_{11} + a_2(\bar{u}_{ik} - \frac{1}{3} \delta_{ik} \bar{u}_{11})^2 + a_3(\bar{u}_{11})^2 \quad (2.39)$$

where the function $\mathcal{F}_s^o(\bar{T}_s)$ is independent of \bar{u}_{ik} , and where a_i are constants. Using equations (2.39) and (2.37) the stress tensor obtained through the thermodynamics is

$$\bar{d}_{ik} = a_1(\bar{T}_s - T_o) \delta_{ik} + 2a_2(\bar{u}_{ik} - \frac{1}{3} \delta_{ik} \bar{u}_{11}) + 2a_3 \delta_{ik} [\bar{u}_{11} - 3a(\phi - \phi_o)] . \quad (2.40)$$

The macroscopic solid equation of motion obtained on the basis of volume averaging is of the form (de la Cruz & Spanos, 1989b)

$$\frac{\partial}{\partial t} (\phi \bar{\rho}_s \bar{u}_i^s) = \partial_k (\bar{t}_{ik}^s) + B_i^s \quad (2.41)$$

where B_i^s is the body force representing the action of the fluid component (essentially the Darcian resistance). For quasi-static processes, $B_i^s = 0$ as discussed in chapter 3. $\langle \bar{t}_{ik}^s \rangle$ is the macroscopic stress tensor (de la Cruz & Spanos, 1989b; Hickey *et al.*, 1993; and derived in chapter 4) which is obtained from volume averaging (to first order) as

$$\langle \bar{t}_{ik}^s \rangle = -\phi_o K_s \alpha_s (\bar{T}_s - T_o) \delta_{ik} + 2\mu_{sd} [\bar{u}_{ik} - \frac{1}{3} \delta_{ik} \bar{u}_{11}] + \phi_o K_s \delta_{ik} \left[\bar{u}_{11} + \frac{\phi - \phi_o}{\phi} \right] \quad (2.42)$$

Assuming that \bar{d}_{ik} is the same as $\langle \bar{t}_{ik}^s \rangle$ and comparing the two using equations (2.40) and

(2.42) de la Cruz *et al.* (1993) obtain

$$a_1 = -\phi_0 K_s \alpha_s \quad (2.43)$$

$$a_2 = \mu_M \quad (2.44)$$

$$a_3 = \frac{1}{2} \phi_0 K_s \quad (2.45)$$

and

$$a = -\frac{1}{3\phi_0} \quad (2.46)$$

Here, K_s is the isothermal bulk modulus of the solid material and α_s is the coefficient of thermal expansion of the solid material, and μ_M is a macroscopic shear modulus of the medium.

The assumed macroscopic solid free energy F_s , equation (2.39), is simply

$$F_s(\bar{T}_s, \bar{u}_{ik}^s) = \phi_0 f_s^0(\bar{T}_s) - \phi_0 K_s \alpha_s (\bar{T}_s - T_0) \bar{u}_{11}^s + \mu_M (\bar{u}_{ik}^s - \frac{1}{3} \delta_{ik} \bar{u}_{ll}^s)^2 + \frac{1}{2} \phi_0 K_s (\bar{u}_{11}^s)^2 \quad (2.47)$$

with

$$\bar{u}_{ik}^s = \bar{u}_{ik}^1 + \frac{1}{3} \delta_{ik} \frac{\phi - \phi_0}{\phi_0} \quad (2.48)$$

From equation (2.35) the macroscopic solid entropy S_s is calculated as

$$S_s = -\frac{\partial F_s(\bar{T}_s, \bar{u}_{ik}^s)}{\partial \bar{T}_s} \quad (2.49)$$

so that using equation (2.47), the macroscopic entropy is

$$S_s = -\phi_o \frac{\partial \mathcal{S}_s^o(T_s)}{\partial T_s} + \phi_o K_s \alpha_s \left[\bar{u}_{11} + \frac{\phi - \phi_o}{\phi_o} \right] \quad (2.50)$$

to first order.

In order to check the validity of the work relation postulated by equation (2.31) the above macroscopic solid entropy equation (2.50), to first order, is obtained by de la Cruz *et al.* (1993) by volume averaging the governing pore scale relation as follows. The microscopic entropy (per unit volume of deformed material denoted by an asterisk) is

$$S_s^* = [S_s^o(T_s) + K_s \alpha_s u_{11}^*] (1 - u_{11}^*) \quad (2.51)$$

The term contained in square brackets is the microscopic entropy S_s^* of the solid material per unit volume of the undeformed material, to first order, as given by equation (2.25) above. The additional term is a first order correction for the volume change associated with the deformation.

Applying the averaging theorems of section 2.2, de la Cruz *et al.* (1993) obtain

$$\begin{aligned} \phi \bar{S}_s &= \frac{1}{V} \int_V S_s^* dV \\ &= \phi_o S_s^o(T_s) (1 - \bar{u}_{11}) + \phi_o K_s \alpha_s \left(\bar{u}_{11} + \frac{\phi - \phi_o}{\phi_o} \right) \end{aligned} \quad (2.52)$$

The entropy of the body, S_s^o , is the same function of temperature at the macroscale and pore scale. For macroscale entropy the value of the averaged solid temperature, \bar{T}_s , is used instead of the pore scale solid temperature, T_s . To relate to a unit volume of unperturbed porous medium, de la Cruz *et al.* (1993) multiply equation (2.52) by

$$\frac{\phi_o \phi_s^o}{\phi_o} = 1 + \bar{u}_{11} \quad (2.53)$$

to yield

$$\bar{S}_s(1 + \bar{u}_{11}) = \phi_0 \mathcal{S}_s(\bar{T}_s) + \phi_0 K_s \alpha_s \left(\bar{u}_{11} + \frac{\phi - \phi_0}{\phi_0} \right) \quad (2.54)$$

which shows that entropy, S_s , given by equation (2.50) is indeed the macroscopic solid entropy, and

$$-\frac{d\mathcal{F}_s^0(\bar{T}_s)}{d\bar{T}_s} = \mathcal{S}_s(\bar{T}_s) \quad (2.55)$$

is the free energy (per unit volume) of the solid material at temperature \bar{T}_s and zero (microscopic) deformation, $u_{ik} = 0$. This is at zero microscopic deformation due to the fact that the free energy, \mathcal{F}_s^0 , of the initial state has the same dependence on temperature at both scales. Furthermore, the entropy result supports the postulated relation (2.31) for the macroscopic work, R_s , and the macroscopic free energy, F_s , relation (2.39).

By an argument similar to that which led to equation (2.47) for the macroscopic free energy, de la Cruz *et al.* (1993) postulate for the macroscopic internal energy, U_s , an expression of the form (to second order)

$$U_s(S_s, \bar{u}_{ik}) = \phi_0 \mathcal{U}_s(S_s) + b_1(S_s - S_s^0) \bar{u}_{11} + b_2(\bar{u}_{ik} - \frac{1}{3} \delta_{ik} \bar{u}_{11})^2 + b_3 \bar{u}_{11}^2. \quad (2.56)$$

To determine the constants b_1 , b_2 , and b_3 , de la Cruz *et al.* (1993) compute the stress from macroscopic internal energy, $U_s(S_s, \bar{u}_{ik})$, i.e.

$$d_{ik} = \frac{\partial U_s(S_s, \bar{u}_{ik})}{\partial \bar{u}_{ik}} \quad (2.57)$$

so that using equation (2.56) gives

$$d_{ik} = b_1(S_s - S_s^0) \delta_{ik} + 2b_2(\bar{u}_{ik} - \frac{1}{3} \delta_{ik} \bar{u}_{11}) + 2b_3 \delta_{ik} \left[\bar{u}_{11} + \frac{\phi - \phi_0}{\phi_0} \right]. \quad (2.58)$$

Substituting equation (2.50), in the form

$$S_1 - S_1^0 = \phi_0 C_v^* \frac{(T_1 - T_0)}{T_0} + \phi_0 K_r \alpha_s \bar{u}_{11}, \quad (2.59)$$

into equation (2.58), where the heat capacity C_v^* enters through the usual thermodynamic relation

$$C_v^* = - T_0 \frac{d^2 \mathcal{F}_1^0(T_0)}{dT_0^2}, \quad (2.60)$$

gives

$$d_{ik} = \delta_1 \phi_0 C_v^* \frac{(T_1 - T_0)}{T_0} \delta_{ik} + 2b_2 (\bar{u}_{1k}^* - \frac{1}{3} \delta_{ik} \bar{u}_{11}^*) + \delta_{ik} [2b_3 + \delta_1 \phi_0 K_r \alpha_s] \left[\bar{u}_{11}^* + \frac{\phi - \phi_0}{\phi_0} \right]. \quad (2.61)$$

Comparison with the stress tensor, equation (2.42), obtained from volume averaging yields the values for δ_1 :

$$\delta_1 = - \frac{K_r \alpha_s T_0}{C_v^*} \quad (2.62)$$

$$b_2 = \mu_M, \quad (2.63)$$

and

$$b_3 = \frac{1}{2} \phi_0 K_r \left[1 + \frac{K_r \alpha_s^2 T_0}{C_v^*} \right]. \quad (2.64)$$

Using the ratio of heat capacities (Zemansky, 1957),

$$\frac{C_v^*}{C_p^*} = \frac{K_M^*}{K_s^*}, \quad (2.65)$$

and equation (2.27) we have

$$b_3 = \frac{1}{2} \phi_0 K_{ad}^s \quad (2.66)$$

The internal energy (2.56) is found to be

$$U_s(S_s, \bar{u}_{ik}^s) = \phi_0 \epsilon_s^e(S_s) - \frac{T_0 K_r \alpha_s}{C_v} (S_s - S_s^0) \bar{u}_{11}^s + \mu_m (\bar{u}_{ik}^s - \frac{1}{3} \delta_{ik} \bar{u}_{11}^s)^2 + \frac{1}{2} \phi_0 K_{ad}^s (\bar{u}_{ik}^s)^2 \quad (2.67)$$

where K_{ad}^s is the adiabatic modulus of compression of the solid material.

The above discussion is a detailed description of how de la Cruz *et al.* (1993) have obtained the governing macroscopic equations describing the contribution of the solid component in the equilibrium thermodynamics of porous media. The relations for the contribution of the fluid component are now reviewed. de la Cruz *et al.* (1993) take the volume average of equation (2.28)

$$\frac{1}{V} \int_V \left\{ \frac{\partial \epsilon_f}{\partial t} + \nabla \cdot \left[v_f (\epsilon_f + p_f) - \kappa_f \nabla T_f + kv \right] \right\} dV = 0 \quad (2.68)$$

and using equation (2.3) and (2.4), obtain

$$\frac{\partial \eta \bar{\epsilon}_f}{\partial t} + \nabla \cdot \left[\eta \overline{v_f (\epsilon_f + p_f)} \right] + \int_{A_b} p_f v_f \cdot n \, dA - \frac{1}{V} \int_V \nabla \cdot \left[\kappa_f \nabla T_f \right] dV + kv = 0 \quad (2.69)$$

where "kv" stands for the kinetic energy and viscous dissipation terms.

The aim is to obtain relations for equilibrium thermodynamics. Therefore the processes considered are assumed to be sufficiently slow that when ϵ_f and p_f appear as factors of the velocity in equation (2.69) they may be replaced by $\bar{\epsilon}_f$ and \bar{p}_f . Also the "kv" terms are negligible for such processes. The term involving temperature is expanded as the sum of a heat flux term and a heat source term (the solid component acting as a source). It is the heat gain per unit time and de la Cruz *et al.* (1993) denote it by $\partial Q_s / \partial t$. Using the volume averaged equation of continuity (de la Cruz & Spanos, 1983) to substitute for $\nabla \cdot v_f$, equation (2.69) becomes

$$\left[\frac{\partial (\eta \bar{e}_f)}{\partial t} - \frac{\bar{e}_f + \bar{p}_f}{\bar{\rho}_f} \frac{\partial}{\partial t} (\eta \bar{\rho}_f) + \bar{p}_f \frac{\partial \eta}{\partial t} \right] - \frac{\delta Q_f}{\delta t} + \bar{v}_f \left[\nabla (\eta \bar{e}_f) - \frac{\bar{e}_f + \bar{p}_f}{\bar{\rho}_f} \nabla (\eta \bar{\rho}_f) + \bar{p}_f \nabla \eta \right] + \eta \bar{v}_f \cdot \nabla \bar{p}_f = 0 \quad (2.70)$$

By virtue of the macroscopic equations of motion (de la Cruz & Spanos, 1989b; Hickey *et al.*, 1993) the last term above contributes solely to kinetic energy and viscous dissipation, and is disregarded. Thus de la Cruz *et al.* (1993) interpret equation (2.70) to mean the following thermodynamic relation,

$$d(\eta \bar{e}_f) = \frac{\bar{e}_f + \bar{p}_f}{\bar{\rho}_f} d(\eta \bar{\rho}_f) - \bar{p}_f d\eta + \delta Q_f. \quad (2.71)$$

The quantity δQ_f can be related to the entropy as follows. Let s_f be the (microscopic) entropy per unit volume of fluid which satisfies the general equation of heat transfer (2.30). Volume averaging, de la Cruz *et al.* (1993) obtain

$$\frac{\partial (\eta \bar{s}_f)}{\partial t} + \nabla \cdot (\eta \bar{s}_f \bar{v}_f) - \frac{1}{V} \int_V \frac{\nabla \cdot (\kappa_f \nabla T_f)}{T_f} dV - \frac{1}{V} \int_V \frac{\nabla \cdot (\bar{\tau}_f \bar{v}_f)}{T_f} dV = 0 \quad (2.72)$$

Assume the temperature distribution is sufficiently smooth and its gradient sufficiently small that the factor $1/T_f$ can be replaced by $1/\bar{T}_f$. Thus with the help of the equation of continuity, equation (2.72) is recast as

$$\left[\frac{\partial (\eta \bar{s}_f)}{\partial t} - \frac{\bar{s}_f}{\bar{\rho}_f} \frac{\partial (\eta \bar{\rho}_f)}{\partial t} \right] + \bar{v}_f \cdot \left[\nabla (\eta \bar{s}_f) - \frac{\bar{s}_f}{\bar{\rho}_f} \nabla (\eta \bar{\rho}_f) \right] - \frac{1}{\bar{T}_f} \frac{\delta Q_f}{\delta t} + \text{viscous term} = 0. \quad (2.73)$$

de la Cruz *et al.* (1993) interpret (2.73) to mean

$$d(\eta \bar{s}_f) = \frac{\bar{s}_f}{\bar{\rho}_f} d(\eta \bar{\rho}_f) + \frac{1}{\bar{T}_f} \delta Q_f. \quad (2.74)$$

Combining equations (2.71) and (2.74) yields

$$d(\eta \bar{e}_f) = \frac{\bar{e}_f - \bar{T}_f \bar{s}_f + \bar{p}_f}{\bar{\rho}_f} d(\eta \bar{\rho}_f) - \bar{p}_f d\eta + \bar{T}_f d(\eta \bar{s}_f) . \quad (2.75)$$

Note that this relation involves only macroscopic quantities. Here $\eta \bar{e}_f$ and $\eta \bar{s}_f$ are internal energy and entropy (of the fluid component) per unit volume of the porous medium. For $\eta = 1$ and $V \rightarrow 0$, de la Cruz *et al.* (1993) recover the familiar thermodynamic relation.

The mass of fluid in a unit volume of deformed porous medium is $\eta \bar{\rho}_f$, which is a variable. To refer to the amount of fluid contained in a unit volume of the "unperturbed" medium, we have to multiply $\eta \bar{e}_f$ by $\eta_0 \rho_f^0 / \eta \bar{\rho}_f$. Defining quantities per unit volume of fluid in the unperturbed configuration

$$U_f = (\eta_0 \rho_f^0 / \eta \bar{\rho}_f) \eta \bar{e}_f \quad (2.76)$$

and

$$S_f = (\eta_0 \rho_f^0 / \eta \bar{\rho}_f) \eta \bar{s}_f \quad (2.77)$$

we find from (2.74) the relation

$$dU_f = \eta p_f \left(\frac{d(\eta \bar{\rho}_f)}{\eta \bar{\rho}_f} - \frac{d\eta}{\eta} \right) + \bar{T}_f dS_f \quad (2.78)$$

where we have used $\eta \approx \eta_0$, $\rho_f \approx \rho_f^0$ in the coefficients (as we are interested in small changes here). For certain purposes (Biot, 1956b, 1956c ; de la Cruz & Spanos, 1989b) it is useful to introduce the fluid displacement vector \bar{u}_f . Using the equation of continuity (for slow processes in the neighborhood of the unperturbed configuration), we can write (2.78) as

$$dU_f = -\eta \bar{p}_f d \bar{u}_{kk}^f + \bar{T}_f dS_f \quad (2.79)$$

where

$$\bar{u}_{kk}^f = \nabla \cdot \bar{u}_f + \frac{\eta - \eta_0}{\eta_0} \quad (2.80)$$

Clearly, equation (2.79) is the fluid counterpart of equation (2.33).

2.5 Internal Energy for Porous Media

In this section a porous medium is regarded as a system consisting of two superposed continua. The internal energy density of such a porous medium and how it is related to the stresses and strains will be discussed. The motivation for such a discussion is that Biot (1941) introduced the assumption of the existence of a potential energy for a porous medium in his description of seismic wave propagation. From this assumption, Biot reduced his number of independent macroscopic parameters, for a homogeneous isotropic system, from five to four (Biot & Willis, 1957). de la Cruz & Spanos (1985) compare their equations obtained through volume averaging to those of Biot (1956b) and deduce a required compatibility condition which would in essence further reduce the number of independent macroscopic parameters. Therefore, it is of interest to see if the compatibility relation obtained by de la Cruz & Spanos (1989b) has any connection with the assumption of the unique energy potential.

With respect to Biot's (1956b) paper on low frequency wave propagation in fluid saturated porous media, a potential energy $W(\nabla \cdot \bar{u}_f, \bar{u}_{ik}^f)$ per unit volume of aggregate is postulated to exist such that

$$-\eta \bar{p}_f = \frac{\partial W}{\partial \nabla \cdot \bar{u}_f} \quad (2.81)$$

and

$$t_{ik}^f = \frac{\partial W}{\partial \bar{u}_{ik}^f} . \quad (2.82)$$

According to Biot (1956b) the consequence of the existence of such a potential is the

equality of two parameters, namely

$$Q = Q' \quad (2.83)$$

where these have been introduced in the stress-strain relations

$$-\eta \bar{p}_f = Q' \nabla \cdot \bar{u}_s + R \nabla \cdot \bar{u}_f \quad (2.84)$$

and

$$t_{ik}^f = A \bar{u}_{ij}^f \delta_{ik} + 2N \bar{u}_{ik}^f + Q \bar{u}_{ij}^f \delta_{ik} \quad (2.85)$$

In the thermodynamic formulation de la Cruz *et al.* (1993) discussed above, the fluid internal energy, U_f , per unit volume of porous media in the unperturbed configuration is given by equation (2.79)

$$dU_f = -\eta \bar{p}_f d\bar{u}_{kk}^f + \bar{T}_f dS_f \quad (2.86)$$

with

$$\bar{u}_{kk}^f = \bar{\nabla} \cdot \bar{u}_f + \frac{\eta - \eta_0}{\eta_0} \quad (2.87)$$

and the solid internal energy, U_s , per unit volume of porous media in the unperturbed configuration is given by equation (2.33),

$$dU_s = \bar{t}_{kk} d\bar{u}_{kk}^s + \bar{T}_s dS_s \quad (2.88)$$

where

$$\bar{u}_{kk}^s = \bar{u}_{kk}^s + \frac{1}{3} \delta_{kk} \frac{\phi - \phi_0}{\phi_0} \quad (2.89)$$

and $\phi = 1 - \eta$. The stresses are given by

$$-\eta \bar{p}_r = \frac{\partial U_f}{\partial \bar{u}_{kk}^f} \quad (2.90)$$

and

$$\tau_{ik}^s = \frac{\partial U_s}{\partial \bar{u}_{ik}^s} . \quad (2.91)$$

Hence, we can write

$$-\eta \bar{p}_r = \frac{\partial (U_f + U_s)}{\partial \bar{u}_{kk}^f} \quad (2.92)$$

and

$$\tau_{ik}^s = \frac{\partial (U_f + U_s)}{\partial \bar{u}_{ik}^s} . \quad (2.93)$$

In this sense the function $U_f + U_s$ may be regarded as an "energy potential" for the porous medium, from which the fluid and solid stresses can be obtained by differentiation with respect to the "strains" \bar{u}_{ik}^f and \bar{u}_{ik}^s . It is seen that equations (2.81) and (2.92) and equations (2.82) and (2.93) are close in form, if we make the following correlations

$$W \rightarrow U_f + U_s , \quad (2.94)$$

$$\nabla \cdot \bar{u}_r \rightarrow \nabla \cdot \bar{u}_r + \frac{\eta - \eta_0}{\eta_0} , \quad (2.95)$$

and

$$\bar{u}_{kk}^s \rightarrow \bar{u}_{kk}^s - \frac{1}{3} \delta_{kk} \frac{(\eta - \eta_0)}{(1 - \eta_0)} . \quad (2.96)$$

In Biot's (1956b) formulation, the variable porosity, η , does not appear explicitly. One

might attempt to introduce at the outset some relation, e.g. (de la Cruz & Spanos, 1989b)

$$\eta - \eta_0 = \delta_s \nabla \cdot \bar{\mathbf{u}}_s - \delta_r \nabla \cdot \bar{\mathbf{u}}_r, \quad (2.97)$$

and use it to eliminate η everywhere, so that $U_r + U_s$ becomes a function of $\nabla \cdot \bar{\mathbf{u}}_r$ and \bar{u}_{ik}^r . Carrying this out with the help of equations (2.86) and (2.88) we would find that

$$\frac{\partial(U_r + U_s)}{\partial \nabla \cdot \bar{\mathbf{u}}_r} = -\eta \bar{p}_r + \delta_r \left[\bar{p}_r + \frac{1}{3} \frac{t_{ii}^r}{(1-\eta)} \right] \quad (2.98)$$

and

$$\frac{\partial(U_r + U_s)}{\partial \bar{u}_{ik}^r} = t_{ik}^r - \delta_s \left[\bar{p}_r + \frac{1}{3} \frac{t_{ii}^r}{(1-\eta)} \right] \delta_{ik}. \quad (2.99)$$

For Biot's (1956b) relations (2.81) and (2.82) to be valid, assuming we identify $\mathbf{W} = \mathbf{U}_r + \mathbf{U}_s$, and Biot's (1956b) average solid and fluid displacements as $\bar{\mathbf{u}}_s$ and $\bar{\mathbf{u}}_r$ respectively, it would then be necessary that $\delta_s = \delta_r = 0$. Given this constraint it appears that the use of an energy potential in the approach of Biot (1956b) would require that no change in porosity occur during deformation. Continuing along the lines of the formulation of Biot (1956b) the energy potential for the porous medium, in this case $U_r + U_s$, should be an exact differential thereby requiring

$$\frac{\partial}{\partial \bar{u}_{ik}^r} \left(-\eta \bar{p}_r + \delta_r \left[\bar{p}_r + \frac{1}{3} \frac{t_{ii}^r}{(1-\eta)} \right] \right) = \frac{\partial}{\partial \nabla \cdot \bar{\mathbf{u}}_r} \left(t_{ik}^r - \delta_s \left[\bar{p}_r + \frac{1}{3} \frac{t_{ii}^r}{(1-\eta)} \right] \delta_{ik} \right). \quad (2.100)$$

Substituting for the fluid pressure and solid stress in terms of strains and performing the differentiation yields no constraint on the δ 's. Therefore, the compatibility condition which was deduced by de la Cruz & Spanos (1989b) through comparison of final equations is not obtained from the use of the energy potential. Furthermore, δ_r and δ_s can be determined from measurable compressibilities as discussed in chapter 3 and are demonstrably non-zero. Therefore there is some ambiguity as to the result if one uses the energy potential as in the context of Biot (1956b).

The sum $U_f + U_s$ refers to the fluid and solid materials in a unit volume of the unperturbed configuration. After a deformation has taken place, each component will have occupied separate regions in space. That is, the original unit volume will have "bifurcated" into (partly overlapping) regions mapped out by the two velocity fields \bar{v}_f and \bar{v}_s . Only the sum of the energies in a unit volume fixed in space can be properly called the internal energy density of the porous medium (de la Cruz *et al.*, 1993). Defining this quantity as

$$\mathbb{W} = (\bar{\phi}\bar{\rho}_s/\phi_0\rho_s^0)U_s + (\eta\bar{\rho}_f/\eta_0\rho_f^0)U_f \quad (2.101)$$

and expanding the solid contribution we have

$$\begin{aligned} \mathbb{W} = & \frac{U_s}{\bar{\phi}\bar{\rho}_s} d(\bar{\phi}\bar{\rho}_s) + \frac{\bar{e}_f - \bar{T}_f\bar{S}_f + \bar{p}_f}{\bar{\rho}_f} d(\eta\bar{\rho}_f) \\ & + \bar{t}_k d\bar{u}_{ik} + \bar{T}_s dS_s - \bar{p}_f d\eta + \bar{T}_f d(\eta\bar{S}_f) \end{aligned} \quad (2.102)$$

It is therefore not possible to obtain the component stresses from such an internal energy by simply differentiating with respect to the strains. This is due to fact that the change in internal energy, represented by equation (2.102), is not solely due to the work done on the material but includes changes associated with flux of material, both fluid and solid, into the volume during deformation.

2.6 Conclusions

The macroscopic thermodynamic relations for the solid and the fluid components developed by de la Cruz *et al.* (1993), starting with the well established thermodynamics of each phase, shows that η enters the macroscopic thermodynamic relations on the same footing as $\eta\bar{\rho}_f$ and \bar{u}_{ik} . Nothing from the pore scale physics would lead one to expect a functional relation $f(\eta\bar{\rho}_f, \bar{u}_{ik}, \eta) = 0$ (de la Cruz *et al.*, 1993). It seems therefore reasonable to regard a relation such as (de la Cruz & Spanos, 1999b)

$$\frac{\partial \eta}{\partial t} = \delta_s \nabla \cdot \bar{v}_s - \delta_f \nabla \cdot \bar{v}_f \quad (2.103)$$

for suitable values of the parameters δ_f and δ_s , as merely selecting particular processes to consider. It is not to be introduced from the beginning as though it were an equation of state.

For Biot's (1956b) relations (2.81) and (2.82) to be valid, assuming we identify $W = U_f + U_s$, and Biot's (1956b) average solid and fluid displacements as \bar{u}_s and \bar{u}_f respectively, it would then be necessary that $\delta_s = \delta_f = 0$. This is not the compatibility condition which was deduced by de la Cruz & Spanos (1985) through comparison of final equations for wave propagation. The other alternative is to associate Biot's $\nabla \cdot \bar{u}_f$ and \bar{u}_{ik}^f with $\nabla \cdot \bar{u}_f + \frac{\eta - \eta_0}{\eta_0}$ and $\bar{u}_{ik}^f - \frac{1}{3} \delta_{ik} \frac{(\eta - \eta_0)}{(1 - \eta_0)}$ derived here. This would imply that Biot's macroscopic displacements are not simply average displacements of the components. Although Biot's (1956b) final equations are of the correct form, his use of the energy potential is questionable.

CHAPTER 3

QUASI-STATIC DEFORMATIONS OF POROUS MEDIA

3.1 Introduction

Quasi-static deformation of porous rock is studied by experts in many fields. In the area of composite materials a considerable amount of work has been published on bounds of "effective" elastic coefficients (Walpole 1966; see also Hashin (1983) for a comprehensive survey). Measurements of various bulk moduli, and derivations of relationships between them have been reported for decades and are still of current interest (see Zimmerman (1991) for a comprehensive exposition). The results from these types of experiments are also used to determine macroscopic parameters required in wave propagation theories (Biot & Willis, 1957; Yew & Jogi, 1976, 1978; Hickey *et al.*, 1993). However, there is concern of whether or not statically determined values for parameters may be applied to dynamic situations (Detourney, 1993; Kämpel, 1991).

The deformation of porous media subjected to mechanical stress is characterized by various parameters. These parameters must reflect the deformation of solid and fluid components as well as the interaction between these components. For example, the components may change in relative proportions during a deformation. Such interactions introduce additional degrees of freedom into the problem, and therefore more material parameters are required for an adequate description.

A description of quasi-static deformations of a porous material consisting of a solid frame completely saturated by a single fluid is presented. The description is based on the quasi-static limit of the low-frequency wave propagation work of de la Cruz & Spanos (1985, 1989b). In the development, the constraint of linearity in both displacements and velocity plays a prominent role. This means that any motion is regarded as a small deviation from the static and uniform unperturbed configuration. The deformations are assumed isothermal, reversible and infinitesimal. No specific assumptions are made as to the shape of the pores or cracks, however the material must behave in a macroscopically homogeneous and isotropic manner. Furthermore, the porous medium is assumed to have a well connected pore structure.

Various quasi-static experiments which are used to quantify the additional degrees of freedom associated with a fluid-filled porous medium are discussed. This leads to the definition of various bulk moduli, "Young's " moduli, "Poisson's" ratio, and shear modulus which are analogous to elasticity. Both drained and undrained compressibilities (bulk moduli) are defined and calculated. Relationships between these various compressibilities are derived and compared to those cited in the literature (Zimmerman, 1986, 1991). The problem of macroscopic shearing is analyzed. Formulas for "Young's modulus" and "Poisson's ratio" for porous media under drained and undrained conditions are derived to provide an alternate method of determining the shear modulus of a porous sample. Other descriptive parameters such as induced pore pressure coefficient and effective stress coefficient are also described which have no analog in elasticity.

3.2 Equations for Quasi-Static Compression

The description is based on the quasi-static limit of the low-frequency wave propagation work of de la Cruz & Spanos (1985; 1989b) but are modified to include the fluid bulk viscosity and to accommodate phenomenological shear modulus and heat conductivities. The theoretical basis for the modification is given in chapter 4. The system of equations is developed on a model which contains no explicit assumption on pore structure. However, since we will be required to control the pore-pressure in some quasi-static deformations, a well connected pore structure is further assumed.

In the following discussion, the parameters and variables are phasic averages, however, the bars have been omitted. The macroscopic equations of motion are combined in the form

$$\frac{\partial^2}{\partial t^2} [\eta_o \rho_f^o u_i + (1-\eta_o) \rho_s^o u_i] = \partial_j \tau_{ij} \quad (3.1)$$

where the stress tensor for the porous medium is given by

$$\begin{aligned}
\tau_{ij} = & -\eta_0(p_r - p_0) \delta_{ij} + \eta_0 \mu_r (v'_{i,j} + v'_{j,i} - \frac{2}{3} v'_{i,r} \delta_{ij}) + \xi_r (\eta_0 v'_{i,r} + \frac{\partial \eta}{\partial t}) \delta_{ij} \\
& + (1 - \eta_0) \mu \left(\frac{\mu_M}{(1 - \eta_0) \mu_0} - 1 \right) \frac{\partial}{\partial t} (u'_{i,j} + u'_{j,i} - \frac{2}{3} u'_{i,r} \delta_{ij}) \\
& + \mu_M (u'_{i,j} + u'_{j,i} - \frac{2}{3} \delta_{ij} u'_{i,r}) + [(1 - \eta_0) K_s u'_{i,r} - K_s (\eta - \eta_0)] \delta_{ij}
\end{aligned} \tag{3.2}$$

An additional equation

$$\frac{\partial \eta}{\partial t} = \delta_s \nabla \cdot v_s - \delta_r \nabla \cdot v_r \tag{3.3}$$

is introduced (de la Cruz & Spanos, 1989b) to complete the system of equations. It is assumed that there are parameters, δ_r and δ_s , characteristic of the medium such that equation (3.3) is valid for low-frequency waves and for quasi-static compressions of the type discussed in this paper. The validity of such an equation and its possible process dependence has been discussed in chapter 2.

All compressions are to be isothermal and performed on a sample which initially sustains a uniform pressure:

$$p^s_r = p^s_s = p_0 \tag{3.4}$$

and for quasi-static processes set

$$v_r = 0 \tag{3.5}$$

Systematically eliminating $\nabla \cdot u_s$ and $\nabla \cdot u_r$ by combining the pressure equations and the continuity equations we find that the mass densities respond to pressure changes according to

$$\rho_r - \rho_r^0 = \frac{\rho_r^0}{K_r} (p_r - p_r^0) \tag{3.6}$$

and

$$\rho_s - \rho_s^0 = \frac{\rho_s^0}{K_s} (p_s - p_f) ; \quad (3.7)$$

and the change in porosity is

$$\eta - \eta_0 = \frac{\delta_r}{K_f \left[1 - \frac{\delta_r}{\eta_0} - \frac{\delta_s}{1 - \eta_0} \right]} (p_r - p_0) - \frac{\delta_s}{K_s \left[1 - \frac{\delta_r}{\eta_0} - \frac{\delta_s}{1 - \eta_0} \right]} (p_s - p_0) \quad (3.8)$$

The total or confining pressure of the porous medium is defined as

$$p = \eta p_r + (1 - \eta) p_s \quad (3.9)$$

so that

$$p - p_0 = \eta_0 (p_r - p_0) + (1 - \eta_0) (p_s - p_0) . \quad (3.10)$$

The condition for static equilibrium is

$$\partial_j \tau_{ij} = 0 \quad (3.11)$$

3.3 Drained Compressional Deformations

The drained compressions are such that the pore-pressure and confining pressure are independently controlled, whereas, later in the undrained compression the pore pressure is a function of confining pressure (figure 3.1). The notation used in the following description is the same as Zimmerman *et al.* (1986) and Zimmerman (1991). To clarify the notation, say in the bulk modulus K_{xy} , the first subscript, x , represents the type of volume measured ($x=b$: total or bulk volume, $x=p$: pore volume) and the second subscript, y , represents the pressure which is incremented ($y=c$: confining or total external pressure, $y=p$: pore-pressure), keeping the other pressure constant.

The drained bulk compression is characterized by the requirement that under a change of the confining pressure, the mass of the solid is conserved, and the fluid pressure $p_r = p_0$ is maintained. Since the equation of continuity can be written as

$$\frac{\partial}{\partial t} [(1-\eta) \rho_s] + \nabla \cdot [(1-\eta) \rho_s \mathbf{v}_s] = 0 \quad (3.12)$$

then in the drained bulk compression, the volume increment must be defined by ascribing the displacement \mathbf{u}_s (and not for example $(1-\eta_0) \mathbf{u}_s$) to each point on the closed surface.

Denoting the bulk modulus for this process by K_{bc} (or compressibility by C_{bc}) one has

$$C_{bc} = K_{bc}^{-1} = -\frac{1}{V_0} \left(\frac{\Delta V}{\Delta p} \right)_{p_r = p_0} \quad (3.13)$$

Here, $\Delta V = V - V_0$ represents the change in volume of the overall sample, V_0 is the initial volume of the sample, the pressure, p_r , of the fluid in the pores is kept constant during the deformation, and Δp represents the change in confining pressure (see figure 3.1).

In term of mass density

$$C_{bc} = K_{bc}^{-1} = \frac{1}{(1-\eta_0) \rho_s^0} \frac{\partial}{\partial p} [(1-\eta) \rho_s], \quad p_r = p_0. \quad (3.14)$$

Using equations (3.7), (3.8) and (3.10), C_{bc} can be readily expressed in terms of δ_r and δ_s as

$$C_{bc} = \frac{1}{(1-\eta_0) K_s} \left[\frac{1 - \frac{\delta_r}{\eta_0}}{1 - \frac{\delta_r}{\eta_0} - \frac{\delta_s}{(1-\eta_0)}} \right]. \quad (3.15)$$

As well as the drained bulk modulus, K_{bc} , discussed above, Zimmerman (1991) also discusses three other drained compressibility tests for porous media and has given relationships among all four drained compressibilities. Hence, it is useful to obtain expressions for such compressibilities in our framework and to verify the relationships.

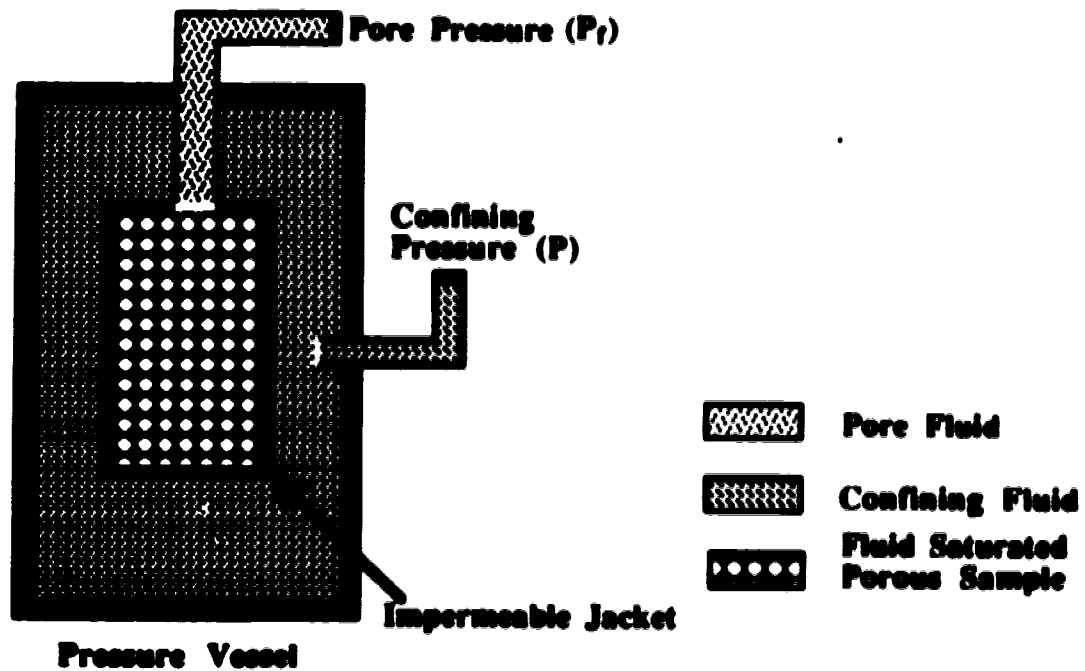


Figure 3.1 Schematic of experimental set up for static compressibility measurements of porous materials. The impermeable jacket around the sample enables the pore-pressure and confining pressure to be controlled independently.

One compressibility commonly referred to in the literature as "pseudo-bulk compressibility" is obtained by measuring the change in bulk volume with a change in pore-pressure. The bulk modulus denoted here by K_{bp} , compressibility by C_{bp} , is defined as

$$C_{bp} = K_{bp}^{-1} = \frac{1}{V_0} \left(\frac{\Delta V}{\Delta p_f} \right)_{p = p_0} \quad (3.16)$$

Here, ΔV represents the change in volume of the overall sample, V_0 is the initial volume of the sample, p represents the confining pressure which is kept constant during the deformation and Δp_f represents the change in pressure of the fluid in the pores. In terms of mass density

$$C_{bp} = K_{bp}^{-1} = \frac{-1}{(1 - \eta_0) \rho_s^2} \frac{\partial}{\partial p_f} [(1 - \eta) \rho_s] , p = p_0 . \quad (3.17)$$

Using equations (3.7), (3.8), (3.10) and (3.14), we find from equation (3.17) that

$$C_{bp} = C_{bc} - C_s + \frac{\frac{\delta_f}{K_f} - \frac{\delta_s}{K_s}}{(1 - \eta_0) \left(1 - \frac{\delta_f}{\eta_0} - \frac{\delta_s}{1 - \eta_0} \right)} \quad (3.18)$$

Comparing equation (3.18) to Zimmerman's (1991) relation 2.1 gives

$$C_{bp} = C_{bc} - C_s \quad (3.19)$$

it is evident that they only become identical if

$$\frac{\delta_s}{\delta_f} = \frac{K_s}{K_f} . \quad (3.20)$$

This constraint has been noted previously by de la Cruz & Spanos (1989b) as a compatibility condition between their theory and that of Biot (1956b). Comparison to Biot (1956b) will be discussed further in chapter 4. Finally, it will be shown that this constraint is equivalent to the frequently used hydrodynamic limit condition, equation (3.77), below.

Another compressibility which is commonly referred to in the literature as the "formation compaction" represents the change in pore volume, ΔV_f , of the sample due to a change in confining pressure. The magnitude of the change in pore volume, ΔV_f , is usually obtained by measuring the volume of fluid exiting the sample during the deformation. Hence, the bulk modulus, K_{pc} , or compressibility, C_{pc} , associated with this process is defined by

$$C_{pc} = K_{pc}^{-1} = - \frac{1}{V_f^0} \left(\frac{\Delta V_f}{\Delta p} \right)_{p=p_f} \quad (3.21)$$

where V_f^0 is the initial volume of fluid contained in the pores, Δp represents the change in

confining pressure, and p_f represents the pressure of the fluid in the pores and is kept constant during the deformation. Since the pore fluid pressure remains constant, we have

$$\begin{aligned}\Delta V_f &= \eta V - \eta_0 V_0 \\ &= \eta_0(V - V_0) + V_0(\eta - \eta_0)\end{aligned}\quad (3.22)$$

to first order, where η is the final porosity and V is the final total volume of the sample. Substituting equation (3.22) into equation (3.21) we obtain

$$C_{pc} = - \left[\frac{(V - V_0)}{V_0 \Delta p} + \frac{(\eta - \eta_0)}{\eta_0 \Delta p} \right], \quad p_f = p_0 \quad (3.23)$$

and using definition (3.13) for C_{bc} and equations (3.8) and (3.10) one obtains

$$C_{pc} = C_{bc} + \frac{\frac{\delta_1}{(1-\eta_0)}}{\eta_0 K_d \left(1 - \frac{\delta_1}{\eta_0} - \frac{\delta_1}{(1-\eta_0)} \right)} \quad (3.24)$$

With the use of equation (3.15) and some algebra one obtains

$$\eta_0 C_{pc} = C_{bc} - C_s \quad (3.25)$$

Equation (3.25) is Zimmerman's (1991) relation 2.7 obtained through the use of the hydrostatic limit and the Betti reciprocal theorem of elasticity adopted for porous media.

The final drained compressibility to be discussed is commonly referred to as the "effective pore compression". It is obtained by measuring the change in pore volume due to a change in pore-pressure. The associated bulk modulus, K_{pp} , or compressibility, C_{pp} , is defined as

$$C_{pp} = K_{pp}^{-1} = \frac{1}{V_f^i} \left(\frac{\Delta V_f}{\Delta p_f} \right)_{p=p_0} \quad (3.26)$$

where V_f^i is the initial volume of fluid contained in the pores, p represents the confining pressure which is kept constant during the deformation, Δp_f represents the change in

pressure of the fluid in the pores, and ΔV_f is the change in pore volume. Substituting equation (3.22) into equation (3.26), so that

$$C_{pp} = \left[\frac{(V - V_o)}{V_o \Delta p_f} + \frac{(\eta - \eta_o)}{\eta_o \Delta p_f} \right], \quad p = p_o \quad (3.27)$$

and using definition (3.16) for C_{bp} and equations (3.8), (3.10) and (3.15), the relation

$$C_{pp} = \frac{C_{bp}}{\eta_o} - C_s \quad (3.28)$$

is obtained. Equation (3.28) may be regarded as the third Zimmerman (1991) relation. If one employs equation (3.19) for C_{bp} , then one obtains Zimmerman's (1991) relation 2.8:

$$\eta_o C_{pp} = C_{bc} - (1 + \eta_o) C_s \quad (3.29)$$

Thus in a simple and straightforward manner we have reproduced all three independent relations given in Zimmerman (1991). These are equations (3.19), (3.25), and (3.28). Of these three only equation (3.19) requires the validity of condition (3.20).

Experimental measurements of the various drained bulk moduli have been reported in the literature. Fatt (1959) obtained measurements for the drained bulk compression, C_{bo} , and the pseudo bulk compressibility, C_{bp} , for Boise sandstone over a range of effective confining pressures ($p - p_f$). The ratio of C_{bp} and C_{bc} were obtained from the measurements as well as using a formula which is equivalent to equation (3.19) presented above, which is subject to constraint (3.20). The ratios of C_{bp} and C_{bc} measured were always smaller than the calculated value, except at zero effective confining pressure where the measured value was larger than the calculated value.

Van der Knapp (1959) experimentally verified relationship (3.25) between C_{pp} and C_{bc} for a Belok sandstone with 15% porosity. The data appear to support this relationship even in the non-linear regime. Zimmerman *et al.* (1986) tested relation (3.25) by comparing his measurements of C_{pp} to measurements of C_{bo} , obtained by King (1969) using acoustical methods, for a Berea sandstone. He concluded that relation (3.19) was valid, particularly at effective pressures not too close to zero.

Measurements on various sands (Hughes & Cooke, 1953) shows that C_{pc} varies exponentially with confining stress. C_{pp} was measured by Fatt (1958) on four different types of sandstones and concluded that this compressibility is a strong function of pressure but no apparent correlation with porosity was evident. Van der Knapp (1959) presents data for C_{pp} on 16 different well consolidated samples consisting of sandstones, granites and limestone (approximate porosity range; 1% to 30 %). He states that the lower the porosity, the higher the compressibility. This observation was more pronounced for some limestone samples. Yew & Jogi (1978) measured the drained bulk compressibility, C_{bc} , of an artificial rock, "Alundum", and three natural sandstones, namely Berea, Pecos and Ohio. The resulting pressure strain curves of Berea and Ohio sandstone showed considerable non-linearity in the low pressure region. Similar non-linear behavior exists in measurements performed on Westerly granite (Nur & Byerlee, 1971; Coyner, 1984; Schmitt & Zoback, 1992).

Let's now consider a uniaxial compression, or a "Young's modulus" measurement. Consider a rectangular block of porous medium with a square cross section of width L before the stress is applied and let the two sides normal to the x axis be subject to constant uniform compressive stress p , i.e. $\tau_{xx} = -p$ and $\tau_{xy} = 0$, with drained condition ($p_f = p_o$) everywhere. The other sides are to be entirely stress free: $\tau_{xz} = \tau_{yz} = 0$ (see figure 3.2). The stress tensor, equation (3.2), for the porous medium subject to a drained boundary condition and for a quasi-static isothermal process is

$$\tau_{ij} = \mu_M (u_{i,j} + u_{j,i} - \frac{2}{3} \delta_{ij} u_{l,l}) + [(1-\eta_o)K_s u_{i,j} - K_s(\eta-\eta_o)] \delta_{ij} . \quad (3.30)$$

Using equation (3.3) for the change in porosity and then integrating with respect to time, we find for the stress tensor under drained conditions to be

$$\tau_{ij} = \mu_M (u_{i,j} + u_{j,i} - \frac{2}{3} \delta_{ij} u_{l,l}) + (1-\eta_o)K_s \left[\frac{1 - \frac{\delta_{ij}}{\eta_o} - \frac{\delta_{ij}}{(1-\eta_o)}}{1 - \frac{\delta_{ij}}{\eta_o}} \right] u_{l,l} \delta_{ij} \quad (3.31)$$

or, in view of equation (3.15) for K_{bo} ,

$$\tau_{ij} = \mu_M (u_{i,j} + u_{j,i} - \frac{2}{3} \delta_{ij} u_{l,l}) + K_{bo} u_{l,l} \delta_{ij} . \quad (3.32)$$

The stress tensor is of the same form as the stress tensor for an elastic solid. The shear modulus is represented by μ_M and the bulk modulus is represented by K_{bc} . The displacement $u^a(x,y)$ satisfying the above boundary conditions, as well as the condition for equilibrium, equation (3.11), is

$$u_x^1 = - \left(\frac{K_{bc} + \frac{1}{3}\mu_M}{3K_{bc}\mu_M} \right) p x , \quad (3.33)$$

$$u_y^1 = \left(\frac{K_{bc} - \frac{2}{3}\mu_M}{6K_{bc}\mu_M} \right) p y . \quad (3.34)$$

and

$$u_z^1 = \left(\frac{K_{bc} - \frac{2}{3}\mu_M}{6K_{bc}\mu_M} \right) p z . \quad (3.35)$$

Defining a Young's modulus for a drained porous medium, E_{bc} , in the conventional manner, i.e. as the ratio of longitudinal stress to the longitudinal strain, where the strain is the fractional change in length of the sample, gives

$$\begin{aligned} E_{bc} &= \frac{(-p)}{(\Delta L/L)_x} \\ &= \frac{3K_{bc}\mu_M}{K_{bc} + \frac{1}{3}\mu_M} \end{aligned} \quad (3.36)$$

More information can be obtained from the uniaxial compression if one measures the change in length of the sample perpendicular to the direction of applied stress, i.e. u_y^1 or u_z^1 . Defining a Poisson's ratio ν_{bc} for a drained porous medium as the ratio of lateral extension to the corresponding longitudinal compression, gives us

$$\begin{aligned} \nu_{bc} &= - \frac{(\Delta L/L)_y}{(\Delta L/L)_x} \\ &= \frac{K_{bc} - \frac{2}{3}\mu_M}{2(K_{bc} + \frac{1}{3}\mu_M)} . \end{aligned} \quad (3.37)$$

It has been shown that for a porous medium under drained conditions or absent of pore fluid the stress tensor is of the same form as for elastic theory and therefore similar relationships between "Young's" modulus, "Poisson's" ratio, drained bulk modulus and shear modulus exist. The expression for "Poisson's" ratio (3.37) has been used by Yew & Jogi (1978) to obtain a value for the shear modulus, using a measurement of the drained bulk modulus and assuming a value for "Poisson's" ratio.

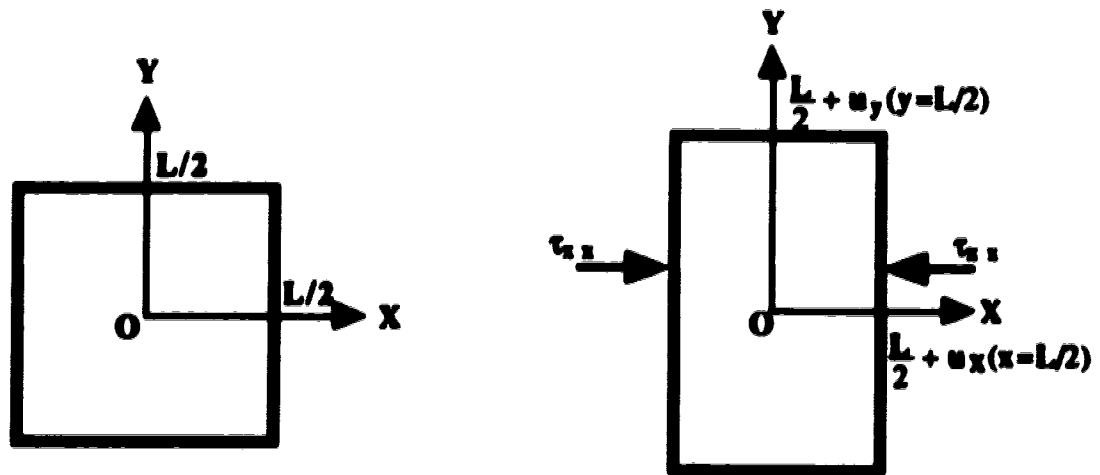


Figure 3.2 The deformation of a block of porous medium with a square cross section of width L on which the faces normal to the x -axis is subject to a uniform compressive stress, $\tau_{xx} = -p$ and the pore fluid is allowed to flow out of the sample, $p_f = p_p$. The change in dimension of the sample is measured in the direction of applied stress (x -direction) and in one direction perpendicular to the direction of applied stress (y -direction).

3.4 Undrained Compressional Deformations

The undrained compression, as defined in this paper, is characterized by the requirement that the masses of the two components enclosed by a surface are separately conserved. In the lab this is accomplished by enclosing the sample in an impermeable but deformable jacket. The conservation of the total mass can be stated more formally by combining the continuity equations for each phase to obtain

$$\frac{\partial \rho}{\partial t} + \nabla \cdot (\rho \mathbf{v}) = 0 \quad (3.38)$$

where

$$\rho = \eta \rho_f + (1-\eta) \rho_s \quad (3.39)$$

and

$$v = [\eta_o \rho_f^o v_f + (1-\eta_o) \rho_s^o v_s] / \rho \quad (3.40)$$

Denoting the bulk modulus for the undrained compression by K_{ud} , or compressibility by C_{ud} , one has

$$C_{ud} = K_{ud}^{-1} = \frac{1}{\rho_o} \left(\frac{\partial \rho}{\partial p} \right)_{q=q_o} \quad (3.41)$$

where p is the medium pressure defined by equation (3.10), and

$$q = \frac{\eta \rho_f}{(1-\eta) \rho_s} \quad (3.42)$$

Let us establish that the undrained process is characterized by q -constant. The conservation of the total enclosed mass can be expressed as

$$[\eta \rho_f + (1-\eta) \rho_s] V = [\eta_o \rho_f^o + (1-\eta_o) \rho_s^o] V_o \quad (3.43)$$

In terms of q and ρ_s , equation (3.43) becomes

$$(1-\eta) \rho_s (1+q) V = (1-\eta_o) \rho_s^o (1+q_o) V_o \quad (3.44)$$

If $q=q_o$, then equation (3.44) gives

$$(1-\eta) \rho_s V = (1-\eta_o) \rho_s^o V_o \quad (3.45)$$

Combining equation (3.45) with equation (3.43) one also obtains

$$\eta \rho_f V = \eta_o \rho_f^o V_o \quad (3.46)$$

thereby implying that the two masses are separately conserved.

Using equations (3.6), (3.7) and (3.8) the change in density may be expressed as

$$\begin{aligned} \rho - \rho_0 = & \left\{ \eta_0 \frac{\rho_f^0}{K_f} + \frac{\delta_r}{K_f \left[1 - \frac{\delta_r}{\eta_0} - \frac{\delta_s}{1 - \eta_0} \right]} (\rho_f^0 - \rho_s^0) \right\} (p_f - p_0) \\ & + \left\{ (1 - \eta_0) \frac{\rho_s^0}{K_s} - \frac{\delta_s}{K_s \left[1 - \frac{\delta_r}{\eta_0} - \frac{\delta_s}{1 - \eta_0} \right]} (\rho_f^0 - \rho_s^0) \right\} (p_s - p_0) \end{aligned} \quad (3.47)$$

and

$$\begin{aligned} \frac{q - q_0}{q_0} = & \left\{ \frac{1}{K_f} + \frac{1}{\eta_0(1 - \eta_0)} \frac{\delta_r}{K_f \left[1 - \frac{\delta_r}{\eta_0} - \frac{\delta_s}{1 - \eta_0} \right]} \right\} (p_f - p_0) \\ & - \left\{ \frac{1}{K_s} + \frac{1}{\eta_0(1 - \eta_0)} \frac{\delta_s}{K_s \left[1 - \frac{\delta_r}{\eta_0} - \frac{\delta_s}{1 - \eta_0} \right]} \right\} (p_s - p_0) . \end{aligned} \quad (3.48)$$

Using equations (3.10) and (3.48), p_f and p_s may be written as functions of p and q . Then substituting into equation (3.47), $\rho - \rho_0$ may be expressed by an equation of the form

$$\rho - \rho_0 = a(p - p_0) + b(q - q_0) \quad (3.49)$$

from which one identifies

$$\begin{aligned} K_{ud} = \frac{\rho_0}{a} \\ = \eta_0 K_f + (1 - \eta_0) K_s + (\delta_r - \delta_s) (K_s - K_f) . \end{aligned} \quad (3.50)$$

The last term in equation (3.50) measures the deviation from the simple average $\eta_0 K_f + (1 - \eta_0) K_s$ due to the combined effect of the solid shear modulus and pore structure on this macroscopic deformation.

Using equations (3.15), (3.18), (3.23) and (3.28) the undrained compressibility may

be written in terms of the four drained compressibilities as

$$C_{ud} = C_{bc} \cdot \frac{C_{bp}C_{ps}}{(C_{pp} + C_f)} \quad (3.51)$$

This expression was given in Zimmerman (1991). C_{ud} of equation (3.51) may be expressed in terms of two drained compressibilities, using relations (3.25) and (3.28) without any constraint. Zimmerman (1991) derives an expression obtained earlier by Gassmann (1951) by using his relations among the four drained compressibilities to represent the undrained bulk modulus in terms of only one drained bulk modulus, i.e.

$$C_{ud} = \frac{\eta_0 C_{bd}(C_f - C_s) + C_d(C_{bc} - C_s)}{\eta_d(C_f - C_s) + (C_{bc} - C_s)} \quad (3.52)$$

This expression can only be obtained in this analysis if one assumes relation (3.20). The requirement of such a constraint has been commented on previously by Brown & Korringa (1975), Rice & Cleary (1976), and Green & Wang (1986).

Let us now consider a uniaxial compression, or a "Young's modulus" measurement on a sample in an undrained configuration. This type of compression can not be performed in the lab exactly as described here. This is because the sample's initial configuration is subject to a uniform pressure configuration (equation 3.4) and therefore, as the stress is applied to the ends of the sample, a possible increase in pore pressure would push the confining jacket outwards and it would therefore separate from the sample.

We again consider a rectangular block of porous medium with a square cross section of width L , before the stress is applied and let the two sides normal to the x axis be subject to constant uniform compressive stress p , i.e. $\tau_{xx} = -p$ and $\tau_{xy} = 0$. The other sides are to be entirely stress-free: $\tau_{xz} = \tau_{yz} = 0$. The stress tensor, equation (3.2), for the porous medium subject to an undrained boundary condition and for a quasi-static isothermal process is

$$\begin{aligned} \tau_{ij} = & -\eta_0(p_f - p_0) \delta_{ij} + \mu M (u_{i,j} + u_{j,i} - \frac{2}{3} \delta_{ij} u_{l,l}) \\ & + [(1 - \eta_0)K_s u_{i,j} - K_d(\eta - \eta_0)] \delta_{ij} \end{aligned} \quad (3.53)$$

Substituting for the fluid pressure (see equation 4.6) we find the stress tensor for the undrained material to be

$$\begin{aligned} \tau_{ij} = & \eta_o K_r u_{1,r} \delta_{ij} + (1-\eta_o) K_s u_{1,r} \delta_{ij} + (K_r - K_s)(\eta - \eta_o) \delta_{ij} \\ & + \mu_M (u_{1,j} + u_{j,1} - \frac{2}{3} u_{1,r} \delta_{ij}) \end{aligned} \quad (3.54)$$

It was shown above (equation 3.42) that the undrained compression is characterized by

$$\frac{\eta p_r}{(1-\eta) p_s} = \frac{\eta_o p_r^o}{(1-\eta_o) p_s^o} \quad (3.55)$$

which can be written to first order as

$$\frac{\eta_o (\rho_r - \rho_s^o) + \rho_s^o (\eta - \eta_o)}{\eta_o \rho_s^o} = \frac{(1-\eta_o)(\rho_s - \rho_s^o) - \rho_s^o (\eta - \eta_o)}{(1-\eta_o) \rho_s^o} \quad (3.56)$$

Using the volume averaged continuity equation for the fluid (4.4) and solid (4.3) the above condition simply states

$$\nabla \cdot \mathbf{u}_s = \nabla \cdot \mathbf{u}_f \quad (3.57)$$

Using condition (3.57) and equation (3.3) for the change in porosity the stress tensor (3.54) may be written in terms of the solid displacement vector only as

$$\begin{aligned} \tau_{ij} = & \left[\eta_o K_r + (1-\eta_o) K_s + (K_r - K_s)(\delta_s - \delta_r) \right] u_{1,r} \delta_{ij} \\ & + \mu_M (u_{1,j} + u_{j,1} - \frac{2}{3} u_{1,r} \delta_{ij}) \end{aligned} \quad (3.58)$$

however, the term in the first square bracket is simply the undrained bulk modulus (3.50). Therefore, the stress tensor has the same form as the strain tensor for an elastic solid, i.e.

$$\tau_{ij} = K_{ud} u_{1,r} \delta_{ij} + \mu_M (u_{1,j} + u_{j,1} - \frac{2}{3} u_{1,r} \delta_{ij}) \quad (3.59)$$

where the shear modulus of the porous sample is represented by μ_M and the bulk modulus is represented by K_{ud} . It will be shown in the next section that the volume of a porous sample remains unchanged (to first order) during a macroscopic shear deformation. Therefore, the drained shear modulus must equal the undrained shear modulus.

Defining a Young's modulus for an undrained porous medium, E_{ud} , in the conventional

manner, i.e. as the ratio of longitudinal stress to the longitudinal strain, where the strain is the fractional change in length of the sample, gives

$$E_{ud} = \frac{(-p)}{(\Delta L/L)_x} \quad (3.60)$$

$$= \frac{3K_{ud}\mu_M}{K_{ud} + \frac{1}{3}\mu_M}$$

Poisson's ratio, ν_{ud} , for an undrained porous medium is the ratio of lateral extension to the corresponding longitudinal compression:

$$\nu_{ud} = -\frac{(\Delta L/L)_y}{(\Delta L/L)_x} \quad (3.61)$$

$$= \frac{K_{ud} - \frac{2}{3}\mu_M}{2(K_{ud} + \frac{1}{3}\mu_M)}$$

The undrained Poisson ratio is used in the work of Rice & Cleary (1976).

It is shown that for a porous medium under undrained conditions the stress tensor is of the same form as for elastic theory and therefore similar relationships between "Young's" modulus, "Poisson's" ratio, bulk modulus and shear modulus exist. However, it should be stated again that undrained uniaxial compression as described here cannot be performed in the lab due to the fact that the sample's increase in pore pressure, during deformation, would push the confining jacket outwards and it would separate from the sample. The problem might be overcome by performing an undrained uniaxial tension test (Schmitt, personal communication)

3.5 Shear Deformation

Consider a rectangular block of a porous medium subject to stresses at the boundary. Let the cross section be a square of width L before the stress is applied and let the four sides be subject to constant uniform shearing stress τ , i.e. $\tau_{xy}=\tau_{yx}=\tau$ and $\tau_{xx}=\tau_{yy}=0$ with the drained condition, $p_f=p_0$ (not a necessary condition as will be shown). The two other sides are to be entirely stress free: $\tau_{zi}=0$ (see figure 3.3). The displacement $u^i(x,y)$ satisfying the above boundary conditions, as well as the condition for static equilibrium, equation (3.11), and vanishing identically when $\tau = 0$, is easily verified to be

$$u_x^i = by, \quad (3.62)$$

$$u_y^i = bx, \quad (3.63)$$

where

$$b = \frac{\tau}{2(1-\eta_0)\mu_M}. \quad (3.64)$$

In particular, the upper right hand corner of the block moves by

$$u_x^i(L/2, L/2) = bL/2, \quad (3.65)$$

$$u_y^i(L/2, L/2) = bL/2, \quad (3.66)$$

and similarly for the other corners. Thus, one diagonal is lengthened from $\sqrt{2}L$ to

$$L_1 = \sqrt{2}L(1+b) \quad (3.67)$$

while the other diagonal is shortened to

$$L_2 = \sqrt{2}L(1-b). \quad (3.68)$$

The volume of the block is therefore unchanged (to first order) and therefore it makes no difference if this deformation is induced with the sample in a drained or undrained configuration. The shear angle θ is given by

$$\theta = \frac{1}{\mu_M} \tau . \quad (3.69)$$

In this sense the bulk shear modulus of the homogeneous medium is μ_M .

Applying a pure shear on a sample as described above is difficult to perform in the laboratory due to the fact that it is difficult not to change the volume. Therefore, it may be best to obtain the macroscopic shear modulus from the drained uniaxial deformation described in section 3.3 .

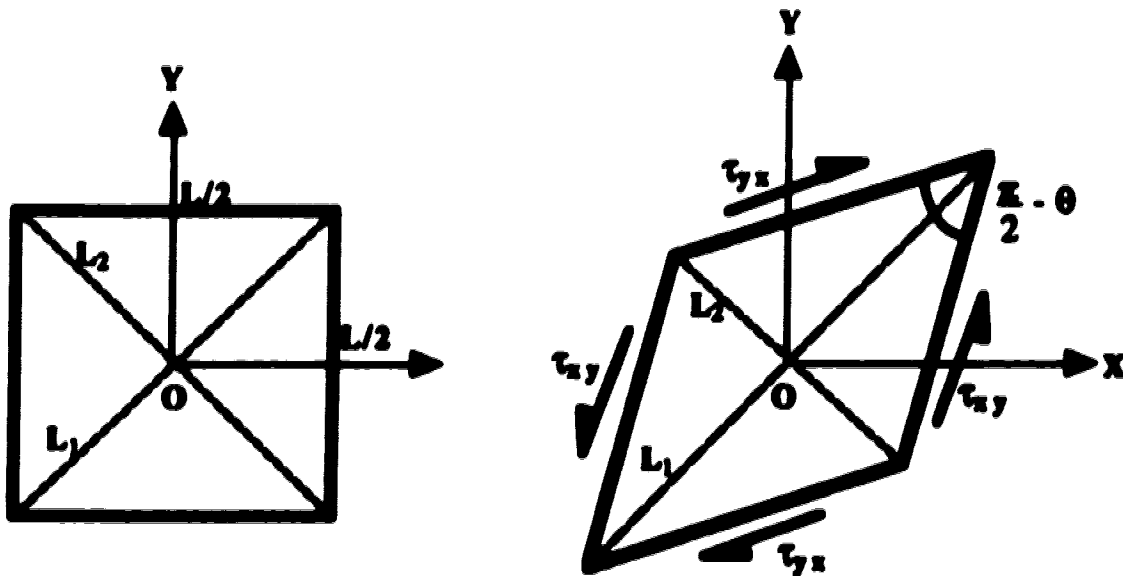


Figure 3.3 The deformation of a block of porous medium with a square cross-section of width L subject to a constant uniform shearing stress $\tau_{xy} = \tau_{yx} = \tau$. The volume of the block is unchanged to first order.

3.6 A Continuous Family of Compressibilities

The drained and the undrained moduli lie within a continuous family of compressibilities which differ by the degree to which the fluid is free to flow out. We define the family of compressibilities, $C(\Theta)$, by

$$C(\Theta) = - \frac{1}{V_0} \frac{\Delta V}{\Delta p} \Big|_{\Theta = \text{const}} \quad (3.70)$$

where ΔV is the the volume change of the overall sample, Δp is the change in confining pressure and where the relative pressure

$$\Theta = \frac{(p_f - p_0)}{(p - p_0)} \quad (3.71)$$

is kept constant during each process. In terms of mass densities, $C(\Theta)$ is given by

$$C(\Theta) = \frac{1}{(1-\eta_0) \rho_s^0} \frac{d}{d p} [(1-\eta) \rho_s] \quad (3.72)$$

Substituting equations (3.7), (3.8) and (3.9) into equation (3.72), the relation for $C(\Theta)$ is found to be

$$C(\Theta) = \frac{1}{(1-\eta_0)(1-\frac{\delta_1}{\eta_0} - \frac{\delta_1}{(1-\eta_0)})} \left\{ \frac{(1-\frac{\delta_1}{\eta_0})}{K_s} - \eta_0 \left[\frac{(\frac{\delta_1}{\eta_0})}{K_f} + \frac{(1-\frac{\delta_1}{\eta_0})}{K_s} \right] \Theta \right\} \quad (3.73)$$

Hence, in terms of drained moduli, we have

$$C(\Theta) = C_{be} - C_{bp} \Theta \quad (3.74)$$

To demonstrate a possible use of $C(\Theta)$, suppose one performs "almost drained" compressions (i.e. $\Theta=0$) for a number of values of Θ . Then the slope of the $C(\Theta)$ vs. Θ , which is C_{bp} , and the intercept, C_{be} , provides all necessary information to determine δ_1 and

δ_r by

$$\delta_r = \eta_o \left[\frac{K_f(K_{bc} - \eta_o K_{bp})}{\eta_o K_{bp}(K_s - K_f) + K_f K_{bc}} \right] \quad (3.75)$$

and

$$\delta_s = \eta_o \left[\frac{K_{bp}((1-\eta_o)K_s - K_{bc})}{\eta_o K_{bp}(K_s - K_f) + K_f K_{bc}} \right]. \quad (3.76)$$

To this point the family of compressibilities is quite general and two independent parameters are required to fully describe this family. However, if one assumes that the "hydrostatic limit", commonly referred to as the unjacketed or matrix bulk modulus, i.e.

$\Theta=1$, is

$$K_{unj} = K(1) = K_s \quad (3.77)$$

then equation (3.73) readily yields equation (3.20). We see that condition (3.20) holds if and only if assumption (3.77) holds.

Nur & Byerlee (1971) present a very strong argument for the value of the unjacketed bulk modulus as given by equation (3.77). This assumption is the "boundary condition" used by Zimmerman (1991) in the description of static deformations and is based on the work of Geertma (1957). This enables Zimmerman (1991) to determine relationships between the four drained compressibilities. It also enables the undrained bulk modulus to be written as a function of one drained bulk modulus. A majority of the previous theoretical analysis (Gasmann, 1951; Geertma, 1957; Biot & Willis, 1957; Carroll, 1979; Carroll & Katsube, 1983; Katsube, 1985; Zimmerman, 1986, 1991) have used this assumption. This assumption is in effect postulating a microscopically homogeneous solid frame (Berryman, 1992). Several authors have recognized the restrictive nature of this assumption (Morland, 1972; Rice & Cleary, 1976; Brown & Korringa, 1985; Green & Wang, 1986; Berryman & Milton, 1991). Biot & Willis (1957) also caution about the use of this assumption and illustrate the reduction of the number of parameters in the work of Biot (1941).

Van der Knapp (1959) performed unjacketed compressibility measurements on a sample of Belait sandstone in an initial unstressed state (i.e. confining pressure and pore pressure were both equal to atmospheric pressure) and an initial stressed state. The values of the unjacketed compressibility for the sample in an initial unstressed state is $2.97 \times 10^{-5} \text{ m}^2/\text{MN}$ ($2.97 \times 10^{-11} \text{ Pa}^{-1}$) and in the prestressed state is $3.44 \times 10^{-5} \text{ m}^2/\text{MN}$ ($3.44 \times 10^{-11} \text{ Pa}^{-1}$). Van der Knapp (1959) states that the difference is within experimental error. Using independent measurements of C_{ps} and C_{bc} and relation (3.25) a value for the solid compressibility is obtained to be $3.02 \times 10^{-5} \text{ m}^2/\text{MN}$ ($3.02 \times 10^{-11} \text{ Pa}^{-1}$) which lies between the obtained values for the unjacketed compressibility.

Fatt (1959) measured the unjacketed bulk compressibility for Boise sandstone with a porosity of 26%. The measured value for the the unjacketed compressibility was $0.22 \times 10^{-6} \text{ psi}^{-1}$ ($3.19 \times 10^{-11} \text{ Pa}^{-1}$), over a pressure range of 2000 ($1.38 \times 10^7 \text{ Pa}$) to 7000 psi ($4.80 \times 10^7 \text{ Pa}$), as compared to the compressibility of quartz or feldspar which is about $0.20 \times 10^{-6} \text{ psi}^{-1}$ ($2.90 \times 10^{-11} \text{ Pa}^{-1}$) (Fatt, 1959). Nur & Byerlee (1971) observe a linear stress strain relation for Westerly granite subject to an unjacketed test. They argue that the compressibility value obtained, $C_{unj} = 2.2 \text{ Mb}^{-1}$ ($2.2 \times 10^{-11} \text{ Pa}^{-1}$), was equal to the compressibility of the dry sample after cracks were closed and therefore support relation (3.77).

Yew & Jogi (1978) measure the unjacketed bulk modulus of an artificial rock "Alundum", a sintered material made up of over 99% Al_2O_3 , and three types of natural sandstones (Berea, Ohio, and Pecos). The axial strain, under unjacketed conditions, varied linearly with pressure over the entire range (0-50 MPa). The measured unjacketed bulk modulus was $8.3 \times 10^{10} \text{ Pa}$ smaller in comparison to the value (Forsythe, 1959) of $3.0 \times 10^{11} \text{ Pa}$ for Al_2O_3 . Berea sandstone is a fine-grained greywacke composed of 99% quartz grains. The measured unjacketed bulk modulus was $4.4 \times 10^{10} \text{ Pa}$ which is larger than the $3.67 \times 10^{10} \text{ Pa}$ value (Weast, 1969) for quartz. Ohio sandstone is a very fine-grained rock. Most of the matrix material is quartz, clay and shale. The measured unjacketed bulk modulus was $3.3 \times 10^{10} \text{ Pa}$ which is less than the $3.67 \times 10^{10} \text{ Pa}$ value (Weast, 1969) for quartz. The Pecos is a reddish brown, calcareous sandstone. Calcareous denotes fine-grained, relatively homogeneous rock composed mainly of calcite. It has a measured unjacketed bulk modulus of $3.7 \times 10^{10} \text{ Pa}$ which is twice as small as the $7.3 \times 10^{10} \text{ Pa}$ value (Forsythe, 1959) of calcite. The use of the assumption (3.77) or

(3.20), $K_{unj} = K_s$, does enable the construction of more simplified relations between poroelastic parameters. However, it receives little support from the above experimental measurements.

There is one other compressibility which can be obtained from an unjacketed test and is usually referred to as the coefficient of fluid content (Biot & Willis, 1957). It refers to the amount of fluid which enters the pores of a unit volume of porous material, during a deformation subject to unjacketed conditions. In the notation used here

$$C'_{unj} = \frac{1}{V_0} \left. \frac{\Delta V_f^\circ}{\Delta p} \right|_{\Theta=1}, \quad \Theta = \frac{P_f - P_0}{p - p_0} \quad (3.78)$$

where Δp is the change in confining pressure and is equal to the change in pore pressure, i.e. $\Theta=1$, V_0 is the initial volume of the sample, and ΔV_f° is the amount of fluid which enters the porous sample. Equation (3.22) used previously for ΔV_f must be modified to account for the change in volume of fluid associated with the increase in pore pressure, hence

$$\Delta V_f^\circ = \eta_d(V - V_0) + V_d(\eta - \eta_0) + C_f V_f^\circ \Delta p_f \quad (3.79)$$

Combining equation (3.79) and equation (3.78) and using definition (3.70) at $\Theta=1$ one obtains,

$$C'_{unj} = \eta_d(C_f - \alpha(1)) + \frac{\eta - \eta_0}{p - p_0} \quad (3.80)$$

Using equations (3.8) and (3.10) one obtains from equation (3.80)

$$C'_{unj} = \eta_d(C_f - \alpha(1)) + \frac{C_f \delta_f - C_s \delta_s}{1 - \frac{\delta_f}{\eta_0} - \frac{\delta_s}{1 - \eta_0}} \quad (3.81)$$

which yields, with the substitution of equation (3.18),

$$C'_{unj} = \eta_d(C_f - \alpha(1)) + (1 - \eta_0)(C_s - \alpha(1)) \quad (3.82)$$

Using the assumption discussed above for the matrix compressibility, equation (3.82) gives

$$C_{unj}^d = \eta_d(C_f - C_s) \quad (3.83)$$

3.7 Induced Pore Pressure Coefficient

A parameter which is deduced from the undrained compression has been described previously in the literature (Skempton 1954; Rice & Cleary 1976; Dropek, Johnson & Walsh 1978; Green & Wang 1986; McTigue 1986; Green & Wang 1990) as the pore-pressure build up coefficient. This parameter is simply the value of Θ for which the family of compressibilities gives C_{un} . For the drained compression the pore-pressure is kept constant, i.e. $\Theta = 0$, and therefore $C(0) = C_{bc}$. By setting $C(\Theta_u) = C_{un}$ in equation (3.74) the induced pore-pressure, Θ_u , is found to be

$$\Theta_u = \frac{C_{un} - C_s}{\eta_d(C_f - C_s)} \quad (3.84)$$

without any assumption as to what the value of $C(\Theta)$ is at $\Theta = 1$. This expression may be obtained from the work of Brown & Korringa (1975) by using their equation 8 which does not involve any assumptions regarding the homogeneity of the solid.

Under the assumption that $C(1) = C_u$, the induced pore pressure coefficient may be written, by substituting the relationship for the undrained in terms of the drained, (i.e. equation (3.52) into equation (3.84)), as a unique function of the drained bulk modulus

$$\Theta_u = \frac{C_{un} - C_s}{\eta_d(C_f - C_s) + C_{bc} - C_s} \quad (3.85)$$

This expression is also obtained by Green & Wang (1986) based on the work of Brown & Korringa (1975) for a material subject to the above assumption. It was also derived by Bishop (1973, 1976) and can be obtained from the equations of Geertman (1957).

Measured values of Θ_u are about one at low effective pressures for both natural and synthetic sandstones (Wang, 1993; Green & Wang, 1986). The value decreases to 0.5 - 0.6 at increased effective pressures (confining pressure minus pore pressure) (Wang,

1993). Mesri *et al.*(1976) observe similar behavior during measurements on Berea sandstone, Salem limestone, Vermont marble and Barre granite. They attribute the rapid decrease in pore-pressure coefficient, with increasing effective pressure, to the closure of crack like pores.

3.8 Coefficient of Effective Stress

The interest in an effective stress law is that it will enable one to predict the value of a given property, i.e. density, porosity, for any combination of pore and confining pressure, having only made measurements of the property without pore pressure (Robin, 1973). The first to recognize the importance of pore pressure was Terzaghi (1923) who developed a model of effective pressure for highly compliant materials such as soils. Others recognized the apparent correlation of earthquakes with injection of fluids in deep wells (Healy *et al.*, 1968) and the possible association of pre and post earthquake phenomena with pore pressure (Nur & Booker, 1972; Nur, 1972). In Terzaghi's (1923) formulation the concept of effective stress is:

$$\tau_{ij}^{\text{eff}} = \tau_{ij} + \chi p_f \delta_{ij} \quad (3.86)$$

where τ_{ij} denotes the applied stress (positive in tension), p_f is the pore pressure (positive in compression), δ_{ij} is the Kronecker delta and χ is the effective stress coefficient. Terzaghi (1923) argued that χ should be equal to the porosity (η) so that the effect of pore pressure is eliminated when porosity goes to zero. However, his experiments supported values of $\chi=1$.

Stimpson (1961) and Geertsma (1957) have suggested that

$$\chi = 1 - \frac{K_{dr}}{K_s} \quad (3.87)$$

where K_s is the bulk modulus of the grains and K_{dr} being the dry or drained bulk modulus of the porous rock. Nur & Byerlee (1971), and Biot & Willis (1957) have derived equation (3.87) for the effective stress coefficient. Garg & Nur (1973) using the theory of interacting continua (TINC) show that the above relation (3.87) is strictly valid only for linear elastic porous rocks (constant K_{dr}). Zimmerman (1986) examines the nature of

effective stress with respect to volumetric bulk and pore strains. The derivation has been carried out within the framework of a micromechanical theory based solely on linear elasticity. His derived value for χ is the same as equation (3.87). He proves that if the total volumetric strains are unique functions of the pressures, then the compressibilities must depend only on the differential pressure. Carroll (1979) and Carroll & Katsube (1983) generalize the effective stress law for anisotropic elastic deformations. Berryman (1992) argues that the effective stress data on fluid transport through porous rocks cannot be explained with theories based on a homogeneous solid frame. Berryman & Milton (1991) generalize the work of Gasmann (1951) to include two solid constituents in the porous frame.

From the equation of effective stress we can write down the equation for an effective pressure as

$$P_{eff} = P - \chi P_r \quad (3.88)$$

where p is the applied pressure and p_r is the pore pressure. It should be noted that the following derivation of effective stress is for quasi-static, reversible, infinitesimal deformations. From the definition of the family of compressibilities (3.70) we can write the fractional volume change of a sample as

$$-\frac{\Delta V}{V_0} = C(\Theta)\Delta p \quad (3.89)$$

where the ratio $\Theta = \frac{P_r P_0}{P - P_0}$ is kept constant. Substituting equation (3.74) for $C(\Theta)$ in equation (3.89) and using the definition for Θ we obtain

$$-\frac{\Delta V}{V_0} = C_{bc} \left(\Delta p - \frac{C_{bp}}{C_{bc}} \Delta p_r \right) . \quad (3.90)$$

We have the effective pressure as

$$P_{eff} = P - \frac{C_{bp}}{C_{bc}} P_r . \quad (3.91)$$

Comparing equation (3.91) to equation (3.88) we have

$$\chi = \frac{C_{bp}}{C_{bc}} . \quad (3.92)$$

If we assume relation (3.77), i.e. $C(1) = C_s$, we can use relation (3.19) for C_{bp} in equation (3.92) to obtain expression (3.87) for χ as derived by the other authors mentioned above.

Nur & Byerlee (1971) plot volumetric strain measurements, performed on Weber sandstone, versus effective pressures. The effective pressure calculated with the use of equation (3.87) for χ describes quite accurately the measured strains, although some scatter in data still exist. Other measurements (Dobrynin, 1985) performed on two consolidated sandstones supports relation (3.87) for the coefficient of effective stress. A value of $\chi = 0.85$ was determined for those two sandstones. Other experimental work (Handin *et al.*, 1963; Brace & Martin, 1968) appears to support a value of $\chi = 1$. These measurements can be explained by relation (3.81) if the bulk modulus of the porous rock is much less than the bulk modulus of the mineral grains. Fatt (1959) presented data which shows that χ decreases from 1.0, when confining pressure equals pore pressure, to about 0.70 when the confining pressure is much larger than the pore pressure.

3.9 Conclusions

Using the static form of a system of equations for seismic waves (de la Cruz & Spanos, 1989b), we show how various poroelastic parameters (see table 3.1) can be calculated in a straightforward manner. The results obtained have many points of contact with those found in the literature. In particular, we verify all identities (see table 3.2) among drained compressibilities given in, e.g., Zimmerman (1991), thus providing an alternative route towards them. In this work we also addressed the problem of macroscopic shearing. Experiments are proposed for the determination of the macroscopic shear modulus, leading to natural expressions for "Young's modulus" and "Poisson's ratio" for the porous medium under drained conditions.

The undrained compressibility is described within the context of this work and its relation to the various drained compressibilities is verified. The description of "undrained Young's modulus" and "undrained Poisson's ratio" leads to relationships with an undrained bulk modulus which are similar to those of elasticity. For greater experimental flexibility we introduce a one parameter family of compressibilities which includes the drained and the undrained compressibilities as members. The family of compressibilities is also used to obtain an expression for the pore-pressure build up coefficient.

Two compressibilities are defined subject to anunjacketed test and are usually referred to as the coefficient of fluid content (Biot & Willis, 1957) and the matrix compressibility. The use of the assumption that the matrix compressibility is equal to the solid grain compressibility does enable the construction of more simplified relations between poroelastic parameter. It also appears to be the assumption responsible for a compatibility condition obtained by de la Cruz & Spanos (1989b) when comparing final equations describing seismic wave propagation to those of Biot (1956b). If parameter values obtained from quasi-static experiments are used in the dynamic equations, it appears that the Biot theory is limited to systems for which $K_{unj} = K_s$. The sensitivity of the phase velocity and attenuation due to deviations from such a constraint will be explored numerically in chapter 4.

Test	Boundary Conditions	Incremental Variable	Measurements	Poroelastic Parameter
Drained	$p_f = p_o$	Δp	ΔV	C_{bc}, K_{bc}^{-1}
		τ_{xx}	$(\Delta L/L)_x$	E_{bc}
	τ_{xx}	$\frac{(\Delta L/L)_y}{(\Delta L/L)_x}$	ν_{bc}	
	Δp	ΔV_f	C_{pc}, K_{pc}^{-1}	
$p = p_o$	Δp_f	ΔV_f	C_{pp}, K_{pp}^{-1}	
	Δp_f	ΔV	C_{bp}, K_{bp}^{-1}	
Shear	$p_f = p_o$ $\tau_{xx} = \tau_{yy} = 0$ $\tau_{xz} = 0$	$\tau_{xy} = \tau_{yx} = \tau$	θ	μM
Undrained	$\frac{\eta p_f}{(1-\eta)p_o} = \frac{\eta_o p_f^o}{(1-\eta_o)p_o^o}$	Δp	ΔV	C_{ud}, K_{ud}^{-1}
		τ_{xx}	$(\Delta L/L)_x$	E_{ud}
		τ_{xx}	$\frac{(\Delta L/L)_y}{(\Delta L/L)_x}$	ν_{ud}
		Δp	$\frac{(p_f - p_o)}{(p - p_o)}$	θ_u
Unjacketed	$\frac{(p_f - p_o)}{(p - p_o)} = 1$	$\Delta p_f, \Delta p$	ΔV	$K(1), K_{unj}$
		$\Delta p_f, \Delta p$	ΔV_f	C'_{unj}

Table 3.1 Various quasi-static tests and associated poroelastic parameters as derived in this chapter.

$C_{bp} = C_{bc} - C_s^*$	$\eta_o C_{pc} = C_{bc} - C_s$	$C_{pp} = \frac{C_{bp}}{\eta_o} - C_s$
$E_{bc} = \frac{3K_{bc}\mu M}{K_{bc} + \frac{1}{3}\mu M}$	$\nu_{bc} = \frac{K_{bc} - \frac{2}{3}\mu M}{2(K_{bc} + \frac{1}{3}\mu M)}$	
$C_{ud} = C_{bc} \cdot \frac{C_{bp}C_{pc}}{(C_{pp} + C_r)}$	$C_{ud} = \frac{\eta_o C_{bc}(C_r - C_s) + C_d(C_{bc} - C_s)^*}{\eta_o(C_r - C_s) + (C_{bc} - C_s)}$	
$E_{ud} = \frac{3K_{ud}\mu M}{K_{ud} + \frac{1}{3}\mu M}$	$\nu_{ud} = \frac{K_{ud} - \frac{2}{3}\mu M}{2(K_{ud} + \frac{1}{3}\mu M)}$	
$\Theta_s = \frac{C_{ud} - C_s}{\eta_o(C_r - C_s)}$	$\Theta_s = \frac{C_{bc} - C_s}{\eta_o(C_r - C_s) + C_{bc} - C_s}^*$	
$C'_{unj} = \eta_o(C_r - C(1)) + (1 - \eta_o)(C_s - C(1))$	$C'_{unj} = \eta_o(C_r - C_s)^*$	
$\chi = \frac{K_{bc}}{K_{bp}}$	$\chi = 1 - \frac{K_{bc}}{K_s}^*$	

Table 3.2 Relations among various quasi-static poroelastic parameters. The * indicates that the relation is only valid if $C(1) = C_s$.

CHAPTER 4

WAVE PROPAGATION IN FULLY SATURATED POROUS MEDIA

4.1 Introduction

The elastic model of wave propagation predicts one dilatational (P) wave and one rotational (S) wave (isotropic media). The waves are non-dispersive and no attenuation is present. The physical parameters introduced are the density, the bulk modulus and the shear modulus. Wave propagation in a viscous compressible fluid is described by the Navier Stokes equation. It predicts one dilatational wave and one rotational wave (assuming isotropy), usually known as the viscous waves, which are attenuated and dispersive in nature. The physical constants present are the density, the bulk modulus, the shear viscosity and the bulk viscosity. Viscoelastic theory is concerned with materials whose response is dependent on all past states of stress (Christensen, 1962). The stress-strain relations involves integrals over all past states of stress or strain and the material properties are represented by relaxation and creep functions. Mechanical models such as the Maxwell model and the Kelvin-Voigt model help one to visualize the behavior of viscoelastic materials. For the majority of viscoelastic materials it is shown that they behave elastically under very rapid deformations and can behave elastically or viscously under very slow deformations. The dispersion relations for dilatational and rotational plane waves propagating in a viscoelastic material are similar in form to those of the elastic case. However, the waves are attenuated and dispersive in nature. It should be mentioned that the governing equation for waves is simply a statement of Newton's second law and that the difference in the above models, i.e. elastic solid, viscous fluid, and viscoelastic, lies solely in the choice of the constitutive relation.

The simplest model utilized for wave propagation in the earth is the elastic solid model. As mentioned previously, this model predicts the existence of one P wave and one S wave and it does not allow for attenuation, and the waves are nondispersive. In the past, attenuation has been added into the single continuum model by allowing the bulk and shear moduli of the medium to be described by complex numbers (simplified viscoelastic approximation). However, it is very difficult to make an association between the measured attenuation and the actual physical mechanism responsible. Furthermore, most physical

systems of interest in exploration geophysics and seismically monitored oil recovery processes involve a single fluid phase or multiple fluid phases in a porous medium, and the extra degrees of freedom introduced in a multicomponent system can not be duplicated by any single continuum model.

The first models for seismic wave propagation in porous media which involved two coupled and interacting continua were proposed by Gassmann (1951a) and Biot (1956b, 1956c). More recently, macroscopic models have been obtained by applying various homogenization schemes to the governing equations at the small scale. Burridge & Keller (1981), use the two-space method of homogenization to construct the macroscopic equations. de la Cruz & Spanos (1985, 1989b) and Pride *et al.* (1992) use a volume averaging method, whereas; Liu & Katsube (1990), Katsube & Carroll (1987a, 1987b), Crochet & Nagdhi (1966), and Green & Nagdhi (1965) use the method of mixtures to construct the macroscopic equations.

In order to utilize any of the above models, both the constitutive properties and macroscopic properties of the porous medium must be determined. Microscopic constitutive properties are easily determined for simple systems, that is, for a porous medium consisting of water and sand, routine measurements determine parameters such as the density of the sand grains or the water, the viscosity of water, and so forth. Macroscopic parameters, such as porosity and permeability, are also easily determined independently of a wave propagation experiment for simple systems. In the past other macroscopic parameters, however, have not been measured independently, so that the wave propagation model was a curve fit to wave propagation experiments in order to determine these parameters.

In this chapter generalizations to the de la Cruz & Spanos (1989b) model are presented. The origin of all the macroscopic parameters needed for the model are described. Independent experiments needed to determine some of the macroscopic parameters are discussed and the conditions under which such values for the parameters may be utilized. Numerical solutions are also presented in order to illustrate some of the important aspects of this wave propagation model as well as the significance of the generalizations.

4.2 Formal Equations of de la Cruz & Spanos (1989b)

In the work of de la Cruz & Spanos (1985, 1989b), the macroscopic continuum equations which describe wave propagation in a fluid filled porous medium have been constructed by using volume averaging (see section 2.1) in conjunction with physical arguments. A porous medium is envisaged here as an elastic matrix whose pores are interconnected and are completely filled with a viscous compressible fluid. The medium is also assumed to be macroscopically homogeneous and isotropic. The steps used to formulate the final macroscopic equations are shown schematically in figure 4.1, along with the model assumptions. This theory appears to have the advantage of relative simplicity and physical transparency. The initial model of de la Cruz & Spanos (1985) did not include the induced mass coefficient which expresses the effect of inertia at the fluid-solid boundaries, but did include a viscous dissipation term within the fluid elements which Biot (1956b, 1956c) neglected. In subsequent work, de la Cruz & Spanos (1989b) included the induced mass coefficient through its basic pore scale origins using the same nomenclature as Biot (1956b), and included thermomechanical coupling. Thermomechanical coupling refers to the first order heating of the phases from compression and the expansion/contraction of the phases due to heating and cooling.

The resulting coupled, first order, macroscopic equations which describe wave propagation in porous media saturated with a single viscous compressible fluid are (as per de la Cruz & Spanos, 1989b):

Equations of motion

$$(1-\eta_0)\rho_s \frac{\partial^2 \bar{u}_s}{\partial t^2} = (1-\eta_0)K_s \nabla(\nabla \cdot \bar{u}_s) - K_s \nabla \eta + (1-\eta_0)\mu_s [\nabla^2 \bar{u}_s + \frac{1}{3} \nabla(\nabla \cdot \bar{u}_s)] \\ - (1-\eta_0) K_s \alpha_s \nabla T_s - \Gamma^{(3)} + \mu_s \partial_k \Gamma_{ik}^{(4)} \quad (4.1)$$

$$\eta_0 \rho_f \frac{\partial}{\partial t} \bar{v}_f = -\eta_0 \nabla \bar{p}_f + \eta_0 [\mu_f \nabla^2 \bar{v}_f + \frac{1}{3} \mu_f \nabla(\nabla \cdot \bar{v}_f)] - \Gamma^{(1)} + \mu_f \partial_k \Gamma_{ik}^{(2)} \quad (4.2)$$

Equations of continuity

$$\frac{(\bar{\rho}_s - \rho_f)}{\rho_f} \cdot \frac{(\eta - \eta_0)}{(1 - \eta_0)} + \nabla \cdot \bar{u}_s = 0 \quad (4.3)$$

$$\frac{1}{\rho_f} \frac{\partial \bar{\rho}_f}{\partial t} + \frac{1}{\eta_0} \frac{\partial \eta}{\partial t} + \nabla \cdot \bar{v}_f = 0 \quad (4.4)$$

Pressure equations

$$\frac{1}{K_s} (\bar{p}_s - p_0) = -\nabla \cdot \bar{u}_s + \frac{(\eta - \eta_0)}{(1 - \eta_0)} + \alpha_s (\bar{T}_s - T_0) \quad (4.5)$$

$$\frac{1}{K_f} \frac{\partial \bar{p}_f}{\partial t} = -\nabla \cdot \bar{v}_f - \frac{1}{\eta_0} \frac{\partial \eta}{\partial t} + \alpha_f \frac{\partial \bar{T}_f}{\partial t} \quad (4.6)$$

Heat equations

$$(1 - \eta_0) \rho_s c_v \frac{\partial \bar{T}_s}{\partial t} - T_0 K_s \alpha_s \left[\frac{\partial \eta}{\partial t} - (1 - \eta_0) \frac{\partial}{\partial t} \nabla \cdot \bar{u}_s \right] - (1 - \eta_0) \kappa_s \nabla^2 \bar{T}_s - \nabla \cdot \kappa_s \mathbf{I}^{(7)} - \mathbf{I}^{(8)} = 0 \quad (4.7)$$

$$\eta_0 \rho_f c_f \frac{\partial \bar{T}_f}{\partial t} - \eta_0 T_0 \alpha_f \frac{\partial \bar{p}_f}{\partial t} - \eta_0 \kappa_f \nabla^2 \bar{T}_f - \nabla \cdot \kappa_f \mathbf{I}^{(5)} - \mathbf{I}^{(6)} = 0 \quad (4.8)$$

Porosity equation

$$\frac{\partial \eta}{\partial t} = \delta_s \nabla \cdot \bar{v}_s - \delta_f \nabla \cdot \bar{v}_f \quad (4.9)$$

Equation (4.9) has been introduced to complete the system of equations. It is assumed that there are parameters, δ_s and δ_f , characteristic of the medium such that equation (4.9) is valid for low-frequency waves and for quasi-static compressions of the type discussed

here. The thermodynamic foundations of these δ 's were discussed in chapter 2 and it is believed that their values may depend on the process which is taking place.

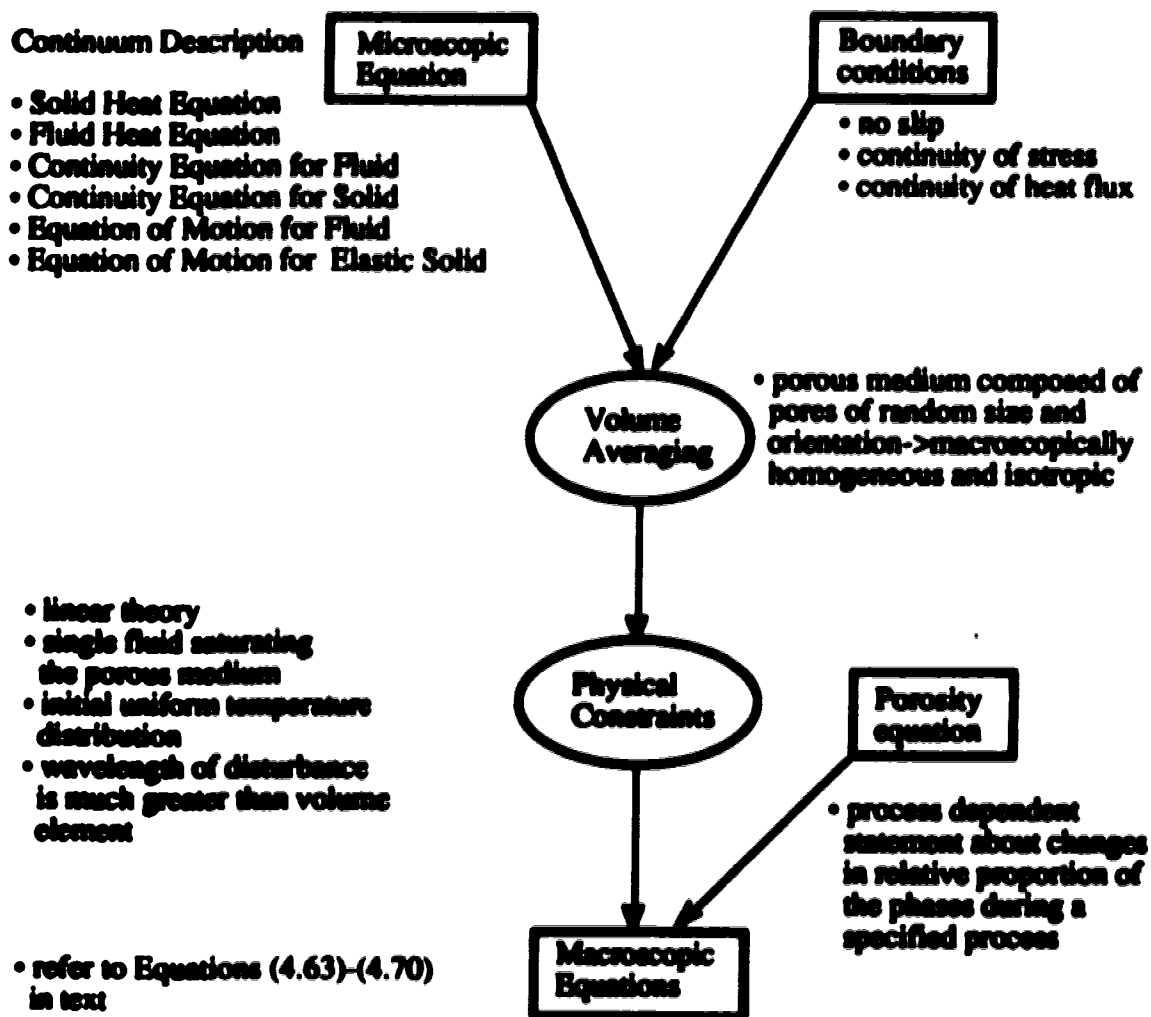


Figure 4.1 Development of the theory.

The integrals (denoted by Γ 's) over fluid-solid interface in the above equations represent the coupling between the constituents and representative expressions in terms of macroscopic observables must be argued for on physical grounds. These expressions

introduce the majority of the macroscopic parameters in the theory, except for porosity. An interpretation of the introduced macroscopic parameters in such expressions may depend on the type of process taking place. These area integrals are not all independent but are related due to the pore scale boundary conditions. The area integrals given by

$$\Gamma_i^{(1)} = \frac{1}{V} \int_{A_B} [(p_T - p_0)\delta_{ik} - \tau_{ik}^*] n_k dA \quad (4.10)$$

and

$$\Gamma_i^{(3)} = -\frac{1}{V} \int_{A_M} [\tau_{ik}^* + p_0 \delta_{ik}] n_k dA \quad (4.11)$$

are related, due to the continuity of stress at the pore scale interface, as

$$\Gamma_i^{(3)} = -\Gamma_i^{(1)} . \quad (4.12)$$

The area integrals given by

$$\Gamma_{ik}^{(2)} = \frac{1}{V} \int_{A_B} (v_k n_i + v_i n_k - \frac{2}{3} v [n_i \delta_{ik}]) dA \quad (4.13)$$

and

$$\Gamma_{ik}^{(4)} = \frac{1}{V} \int_{A_M} (u_k n_i + u_i n_k - \frac{2}{3} u [n_i \delta_{ik}]) dA \quad (4.14)$$

are related by

$$\frac{\partial}{\partial t} \Gamma_{ik}^{(4)} = -\Gamma_{ik}^{(2)} \quad (4.15)$$

on account of the continuity of displacements at the pore scale interface. The following two area integrals

$$\Gamma^{(6)} = \frac{1}{V} \int_{A_{th}} \kappa_f \nabla T_f \cdot dA \quad (4.16)$$

and

$$\Gamma^{(8)} = \frac{1}{V} \int_{A_{sf}} \kappa_s \nabla T_s \cdot dA \quad (4.17)$$

are related by

$$\Gamma^{(6)} = -\Gamma^{(8)} \quad (4.18)$$

due to the continuity of heat flux

Finally, the the two area integrals given by

$$\Gamma^{(5)} = \frac{1}{V} \int_{A_{th}} (T_f - T_o) dA \quad (4.19)$$

and

$$\Gamma^{(7)} = \frac{1}{V} \int_{A_{sf}} (T_s - T_o) dA \quad (4.20)$$

are related by

$$\Gamma^{(5)} = -\Gamma^{(7)} \quad (4.21)$$

because the temperatures of the two components are the same on the interface.

4.3 Discussion of Fluid Bulk Viscosity

The equations presented above are generalized to include fluid bulk viscosity, ξ_f , (Hickey *et al.*, 1991). The constitutive equation for a Newtonian fluid (pore scale) is

$$\sigma_{ik}^f = p_f \delta_{ik} + \rho_f v_i v_k - \bar{\sigma}_{ik}^f, \quad (4.22)$$

where the contribution in stress due to the viscosity, $\bar{\sigma}_{ik}^f$, is

$$\bar{\sigma}_{ik}^f = \mu_f \left(\frac{\partial v_i}{\partial x_k} + \frac{\partial v_k}{\partial x_i} - \frac{2}{3} \delta_{ik} \frac{\partial v_l}{\partial x_l} \right) + \xi_f \delta_{ik} \frac{\partial v_l}{\partial x_l}. \quad (4.23)$$

de la Cruz & Spanos (1989b) assumed from the outset that ξ_f , the bulk viscosity, was zero. Hence by volume averaging the last term in equation (4.23) the macroscale effect of the bulk viscosity can be determined. Substituting the constitutive relation into the equation of motion and applying the volume averaging procedure, from section 2.1, to the term containing bulk viscosity yields

$$\left\langle \frac{\partial}{\partial x_i} \xi_f \frac{\partial v_l}{\partial x_l} \right\rangle = \frac{\partial}{\partial x_i} \left\langle \xi_f \frac{\partial v_l}{\partial x_l} \right\rangle + \frac{1}{V} \int_{A_{fb}} \xi_f \frac{\partial v_l}{\partial x_l} n_i dA \quad (4.24)$$

Applying the averaging theorem (2.4) to the first term on the right hand side of equation (4.24) yields

$$\frac{\partial}{\partial x_i} \left\langle \xi_f \frac{\partial v_l}{\partial x_l} \right\rangle = \frac{\partial}{\partial x_i} \left[\xi_f \frac{\partial}{\partial x_l} (\eta \bar{v}_l^f) + \frac{1}{V} \int_{A_{fb}} \xi_f v_l n_i dA \right]; \quad (4.25)$$

since $v_l n_i dA$ is the time rate of volume swept out by the fluid velocity v_l of the boundary surface element, we can evaluate the area integral yielding

$$\frac{\partial}{\partial x_i} \left\langle \xi_f \frac{\partial v_l}{\partial x_l} \right\rangle = \frac{\partial}{\partial x_i} \left[\xi_f \frac{\partial}{\partial x_l} (\eta \bar{v}_l^f) + \frac{\partial}{\partial t} (\xi_f \eta) \right]. \quad (4.26)$$

Substituting equation (4.26) into equation (4.24) the macroscopic expression representing the contribution of bulk viscosity is

$$\left\langle \frac{\partial}{\partial x_i} \xi_r \frac{\partial v_j}{\partial x_i} \right\rangle = \frac{\partial}{\partial x_i} \left[\xi_r \frac{\partial}{\partial x_i} (\eta \bar{v}) + \frac{\partial}{\partial x} (\xi_r \eta) \right] + \frac{1}{V} \int_{A_{fs}} \xi_r \frac{\partial v_j}{\partial x_i} n_r dA \quad (4.27)$$

Two additional terms in the fluid macroscopic equation of motion (4.2) are required. The area integral term on the right hand side of equation (4.27) is included in the macroscopic terms which describe macroscopically viscous and inertial drag across all fluid-solid interfaces. This is accounted for by replacing expression for the viscous stress tensor τ_{ik}^f in the area integral $I_i^{(1)}$ (equation, 4.10) of de la Cruz & Spanos (1989b) by $\tilde{\sigma}_{ik}^f$ of equation (4.23).

4.4 Generalized Macroscopic Shear Deformations

In the work of de la Cruz & Spanos (1985, 1989b) the shear modulus of the porous material turned out to be equal to the volume fraction of solid times the shear modulus of the solid component. In that description, the pore structure and packing of the grains did not alter the shear strength of the overall material as long as it did not alter the porosity. The influence of pore structure on shear stresses is accounted for by the surface integrals $I_{ik}^{(4)}$ and $I_{ik}^{(2)}$, which were believed to be zero by de la Cruz & Spanos (1985, 1989b). In this section the macroscopic shear modulus μ_M is introduced as a phenomenological parameter (but is none the less well-defined in terms of pore-scale quantities).

Formal arguments permit one to write the additional shear strain associated with the coupling at the pore scale interfaces, in the notation of de la Cruz & Spanos (1989b),

$$I_{ik}^{(2)}(1-\eta_0) = -c_1 \frac{\partial}{\partial x} \left[\bar{u}_{i,k} + \bar{u}_{k,i} - \frac{2}{3} \bar{u}_{l,l} \delta_{ik} \right] - c_2 \left[\bar{v}_{i,k} + \bar{v}_{k,i} - \frac{2}{3} \bar{v}_{l,l} \delta_{ik} \right] \quad (4.28)$$

where c_1 and c_2 (a temporary notation) are some dimensionless quantities. Given condition (4.15) the additional shear strain in the solid due to coupling is

$$\Gamma_{ik}^{(4)}(1-\eta_o) = c_1 \left[\bar{u}_{i,k} + \bar{u}_{k,i} - \frac{2}{3} \bar{u}_{i,r} \delta_{ik} \right] + c_2 \left[\bar{u}_{i,k} + \bar{u}_{k,i} - \frac{2}{3} \bar{u}_{i,r} \delta_{ik} \right] \quad (4.29)$$

The second term on the right hand side of equation (4.29) is proportional to fluid displacements. At the beginning it was assumed that the fluid is a Newtonian fluid implying that shear stresses are related to the shear rate i.e., proportional to velocity. Therefore, this will impose that $c_2=0$.

Defining μ_M as

$$\mu_M = (1-\eta_o)\mu_o(1+c_1) \quad (4.30)$$

the generalization requires that $(1-\eta_o)\mu_o$ be replaced by μ_M in equation (4.1). At the same time, equation (4.2), the fluid equation of motion, acquires a new term involving space derivatives of the solid velocity. The new term

$$-(1-\eta_o)\mu_o \left(\frac{\mu_M}{(1-\eta_o)\mu_o} - 1 \right) \frac{\partial}{\partial x_k} \left[\bar{v}_{i,k} + \bar{v}_{k,i} - \frac{2}{3} \bar{v}_{i,r} \delta_{ik} \right] \quad (4.31)$$

arises from equation (4.15) which fails to vanish unless $c_1 = 0$, a condition which was used in de la Cruz & Spanos (1989b) but which is now regarded as being too restrictive. An approximate value for the macroscopic shear modulus can be obtained from quasi-static experiments as described in section 3.5 or indirectly from a quasi-static uniaxial test as described in section 3.3.

4.5 Generalized Macroscopic Heat Conduction

In analogy with the generalization of the shear modulus, the macroscopic heat conductivities can be introduced as phenomenological parameters and are related to component heat conductivities κ_i , κ_o according to

$$\kappa_M = \eta_o \kappa_i (1+c_i) \quad (4.32)$$

and

$$\kappa_M^t = (1 - \eta_o) \kappa_s (1 + c_s) \quad (4.33)$$

where the dimensionless constants c_s , c_f reflect the pore scale behavior through the assumed relation

$$\frac{1}{V} \int_{A_{th}} (T_f - T_o) d\vec{A} = \eta_o c_f \nabla T_f - (1 - \eta_o) c_s \nabla T_s \quad (4.34)$$

so that from relation (4.21), one has

$$\frac{1}{V} \int_{A_M} (T_s - T_o) d\vec{A} = (1 - \eta_o) c_s \nabla T_s - \eta_o c_f \nabla T_f \quad (4.35)$$

These generalizations will produce additional terms in the averaged heat equations (4.7) and (4.8) as well introduce two additional macroscopic parameters. Nozad *et al.* (1985) also constructed the basis for a two-equation model of transient heat conduction in porous media using volume averaging. However, no attempt was made to evaluate the area integrals. Given that two additional macroscopic parameters, defined by (4.32) and (4.33), come about due to the effect of pore structure on heat conduction through the porous medium, the two macroscopic heat conductivities might be related but there is no argument for such a relationship at this time.

In most studies of heat transfer in porous medium filled with a static fluid (Verma *et al.*, 1991; Zimmerman, 1989; Haug, 1971; Woodside & Messmer, 1961a, 1961b; among others) a one-equation model is used and only one effective thermal conductivity parameter, usually referred to as the stagnant effective thermal conductivity (Haug, 1971; Hsu & Cheng, 1990), is required. This model is based on the assumption that the energy transport process can be characterized by a single temperature (Nozad *et al.*, 1985). This assumption is referred to as "local thermal equilibrium" (Nozad *et al.*, 1985; Zarotti & Carbonell, 1984). By reducing their two-equation model to a one-equation model Nozad *et al.* (1985) show that

$$\nabla^2 [\eta_o \kappa_f + (1 - \eta_o) \kappa_s] T + \nabla \cdot \frac{1}{V} \int_{A_o} \kappa_f (T_f - T_o) - \kappa_s (T_s - T_o) dA = \nabla \cdot (\kappa_M \nabla T) \quad (4.36)$$

where \bar{T} is the characteristic single temperature and κ_d is the stagnant effective thermal conductivity. Applying such an approach to the present analysis would lead to only one degree of freedom, which would be related to the stagnant effective thermal conductivity as

$$\eta_o c_f - (1 - \eta_o) c_s = \frac{\kappa_d - [\eta_o \kappa_f + (1 - \eta_o) \kappa_s]}{\kappa_f - \kappa_s} \quad (4.37)$$

The generalization to include convection has been addressed by Yoshida *et al.* (1990) and Hsu & Cheng (1990). This generalization still contains only one effective thermal conductivity. Huang (1971) states that with the flow rates normally observed in thermal processes, stagnant effective thermal conductivities are usually adequate to describe the conductive heat transfer.

4.6 Evaluation of the Area Integrals $I_i^{(1)}$ and $I_i^{(3)}$

When the fluid equation of motion is volume averaged one obtains the surface integral

$$I_i^{(1)} = \frac{1}{V} \int_{\Lambda_b} [(p_f - p_o) \delta_{ik} - \tau_{ik}^f] n_k dA \quad (4.38)$$

and the corresponding surface integral for the solid is

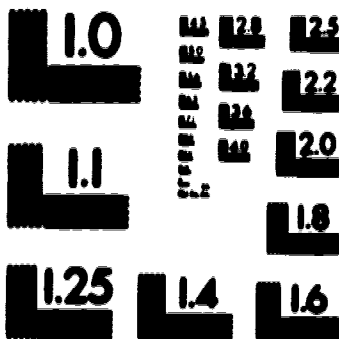
$$I_i^{(3)} = - \frac{1}{V} \int_{\Lambda_s} [\tau_{ik}^s + p_o \delta_{ik}] n_k dA \quad (4.39)$$

These integrals are opposites of each other and describe the force per unit volume exerted by one continuum on the other across the interfaces due to any motion. de la Cruz & Spanos (1989b) argue that this body force may be expanded as follows;

$$\frac{1}{V} \int_{\Lambda_f} [(p_f - p_o) \delta_{ik} - \sigma_{ik}^f] n_k dA = \frac{\eta_o \mu_f}{K} (\bar{v}_f - \bar{v}_s) - \rho_{12} \frac{\partial}{\partial t} (\bar{v}^f - \bar{v}^s) \quad (4.40)$$

2

PM-1 3 1/2"x4" PHOTOGRAPHIC MICROCOPY TARGET
NBS 1910a ANSI/ISO G2 EQUIVALENT



PRECISIONSM RESOLUTION TARGETS

Physically, the first term in the expansion represents the momentum transfer between the fluid and solid across the solid-fluid interfaces during wave propagation. This is a significant attenuation mechanism which is known as Darcian resistance. It is dependent on the relative solid-fluid velocity (due to invariance) and is therefore also dependent on the relative phase angles. It becomes the dominant attenuation mechanism at low viscosities (Hickey, 1990).

The parameter K is a scalar quantity, as long as the volume elements are assumed large enough that the porous medium is macroscopically homogeneous and isotropic. Permeability is also a parameter used to quantify the resistance to flow of a fluid through a porous medium. It is a function of the size, orientation, distribution, and connectivity of the pores. It has been introduced previously in Darcy's equation,

$$\mathbf{q}_f = \frac{-K}{\mu_f} (\nabla p_f - \rho_f \mathbf{g}) \quad (4.41)$$

which is based on a classical experiment performed by Darcy (1856). The fluid pressure is denoted by p_f and has units Pa, μ_f is the fluid viscosity in Pa s, \mathbf{q} is the Darcy velocity in m/s, ρ_f is the density of the fluid in kg/m³, \mathbf{g} is the acceleration due to gravity in m/s², and K is the permeability in m². There are several methods of measuring permeability based on different forms of Darcy's equation. Most are performed by flowing a fluid of known viscosity through a porous medium at a specified pressure gradient and measuring the flow rate. Utilizing these measured values and the above equation one can calculate the permeability of the medium. Given the condition that the wavelength of disturbance be orders of magnitude larger than the pore scale de la Cruz & Spanos (1985, 1989b) suggest that the permeability value obtained through a Darcy experiment might be used as an estimate for the parameter, K , in the expansion (4.40). However, it is important to remember that this parameter is introduced to represent the momentum transfer between the fluid and solid components during a seismic disturbance. As an extreme example consider a porous medium having a disconnected pore space. In such a material the Darcy permeability would be zero. However, during a seismic disturbance there could still be momentum transfer between the solid and fluid components.

Biot (1956c) extended the notion that fluid-flow through a porous medium could deviate from Poiseuille type flow during the passage of a seismic wave. In order to

account for such flow behavior, Biot (1956c) introduced a "dynamic viscosity operator" which is of importance in regions other than low frequency (Warner, 1990). The theory was divided into two regimes, a high and a low frequency regime. In the high frequency regime (Biot, 1956c), the fluid-flow is not of the Poiseuille type and the dynamic viscosity operator is of importance. In the low frequency regime (Biot, 1956b) the fluid-flow is Poiseuille type and the dynamic viscosity operator is simply equal to one. In order to quantify the separation of these two regions a "viscous penetration depth" (Warner, 1986) is defined by

$$\delta = \left(\frac{2\mu r}{\rho r \omega} \right)^{1/2} \quad (4.42)$$

It is argued that the fluid is viscously locked to the solid matrix if it is within a distance less than a viscous penetration depth from the pore wall. The critical frequency separating the two regimes, defined as the frequency at which the viscous penetration depth is equal to one pore radii, is given by

$$\omega_c = \frac{2\mu}{\rho r R^2} \quad (4.43)$$

where R is a typical pore radius. For frequencies larger than the critical frequency, the viscous penetration depth becomes smaller and the flow deviates from Poiseuille flow.

Biot (1956c) constructed a model of a fluid contained within an oscillating duct, of radius a , and subjected to an oscillatory pressure gradient. From this model he obtained the following expression for the dynamic viscosity operator, $F(\psi)$, as

$$F(\psi) = \frac{1}{4} \frac{\kappa T(\psi)}{1 - \frac{2}{i\psi} T(\psi)} \quad (4.44)$$

where $T(\kappa)$ can be written in terms of Kelvin functions as

$$T(\psi) = \frac{\text{ber}' \psi + i \text{ber}' \psi}{\text{ber} \psi + i \text{bei} \psi} \quad (4.45)$$

and

$$\psi = a \left(\frac{\omega \rho_f}{\mu_f} \right)^{\frac{1}{2}} \quad (4.46)$$

The dynamic viscosity operator will be complex valued in most cases. For application to porous media Biot (1956c) accounts for the size of the pores and geometry of the pore structure by assuming a to be some characteristic parameter. This requires that the frequency correction be the same for all pores and therefore does not account for a medium with a distribution of pore sizes. The above expression, although quite complicated, does not account for the geometry of the pore structure for a medium with a distribution of pore sizes.

Johnson *et al.* (1987) derived an expression for the dynamic viscosity operator. In its simplest form (after Warner, 1990), this expression is

$$F(\omega) = \left(1 + \frac{4\alpha^2 K^2 \rho_f^2 \omega}{\mu_f \Lambda^2 \eta_0^2} \right)^{\frac{1}{2}} \quad (4.47)$$

which requires a measurement of the Darcy permeability of the medium, K , as well as additional measurements of tortuosity (high frequency limit), α , and of the characteristic throat size, Λ .

The second term in the expansion (4.40) accounts for non-steady flow between phases. de la Cruz & Spanos (1989b) argue that inertial coupling can be accounted for by an extra term that is proportional to the relative acceleration. They have used the symbol ρ_{12} because, when comparison with Biot's (1956b) theory is meaningful, it is exactly the induced mass coefficient, ρ_{12} , of Biot.

Landau and Lifshitz (1975b) derived an expression for ρ_{12} based on a model of a rigid sphere oscillating in an incompressible perfect fluid. This discussion yields an upper bound for ρ_{12} , namely $\rho_{12} < 0$, which is determined by the directions of the applied forces and should therefore extend to more general cases. Yih (1969) generalized the problem for a viscous fluid which introduced an additional term dependent on frequency and viscosity.

Assuming that the porous medium can be regarded as a collection of spheres (radius of b) and neglecting interaction between spheres, the induced mass coefficient may be written as (Mochizuki, 1982)

$$\rho_{12}(\omega) = -(\alpha(\omega) - 1)\eta_o\rho_f . \quad (4.48)$$

The coefficient, α , is

$$\alpha(\omega) = 1 - \Gamma(\omega) (1 - 1/\eta_o) \quad (4.49)$$

with

$$\Gamma(\omega) = \frac{1}{2} + \frac{2}{4} \sqrt{\frac{2\mu_f}{b^2\rho_f\omega}} . \quad (4.50)$$

Johnson *et al.* (1987) write the dynamic tortuosity $\alpha(\omega)$ as

$$\alpha(\omega) = \alpha + \frac{i\mu_f\eta_o}{\omega K\rho_f^2} F(\omega) ; \quad (4.51)$$

therefore α is the high frequency limit of $\alpha(\omega)$. More elaborate functions for the dynamic tortuosity are derived by Johnson *et al.* (1987) by accounting for the fractal nature of the pore surfaces. In general, α is restricted to be greater than unity and depends on the topology of the interconnected pore spaces.

Bedford *et al.* (1984) consider an idealized porous medium composed of cylindrical pores oriented in a random fashion, and calculates the induced mass coefficient as a function of frequency. If the simplification is made that the cylindrical pores are aligned so that their axes are in three perpendicular directions and one axis parallel to the motion, then in the low frequency limit the induced mass coefficient, ρ_{12} , is

$$\rho_{12} = -\frac{\eta_o\rho_f}{3} . \quad (4.52)$$

The tortuosity, α (high frequency limit) is also related to electrical conductivity of a porous medium. Assuming that the solid is an insulator the relation is (Brown, 1980)

$$\alpha = \eta_o \Omega \quad (4.53)$$

where Ω is the ratio of the electrical conductivity of the porous medium to the electrical conductivity of the pore fluid.

Johnson (1980) applies the Biot theory to fused glass bead samples filled with a superfluid. He shows that the tortuosity, α , as defined by equation (4.50), can be obtained from measurements of the 2nd P-wave velocity, using the following relationship

$$\alpha^{1/2} = \frac{v(\text{slow wave or fourth sound})}{v(\text{fluid})} \quad (4.54)$$

Velocity measurements on a set of fused glass bead samples, of various porosities ranging from 10.5% to 33.5% , saturated with ^4He superfluid (Johnson *et al.*,1982) shows that tortuosity decreases as porosity increases. Values obtained for tortuosity ranged from 3.84 down to 1.75. The values obtained from the use of the superfluid agree with values obtained from electrical conductivity measurements on these fused glass bead samples. Using 2nd P-wave velocity measurements on water filled fused glass bead samples (Piona, 1980), and relation (4.54) Dutta (1980) predicted tortuosity values of 2.1, 2.2, and 3.3 for Piona's three samples.

The importance of the induced mass, ρ_{12} , and dynamic viscosity on wave velocities and their relation to tortuosity are still under investigation (Champoux & Stinson, 1992). It is probably not possible to measure the induced mass without resorting to a wave propagation experiment, since its origins lie in the relative accelerations which occur during wave propagation. Furthermore, many of the investigations discussed above utilize a rigid frame approximation. The consequences of such an approximation are not obvious. The expressions for the induced mass being dependent on only the fluid density might be associated with such an approximation.

4.7 Evaluation of the Area Integrals $I^{(6)}$ and $I^{(8)}$

An additional parameter is introduced when de la Cruz & Spanos (1989b) explicitly take into account thermo-mechanical coupling. The physical argument for its introduction is very similar to that for the permeability, aside from the fact that it deals with heat conduction rather than momentum transfer across the solid-fluid interfaces.

When the equations describing the thermomechanics of the components (fluid and solid) are volume averaged, de la Cruz & Spanos (1989b) obtain a pair of surface integrals, $I^{(6)}$ and $I^{(8)}$. These two integrals are equal and opposite and represent the heat transfer from one component to the other across the microscopic interfaces. Hence, the fluid component acts as an additional heat source for the solid and vice-versa. As discussed by de la Cruz & Spanos (1989b), these heat exchange terms between components should vanish if and only if the macroscopic component temperatures are equal ($\bar{T}_f = \bar{T}_s$). It is therefore argued by de la Cruz & Spanos (1989b), that these terms may be represented by a first order scalar proportional to $(\bar{T}_s - \bar{T}_f)$ and therefore they obtain

$$I^{(6)} = \int_{\Lambda_s} \kappa_f \nabla T_f \cdot d\vec{\Lambda} = \gamma(\bar{T}_s - \bar{T}_f) \quad (4.55)$$

where γ is the positive empirical parameter. The heat transfer between components represented by this term should contribute to the attenuation of the dilatational waves.

The surface coefficient of heat transfer, γ , is estimated by

$$\gamma = O[\kappa A/(VL)] \quad (4.56)$$

where κ is the effective conductivity between the fluid and solid, A is the interfacial surface area between the fluid and the solid within the volume, V is the averaging volume, and L is the characteristic pore scale length.

In order to evaluate in what frequency regime thermomechanical coupling is most important, Hickey *et al.* (1991) examine the rates at which different heating mechanisms are occurring. Using order of magnitude approximations, a bound on the physical system

of interest is established in terms of a dimensionless quantity. The frequency below which there will be approximate equality of the two temperatures is approximated as

$$\omega_{CT} = \frac{\gamma}{\rho c} \quad (4.57)$$

where ρc is some effective value for the medium. A dimensionless quantity is then defined as the ratio of ω_{CT} to the frequency of deformation. Based on crude estimates for the surface are per unit volume of porous media, figure 4.2 (after Hickey *et al.*, 1991) is a plot of the dimensionless quantity equated to unity versus the three variables, frequency, surface coefficient of heat transfer, and the effective heat capacity. The upper left portion of the graph represents the combination of parameters where the wave is oscillating in a characteristic time which is less than the time required for significant transfer of thermal energy between the phases. Conversely, the lower right portion of the graph represents the combination of parameters where the wave is propagating in a characteristic time which is greater than the time for the significant transfer of thermal energy between the phases.

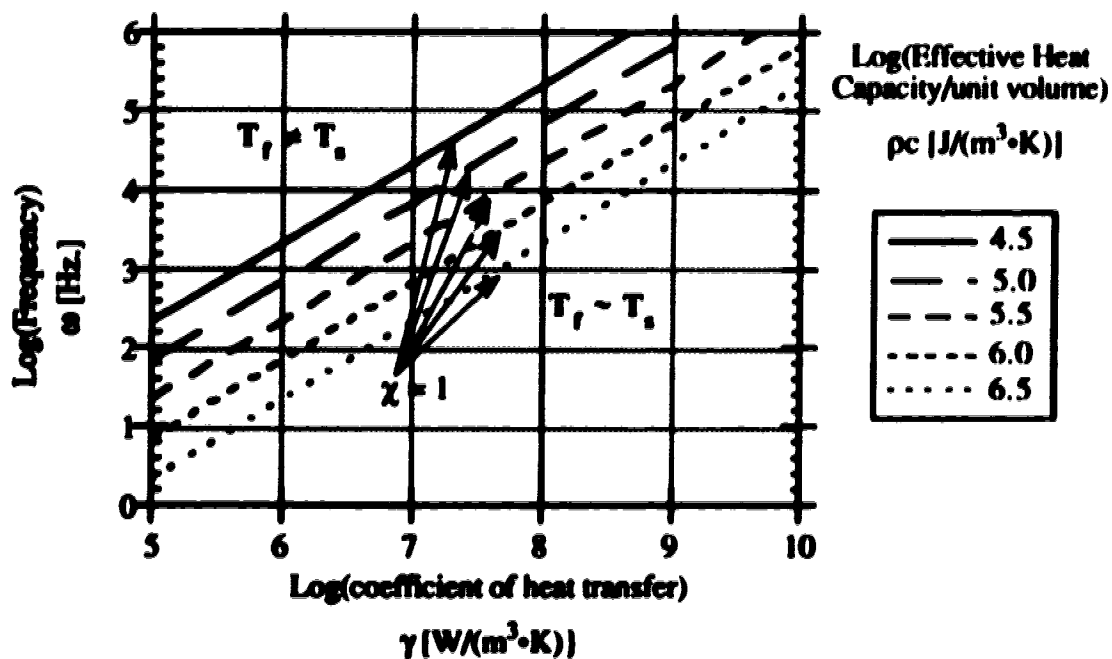


Figure 4.2 Illustration of different possible thermal regimes of a porous medium during

a seismic disturbance.

Intercomponent heat conduction is present only when thermomechanical coupling is included and induces significant changes in attenuation of the 1st P-wave within the seismic frequency range. It can be approximated by equation (4.56) and becomes more important for small pore sizes. The frequency at which the equality of component temperatures exists depends on γ . No independent experiment for measuring this parameter exists at this time. It should be related to the stagnant effective thermal conductivity.

4.8 Solid Compliance Factor (δ_s) and Fluid Compliance Factor (δ_f)

From the thermodynamics (de la Cruz *et al.*, 1993) discussed in chapter 2, the porosity, η , enters the macroscopic description on the same footing as displacements and density. In order to obtain a complete set of equations describing the propagation of a dilatational wave de la Cruz & Spanos (1989b) adopted relation (4.9). It is argued that such a relation is a process dependent statement and suitable values of δ_s and δ_f will depend on the process considered. Using the above relationship (4.9), de la Cruz & Spanos (1989b) considered the case where the two average pressures, \bar{p}_s and \bar{p}_f , are regarded as approximately equal. Neglecting thermal effects in equations (4.5) and (4.6) they obtain a relationship for $\frac{\partial \eta}{\partial t}$ with the following definite expressions for δ_s and δ_f :

$$\delta_s = \frac{\eta_0 (1 - \eta_0)}{K_f \left[\frac{\eta_0}{K_f} + \frac{1 - \eta_0}{K_s} \right]} \quad (4.58)$$

and

$$\delta_f = \frac{\eta_0 (1 - \eta_0)}{K_s \left[\frac{\eta_0}{K_f} + \frac{1 - \eta_0}{K_s} \right]} \quad (4.59)$$

Although equation (4.9) probably represents the simplest physical statement concerning change in porosity and change in volume of the two phases, the measurement of the compliance factors by an independent experiment is not straightforward. In chapter 3 the problem was reformulated so that the compliance factors are defined in terms of two more physically transparent macroscopic parameters, namely, an undrained bulk modulus,

K_{ud} , and a drained bulk modulus, K_{bc} , which are well known in the geophysical literature. The undrained bulk modulus is defined as the bulk modulus measured by compressing the porous sample where the fluid is not permitted to flow across the closed surface at which the compression takes place. The drained bulk modulus is defined as the measured bulk modulus when fluid is permitted to flow across the closed surface at which the compression takes place. Hence, both of these macroscopic parameters are measurable in a static experiment if a sample of the porous medium is readily available. The relationships between the static compliance factors and the drained and undrained bulk moduli are

$$\delta_s = (1-\eta_o) \frac{(K_s - K_{ud})(K_s - K_{bc}/(1-\eta_o))}{(K_s - K_f)(K_s - K_{bc})} \quad (4.60)$$

and

$$\delta_r = \eta_o \frac{K_s(K_{ud} - K_f) - K_{bc}(K_s - K_f)}{(K_s - K_f)(K_s - K_{bc})} \quad (4.61)$$

Assuming that the bulk modulus value obtained in a hydrostatic unjacketed experiment, i.e. K_{unj} , is the value for the bulk modulus of the solid matrix (see section 3.6) then one needs only to measure the drained bulk modulus of the porous medium, and obtain the compliance factors through

$$\delta_r = \frac{\eta_o[(1-\eta_o)K_s - K_{bc}]}{(1-\eta_o)K_s - K_{bc} + \frac{\eta_o K_s^2}{K_f}} \quad (4.62)$$

and compatibility condition (3.20).

Of course, values obtained for the δ 's from static experiments should only be considered as an estimate. If the processes controlling the compression of the sample differ then this will be reflected in the values of the δ 's. The process dependence of the values of the δ 's is illustrated in the description of macroscopic capillary pressure between two fluid phases in a porous medium.

4.9 Generalized Equations for Wave Propagation in a Porous Medium Saturated by One Fluid

Modifications to the system of equations governing low frequency wave propagation in a porous medium which is saturated by a single fluid, as described in the previous sections of this chapter, are incorporated resulting in the following system of equations:

Equations of motion

$$(1-\eta_0)\rho_s \frac{\partial^2 \bar{u}_s}{\partial t^2} = (1-\eta_0)K_s \nabla[\nabla \cdot \bar{u}_s - \frac{\eta - \eta_0}{1-\eta_0}] + \mu_M [\nabla^2 \bar{u}_s + \frac{1}{3} \nabla(\nabla \cdot \bar{u}_s)] \\ + \frac{\mu \eta_0^2}{K} (\bar{v}_f - \bar{v}_s) - \rho_{12} \frac{\partial}{\partial t} (\bar{v}_f - \bar{v}_s) - (1-\eta_0)K_s \alpha_s \nabla \bar{T}_s \quad (4.63)$$

$$\eta_0 \rho_f \frac{\partial \bar{v}_f}{\partial t} = -\eta_0 \nabla \bar{p}_f + \eta_0 \mu_f [\nabla^2 \bar{v}_f + \frac{1}{3} \nabla(\nabla \cdot \bar{v}_f)] + \eta_0 \xi_f \nabla [\nabla \cdot \bar{v}_f + \frac{1}{\eta_0} \frac{\partial \eta}{\partial t}] \\ - \frac{\mu_f}{\mu_s} [\mu_M - (1-\eta_0)\mu_s] \frac{\partial}{\partial t} [\nabla^2 \bar{u}_s + \frac{1}{3} \nabla(\nabla \cdot \bar{u}_s)] - \frac{\mu \eta_0^2}{K} (\bar{v}_f - \bar{v}_s) + \rho_{12} \frac{\partial}{\partial t} (\bar{v}_f - \bar{v}_s) \quad (4.64)$$

Equations of continuity

$$\frac{(\bar{\rho}_s - \rho_s^0)}{\rho_s^0} - \frac{(\eta - \eta_0)}{(1-\eta_0)} + \nabla \cdot \bar{u}_s = 0 \quad (4.65)$$

$$\frac{1}{\rho_f^0} \frac{\partial \bar{p}_f}{\partial t} + \frac{1}{\eta_0} \frac{\partial \eta}{\partial t} + \nabla \cdot \bar{v}_f = 0 \quad (4.66)$$

Pressure equations

$$\frac{1}{K_s} (\bar{p}_s - p_0) = -\nabla \cdot \bar{u}_s + \frac{(\eta - \eta_0)}{(1-\eta_0)} + \alpha_s (\bar{T}_f - T_0) \quad (4.67)$$

$$\frac{1}{K_f} \frac{\partial \bar{p}_f}{\partial t} = -\nabla \cdot \bar{v}_f - \frac{1}{\eta_0} \frac{\partial \eta}{\partial t} + \alpha_f \frac{\partial \bar{T}_f}{\partial t} \quad (4.68)$$

Heat equations

$$(1 - \eta_0)\rho_s c_v \frac{\partial \bar{T}_s}{\partial t} + (1 - \eta_0)T_0 K_s \alpha_s \frac{\partial}{\partial t} \left[\nabla \cdot \bar{u}^s - \frac{\eta - \eta_0}{1 - \eta_0} \right] - \kappa_M^s \nabla^2 \bar{T}_s + \frac{\kappa_f}{\kappa_f} [\kappa_M^f - \eta_0 \kappa_f] \nabla^2 \bar{T}_f - \gamma (\bar{T}_f - \bar{T}_s) = 0 \quad (4.69)$$

$$\eta_0 \rho_f c_f \frac{\partial \bar{T}_f}{\partial t} - \eta_0 T_0 \alpha_f \frac{\partial \bar{p}_f}{\partial t} - \kappa_M^f \nabla^2 \bar{T}_f + \frac{\kappa_f}{\kappa_s} [\kappa_M^s - (1 - \eta_0) \kappa_s] \nabla^2 \bar{T}_s + \gamma (\bar{T}_f - \bar{T}_s) = 0 \quad (4.70)$$

Porosity equation

$$\frac{\partial \eta}{\partial t} = \delta_s \nabla \cdot \bar{v}_s - \delta_f \nabla \cdot \bar{v}_f \quad (4.71)$$

Comparison with Biot's theory (1956b, 1956c) is possible by neglecting thermomechanical coupling and bulk viscosity. Assuming the correlation between variables of this work and the Biot (1956b) theory (cf. table 4.1) the equations 6.7 of Biot are written as

$$(1 - \eta_0)\rho_s \frac{\partial^2 \bar{u}_s}{\partial t^2} = N \nabla^2 \bar{u}_s + \nabla[(A + N)\nabla \cdot \bar{u}_s + Q \nabla \cdot \bar{u}_f] + \frac{\mu \eta_0^2}{K} (\bar{v}_f - \bar{v}_s) - \rho_{12} \frac{\partial}{\partial t} (\bar{v}_f - \bar{v}_s) \quad (4.72)$$

and

$$\eta_0 \rho_f \frac{\partial^2 \bar{u}_f}{\partial t^2} = \nabla[Q \nabla \cdot \bar{u}_s + R \nabla \cdot \bar{u}_f] - \frac{\mu \eta_0^2}{K} (\bar{v}_f - \bar{v}_s) + \rho_{12} \frac{\partial}{\partial t} (\bar{v}_f - \bar{v}_s) \quad (4.73)$$

Assuming that equations (4.72) and (4.73) are identical to equations (4.63) and (4.64) respectively then equating coefficients results in relationships between parameters which are presented in table 4.2. Furthermore, two terms present in the fluid equation motion

derived here are not present in the Biot formulation. One of the terms is a Brinkman type term and represent viscous dissipation within the fluid which is not directly related to relative fluid-solid motions. The other term was the additional coupling term introduced into the fluid equation motion as a consequence of the generalization of the shear modulus (section 4.4).

Biot	Present work
u	\bar{u}_s
U	\bar{u}_f
p	\bar{p}_f
k	K
$\mu, (\mu F(\kappa))$	μ_f
β	η_0
ρ_{12}	ρ_{12}

Table 4.1 Relationship in notation of variables and some parameters between the Biot theory and this work.

Biot	Present work
Q'	$K_f \delta_s$
Q	$K_s \delta_f$
N	μ_M
R	$\eta_0 K_f \left(1 - \frac{\delta_f}{\eta_0}\right)$
A	$(1 - \eta_0) K_f \left(1 - \frac{\delta_s}{1 - \eta_0}\right) - \frac{2}{3} \mu_M$

Table 4.2 Comparison of coefficients for the Biot theory and the work presented here. The expression in parenthesis is with comparison to the Biot high frequency theory.

In addition, Biot's assumption of a unique energy potential imposes the following constraint on his parameters:

$$Q=Q' \quad (4.74)$$

in the context of such a comparison this imposes the condition (previously obtained in chapter 3 as equation (3.20))

$$\frac{\delta_z}{\delta_r} = \frac{K_z}{K_r} \quad (4.75)$$

for the two theories to describe equivalent physical systems. It should be emphasized that the use of such an energy potential, from a thermodynamic point of view, leads to somewhat ambiguous conclusions as discussed previously in chapter 2.

Methods for the measurement of the elastic coefficients, A, N, Q, and R, of Biot's theory were described by Biot & Willis (1957). The elastic coefficients are related to the quasi-static values (notation has been changed to correspond to the present work and definitions of the various parameters are given in chapter 3) of jacketed compressibility coefficient, C_{bc} (defined by equation 3.13), the unjacketed compressibility coefficient, C_{unj} (defined by equation 3.77), the coefficient of fluid content, C_{unj}^f (defined by equation 3.78), and the shear modulus of the bulk material, μ_M (defined by equation 3.69). For what they consider to be the most general case they assume that the above four quasi-static parameters are independent and obtain the relationships for the elastic parameters which are presented in table 4.3. Using the quasi-static description presented in chapter 3 relationships for Biot's A, N, Q and R are determined and presented in table 4.4. It was shown previously, in chapter 3, that even under general quasi-static conditions the above static compressibility coefficients are not independent. For example the coefficient of fluid content, C_{unj}^f is related to the unjacketed compressibility, C_{unj} by equation (3.82). Substituting for C_{unj}^f using equation (3.83), in the expressions of Biot & Willis (1957), table 4.2, and comparing to the expressions obtained here, table 4.4, the expressions for A, Q, and are equal only if

$$C_{unj} = C_s \quad (4.76)$$

which is the necessary quasi-static assumption for condition (4.75) to hold. Under such an assumption, the determination of Biot's elastic coefficients requires only two independent quasi-static measurements and the corresponding relations are presented in table 4.5.

$$\begin{aligned}
 N &= \mu_M \\
 R &= \frac{\eta_0^2}{C_{unj}^d + C_{unj} - C_{unj}^2/C_{bc}} \\
 Q &= \frac{\eta_0(1-\eta_0 - C_{unj}/C_{bc})}{C_{unj}^d + C_{unj} - C_{unj}^2/C_{bc}} \\
 A &= \frac{C_{unj}^d/C_{bc} + \eta_0^2 + (1-2\eta_0)(1-C_{unj}/C_{bc})}{C_{unj}^d + C_{unj} - C_{unj}^2/C_{bc}} \cdot \frac{2}{3}\mu_M
 \end{aligned}$$

Table 4.3 Elastic coefficients for the Biot theory in terms of quantities measurable in quasi-static experiments as derived by Biot & Willis (1957).

$$\begin{aligned}
 N &= \mu_M \\
 R &= \frac{\eta_0^2}{(1-\eta_0)C_s + \eta_0 C_f - C_{unf} C_f / C_{bc}} \\
 Q &= \frac{\eta_0(1-\eta_0 - C_f / C_{bc})}{(1-\eta_0)C_s + \eta_0 C_f - C_{unf} C_f / C_{bc}} \\
 A &= \frac{(1-\eta_0)^2 + \eta_0 C_f / C_{bc} - (1-\eta_0) C_{unf} / C_{bc}}{(1-\eta_0)C_s + \eta_0 C_f - C_{unf} C_f / C_{bc}} \cdot \frac{2}{3}\mu_M
 \end{aligned}$$

Table 4.4 Elastic coefficients for the Biot theory in terms of quantities measurable in quasi-static experiments described in chapter 3.

$$\begin{aligned}
 N &= \mu_M \\
 R &= \frac{\eta_0^2}{(1-\eta_0)C_s + \eta_0 C_f - C_s^2/C_{bc}} \\
 Q &= \frac{\eta_0(1-\eta_0 - C_s^2/C_{bc})}{(1-\eta_0)C_s + \eta_0 C_f - C_s^2/C_{bc}} \\
 A &= \frac{(1-\eta_0)^2 + \eta_0 C_f/C_{bc} - (1-\eta_0)C_s^2/C_{bc}}{(1-\eta_0)C_s + \eta_0 C_f - C_s^2/C_{bc}} - \frac{2}{3}\mu_M
 \end{aligned}$$

Table 4.5 Elastic coefficients for the Biot theory in terms of quantities measurable in quasi-static experiments under the condition that $C_{unj} = C_s$. For such a condition the expression obtained from this work and the work of Biot & Willis (1957) are the same.

Ignoring the inconsistencies in the Biot theory from a thermodynamic viewpoint, the comparison of Biot's (1956b) equations and the system of equations derived here reveals that the assumption of an energy potential as put forth by Biot is much more restrictive than was previously thought. This restrictive nature becomes evident if quasi-static measurements are used for the elastic coefficients in the wave propagation theory. It appears that the expressions for the elastic coefficients in terms of measurable quasi-static values given by Biot & Willis (1957) are only valid in the case where $C_{unj} = C_s$.

4.10 Numerical Examples

The numerical examples were programmed in FORTRANVS and executed on the University of Alberta mainframe computer. The steps taken to obtain the final phase velocity and attenuation values are outlined in figure 4.3. To study the propagation of a rotational wave the system of equations for the vector potential ψ is considered. The equations of motion are not coupled to the heat equations in this case, indicating that thermomechanical coupling as proposed here does not affect the rotational waves. Also the generalization to include bulk viscosity does not affect the rotational waves. The resulting dispersion relation yields two distinct physical solutions, thereby implying the presence of two rotational waves.

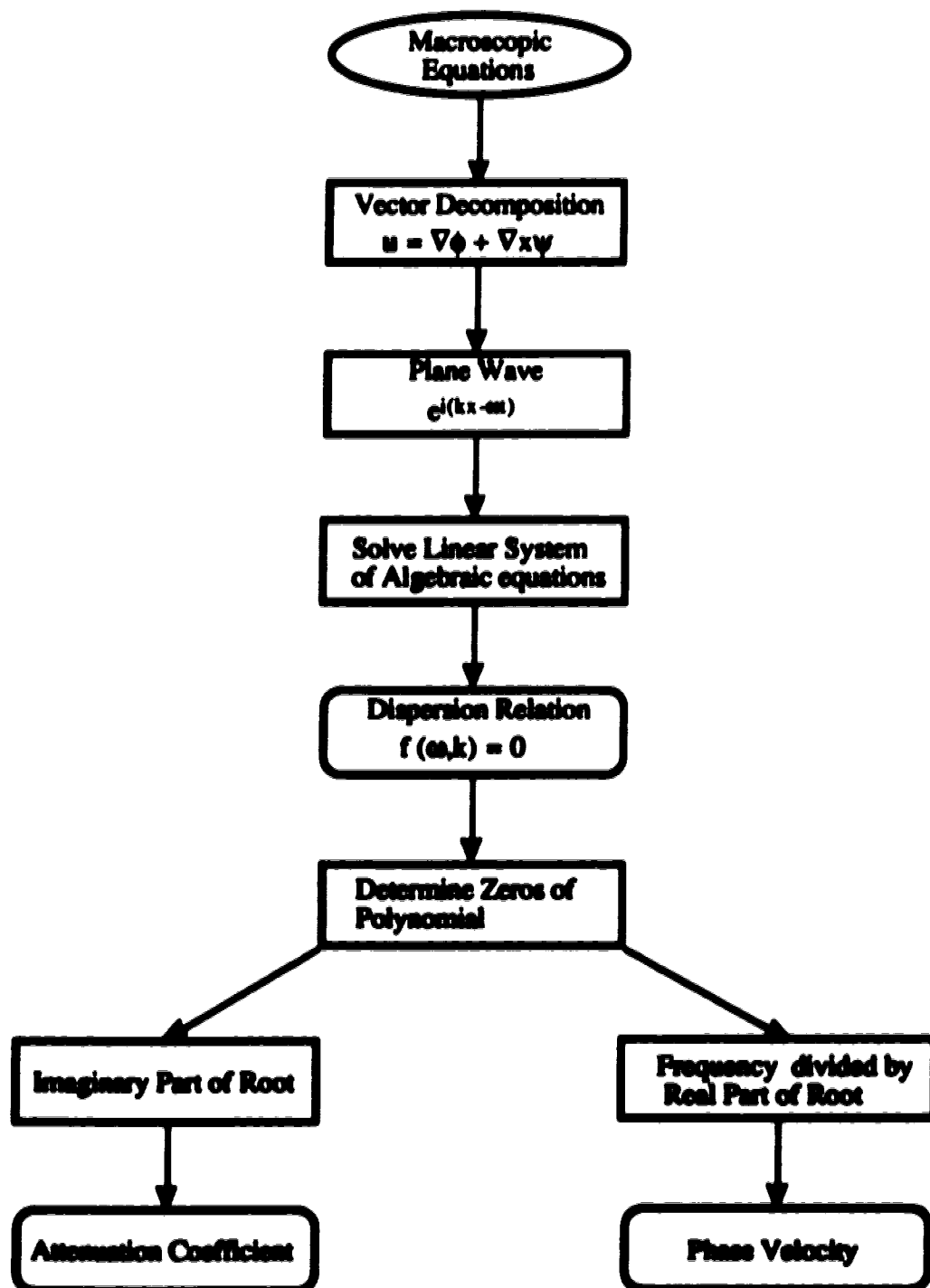


Figure 4.3 Schematic for numerical procedure used to calculate attenuation and phase velocity of various modes.

The description of dilatational waves is obtained by studying the system of equations for the scalar potential ϕ . Due to the complexity of this determinant a numerical solution with numerical consistency checks, in various limiting cases, was constructed. The method of obtaining a solution for the dilatational waves is structured on the cofactor expansions of determinants (Campbell, 1977). For the non-thermal dilatational waves, the dispersion relation implies the presence of two dilatational waves. When thermomechanical coupling is included the dispersion relation suggests the presence of four dilatational waves. Two of these waves are primarily mechanical in nature whereas the other two are primarily thermal. These four waves converge to two waves, i.e. first and second sound, in the solid and/or fluid limits (Hickey, 1990).

The numerical solutions are used to illustrate the significance of the generalizations carried out previously in this chapter, i.e. incorporation of bulk viscosity, generalization of shear modulus, and generalization of heat conductivities. Also, to show how the phase velocity and attenuation of the waves change when δ_s and δ_T values deviate from values obtained from quasi-static experiments. The importance of other macroscopic parameters such as permeability and induced mass coefficient are also examined.

The model used consists of a porous skeleton made up of quartz grains and has macroscopic properties similar to a consolidated Berea sandstone. The physical and thermal parameters for this model are presented in table 4.6. Three different saturating fluids are considered. First, water is used to represent a fairly incompressible and inviscid fluid. Physical and thermal parameters as well as macroscopic parameters which are dependent on the fluid are presented in table 4.7. Second, air is used to represent a compressible and inviscid fluid (cf. table 4.8 for parameters); and third, bitumen is used to represent the compressible and viscid fluid (c.f. table 4.9 for parameters). The induced mass coefficient is approximated using equation (4.52), and an order of magnitude estimate is obtained for the coefficient of heat transfer by using equation (4.56).

Property	Symbol	Value	SI units
Solid constituent			
Density	ρ_s	2650	kg/m ³
Bulk Modulus	K_s	3.3×10^{10}	Pa
Shear modulus	μ_s	2.3×10^{10}	Pa
Specific heat	C_v	755	J(kg°C) ⁻¹
Thermal expansion	α_s	3.4×10^{-7}	°C ⁻¹
Thermal Conductivity	κ_s	8.4	W(m°C) ⁻¹
Macroscopic			
Ambient temperature	T_o	20	°C
Porosity	η_o	.25	
Permeability	K	1.0×10^{-13}	m ²
Shear modulus	μ_M	4.9×10^9	Pa
Drained bulk modulus	K_{bc}	7.1×10^9	Pa
Macroscopic solid thermal conductivity	κ_M^s	4.2	W(m°C) ⁻¹

Table 4.6 Physical properties for Berea sandstone. The constituent properties are assumed to be those of quartz and the values of the macroscopic properties are similar to those of a consolidated Berea sandstone.

Property	Symbol	Value	SI units
Fluid constituent			
Density	ρ_f	1000	kg/m^3
Bulk Modulus	K_f	2.2×10^9	Pa
Shear viscosity	μ_f	1.0×10^{-3}	Pa s
Bulk viscosity	ξ_f	2.8×10^{-3}	Pa s
Specific heat	C_p^f	4180	$\text{J}(\text{kg}^\circ\text{C})^{-1}$
Thermal expansion	α_f	2.0×10^{-4}	$^\circ\text{C}^{-1}$
Thermal Conductivity	κ_f	0.6	$\text{W}(\text{m}^\circ\text{C})^{-1}$
Macroscopic			
Induced mass	ρ_{12}	-83.0	kg/m^3
Coefficient of heat transfer	γ	1.0×10^{12}	$\text{W}(\text{m}^3^\circ\text{C})^{-1}$
Macroscopic fluid thermal conductivity	κ_M^f	$\frac{2}{3}\eta_o\kappa_f$ (0.1)	$\text{W}(\text{m}^\circ\text{C})^{-1}$
Stagnant effective thermal conductivity	κ_{eff}	4.5	$\text{W}(\text{m}^\circ\text{C})^{-1}$

Table 4.7 Physical properties for water and the properties of the porous medium which are dependent on the pore fluid.

Property	Symbol	Value	SI units
Fluid constituent			
Density	ρ_f	1.21	kg/m^3
Bulk Modulus	K_f	1.5×10^5	Pa
Shear viscosity	μ_f	1.8×10^{-5}	Pa s
Bulk viscosity	ξ_f	3.5×10^{-5}	Pa s
Specific heat	C_p^f	1000	$\text{J}(\text{kg}^\circ\text{C})^{-1}$
Thermal expansion	α_f	3.4×10^{-3}	$^\circ\text{C}^{-1}$
Thermal Conductivity	κ_f	2.5×10^{-2}	$\text{W}(\text{m}^\circ\text{C})^{-1}$
Macroscopic			
Induced mass	ρ_{12}	-0.1	kg/m^3
Coefficient of heat transfer	γ	1.0×10^{12}	$\text{W}(\text{m}^3^\circ\text{C})^{-1}$
Macroscopic fluid thermal conductivity	κ_M^f	$\frac{2}{3}\eta_o\kappa_f$ (4×10^{-3})	$\text{W}(\text{m}^\circ\text{C})^{-1}$
Stagnant effective thermal conductivity	κ_{eff}	2.4	$\text{W}(\text{m}^\circ\text{C})^{-1}$

Table 4.8 Physical properties for air and the properties of the porous medium which are dependent on the pore fluid.

Property	Symbol	Value	SI units
Fluid constituent			
Density	ρ_f	990	kg/m ³
Bulk Modulus	K_f	1.8×10^9	Pa
Shear viscosity	μ_f	1000	Pa s
Bulk viscosity	ξ_f	5000	Pa s
Specific heat	C_p^f	1670	J(kg°C) ⁻¹
Thermal expansion	α_f	3.0×10^{-4}	°C ⁻¹
Thermal Conductivity	κ_f	0.1	W(m°C) ⁻¹
Macroscopic			
Induced mass	ρ_{12}	-82.5	kg/m ³
Coefficient of heat transfer	γ	1.0×10^{12}	W(m ³ °C) ⁻¹
Macroscopic fluid thermal conductivity	κ_M^f	$\frac{2}{3}\eta_0\kappa_f$ (0.02)	W(m°C) ⁻¹
Stagnant effective thermal conductivity	κ_{eff}	?	W(m°C) ⁻¹

Table 4.9 Physical properties for bitumen and the properties of the porous medium which are dependent on the pore fluid.

In general, both the phase velocity and attenuation of the P and S waves are functions of frequency. The phase velocity of the various modes, for the three different parameters sets considered, are presented in table 4.10. The phase velocities of the 1st P wave, 1st S wave and 2nd S wave are found to be approximately constant in the frequency range of 0 - 1000 Hz. The actual frequency dependence of the 2nd P wave is shown in figure 4.4. For the air saturated and bitumen saturated cases, the magnitude of the phase velocity is less but the frequency dependence is similar.

Fluid	1st P wave (m/s)	1st S wave (m/s)	2nd P wave (m/s)	2nd S wave (m/s)
Water	2857.0	1479.8	[0.1-26.5]	2.4
Air	2618.9	1570.0	[0.2-6.5]	35.8
Bitumen	2806.6	1480.7	[0.002-0.08]	7.9

Table 4.10 Phase velocities of the various seismic waves propagating through a porous medium saturated with the specified fluid. If the mode is significantly dispersive, the numbers in parentheses are the range of phase velocities for a frequency range 1 - 1000 Hz.

The attenuation and $1000/Q$ of the 1st P wave as a function of frequency for the water, bitumen, and air filled cases, are shown in figure 4.5, figure 4.6 and figure 4.7 respectively. All three cases show an increasing attenuation with frequency and a $1000/Q$ which increases approximately linearly with frequency. In the water and air filled cases there is significant relative motion between the solid and fluid thereby making the Darcian resistance the important attenuation mechanism. In the bitumen case, due to its high viscosity, the fluid and solid are locked together and very little relative flow occurs. Therefore, for the bitumen case the Darcian resistance mechanism is not important and the mechanism responsible for the attenuation is described by the Brinkman type term in the fluid equation as well as the bulk viscosity. From the figures it is seen that both mechanisms exhibit a similar frequency dependence.

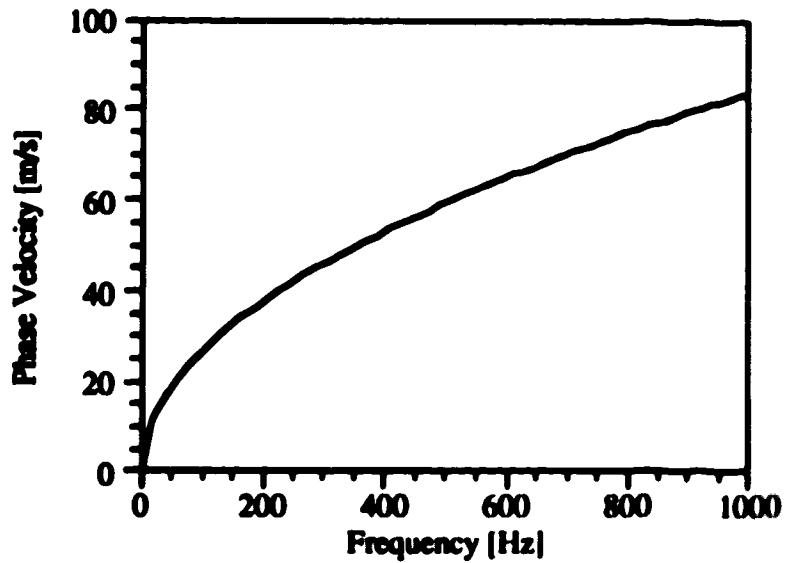


Figure 4.4 Phase velocity versus frequency for the 2nd P wave. Both the non-thermal and thermal (with thermomechanical coupling) exhibit similar frequency dependence. The saturating fluid is water.

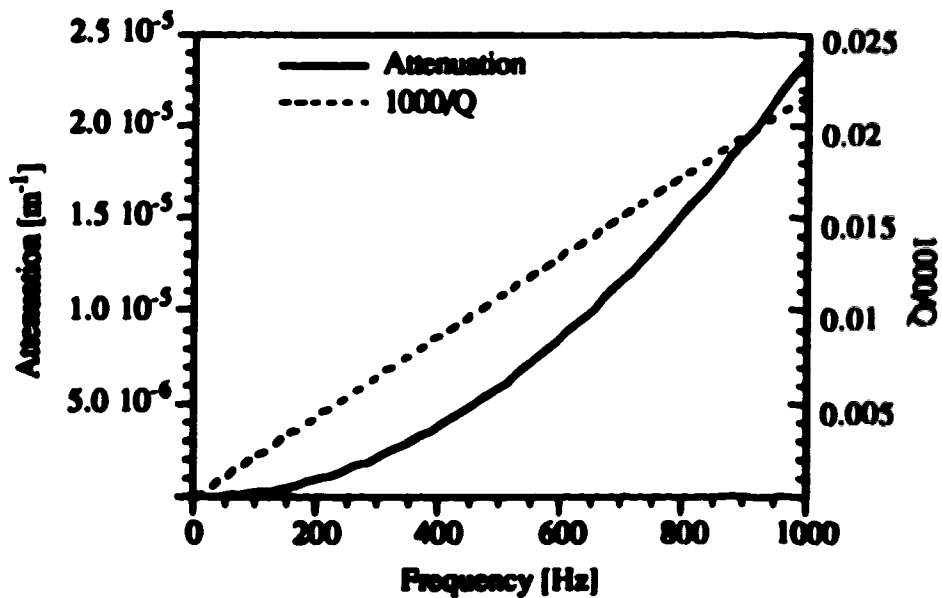


Figure 4.5 Attenuation and inverse Q versus frequency for the 1st P wave. Inverse Q exhibits an approximate linear relationship versus frequency. The saturating fluid is water.

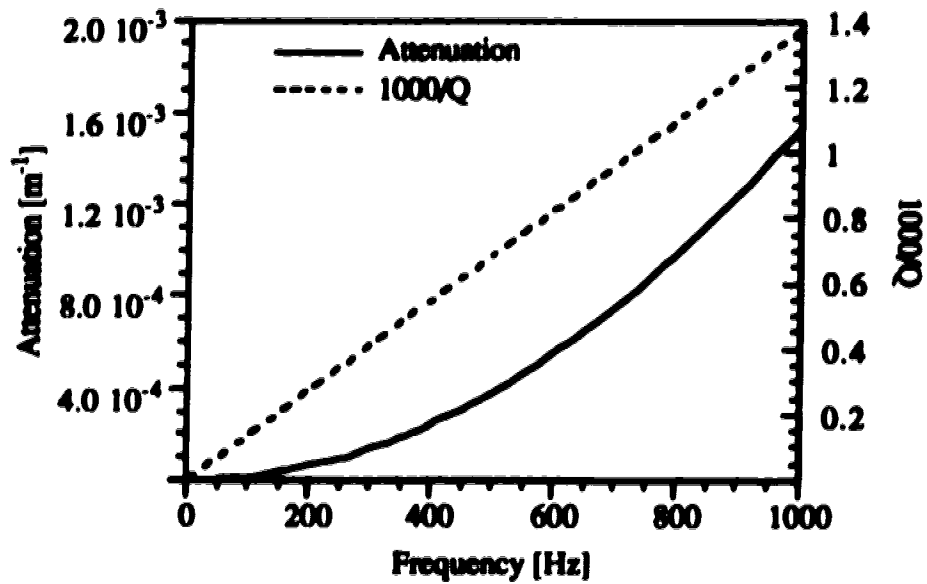


Figure 4.6 Attenuation and inverse Q versus frequency for the 1st P wave. Inverse Q exhibits an approximate linear relationship versus frequency. The saturating fluid is bitumen.

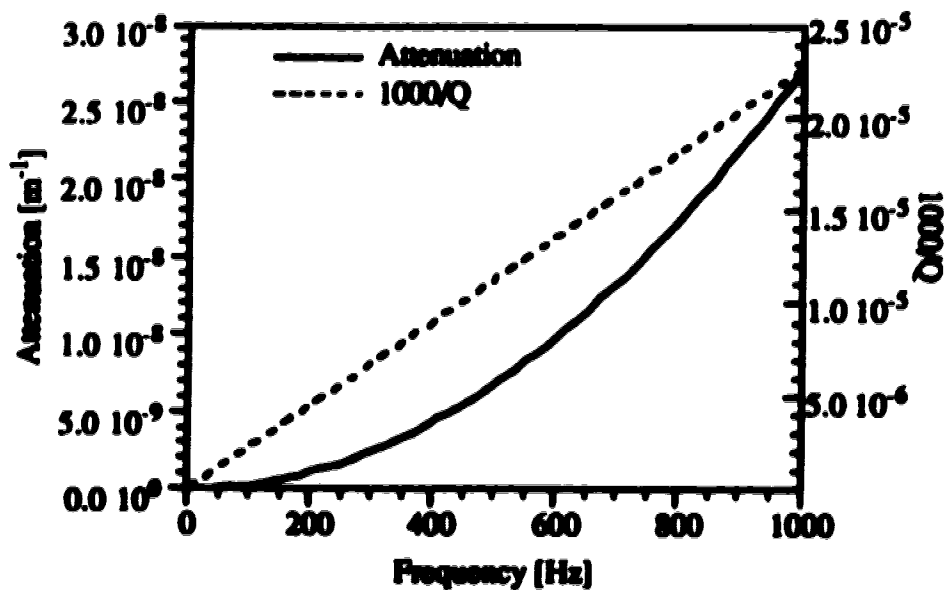


Figure 4.7 Attenuation and inverse Q versus frequency for the 1st P wave. Inverse Q exhibits an approximate linear relationship versus frequency. The saturating fluid is air.

The attenuation and $1000/Q$ of the 1st S wave as a function of frequency for the water, bitumen and air filled cases are presented in figure 4.8, figure 4.9 and 4.10 respectively. The frequency dependence of the 1st S wave is similar to the 1st P wave and the mechanisms responsible in each case are the same as discussed for the 1st P wave. However, for shear waves the bulk viscosity, ξ_r , does not contribute to the attenuation. Although the mechanisms responsible are the same and the frequency dependence is similar, it is interesting to calculate the ratio of $1000/Q$ for the 1st S wave to $1000/Q$ for the 1st P wave. In the water filled case a large ratio, ~ 13 , is obtained whereas in the air filled case the ratio is ~ 1 and in the bitumen case the ratio is small at ~ 0.7 .

The attenuation and $1000/Q$ of the 2nd P wave as a function of frequency for the bitumen case is presented in figure 4.11. The frequency dependence of the attenuation is different than the 1st P and S wave; however, the $1000/Q$ still increases in a linear fashion with increasing frequency. For the case of the water (figure 4.12) filled porous medium the $1000/Q$ of the 2nd P wave is different in that it decreases in an approximate linear fashion with increasing frequency. In the air filled case (figure 4.13) $1000/Q$ of the 2nd P wave also decreases with increasing frequency, but the overall change over the frequency range considered is very small. For the water and air filled samples the fluid and solid are not viscously coupled as opposed to the bitumen sample. This coupling is the cause for the different behavior observed in $1000/Q$. In comparing attenuation and $1000/Q$ it should be remembered that the 2nd P-wave is dispersive.

Introducing thermomechanical coupling into the problem does not affect the rotational waves. The phase velocities of the four different dilatational waves are presented in table 4.11. Upon comparison of these phase velocity values with those without thermal effects, i.e. table 4.10, it is evident that thermomechanical coupling has little influence on the phase velocities for the models considered in the frequency range of 0-1000 Hz. The attenuation of the 1st and 2nd P wave is increased by less than 1%.

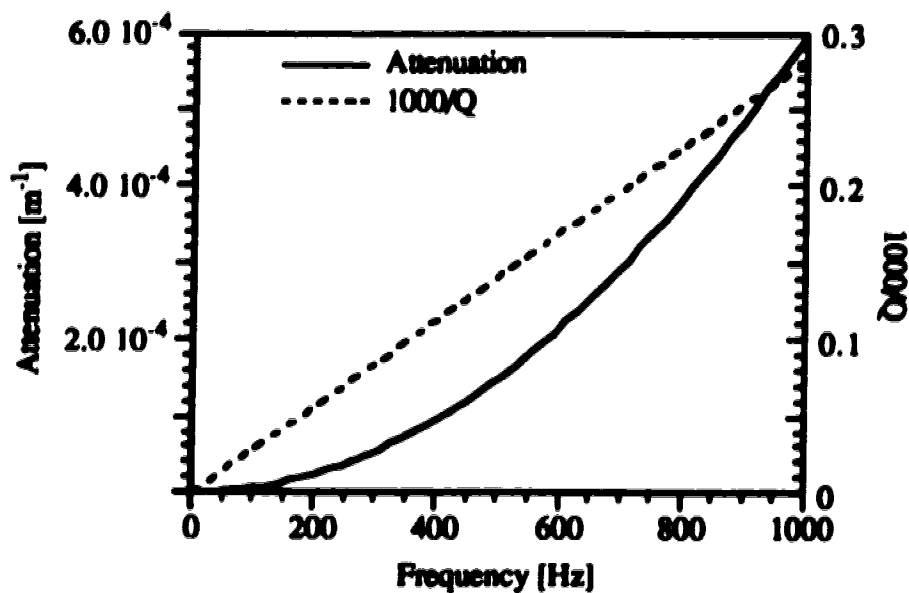


Figure 4.8 Attenuation and inverse Q versus frequency for the 1st S wave. Inverse Q exhibits an approximate linear relationship versus frequency and is about an order of magnitude larger than the 1st P wave. The saturating fluid is water.

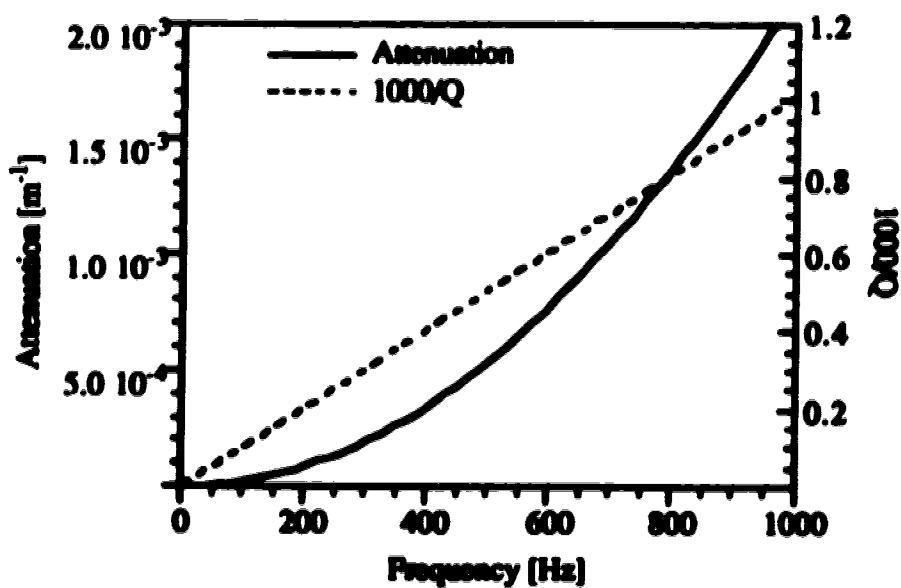


Figure 4.9 Attenuation and inverse Q versus frequency for the 1st S wave. Inverse Q exhibits an approximate linear relationship versus frequency and is the same order of magnitude as the 1st P wave. The saturating fluid is bitumen.

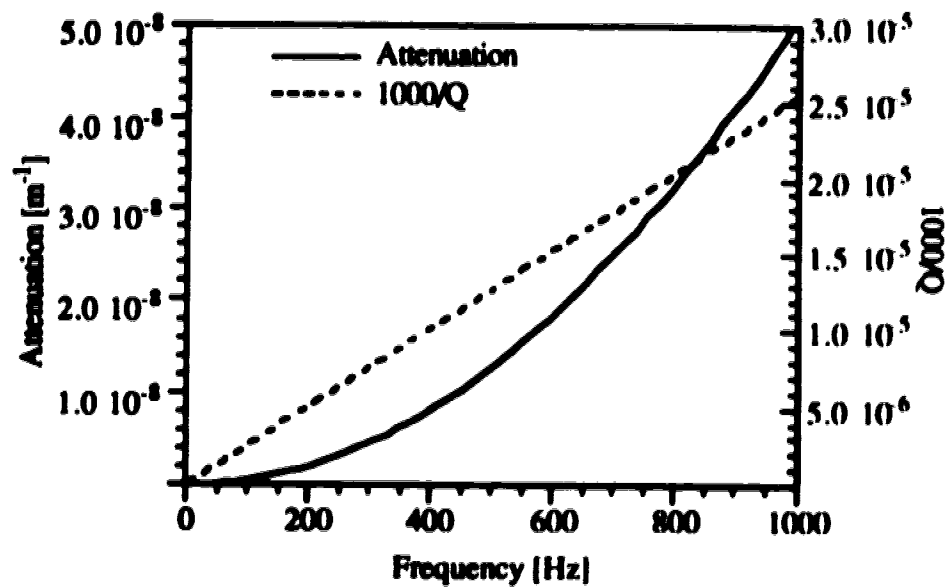


Figure 4.10 Attenuation and inverse Q versus frequency for the 1st S wave. Inverse Q exhibits an approximate linear relationship versus frequency and is the same order of magnitude as the first P wave. The saturating fluid is air.

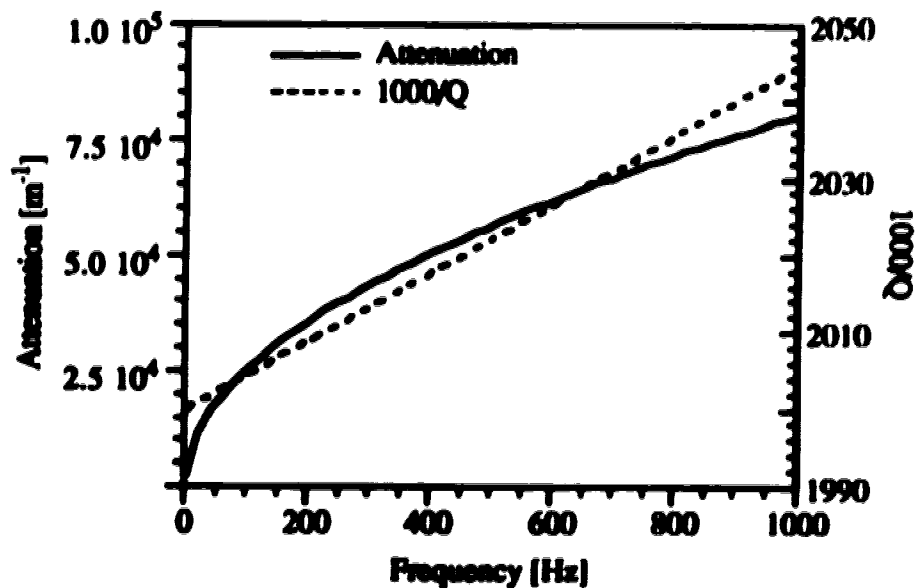


Figure 4.11 Attenuation and inverse Q versus frequency for the 2nd P wave. Inverse Q exhibits an approximate linear relationship versus frequency. The saturating fluid is bioeman.

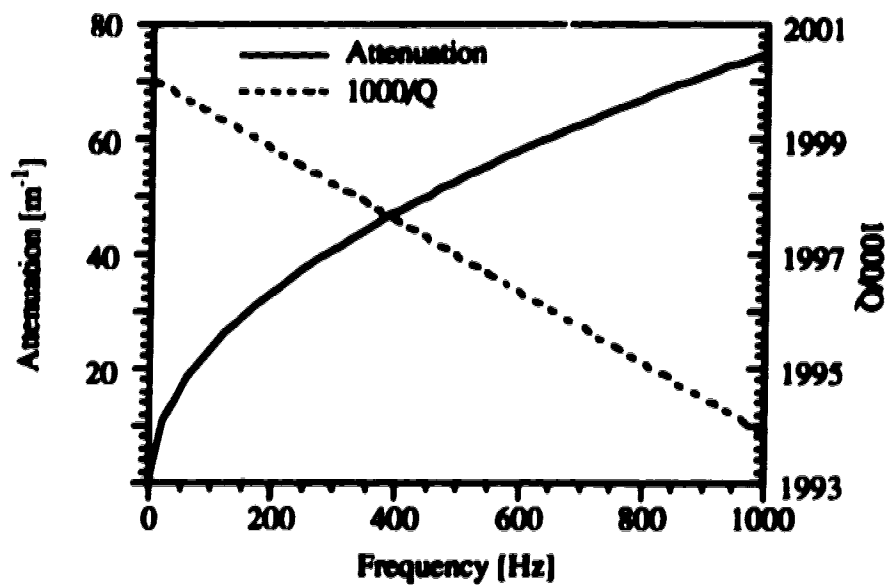


Figure 4.12 Attenuation and inverse Q versus frequency for the 2nd P wave. Attenuation increases with frequency as is expected, however, inverse Q, remains approximately constant with increasing frequency. The saturating fluid is water.

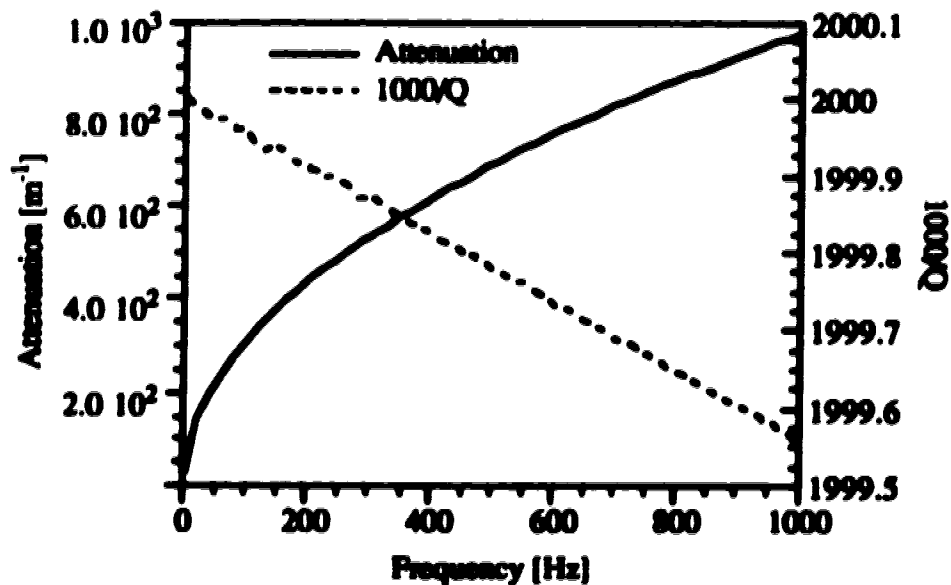


Figure 4.13 Attenuation and inverse Q versus frequency for the 2nd P wave. Inverse Q exhibits a linear relationship versus frequency. The saturating fluid is air.

Fluid	1st P wave (m/s)	2nd P wave (m/s)	3rd P wave (m/s)	4th P wave (m/s)
Water	2857.3	[0.1-26.6]	0.6	[0.003-0.05]
Air	2618.9	[0.2-6.5]	133.3	[0.006-0.20]
Bitumen	2807.3	[0.005-0.2]	0.7	0.003-0.08]

Table 4.11 Phase velocities for the various seismic P waves propagating through a porous medium saturated with the specified fluid when thermomechanical coupling is included. If the mode is significantly dispersive, the numbers in parentheses are the range of phase velocities for a frequency range 1 - 1000 Hz.

Bulk viscosity was introduced formally into the equations of de la Cruz & Spanos (1989b) in section 4.3. It does not affect the rotational waves but it should contribute significantly to the attenuation of the dilatational waves. The significance of bulk viscosity in a water filled sample is illustrated figure 4.14 which shows attenuation as a function of frequency for various ratios of bulk to shear viscosities. The effect of bulk viscosity is minimal for such a model but it does appear for large ratios and is larger at higher frequencies. This small effect of bulk viscosity is due to the fact that water is fairly incompressible and since it has a small shear viscosity it may flow before it actually compresses. In the case where the fluid is highly viscous, as for bitumen (figure 4.15), although it is fairly incompressible its viscosity impedes it from flowing and the effect of bulk viscosity is much larger. To further illustrate the coupling between flow and the effects of bulk viscosity, figure 4.16 is a graph of normalized attenuation versus the ratio of bulk to shear viscosity for various permeabilities. Normalization is carried out with respect to the attenuation when the bulk viscosity is assumed to be zero. As the flow is restricted, i.e. small permeabilities, the attenuation increases as the ratio of bulk to shear viscosity increases.

The compressibility of the frame also has an effect on the role which bulk viscosity plays. Figure 4.17 is a graph of normalized attenuation versus the ratio of bulk to shear viscosity for various values of drained bulk moduli. In this graph "unconsolidated" refers to a low value of drained bulk modulus, the actual value is the one presented in table 4.6,

and "highly consolidated" is a drained bulk modulus equal to the weighted by volume fraction of the solid component ($K_{bc} = (1 - \eta_s)K_s$). As the frame becomes more compressible, the fluid must support more of the deformation as the wave passes and will therefore compress by a greater amount and due to the bulk viscosity the attenuation will increase. This is illustrated in figure 4.17 by an increase in attenuation with decreasing drained bulk modulus. The change in attenuation due to the extra compressibility of the frame is much smaller than the effect of restricting the fluid shown in figure 4.16.

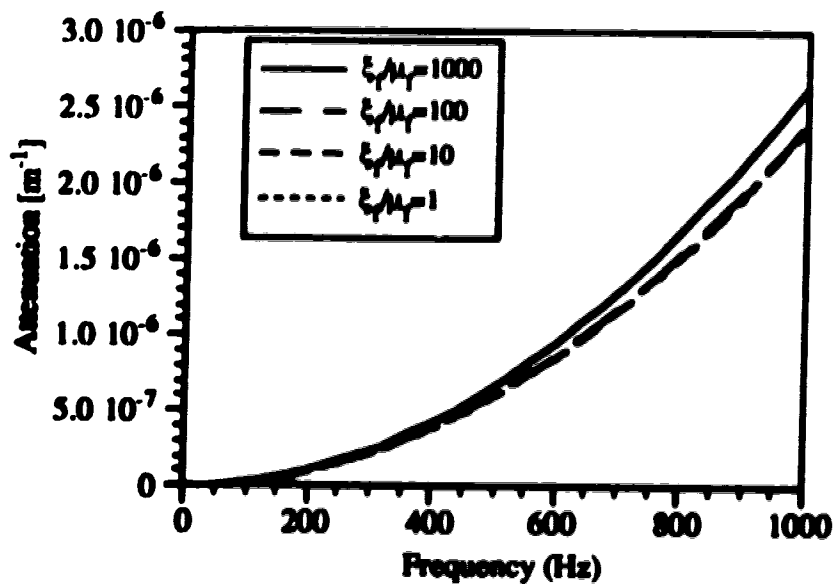


Figure 4.14 Attenuation versus frequency for the 1st P wave for several ratios of bulk viscosity to shear viscosity. Water has a measured viscosity ratio of 2.3.

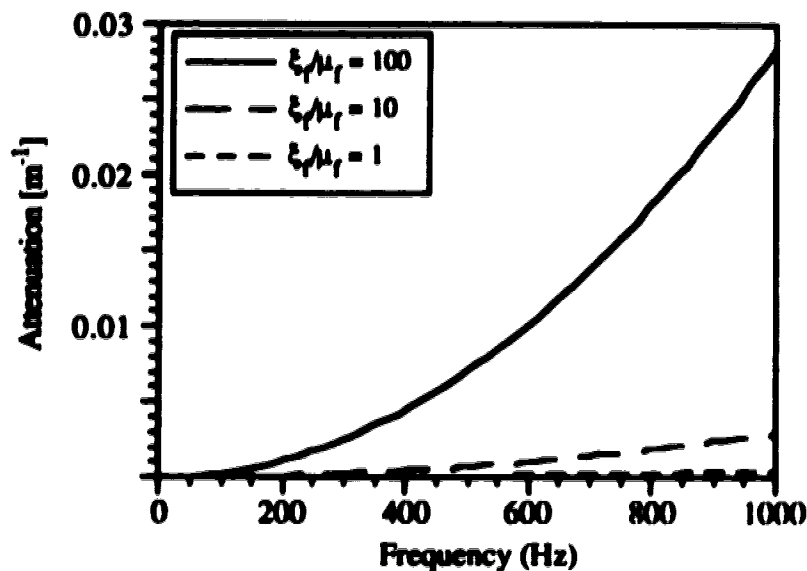


Figure 4.15 Attenuation versus frequency for the 1st P wave for several ratios of bulk viscosity to shear viscosity. The effect of bulk viscosity is much larger than for water case. Bitumen has a measured ratio of 5 but is strongly temperature dependent.

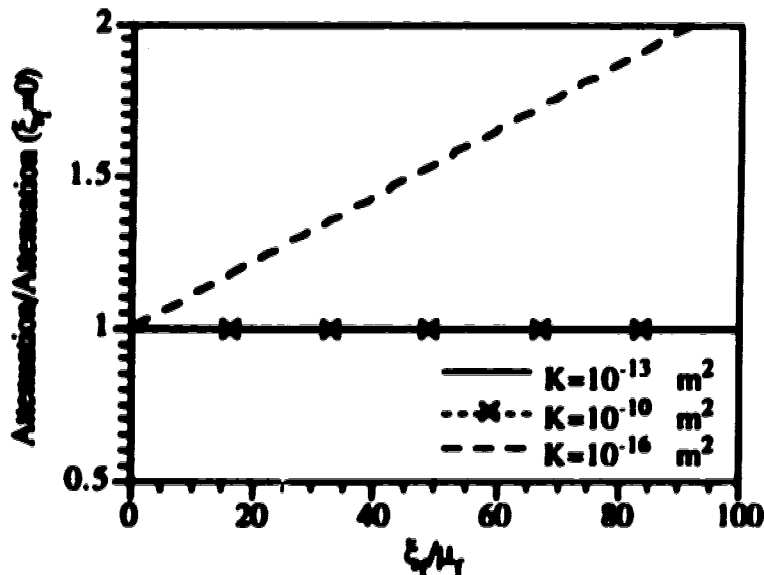


Figure 4.16 Normalized 1st P wave attenuation versus ratio of bulk viscosity to shear viscosity for three different permeabilities. Bulk viscosity effects become important at very low permeabilities. Frequency is 100 Hz and the saturating fluid is water.

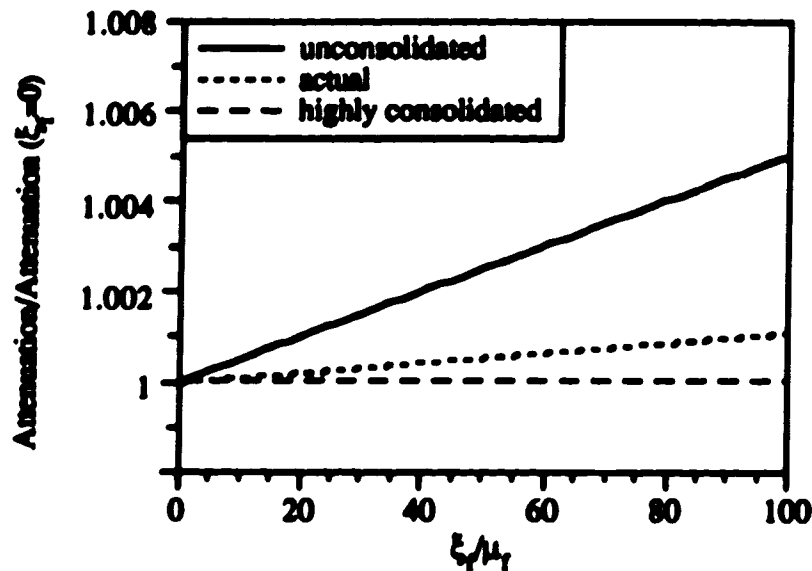


Figure 4.17 Normalized 1st P wave attenuation versus ratio of bulk viscosity to shear viscosity for three different values of drained bulk modulus, K_{b0} . Changes in attenuation due to bulk viscosity are greater in materials with small values of K_{b0} . Frequency is 100 Hz and the saturating fluid is water.

The generalization to the macroscopic shearing of a porous medium and the introduction of a material shear modulus was conducted in section 4.4. As a consequence of this generalization, there appeared an additional term in the equation of motion for the fluid which only vanishes if $\mu_M = (1 - \eta_0)\mu_s$; and it should contribute to attenuation of the waves. The introduction of the material shear modulus affects both dilatational and rotational waves. The phase velocity and attenuation, as a function of normalized material shear modulus, of the 1st P wave, 1st S wave and 2nd P wave propagating in a water filled sample are presented in figures 4.18, 4.19 and 4.20 respectively. The phase velocity of the 1st P wave and 1st S wave increases dramatically with increasing material shear modulus. The increase in the phase velocity of the 2nd P wave is less substantial. The attenuation of the 1st P wave exhibits a minimum in the low material shear modulus regime and increases continually afterwards. Given that the saturating fluid is water, the attenuation is controlled by the relative motion of the fluid and solid. Making the solid more rigid will cause larger relative motion between the component phases thereby increasing the attenuation of the 1st P wave. The attenuation of the 1st S wave increases with decreasing material shear

modulus. In the low material shear modulus regime the attenuation increases very rapidly, which is not surprising since this mode must vanish as the shear strength of the material vanishes. The attenuation of the 2nd P wave also increases with decreasing material shear modulus; however the increase is not as rapid as the 1st S wave.

The 1st S wave attenuation versus frequency for three values of material shear modulus is presented in figure 4.21. The associated $1000/Q$ is shown in figure 4.22. Here "rigid" refers to material shear modulus value equal to a weighted by volume of the solid portion ($\mu_M = (1-\eta_0)\mu_s$), "actual" is the value in table 4.6, and "compliant" refers to a small value of material shear modulus. The attenuation of the 1st S wave increases with frequency but much larger increases are observed for a compliant sample. Quite interesting is the behavior of $1000/Q$. Although the attenuation is a strong function of material shear modulus, $1000/Q$ increases with frequency but does not appear to have the material shear modulus dependence.

Saturating the porous sample with a viscous fluid reduces the amount of relative motion between phases and the dominant attenuation mechanism changes. Figure 4.23 shows the phase velocity and attenuation of the 1st P wave as a function of normalized material shear modulus for a bitumen filled sample. The phase velocity dependence on material shear modulus is quite similar to the water filled case (figure 4.18). The attenuation, however, is much different. For the bitumen case, the attenuation decreases with increasing material shear modulus which is opposite to what occurs for the water filled case. As mentioned previously, for a bitumen filled sample, the fluid and solid are locked together. By increasing the material shear strength there is less shear deformation and therefore less shearing of the fluid which in turn would cause a reduction in attenuation. The presence of a viscous saturating fluid on the 1st S wave is illustrated by a graph of attenuation and phase velocity versus normalized material shear modulus (figure 4.24). The dependence of phase velocity on material shear modulus is the same as in the water filled case (figure 4.19). The attenuation as a function of material shear modulus is also the same as in the water filled case, i.e. increases with decreasing material shear modulus. However, for the bitumen filled case, the attenuation increase at low material shear modulus is much faster.

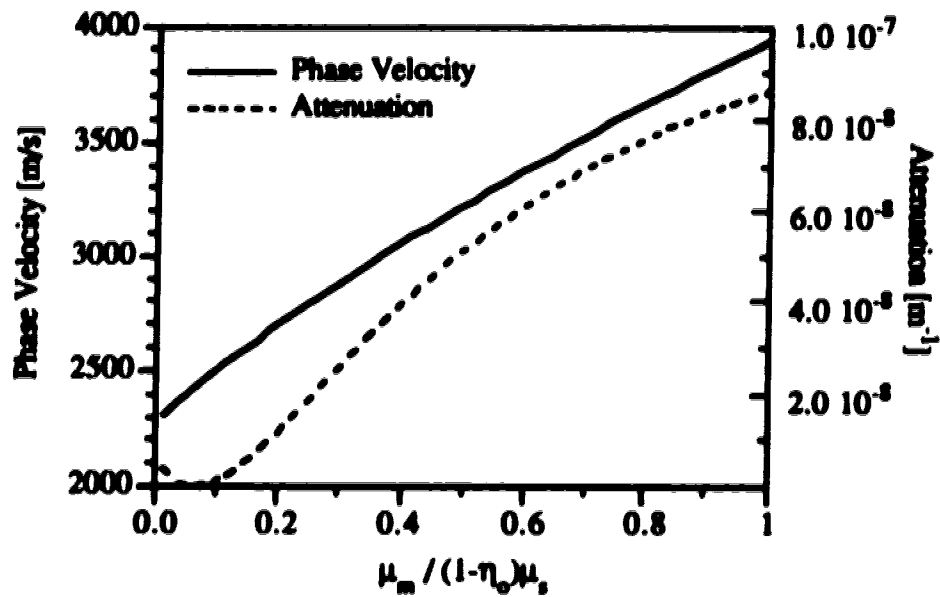


Figure 4.18 Phase velocity and attenuation of the 1st P wave versus a normalized material shear modulus. Saturating fluid is water and the frequency is 100 Hz.

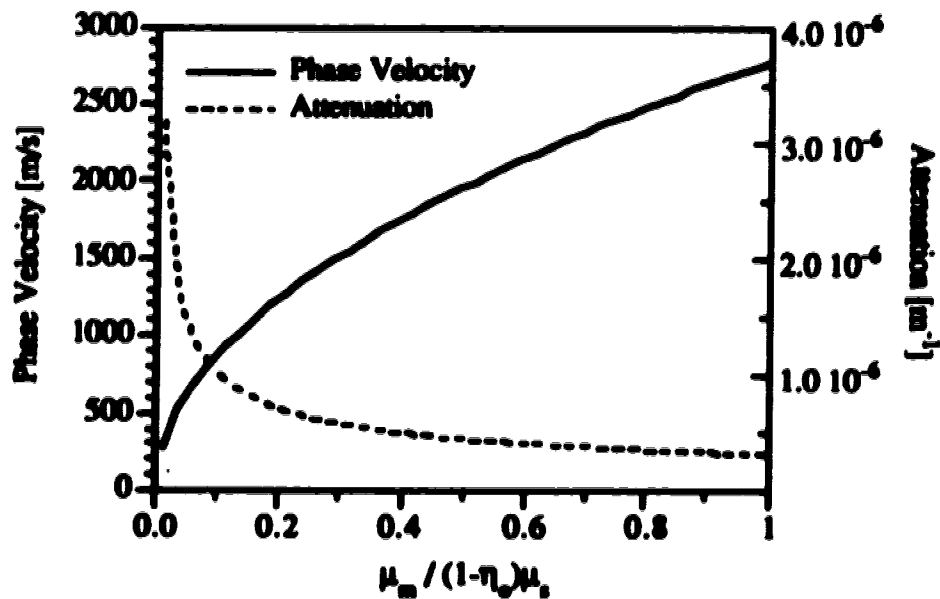


Figure 4.19 Phase velocity and attenuation of the 1st S wave versus a normalized material shear modulus. Saturating fluid is water and the frequency is 100 Hz.

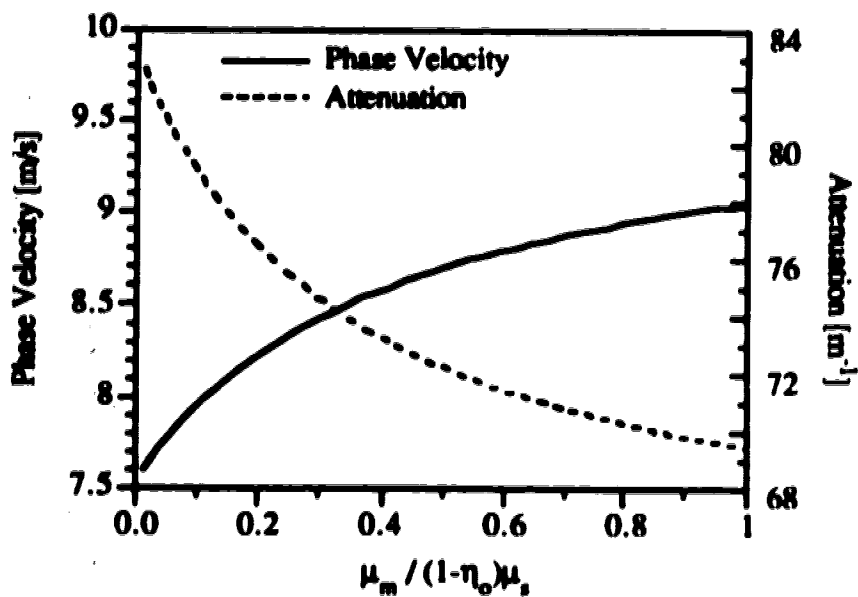


Figure 4.20 Phase velocity and attenuation of the 2nd P wave versus normalized material shear modulus. The saturating fluid is water and the frequency is 100 Hz.

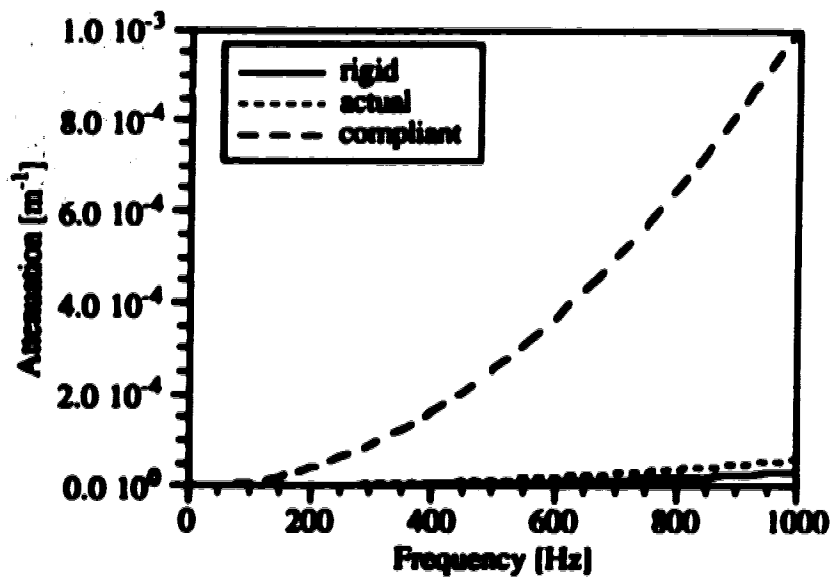


Figure 4.21 Attenuation of the 1st S wave versus frequency for three different values to material shear modulus, μ_M . The saturating fluid is water.

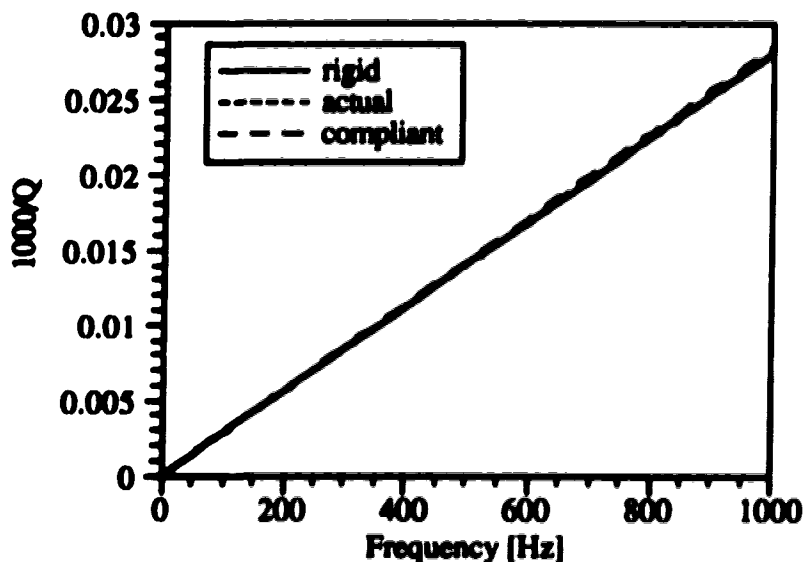


Figure 4.22 Inverse Q of the 1st S wave versus frequency for three different values to material shear modulus, μ_M . Inverse Q exhibits an approximate linear relationship versus frequency and is independent of the values of μ_M . The saturating fluid is water.

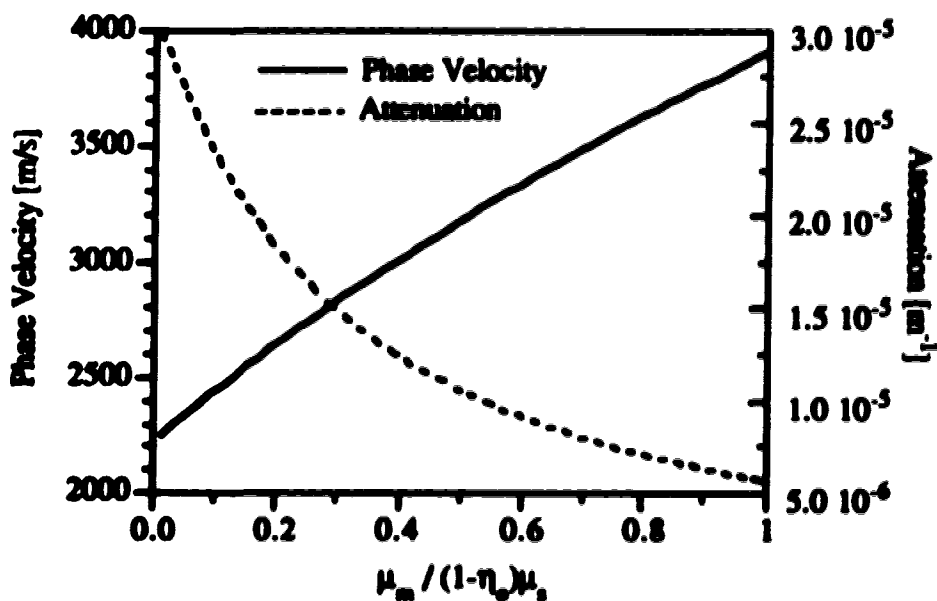


Figure 4.23 Phase velocity and attenuation of the 1st P wave versus a normalized material shear modulus. Phase velocity increases and the attenuation decreases as the frame becomes more rigid. Saturating fluid is bitumen and frequency is 100 Hz.

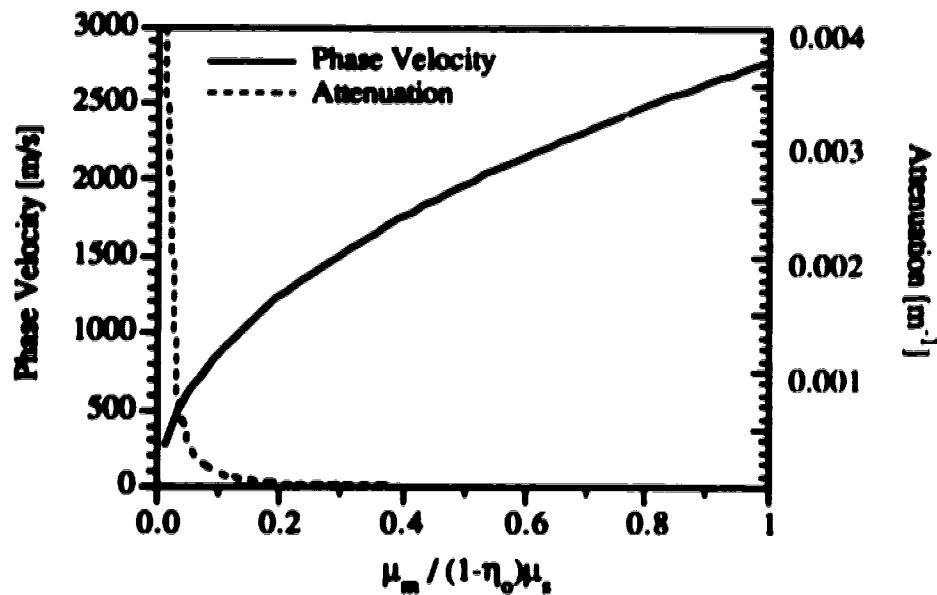


Figure 4.24 Phase velocity and attenuation of the 1st S wave versus a normalized material shear modulus. Phase velocity increases and the attenuation tends to zero as the frame becomes more rigid. Saturating fluid is bitumen and the frequency is 100 Hz.

In order to obtain a complete set of equations describing the propagation of dilatational waves de la Cruz & Spanos (1989b) introduced

$$\frac{\partial \eta}{\partial t} = \delta_s \nabla \cdot \bar{v}_s - \delta_r \nabla \cdot \bar{v}_r$$

where δ_s and δ_r are dimensionless empirical parameters. It was argued (see section 4.8) that such a relation is a process dependent statement and suitable values of δ_s and δ_r will depend on the process considered. Previous numerical studies (Hickey, 1990) have constrained δ_s and δ_r to a narrow range of values on the basis that the theory yield solutions for waves with positive attenuation. In chapter 3, the quasi-static deformation of porous media was described and expressions for δ_s and δ_r in terms of two bulk moduli were obtained (see section 4.7). If the porous medium behaves rather uniquely in an unjacketed test, then only one macroscopic bulk measurement is required. This measurement is usually a drained bulk modulus measurement.

Assuming this unique unjacketed behavior, the sensitivity of the phase velocity and attenuation of the 1st P wave and 2nd P wave to variation of values obtained from drained static experiments, as estimates for δ_s and δ_f , are presented in figures 4.25 and 4.26 respectively. The drained bulk modulus has been normalized by volume fraction times solid component bulk modulus, and the ratio corresponding to the actual measured K_{bc} is about 0.2. The phase velocity of the 1st P wave increases with increasing drained bulk modulus in a near linear fashion. The 1st P wave attenuation shows a minimum in the low drained bulk modulus regime and then increases with increasing drained bulk modulus. This type of 1st P wave attenuation dependence was previously noted for variations in material shear modulus (figure 4.18). The 2nd P wave attenuation decreases and the phase velocity increases when the drained bulk modulus increases. The attenuation of the 1st P wave as a function of frequency for three different values of drained bulk modulus is shown in figure 4.27. The attenuation increases with frequency as usual but the overall increase over the chosen frequency range is much larger for higher values of drained bulk modulus. No variation in 1st P wave velocity with frequency is observed for the three different values of drained bulk modulus.

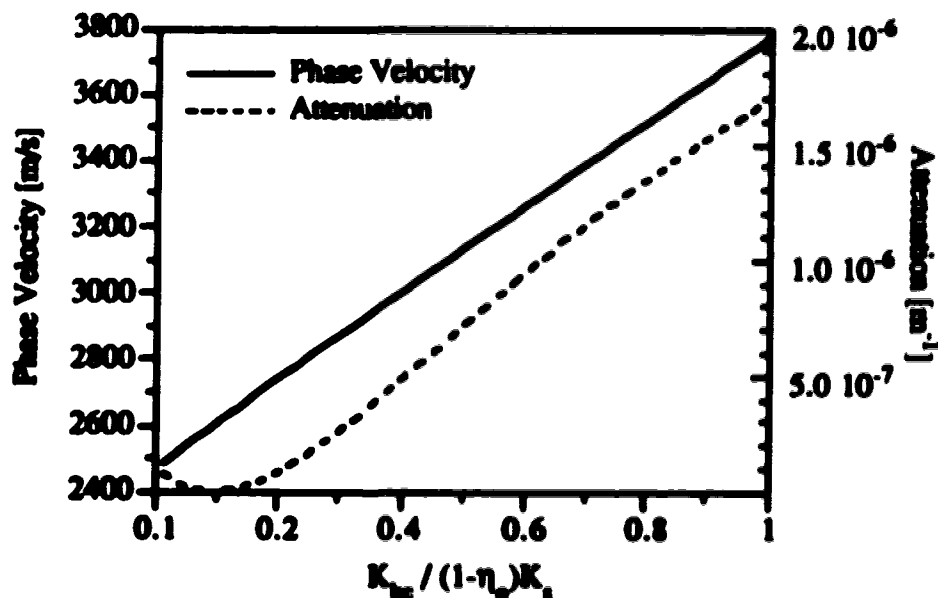


Figure 4.25 Phase velocity and attenuation of the 1st P wave versus a normalized drained bulk modulus. Phase velocity increases (~linear) as a function of drained bulk modulus. The attenuation has a minimum in the compressible regime. Saturating fluid is water and the frequency is 100 Hz.

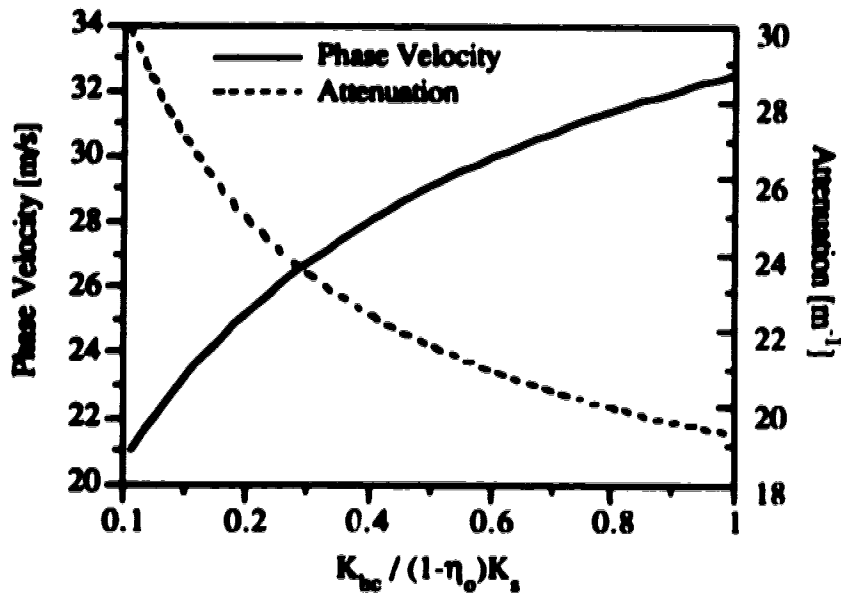


Figure 4.26 Phase velocity and attenuation of the 2nd P wave versus a normalized drained bulk modulus for a frequency of 100 Hz. Saturating fluid is water and the frequency is 100 Hz.

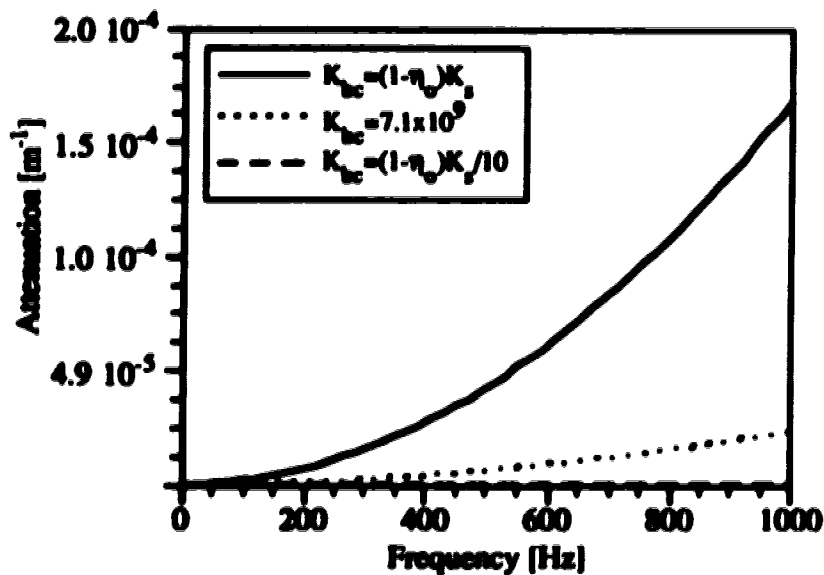


Figure 4.27 Attenuation versus frequency for the 1st P wave for several values of drained bulk modules. The largest increase in attenuation corresponds to the largest value of drained bulk modules. The saturating fluid is water.

The presence of a viscous saturating fluid changes the dependence of the attenuation on drained bulk modulus. Figure 4.28 shows the phase velocity and attenuation of the 1st P wave as a function of the normalized drained bulk modulus. Again the phase velocity increases approximately linearly with increasing drained bulk modulus. The attenuation dependence is considerably different, as compared to the water filled case, in that it decreases with increasing drained bulk modulus. Again, this change in attenuation dependence when the saturating fluids are changed is very similar to what occurred with the material shear modulus as previously discussed above. It is not totally surprising that some similarities exist in the dependencies of the P wave phase velocity and attenuation on material shear modulus and drained bulk modulus.

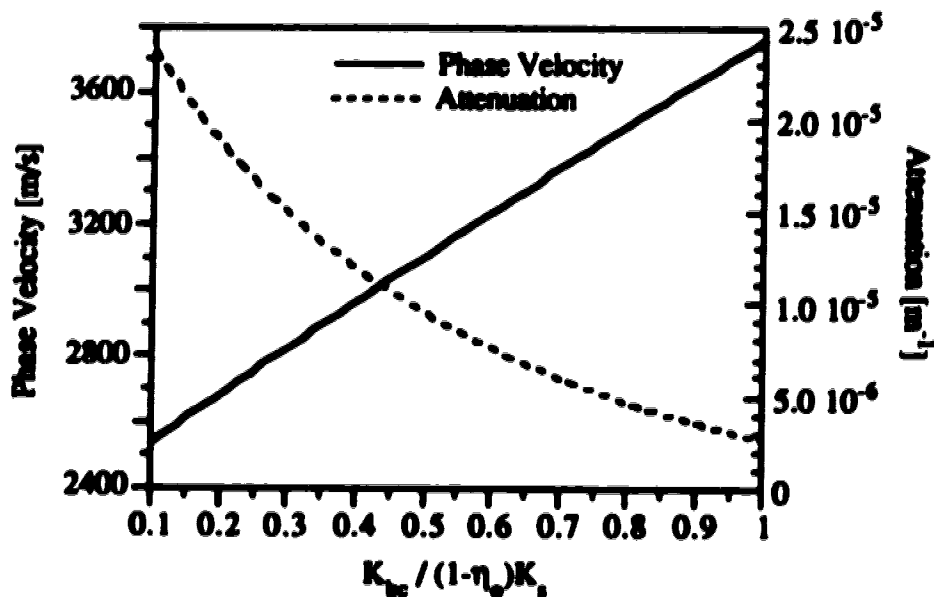


Figure 4.28 Phase velocity and attenuation of the 1st P wave versus a normalized drained bulk modulus. Phase velocity increases (~linear) and the attenuation decreases as the frame becomes less compressible. Saturating fluid is bitumen and the frequency is 100 Hz.

In the above calculations of δ_v and δ_r using the drained bulk modulus, it was assumed that the material deformed during an unjacketed experiment such that the measured value of the bulk modulus would simply equal the bulk modulus of the solid component phase. The use of such an assumption greatly reduces the problem of obtaining values for δ_v and δ_r . It

is therefore of interest to examine the sensitivity of the P waves to variations ofunjacketed bulk modulus. Figure 4.29 illustrates the dependence of the 1st P wave phase velocity and attenuation to variations in unjacketed bulk modulus. A lower bound on the unjacketed bulk modulus is required which is

$$K_{bc} \leq (1-\eta_o)K_{unj} . \quad (4.77)$$

The phase velocity decreases when the unjacketed bulk modulus decreases from a value equal to that of solid bulk modulus. The overall change in velocity over the range of unjacketed bulk modulus considered is about 10%. The attenuation behavior is more complex. Decreasing the unjacketed bulk modulus causes a small initial increase in attenuation. Decreasing the value of unjacketed bulk modulus to less than 50% its maximum causes a very fast decrease in attenuation. The 2nd P wave phase velocity and attenuation are shown as functions of unjacketed bulk modulus in figure 4.30. The phase velocity decreases when the unjacketed bulk modulus approaches the solid bulk modulus value. An overall change of about 20% is observed. It is interesting to note that increasing the unjacketed bulk modulus causes a decrease in the 2nd P wave velocity, but that increasing the drained bulk modulus causes an increase in phase velocity (figure 4.26). Similarly, the attenuation of the 2nd P wave increases as the unjacketed bulk modulus increases, whereas in figure 4.26, the attenuation decreases with increasing drained bulk modulus.

The dependence of the phase velocity and attenuation of the 1st P wave on unjacketed bulk modulus when the saturating fluid is highly viscous, i.e. bitumen, is shown in figure 4.31. The phase velocity dependence is similar to the water filled case (figure 4.29). The attenuation decreases with increasing unjacketed bulk modulus. This dependence is opposite to what is observed in figure 4.29 for a water filled sample. This dramatic change in attenuation dependence when the viscosity of the fluid is changed has also been observed for the drained bulk modulus and the material shear modulus and the same explanation may be used here.

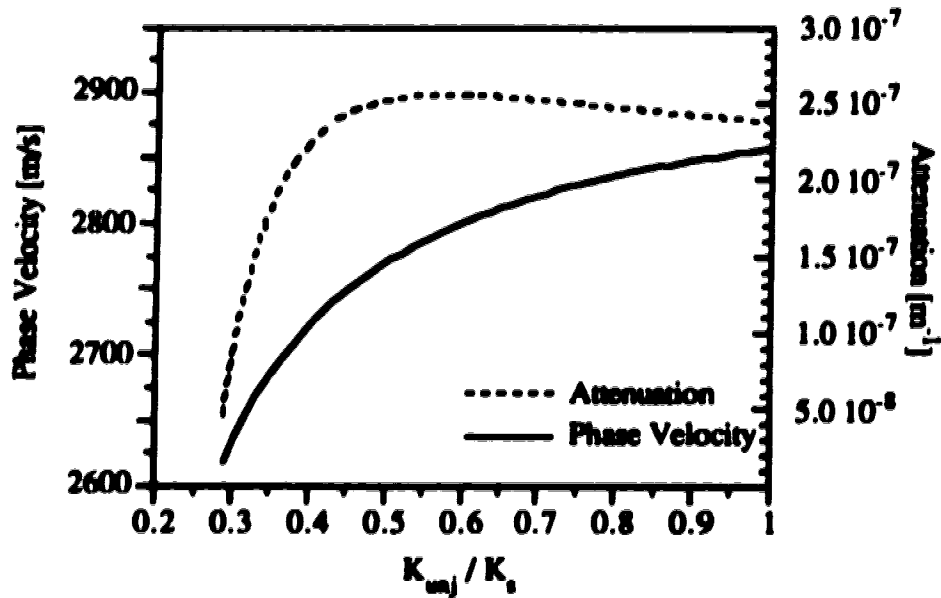


Figure 4.29 Phase velocity and attenuation of the 1st P wave versus normalized unjacketed bulk modulus. The saturating fluid is water and frequency is 100 Hz.

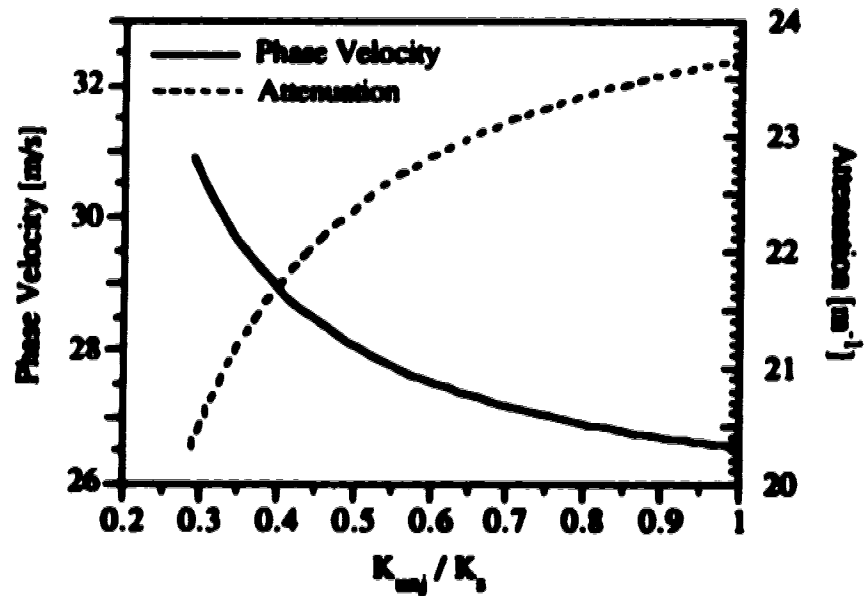


Figure 4.30 Phase velocity and attenuation of the 2nd P wave versus normalized unjacketed bulk modulus. The saturating fluid is water and frequency is 100 Hz.

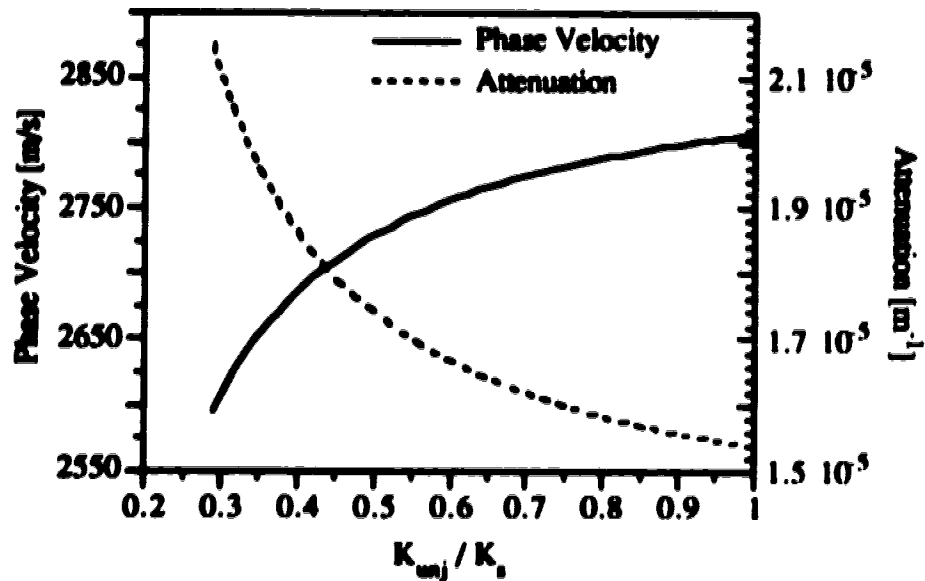


Figure 4.31 Phase velocity and attenuation of the 1st P wave versus normalized unjacketed bulk modulus. The saturating fluid is bitumen and frequency is 100 Hz.

The permeability, K , is a parameter which enters the theory through an area integral expansion that was discussed in section 4.5. It appears in the coefficient which represents the momentum transfer between the fluid and solid across the solid-fluid interfaces during wave propagation. Given the condition that the wavelength of disturbance be orders of magnitude larger than the pore scale, de la Cruz & Spanos (1985, 1989b) suggest that the permeability value obtained through a Darcy experiment might be used as an estimate for the parameter K . Biot (1956c) and others also discussed the notion that fluid-flow through a porous medium could deviate from Poiseuille type flow during the passage of a seismic wave and therefore a constant Darcy permeability would not always be appropriate. The Biot theory was divided into two regimes, a high and a low frequency regime. In the low frequency regime (Biot, 1956b) the fluid-flow is Poiseuille type and the Darcy permeability is adequate. In the high frequency regime (Biot, 1956c), the fluid-flow is not of the Poiseuille type and the Darcy permeability is not adequate. In order to quantify the separation of these two regions a "viscous penetration depth" (Warner, 1986) is defined as

$$\delta = \left(\frac{2\mu_f}{\rho_f \omega} \right)^{\frac{1}{2}} \quad (4.77)$$

It is argued that the fluid is viscously locked to the solid matrix if it is within a distance less than a viscous penetration depth from the pore wall. The critical frequency separating the two regimes, defined as the frequency at which the viscous penetration depth is equal to one pore radii, is given by

$$\omega_c = \frac{2\mu_f}{\rho_f R^2} \quad (4.78)$$

where R is a typical pore radius. For frequencies larger than the critical frequency the viscous penetration depth becomes smaller than the pore radius. The fluid-flow will then deviate from Poiseuille flow and the Darcy permeability cannot be used.

Numerical illustrations of the permeability dependence of the phase velocity and attenuation of the 1st P wave and 1st S wave are shown in figures 4.32 and 4.33 respectively. For this water filled case, a maximum in attenuation of the 1st P and 1st S wave is observed for a permeability near 10^{-10} m^2 . The phase velocity of these waves experience the greatest rate of change near this permeability value. The change in phase velocity of the 1st P wave between the high and low permeability limits is less than 1%. The phase velocity of the 1st S wave is about 5% larger in the high permeability regime. The maximum in attenuation and abrupt changes in velocity corresponds to a permeability (being proportional to R^2) value which makes the critical frequency approximately the same as the disturbance, i.e. 100 Hz. Therefore, according to Biot (1956c) the fluid-flow is not of the Poiseuille type for permeability values greater than 10^{-10} m^2 and the Darcy permeability is not adequate. In the more typical permeability range, 10^{-12} - 10^{-15} m^2 , which is within the low frequency regime for this particular sample the phase velocities are approximately constant and the attenuation increases with increasing permeability.

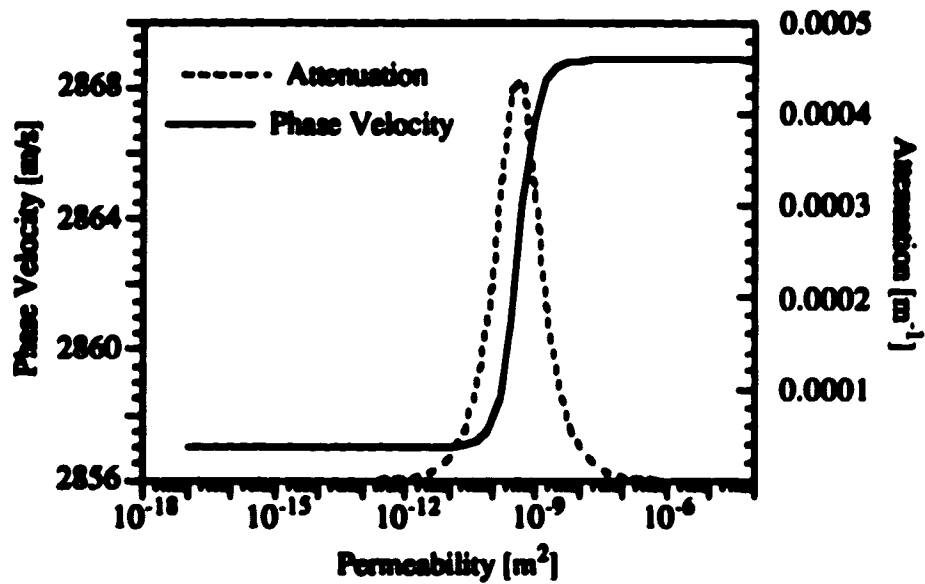


Figure 4.32 Phase velocity and attenuation of the 1st P wave versus permeability. The saturating fluid is water and the frequency is 100 Hz.

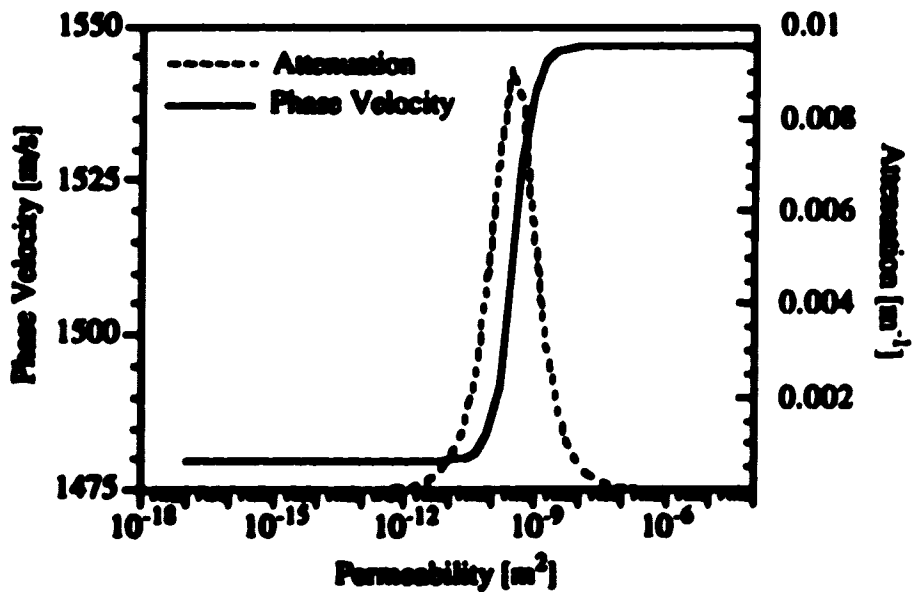


Figure 4.33 Phase velocity and attenuation of the 1st S wave versus permeability. The saturating fluid is water and the frequency is 100 Hz.

The phase velocity and attenuation of the 2nd P wave versus permeability for the water filled sample is shown in figure 4.34. The dependence on permeability is different than the 1st P wave (see figure 4.32). The 2nd P wave vanishes in the low permeability limit since its phase velocity tends to zero and its attenuation goes to infinity. This is because the solid and fluid are viscously locked together in the low permeability regime. A large increase in 2nd P wave phase velocity, on the order of 1000 m/s, occurs at a permeability of 10^{-10} m^2 . As mentioned previously, this permeability corresponds to the transition between Biot's low and high frequency regimes. For permeability values greater than 10^{-10} m^2 the solid and fluid are viscously uncoupled which allows for the propagation of the 2nd P wave.

The frequency / permeability effect on the crossover frequency as observed from phase velocity and attenuation of the 1st P wave is shown in figures 4.35 and figures 4.36. The magnitude of the change in phase velocity of the 1st P wave, associated with the mass coupling, is not altered by changing the frequency but the transition region is shifted to larger frequencies for smaller permeabilities as displayed in figure 4.35. Major changes in attenuation occur at large frequencies (figure 4.36) and decreasing the permeability causes the changes to move to higher frequencies. This behavior is simply due to the fact that lower permeabilities, and therefore small pores, requires higher frequencies for the fluid and solid to become decoupled.

Saturating the sample with a less viscous fluid, e.g air, causes the attenuation peak of the 1st P wave (figure 4.37) and 1st S wave (figure 4.38) to move to the larger permeability values 10^{-8} m^2 . Therefore, a crossover frequency of 100 Hz for the air filled sample requires a permeability of 10^{-8} m^2 . The change in 1st P wave phase velocity is smaller than in the water filled case. The phase velocity of the 1st S wave shows no discernible change. It should be noted that the crossover frequency as modelled by Biot (1956c) is controlled by the ratio of fluid viscosity to fluid density and not simply the fluid viscosity.

The numerical examples illustrating the importance of permeability shows two distinct regimes. These are better known as Biot's high and low frequency regimes and are characterized by different fluid-flow behavior. In the low frequency regime the fluid is viscously locked to the solid frame and therefore the phase velocities are lower due to the

additional drag force and higher effective mass. In the high frequency regime the fluid and solid are uncoupled thereby reducing the effective mass and as a consequence larger phase velocities are observed. Other recent models (Dvorkin & Nur, 1993) have been proposed which include local flow. These models predict very different frequency / permeability behavior. In the local flow models the transition in velocity from a low frequency regime to high frequency regime is related to relaxation of the fluid. In the high frequency regime there is insufficient time for the fluid pressure to equilibrate and the fluid is therefore in an unrelaxed state. Whereas in the low frequency regime the fluid pressure has sufficient time to equilibrate and the fluid is in a relaxed state. The characteristic frequency in these models is due to fluid relaxation and therefore it moves to higher frequencies with increasing permeability. This is the opposite as what has been shown here. However, the models do not contradict one another. One must remember that the values for compliances of the porous medium, i.e. δ_s , δ_f and μ_M , have been obtained from quasi-static measurements which do not incorporate relaxation. The relaxation phenomena in the work of Dvorkin & Nur (1993) can be accounted for in this work by altering the values of δ_s and δ_f . The macroscopic shear modulus will not be altered by the work of Dvorkin & Nur (1993).

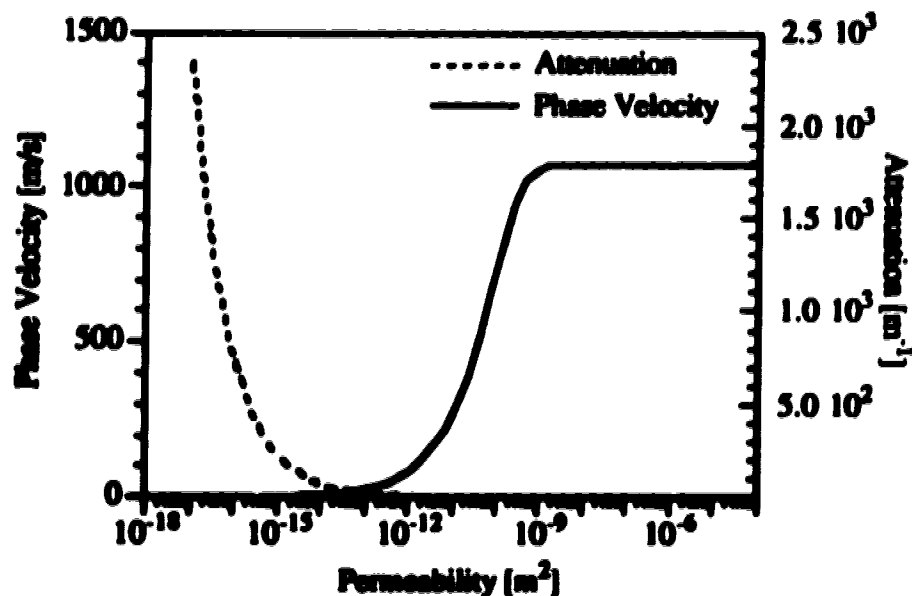


Figure 4.34 Phase velocity and attenuation of the 2nd P wave versus permeability. The saturating fluid is water and the frequency is 100 Hz.

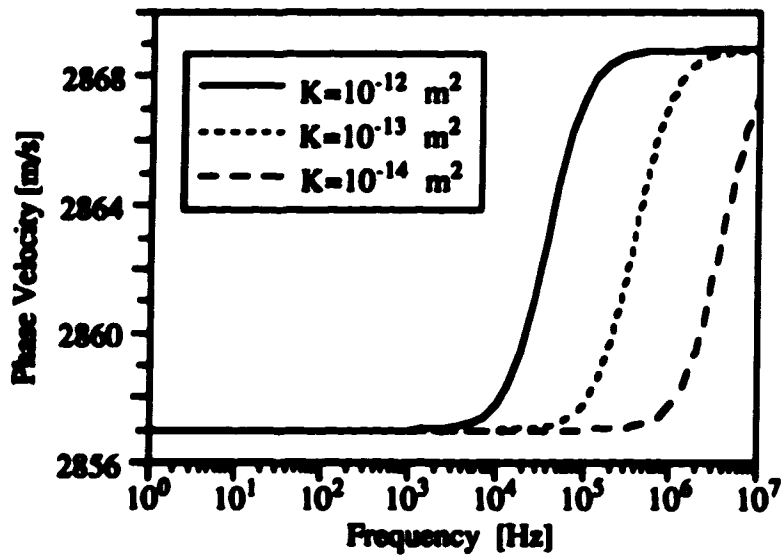


Figure 4.35 1st P wave phase velocity versus frequency for three values of permeability. Increasing the permeability moves the abrupt but small change in velocity to higher frequency. Water is the saturating fluid.

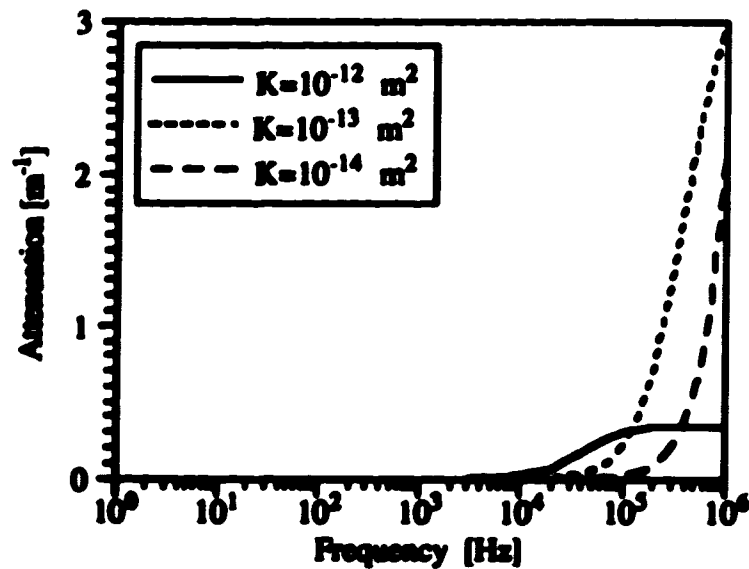


Figure 4.36 1st P wave attenuation versus frequency for three values of permeability. Increasing the permeability moves the change in attenuation to higher frequency. Water is the saturating fluid.

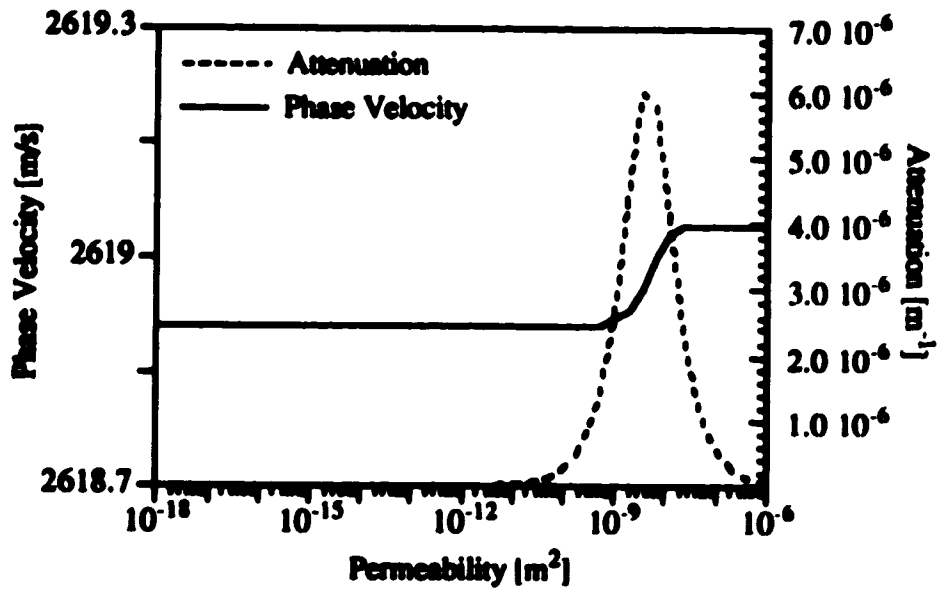


Figure 4.37 Phase velocity and attenuation of the 1st P wave versus permeability. The saturating fluid is air and the frequency is 100 Hz.

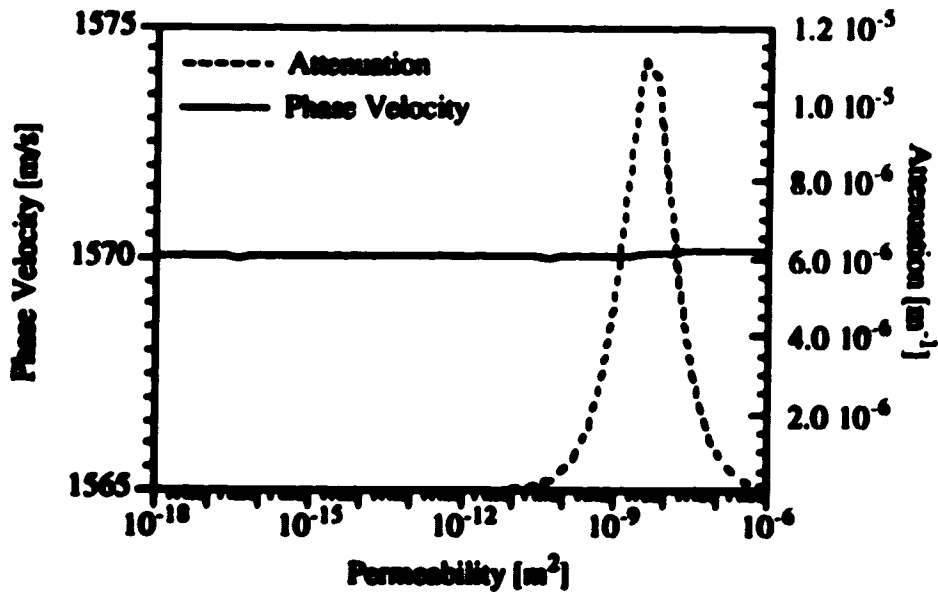


Figure 4.38 Phase velocity and attenuation of the 1st S wave versus permeability. The saturating fluid is air and the frequency is 100 Hz.

The induced mass coefficient is introduced to account for inertial coupling between phases. A large amount of work has been published which links the induced mass coefficient to a parameter characteristic of the solid frame, known as tortuosity (see section 4.5). In most cases this tortuosity parameter must be calculated from wave propagation data. Given the expressions developed in the literature for the induced mass coefficient it appears that a conservative range of values would be

$$-\eta_0 \rho_f \leq \rho_{12} \leq 0 \quad . \quad (4.78)$$

The 1st P wave phase velocity versus frequency is displayed in figure 4.39 for three different values of induced mass coefficient. The induced mass coefficient values correspond to the lower, median, and upper value of the above range (4.78). The phase velocity of the 1st P wave increases as the frequency exceeds 100 kHz. The increase is larger as the induced mass coefficient approaches zero. However, the actual change is less than 1%. The change in phase velocity occurs due to the uncoupling of the fluid and solid. For the frequencies below 100 kHz the solid and fluid are coupled together, the effective mass is large, which manifest itself in a low velocity. At frequencies larger than 100 kHz the solid and fluid become uncoupled, reducing the effective mass, and an increase in velocity is observed. The attenuation of the 1st P wave is displayed in figure 4.40. Similar to the phase velocity the attenuation increases as the frequency approaches the hundreds of kilohertz. The increase in attenuation is larger as the induced mass coefficient approaches zero. The magnitude of attenuation increases by a factor of five over the specified range (4.78) for a frequency of one megahertz.

The phase velocity and attenuation of the 1st S wave versus frequency for three values of induced mass coefficient are shown in figure 4.41 and 4.42 respectively. The phase velocity increases in the high frequency regime, and the increases are larger for values of induced mass coefficient closer to zero. The attenuation also increases in the high frequency regime. The attenuation at one megahertz is about five times larger for the induced mass coefficient equal to zero as compared to the lower bound of the induced mass coefficient. The phase velocity and attenuation of the 2nd P wave versus frequency for three values of induced mass coefficient are shown in figures 4.43 and 4.44 respectively. Decreasing the value of the induced mass coefficient causes a 20% increase in attenuation and a 30% increase in phase velocity at the higher frequency.

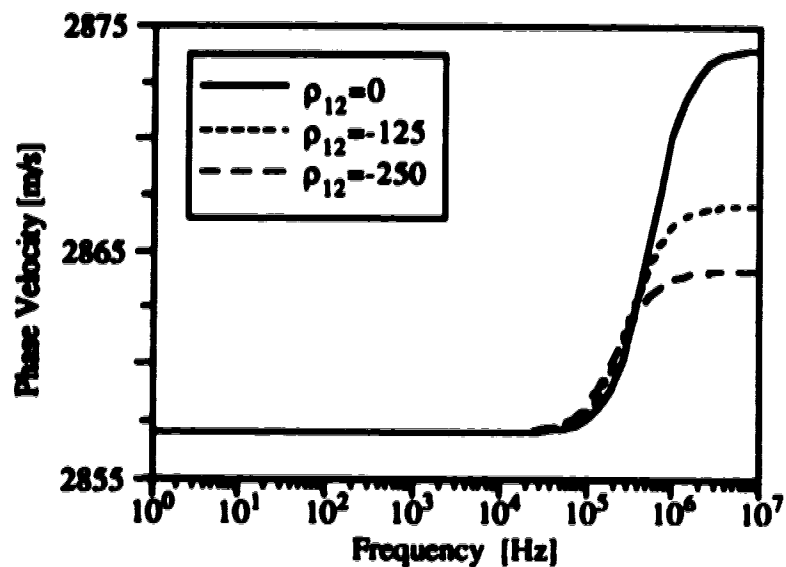


Figure 4.39 1st P wave phase velocity versus frequency for three values of induced mass coefficient. Phase velocity increases with increasing frequency reaching a maximum which is larger for smaller ρ_{12} (magnitude). Water is the saturating fluid.

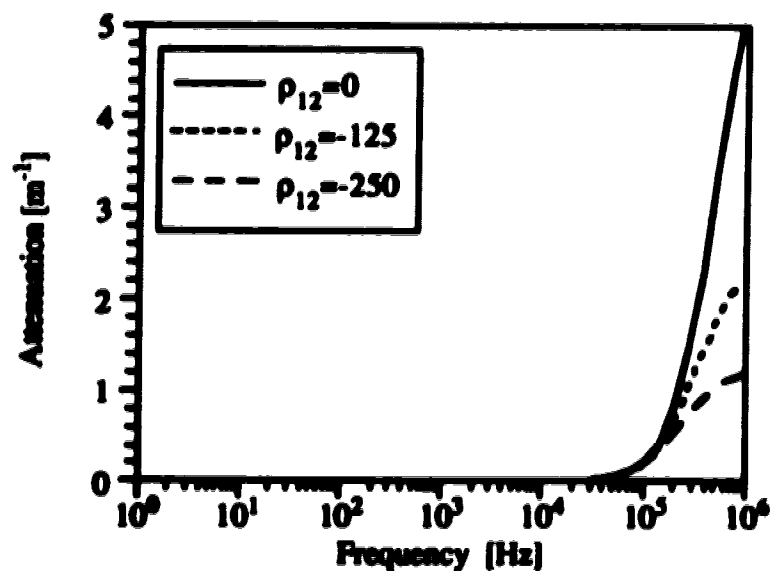


Figure 4.40 1st P wave attenuation versus frequency for three values of induced mass coefficient. Decreasing the magnitude of the induced mass coefficient causes a much larger increase in attenuation at higher frequency. Water is the saturating fluid.

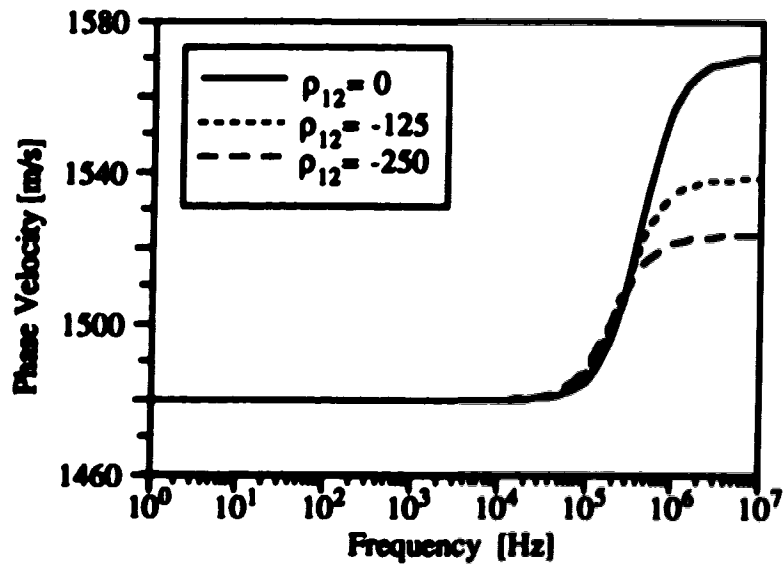


Figure 4.41 1st S wave phase velocity versus frequency for three values of induced mass coefficient. Phase velocity increases with increasing frequency reaching a maximum which is larger for smaller ρ_{12} (magnitude). Water is the saturating fluid.

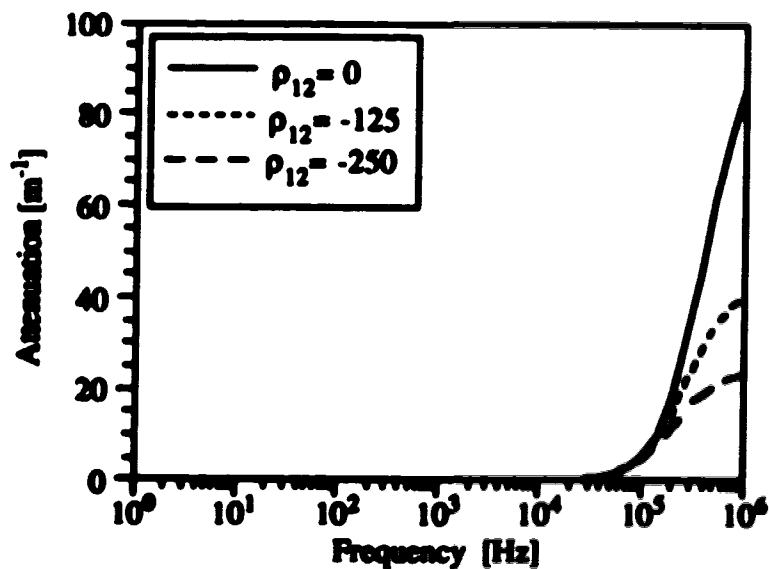


Figure 4.42 1st S wave attenuation versus frequency for three values of induced mass coefficient. Decreasing the magnitude of the induced mass coefficient causes a much larger increase in attenuation at higher frequency. Water is the saturating fluid.

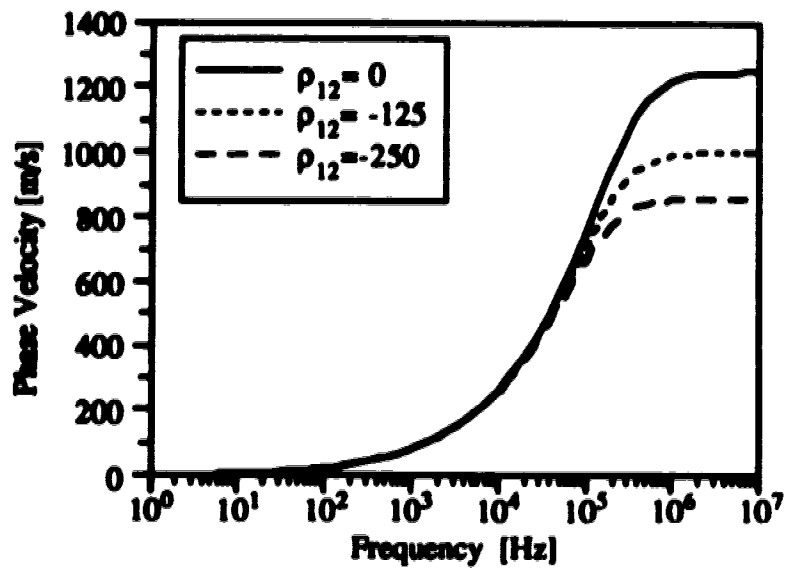


Figure 4.43 2nd P wave phase velocity versus frequency for three values of induced mass coefficient. Phase velocity increases with increasing frequency reaching a maximum which is larger for smaller ρ_{12} (magnitude). Water is the saturating fluid.

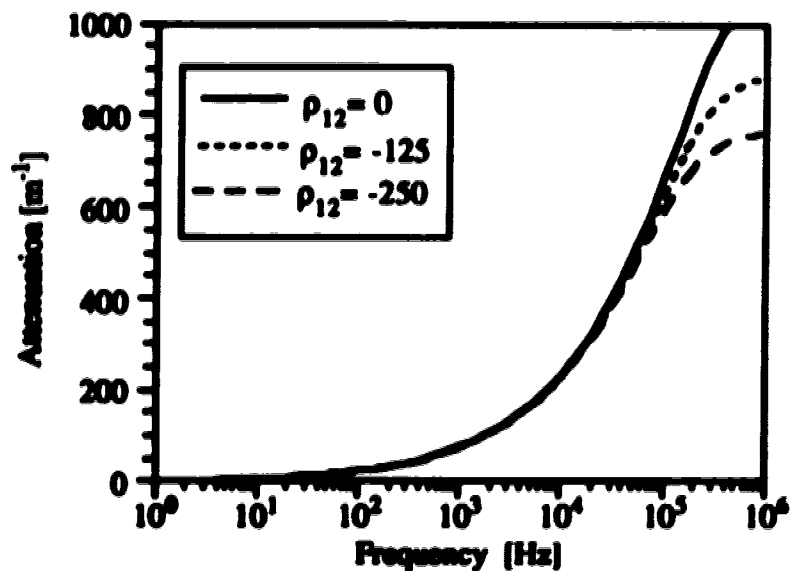


Figure 4.44 2nd P wave attenuation versus frequency for three values of induced mass coefficient. Decreasing the magnitude of the induced mass coefficient causes a slightly larger increase in attenuation at higher frequency. Water is the saturating fluid.

For an air filled sample, i.e. less viscous saturating fluid, the dependence of the phase velocity and attenuation on frequency is similar to the water filled sample; however, the magnitudes of the actual changes are much smaller.

The coefficient of heat transfer, γ , was introduced when thermomechanical coupling was accounted for. It is only present in the description of the dilatational waves. Its effect on the phase velocity and attenuation of the 1st P wave is illustrated by figure 4.45. This figure shows the normalized attenuation and normalized phase velocity as a function of coefficient of heat transfer for a bitumen filled sample and a frequency of 100 Hz. The phase velocity and attenuation are normalized by dividing by the corresponding values without thermomechanical coupling; the later values are referred to as "non-thermal". The attenuation exhibits a maximum and the phase velocity decreases sharply at a coefficient of heat transfer value of $10^8 \text{ W (m}^3\text{C)}^{-1}$. For coefficient of heat transfer values less than $10^8 \text{ W (m}^3\text{C)}^{-1}$ the wave is propagating as an adiabatic process. For values larger than $10^8 \text{ W (m}^3\text{C)}^{-1}$ the wave is propagating primarily as an isothermal process.

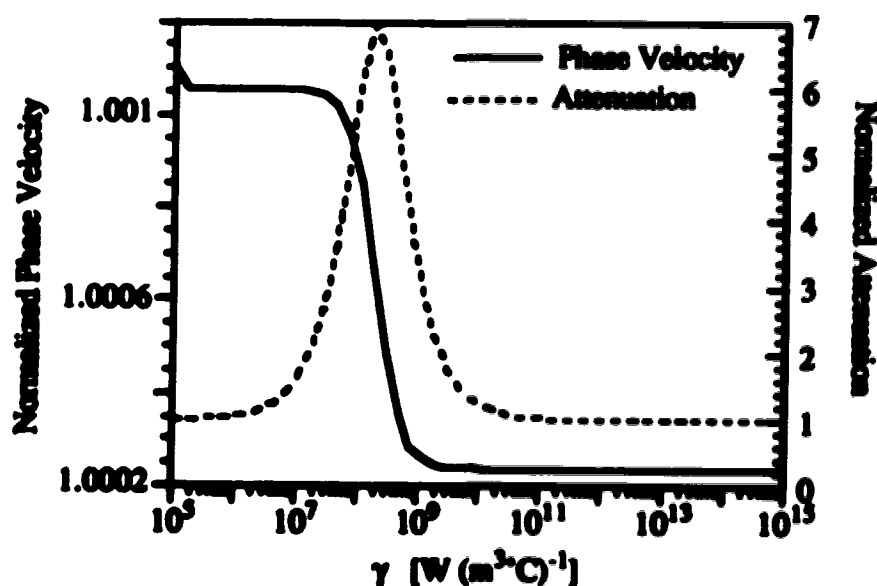


Figure 4.45 Normalized phase velocity and attenuation of the 1st P wave versus coefficient of heat transfer. Normalization was performed by dividing by respective non-thermal quantities. The saturating fluid is bitumen and the frequency is 100 Hz.

Thermomechanical coupling was introduced to describe the first order heating of the phases from compression and the expansion/contraction of the phases due to heating and cooling; it should therefore be strongly dependent on the thermal expansion coefficients of the phases. Figure 4.46 shows the 1st P wave phase velocity and attenuation (normalized with respect to non-thermal values) versus the fluid thermal expansion, α_f . Both the phase velocity and attenuation increase as the fluid thermal expansion is increased. The phase velocity increases by about 6% whereas the attenuation increases by about two and a half times with an order of magnitude increase in fluid thermal expansion. The normalized phase velocity and normalized attenuation of the 1st P wave versus solid thermal expansion is shown in figure 4.47. Here, the phase velocity increases by about 12% and the attenuation decreases by about 30% as the solid thermal expansion increases over three orders of magnitude.

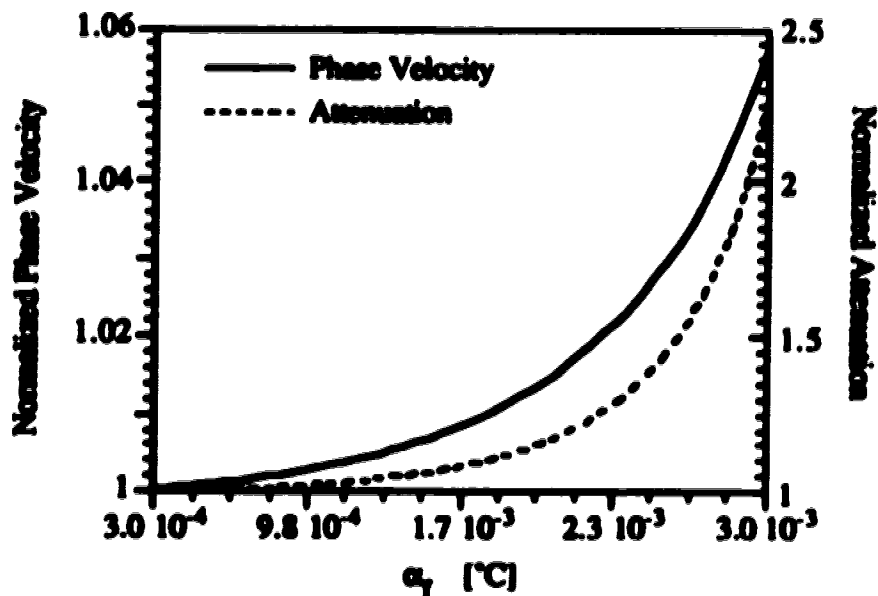


Figure 4.46 Normalized phase velocity and attenuation of the 1st P wave versus fluid thermal expansion. Normalization was performed by dividing by respective non-thermal quantities. The saturating fluid is bitumen and the frequency is 100 Hz.

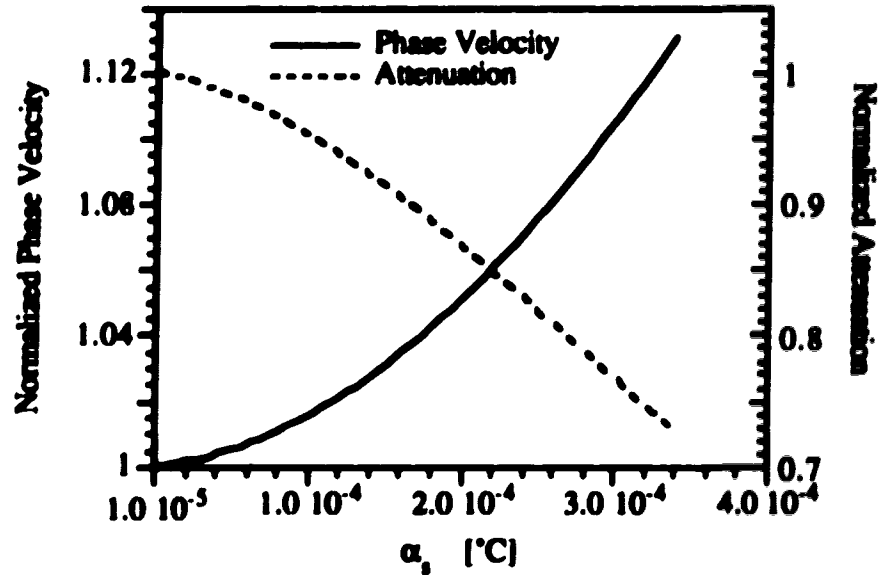


Figure 4.47 Normalized phase velocity and attenuation of the 1st P wave versus solid thermal expansion. Normalization was performed by dividing by respective non-thermal quantities. The saturating fluid is bitumen and the frequency is 100 Hz.

The generalization of the macroscopic heat equations in section 4.6 introduced two macroscopic heat conductivities. Numerical studies for the three models considered here show no changes in attenuation or phase velocity due to variations in macroscopic fluid thermal conductivity or macroscopic solid thermal conductivity. The coefficient of heat transfer was adjusted so that the thermal solutions differed substantially from non-thermal solutions; however, no changes in the phase velocity and attenuation of the 1st and 2nd P waves were observed due to variations in the macroscopic heat conductivities. Finally different values of solid and fluid thermal expansion were used such that thermomechanical coupling was important. Again, in these cases no variation in phase velocity and attenuation was observed due to changes in solid and fluid macroscopic thermal conductivities.

4.11 Conclusions

The theory for wave propagation in porous media developed by de la Cruz and Spanos (1985, 1989b) is based on the fundamental equations governing each component at the pore scale. Assuming the structures are much smaller than the wavelength of disturbance, the macroscopic equations are obtained by volume averaging the component equations and appropriate boundary conditions. The system of equations (4.63) to (4.71) displayed in section 4.8 differ from the system of de la Cruz & Spanos (1989b) in two respects. Firstly, the fluid bulk viscosity is now included. Secondly, macroscopic shear modulus μ_M and heat conductivities κ_M^f , κ_M^s are introduced as phenomenological parameters (but are none the less well-defined in terms of pore-scale quantities). The complete set of coupled macroscopic equations now contains eight empirical parameters, namely; permeability, K , induced mass coefficient, ρ_{12} , solid compliance factor, δ_s , fluid compliance factor, δ_f , macroscopic shear modulus μ_M , heat conductivities κ_M^f , κ_M^s , and the coefficient of heat transfer, γ .

The theory predicts two rotational and four dilatational waves when thermomechanical coupling is included. The rotational waves are unaffected by thermomechanical coupling. The character of these waves is dependent on the properties of the fluid and solid components and the coupling between the two. For the cases studied, thermomechanical coupling has minimal effect on the attenuation and phase velocity of the 1st and 2nd P wave. The phase velocities of the 1st S and P waves are frequency independent, within the frequency range (0-1000 Hz), for the cases considered. The attenuation of the 1st S and P waves is usually a non-linear function of frequency whereas $1000/Q$ increases linearly with frequency. The 2nd P wave velocity increases with frequency and its $1000/Q$ increases linearly with frequency when the saturating fluid is very viscous. For low viscosity fluids the 2nd P wave $1000/Q$ is approximately constant.

An investigation of the empirical parameters using numerical simulations, illustrates that the bulk viscosity, ξ_f , increases the attenuation of the 1st P wave and its effect becomes more significant when the saturating fluid has a large viscosity. Furthermore, effects of bulk viscosity are larger in samples with small values of drained bulk modulus or small permeabilities. The material shear modulus, μ_M , alters the values of phase velocity and

attenuation for both rotational and dilatational waves. The change in attenuation of the 1st P wave with respect to changes in material shear modulus differ substantially, depending on the viscosity of the saturating fluid.

Utilizing quasi-static experiments, the solid compliance factor, δ_s , and fluid the compliance factor, δ_f may be determined from values of a drained bulk modulus, K_{de} and an unjacketed bulk modulus, K_{unj} . Using this approach assumes that the processes governing the compression of the samples during static loading or wave propagation are sufficiently similar. Numerical simulations show that significant changes in phase velocity and attenuation occurs when the drained bulk modulus deviates from the quasi-static value. Changes in attenuation of the 1st P wave due to changes in drained bulk modulus is dependent on the viscosity of the saturating fluid. Another assumption commonly used in the literature is that the unjacketed bulk modulus, K_{unj} is simply equal to the bulk modulus of the solid component. Such an assumption greatly simplifies the problem because now one only requires a measurement of drained bulk modulus. Numerical calculations show that the phase velocity and attenuation of the dilatational waves are very sensitive to changes in the value of the unjacketed bulk modulus. As in the case of the drained bulk modulus, changes in attenuation with respect to changes in the unjacketed bulk modulus, are dramatically different for saturating fluids of different viscosities.

Permeability, K , has significant effects on the attenuation of both rotational and dilatational waves within the seismic frequency range but requires large permeabilities for the cases studied. Changes in phase velocities can be neglected for the cases studied. The induced mass coefficient, ρ_{12} , only becomes important at frequencies in excess of 10^4 Hz and therefore can be considered unimportant for seismic waves. In laboratory experiments, especially if the 2nd P wave is of interest, a value for the induced mass coefficient will be required.

The intercomponent conduction coefficient, γ , is only present when thermomechanical coupling is included. This parameter can change the attenuation of the P waves but has little effect on the phase velocity for the model considered. The frequency at which component temperatures are equal is dependent on this parameter. Generalization of the heat equations

introduced the macroscopic heat conductivities κ_M^f and κ_M^s . These two parameters appear unimportant with respect to altering the phase velocity and attenuation of the dilatational waves.

It is natural to seek connection with Biot's theory. This was done in section 4.6 . In particular the consequence of assuming an energy potential in the sense of Biot (1941) was investigated. While this assumption appears to be a useful approximation in specific circumstances, the consequences are much more restrictive than were previously cited. This restrictive nature becomes evident if quasi-static measurements are used for the elastic coefficients in the wave propagation theory. It appears that the expressions for the elastic coefficients in terms of measurable quasi-static values given by Biot & Willis (1957) are only valid in the case where $C_{ijkl} = C_{ij}$.

CHAPTER 5

SEISMIC WAVE PROPAGATION FOR PERMEABLE MEDIA CONTAINING TWO FLUID PHASES

5.1 Introduction

Modelling oil reservoirs with a seismic wave theory which allows for only one fluid phase in the porous medium does not adequately describe the physical processes occurring, especially in extreme circumstances, where the properties of the two fluids differ substantially (Hickey *et al.*, 1991). In this chapter, the form of the macroscopic equations governing the interaction of three phases (two fluid phases and one solid phase) and their influence on seismic wave propagation is examined. The motivation for this study is that there are many environments in which the rock masses contain more than one fluid. There are many naturally existing examples such as the vadose zone where water and air are contained within the rock mass. A large number of oil reservoirs naturally contain multiple fluids, such as water, oil and gas. One of the fluids may be at connate or irreducible saturation under certain conditions. Given the particular adhesive nature of the solid framework, it may be preferentially wetted by one of the fluids. Another interesting example is geothermal reservoirs, where the fluids are water and steam.

Man induced processes produce many examples of multiple fluid-filled rock masses. These include many types of groundwater contamination, such as the seepage of oil (the two fluids are immiscible) into an aquifer. Other processes which are related to the production of oil and gas are, for example, initial pumping of oil from a reservoir reduces the reservoir pressure enabling gas to come out of solution, secondary recovery techniques such as water flooding of light oil reservoirs, or more complicated enhanced oil recovery techniques such as steam flooding produce multiple fluid-filled rocks. Although, the naturally occurring system must be examined and quantified for construction purposes, it is the monitoring of man induced systems which necessitates the need for knowledgeable and quantifiable observational techniques.

The influence of multiple (usually two) fluids saturating a porous medium on the character (phase velocity and attenuation) of sound waves has been studied in the

laboratory for quite some time. Changes in phase velocity and attenuation of sound waves, due to changes in saturation, are observed to be greatest at very low saturations or near complete saturation.

Knight & Dvorkin (1992) measured various seismic and electrical properties of sandstones at very low saturations. They contend that although seismic and electrical properties vary with saturation throughout the entire range, the dependence at low saturation is distinctly different than at higher saturations. They attribute the decrease in velocity and rapid increase in attenuation (as measured by Pandit & King, 1979; Clark *et al.*, 1980; Murphy, 1982) of P-waves with increasing saturation to a reduction in grain contact stiffness due to the absorption of water at the grain contacts. It is concluded that this phenomenon exists over a range of saturations corresponding to the transition from a dry surface, to the coverage by adsorbed surface water, and then to the appearance of bulk water.

Knight & Nolen-Hoeksema (1990) investigated the variation in elastic wave velocities with saturation (water-air) during a continuous imbibition/drainage experiment. The compressional wave velocity, V_p , and the shear wave velocity, V_s , are concurrently measured using the ultrasonic transmission technique. The resonant frequency for the compressional source is 1 MHz and the shear wave source is 600 kHz. The saturation during imbibition is altered through the absorption of water vapour, and by soaking in deionized water. A maximum water saturation of 90% is obtained through this method. For the drainage part of the experiment the saturation is altered by drying the sample. Actual values of saturation are obtained by weighing the sample and no method is used to ascertain uniformity of saturation.

During imbibition, V_p decreases gradually with increasing water saturation up to about 80% saturation at which time V_p increases sharply. During drainage V_p decreases gradually as water saturation decreases. V_p values obtained during drainage are larger than those obtained during imbibition for saturations of 90% (maximum attained saturation) down to about 40%. Below 40% saturation the velocities are similar for both imbibition and drainage.

V_s exhibits a similar dependence on saturation and method of saturating as V_p . The values of V_s are similar for saturations up to about 50% water saturation for both imbibition and drainage. At larger saturations, V_s values measured during drainage increase gradually with increasing saturation and are larger than the values measured during imbibition. V_s during imbibition increases sharply at a saturation of about 70%, it is also noted that a sudden large drop in the amplitude occurs just prior to the increase in V_s and V_p . This decrease is so large that it inhibited collection of V_s data in that range.

Khalatbari *et al.* (1991) use the ultrasonic pulse transmission (1 MHz shear wave transducer) to investigate the effects of fluid viscosity and saturation on P-wave and S-wave velocities in Fontainebleau sandstone. The P-wave data is obtained from S-wave converted to P-wave. The saturating fluid is glycerol and the viscosity effect is modelled by varying the temperature. Measurements are performed at 8 saturations ranging from oven dry to 100% saturated. The P-wave velocity increases continuously with increasing saturation as opposed the work of Knight & Nolen-Hoeksema (1990). The P-velocity of the fully saturated is ~55% larger than the dry value and appears to be independent of viscosity. The S-wave data looks similar to the P-wave data. The S-velocity of the fully saturated sample is ~45% larger than the dry value and appears to be independent of viscosity.

Vo-Thanh (1991) measured the shear wave attenuation and velocity of a Berea sandstone partially saturated with glycerol over a range of temperatures (-80 °C to 80 °C). The range in temperature is primarily used to obtain a range of viscosities. The measurements were performed using the resonant bar technique, with resonant frequencies being in the range of 1500 Hz to 3100 Hz, at seven discrete glycol saturations of 0, 13, 23, 36, 49 and 69%.

V_s showed a strong temperature dependence except in the dry sample. V_s decreases with increasing temperature, the change being more dramatic at higher saturations. Actual graphs of V_s versus saturation show that the velocity increases gradually with increasing saturation for temperatures less than about -30°C. For temperatures greater than this, the velocity decreases with increasing saturation.

Yin *et al.* (1992) measure the effects of partial liquid/gas saturation on the extensional wave attenuation in Berea sandstone. The resonant bar method is utilized to obtain measurements on two samples with different boundary conditions (enclosing jackets), to examine such dependence. Both samples have similar non-zero extensional quality factor, Q_E^1 , which remains constant from 20% to 70% brine saturation (little data exist below 20%). At larger saturations a maximum in Q_E^1 is observed. These maxima are strongly dependent on the boundary conditions. The sample with a "constant pressure" boundary has the larger peak and is located at about 97% saturation, whereas the other sample with the "no flow" boundary has a smaller peak at a brine saturation of about 85%.

Measurements were also performed for increasing (imbibition) and decreasing (drainage) brine saturation. During drainage a peak in Q_E^1 is observed at about 85% brine saturation. The attenuation peak for imbibition appears to shift to a higher saturation however the data are somewhat sparse. The explanation presented was that the gas selectively fills larger pores during drainage but smaller pores during imbibition.

Yin *et al.* (1992) also use the forced deformation measurement technique to measure the frequency dependence as well as saturation dependence of extensional wave attenuation. The saturation dependence of Q_E^1 is similar to what is observed using the resonant bar method. Basically Q_E^1 is constant for saturations between 20 and 80% with a maximum in Q_E^1 occurring near the 95% saturation. Measurements made at 2000 Hz, 700 Hz, and 100 Hz illustrate a strong dependence on frequency. Firstly, Q_E^1 is larger at higher frequencies for all saturations. Secondly, the maximum in Q_E^1 decreases dramatically with decreasing frequency such that no maximum in Q_E^1 is observed frequency of 100 Hz.

Paffenholz & Burkhardt (1989) studied the absorption and moduli of partially water saturated sedimentary rocks for longitudinal (frequencies between 0.03 and 300 Hz) and torsional (frequencies between 0.03 and 100 Hz) deformations. Attention was placed on securing small (10^{-6}) strain amplitudes. "Young's" moduli and shear moduli decrease with increasing water saturation from 0 to 50 % and are then independent of water content.

Several samples exhibit a maximum in Q_G^1 as a function of frequency. The peak becomes larger in magnitude and moves towards lower frequencies as the saturation is increased. No peaks are observed in the shear quality factor, Q_S^1 , for these samples. A quartzite sample has two peaks, one at low frequency and one at high frequency in both Q_G^1 and Q_S^1 . Both peaks increase in magnitude and the high frequency peak moves to lower frequency as the saturation is increased.

Bacri & Salin (1986, 1990) present experimental data, for an oil-water saturated porous medium, which were collected using the ultrasonic pulse transmission technique (frequency of 400 kHz). Velocity data are collected during drainage from 100% water saturation to an irreducible water saturation of about 35%. The velocity decreases continuously with decreasing water saturation. The change in velocity is about 10% over the range of saturation. During the injection of water into a fully oil saturated sample (imbibition) the velocity decreases with increasing water saturation. The velocity at full oil saturation (zero water saturation) is about 10% larger than the velocity at residual oil saturation (75% water saturation). Velocities during imbibition are larger than the velocities obtained during drainage for water saturations between 35 and 60%.

Domenico (1976) using the pulse transmission technique measured ultrasonic (peak frequency of about 200 kHz) compressional and shear wave velocities in samples of unconsolidated Ottawa sand and fused glass beads. The samples are saturated with brine (water and salt solution) and nitrogen gas. The samples are saturated by two methods, imbibition and "flow". In the flow technique brine and nitrogen are mixed prior to injection. A profile of the saturation along the sample is measured using an X-ray absorption technique. It shows variations in saturation, with larger variations at low saturations. In the imbibition technique the sample is first prepared by flow, then the pore pressure is increased by further injection of brine. The X-ray measurements show a more uniform saturation profile.

Ultrasonic measurements are taken on samples which are dry, and at seven other saturations ranging from about 50 to 100% brine saturation. For the Ottawa sand sample saturated by "flow" the compressional wave velocity remains fairly constant (~4100 ft/sec) up to about a 85% brine saturation where it increases very quickly to near maximum

velocity (~6800 ft/sec) at 97% saturation. Measured shear wave velocities decrease uniformly with increasing saturation from 2744 ft/sec for 0% saturation (dry) to 2628 ft/sec for 100% brine saturated sample.

The glass bead sample is used to illustrate the dependence of the velocity on the method of saturation, i.e. imbibition and "flow". The compressional wave velocity, at comparable saturation (~95%), is larger when the sample filled by "flow" than when the sample is filled by imbibition process. The shear wave velocity appears to be independent of the method of filling. It is argued that when the sample is filled by "flow", the gas preferentially seeks the larger pores, whereas during imbibition the water and gas are more uniformly distributed within the pores.

Although seismic properties vary with saturation throughout the entire range, the dependence at low saturation is distinctly different from that at higher saturations (Knight & Dvorkin, 1992). In the very low saturation range, rapid decreases in V_p and V_s and associated increases in Q_p^1 and Q_s^1 are observed with the addition of a small amount of water. At intermediate saturations both P and S waves appear to have a similar dependence on saturation, i.e. small decreases in phase velocity and slight increases in Q^1 with increasing saturation. At near complete saturation, the phase velocity and Q^1 for the waves depend upon the method by which the sample was saturated. The phase velocities, for a water-air system, are larger when the sample is prepared through a drainage process as compared to values from a sample prepared by the imbibition process. The P-wave appears to exhibit this process dependence more strongly than do the S-waves.

Theoretical modelling of wave propagation for permeable media containing two fluid phases can be grossly subdivided in two categories based upon the approach used: One approach is to utilize a theory for a fully saturated porous media, such as Biot (1956b, 1956c), and account for the multiple fluid phases by replacing the original fluid parameters and some of the macroscopic parameters with "effective" parameters (Domenico, 1974; White, 1975; Dutta & Seriff, 1979; Dutta & Ode, 1979a, 1979b; Mochizuki, 1982; Barryman & Thigpen, 1985; Barryman *et al.*, 1988; Smoulders *et al.*, 1992; Pride *et al.*, 1992). These effective parameters are constructed based upon specific assumptions about the interactions of the two fluid phases, or through micro-mechanical modeling (Brandt, 1955; Murphy *et al.*, 1984, 1986). The other approach is to obtain a general description

whereby the fluids are treated independently, with the use of some type of homogenization scheme (Thigpen & Berryman, 1985; Garg & Nayfeh, 1986; Santos *et al.*, 1990a, 1990b; Hawkins & Bedford, 1992) or through micro-mechanical modeling (Mavko & Nur, 1979). The governing system of equations in these formulations contains numerous parameters which are not well understood and experimental procedures for their measurements are usually not presented .

In this chapter low frequency wave propagation through a porous medium saturated by two fluids will be discussed. First, an approximation will be obtained by using the equations presented in chapter 4 and the assumption that the two fluids form a composite or effective fluid. Suitable expressions for the effective parameters of the composite fluid will be derived and the underlying assumptions clearly stated. Brief discussions about the effects on various macroscopic parameters are also presented. This analysis is based completely on descriptions obtained from volume averaging. Second, the governing equations will be derived for the general case of wave propagation through a porous medium saturated by two fluids. Volume averaging is used to construct the basic equations and the approach parallels that of chapter 4 (see figure 4.1). The expansion of the interaction integrals will be discussed and some insight into the parameters introduced will be given.

5.2 Composite Fluid Model

An approximation of the dynamics of porous media saturated by two fluids can be obtained by utilizing a composite fluid model and the equations derived in chapter 4. In order to model the two-fluid mixture as a single fluid, the fluid density, ρ_f , fluid bulk modulus, K_f , fluid bulk viscosity, ξ_f , and the fluid shear viscosity, μ_f , in the equations presented in chapter 4 become representative "effective" parameters.

In the description of a porous medium saturated by two fluids, several new macroscopic quantities will enter the description naturally through the use of the volume averaging procedure and will be defined at the outset. The volume fraction of fluid l is defined as

$$\eta_i = \frac{V_i}{V}, \quad i = 1, 2, \dots \quad (5.1)$$

where V_i is the volume of fluid i within the volume V of porous media. For the two-fluid model considered here the volume fractions of the fluids and the porosity are simply related by

$$\eta = \eta_1 + \eta_2 \quad (5.2)$$

The fluid saturation, denoted by S_i , which represents the volumetric proportions of fluids is given by

$$S_i = \frac{V_i}{V}, \quad i = 1, 2, \dots \quad (5.3)$$

and is simply related to volume fractions through the porosity by

$$\eta_i = \eta S_i \quad (5.4)$$

Substituting equation (5.4) into equation (5.2) gives

$$S_1 + S_2 = 1 \quad (5.5)$$

which can be used to replace S_2 by $(1 - S_1)$ whenever it appears.

The density of the fluid will be expressed as

$$\rho_f = S_1 \rho_1 + (1 - S_1) \rho_2 \quad (5.6)$$

where ρ_1 and ρ_2 are the mass densities of fluid one and two respectively. The fluid bulk modulus will in general fall between to an upper limit, K_f^U , given by

$$K_f^U = S_1 K_1 + (1 - S_1) K_2 \quad (5.7)$$

and a lower limit, K_f^L , given by

$$\frac{1}{K_f} = \frac{S_1}{K_1} + \frac{(1-S_1)}{K_2} \quad (5.8)$$

Let us however, derive a unique expression, starting with the usual definition of fluid bulk modulus

$$K_f^{-1} = -\frac{1}{V_f} \frac{\Delta V_f}{\Delta p_f} \quad (5.9)$$

and assume that the volume averaged pressures in each fluid phase are the same, ie.

$$p_f = p_1 = p_2 \quad (5.10)$$

This implies that surface tension does not play a significant role in the compression of the two fluid phases. The change in total fluid volume may be written as

$$\Delta V_f = \Delta V_1 + \Delta V_2 \quad (5.11)$$

Substituting equation (5.11) into equation (5.9) and using the assumption of equality of pressures (5.10) yields

$$K_f^{-1} = -\frac{1}{V_f} \frac{\Delta V_1}{\Delta p_1} - \frac{1}{V_f} \frac{\Delta V_2}{\Delta p_2} \quad (5.12)$$

Utilizing equation (5.3) and the definition of the bulk modulus for fluid one and two, equation (5.12) gives

$$\frac{1}{K_f} = \frac{S_1}{K_1} + \frac{(1-S_1)}{K_2} \quad (5.13)$$

which is simply the lower bound presented above. If surface tension plays a significant role in the compression of the fluid composite, then the bulk modulus would be larger, since additional forces would be required to deform the interface between the fluids.

When bulk viscosity is included the total fluid-pressure is altered. Assuming a time harmonic deformation of the form $e^{i\omega t}$ the total fluid-pressure is related to the dilation of the fluid as (trace of the fluid viscosity tensor)

$$-(p_f - p_f^0) = K_f^* \nabla \cdot \mathbf{u}_f \quad (5.14)$$

where

$$K_f^* = K_f + i\omega \xi_f \quad (5.15)$$

Assuming that the total fluid-pressure of the component fluids are equal, the fluid composite average for the operator K_f^* is similar to the bulk modulus above, namely

$$\frac{1}{K_f^*} = \frac{S_1}{K_1^*} + \frac{(1-S_1)}{K_2^*} \quad (5.16)$$

The construction of a total effective viscosity for a fluid composite, with negligible surface tension and where only fluid one contacts the solid matrix, has been presented by Udey & Spanos (1993). Their analysis begins with the equations of motion (developed by de la Cruz & Spanos, 1983; others) governing flow of two immiscible fluids

$$\frac{\mu_1}{K_{11}} \mathbf{q}_1 - \frac{\mu_1}{K_{12}} \mathbf{q}_2 = -\nabla P_1 \quad (5.17)$$

and

$$\frac{\mu_2}{K_{22}} \mathbf{q}_2 - \frac{\mu_2}{K_{21}} \mathbf{q}_1 = -\nabla P_2 \quad (5.18)$$

where \mathbf{q}_i are the Darcy flow velocities, μ_i are the fluid viscosities, and K_{ij} are generalized permeabilities. These generalized permeabilities are phenomenological parameters but are none the less well-defined in terms of pore scale quantities. Assuming that surface tension is zero, it is possible to define a single pressure for the fluid composite, i.e. equation (5.10). With such an assumption Udey & Spanos (1993) show that

$$\frac{1}{K_{12}} = \frac{\mu_2}{\mu_1 K_{21}} \quad (5.19)$$

Furthermore, assuming that only fluid one contacts the solid matrix, Udey & Spanos (1993), show that

$$\frac{1}{K_{21}} = \frac{S_2}{S_1} \frac{1}{K_{22}} \quad (5.20)$$

$$\frac{1}{K_{22}} = \frac{1}{B(S_1) K} \quad (5.21)$$

and

$$\frac{1}{K_{11}} = \frac{1}{S_1^2 A(S_1) K} + \frac{S_2^2 \mu_2}{S_1^2 \mu_1} \frac{1}{B(S_1) K} \quad (5.22)$$

where A and B are functions of saturation and K is the absolute permeability. Therefore assuming that surface tension is negligible and that only fluid one contacts the solid it is possible to write the above equations (5.17) and (5.18) in the form of Muskat's equations, namely

$$q_1 = - \frac{K_{r1} K}{\mu_1} \nabla P_1 \quad (5.23)$$

and

$$q_2 = - \frac{K_{r2} K}{\mu_2} \nabla P_2 \quad (5.24)$$

where the relative permeabilities, K_{r1} and K_{r2} , are related to the functions A and B by

$$K_{r1} = S_1 A(S_1) \quad (5.25)$$

and

$$K_{r2} = \frac{\mu_2}{\mu_1} S_2 A(S_1) + B(S_1) \quad . \quad (5.26)$$

The total Darcy velocity as given by Udey & Spanos (1993) is

$$q = q_1 + q_2 \quad (5.27)$$

which can be written with the use of equations (5.23) and (5.24) as

$$q = -K \left(\frac{K_{r1}}{\mu_1} + \frac{K_{r2}}{\mu_2} \right) \nabla P \quad . \quad (5.28)$$

This enables the extraction of an effective viscosity for the two fluid composite $\mu_f(S_1)$. The total effective viscosity may be viewed in terms of contributions of two relative permeability functions

$$\mu_f(S_1) = \frac{K_{r1}(S_1)}{\mu_1} + \frac{K_{r2}(S_1)}{\mu_2} \quad (5.29)$$

or alternatively as a weighted average of the viscosities of the fluid components

$$\frac{1}{\mu_f(S_1)} = \frac{A(S_1)}{\mu_1} + \frac{B(S_1)}{\mu_2} \quad . \quad (5.30)$$

The induced mass coefficient, ρ_{12} , is a macroscopic parameter which was discussed in section 4.6. Various expressions for the induced mass coefficient developed in the literature contain the fluid density and the fluid viscosity. To obtain an estimate of the induced mass coefficient the above effective fluid density and effective fluid viscosity should be used. This is a crude approach and the models (or assumptions) used to obtain the expressions for the induced mass coefficient should be compared to the assumptions underlying the derivation of the effective parameters for compatibility.

The saturation dependence of seismic properties at low saturation is distinctly different than at higher saturations. Furthermore, seismic properties are observed to be dependent on the method of saturation. Therefore, caution must be taken if the compliance factors

(δ_s and δ_f) are to be determined from quasi-static measurements. In the drained compressibility experiments, the sample should be filled to the appropriate saturation and with the correct fluid wetting the solid. A measurement on an oven dried sample should not be used as the drained bulk modulus. The usual hydrostatic compression assumption

$$K(1) = K_s \quad (5.31)$$

should be ignored and the required second measurement should consist of an undrained compression experiment. This type of measurement will at least incorporate changes in saturation due the different compressibilities of the pore fluids and the interaction with the solid matrix.

Using the above expressions for the fluid parameters in the equations derived in chapter 4 should give an approximation of the dynamics of porous media saturated by two fluids. It is important to realize that assuming negligible surface tension and selective wetting of the solid matrix are not sufficient conditions for writing the two interacting fluids as a single fluid. An underlying assumption must also be made with respect to the relative magnitudes and phase of the velocity fields for the individual fluids. Given the different compressibilities of the fluids we are no more justified in using the effective fluid approximation than we would be to write the interacting solid and fluid continua presented in chapter 4 as say an effective solid.

5.3 Derivation of Governing Equations for Wave Propagation Through a Porous Medium Containing Two Fluid Phases

5.3.1 Introduction

Macroscopic equations governing seismic waves in porous media should reflect the properties and behavior of the constituent materials and their interaction. Hence in attempts to construct these equations it is important to maintain a strong connection with the well established equations governing the behavior of the microscopically segregated components, which interact at the numerous interfaces in accordance with suitable boundary conditions. From this point of view some averaging scheme is, therefore, unavoidable. Through the use of volume averaging de la Cruz & Spanos (1965, 1969b)

proposed a system of equations for low frequency seismic waves propagating in homogeneous porous media saturated with a single fluid phase. These equations were further generalized and presented in chapter 4.

The porous medium considered in this section consists of a homogeneous isotropic elastic solid and the pore space is filled with two immiscible viscous fluids. The pores are assumed to be of random sizes, shapes, orientations, and orders of magnitude smaller in scale than the wavelengths of the waves being considered. The three components are assumed to be microscopically homogeneous as well as macroscopically homogeneous in that the unperturbed proportions of the three phases do not vary with position. Furthermore, the porous matrix is assumed to have a uniform porosity at the macroscale and the fluid phases are assumed to be uniformly distributed in order to avoid the additional macroscopic parameters which are required when porosity gradients or saturation gradients are present. The deformations will be assumed such that thermomechanical coupling can be ignored.

5.3.2 Volume Averaging of Pore scale Equations

The steps required to formally recast the pore scale equations in a macroscopic form, using the volume averaging technique, as outlined in chapter 2, are given. In the equations a subscript or bracketed superscript 1 will correspond to fluid one, a subscript or bracketed superscript 2 will correspond to fluid two, and a subscript or bracketed superscript s, will correspond to the solid material which makes up the porous skeleton.

New macroscopic variables which enter the description naturally through the use of the volume averaging procedure were discussed in section 5.2. For example, the volume fraction of fluid one, η_1 , enters in the relation between two averaged quantities obtained through volume averaging, namely

$$\langle \mathbf{g}_1 \rangle = \eta_1 \bar{\mathbf{g}}_1 . \quad (5.32)$$

In fluid flow experiments it is common to use saturation, which is related to volume fractions through the porosity as given by equation (5.4). In the case considered here the

porosity will vary due to the fact that the frame is deformable and therefore volume fractions will be used.

The volume average of the continuity equation for fluid one is

$$\frac{1}{V} \int_V \left(\frac{\partial \rho_1}{\partial t} + \nabla \cdot (\rho_1 \mathbf{v}_1) \right) dV = 0 . \quad (5.33)$$

Applying the theorems (2.4) and (2.5) to equation (5.33) yields

$$\begin{aligned} & \frac{\partial}{\partial t} \left[\frac{1}{V} \int_V \rho_1 dV \right] - \frac{1}{V} \int_{A_{12}} \rho_1 \mathbf{v}_1 \cdot \mathbf{n} dA - \frac{1}{V} \int_{A_{1S}} \rho_1 \mathbf{v}_1 \cdot \mathbf{n} dA \\ & + \nabla \cdot \left[\frac{1}{V} \int_V (\rho_1 \mathbf{v}_1) dV \right] + \frac{1}{V} \int_{A_{12}} \rho_1 \mathbf{v}_1 \cdot \mathbf{n} dA + \frac{1}{V} \int_{A_{1S}} \rho_1 \mathbf{v}_1 \cdot \mathbf{n} dA = 0 \end{aligned} \quad (5.34)$$

where A_{12} is the surface area between fluid one and fluid two, and A_{1S} is the surface area between fluid one and the solid. In this case the area integral terms which arise from the volume averaging theorems exactly cancel and rewriting equation (5.34) using equations (2.1) and (5.32) one obtains

$$\frac{\partial}{\partial t} \eta_1 \bar{\rho}_1 + \frac{\partial}{\partial x_i} (\eta_1 \overline{\rho_1 v_i^{(1)}}) = 0 . \quad (5.35)$$

Under the assumption that the unperturbed velocity for fluid one is zero ($\bar{\mathbf{v}}_1^0 = 0$) and keeping only first order terms, equation (5.35) may be rewritten as

$$\eta_1^0 \frac{\partial}{\partial t} \bar{\rho}_1 + \rho_1^0 \frac{\partial}{\partial t} \eta_1 + \eta_1^0 \rho_1^0 \nabla \cdot \bar{\mathbf{v}}_1 = 0 . \quad (5.36)$$

Similarly, the linear macroscopic continuity equation for fluid two is

$$\eta_2^0 \frac{\partial \bar{p}_2}{\partial t} + \rho_2^0 \frac{\partial \eta_2}{\partial t} + \eta_2^0 \rho_2^0 \nabla \cdot \bar{v}_2 = 0 \quad (5.37)$$

For the solid phase the volume average of the continuity equation is the same as in chapter 4, i.e.

$$\frac{\bar{\rho}_s - \rho_s^0}{\rho_s^0} - \frac{\eta - \eta_0}{1 - \eta_0} + \nabla \cdot \bar{v}_s = 0 \quad (5.38)$$

where η is the porosity of the deformed porous medium.

The definition of bulk modulus (with reference to an isothermal process) for fluid one can be written for small deformations as

$$K_1 = \frac{p_1 - p_1^f}{\left(\frac{\rho_1 - \rho_1^f}{\rho_1^0} \right)} \quad (5.39)$$

Volume averaging equation (5.39) and keeping only first order terms leads to

$$K_1 = \frac{\bar{p}_1 - p_1^f}{\left(\frac{\bar{\rho}_1 - \rho_1^f}{\rho_1^0} \right)} \quad (5.40)$$

Taking the derivative with respect to time and substituting for the density using equation (5.36), the pressure equation for fluid one is

$$\frac{1}{K_1} \frac{\partial \bar{p}_1}{\partial t} = -\nabla \cdot \bar{v}_1 - \frac{1}{\eta_1^0} \frac{\partial \eta_1}{\partial t} \quad (5.41)$$

Similarly, for fluid two we have

$$\frac{1}{K_2} \frac{\partial \bar{p}_2}{\partial t} = -\nabla \cdot \bar{v}_2 - \frac{1}{\eta_2^0} \frac{\partial \eta_2}{\partial t} \quad (5.42)$$

and for the solid the pressure equation we have

$$\frac{1}{K_s}(\bar{p}_s - p_f) = -\nabla \cdot \bar{u}_s + \frac{(\eta - \eta_0)}{(1 - \eta_0)} \quad (5.43)$$

Applying the volume averaging procedure to the equation of motion for fluid one gives

$$\begin{aligned} \rho_1^o \frac{\partial}{\partial t} \langle v_i^{(1)} \rangle &= \frac{\partial}{\partial x_k} \langle \tau_{ik}^{(1)} \rangle - \frac{\partial}{\partial x_i} \langle p_1 \rangle - \frac{1}{V} \int_{\Lambda_{s1}} [(p_1 - p_f) \delta_{ik} - \tau_{ik}^{(1)}] n_k dA \\ &\quad - \frac{1}{V} \int_{\Lambda_{s2}} [(p_1 - p_f) \delta_{ik} - \tau_{ik}^{(1)}] n_k dA \quad (5.44) \end{aligned}$$

The two area integrals in equation (5.44) represent the forces (per unit volume) exerted on fluid one by the solid matrix and fluid two respectively due to any motions. From the macroscopic fluid one point of view, it is simply a body force (de la Cruz & Spanos, 1989b).

The average viscosity stress tensor (assuming a Newtonian fluid) is

$$\begin{aligned} \langle \tau_{ik}^{(1)} \rangle &= \xi_1 \frac{\partial \langle v_j^{(1)} \rangle}{\partial x_j} \delta_{ik} + \mu_1 \left[\frac{\partial \langle v_i^{(1)} \rangle}{\partial x_k} + \frac{\partial \langle v_k^{(1)} \rangle}{\partial x_i} - \frac{2}{3} \frac{\partial \langle v_j^{(1)} \rangle}{\partial x_j} \delta_{ik} \right] + \xi_1 \frac{1}{V} \int_{\Lambda_{s1}} v_j^{(1)} n_j \delta_{ik} dA \\ &\quad + \xi_1 \frac{1}{V} \int_{\Lambda_{s2}} v_j^{(1)} n_j \delta_{ik} dA + \mu_1 \frac{1}{V} \int_{\Lambda_{s1}} (v_i^{(1)} n_k + v_k^{(1)} n_i - \frac{2}{3} \delta_{ik} v_j^{(1)} n_j) dA \\ &\quad + \mu_1 \frac{1}{V} \int_{\Lambda_{s2}} (v_i^{(1)} n_k + v_k^{(1)} n_i - \frac{2}{3} \delta_{ik} v_j^{(1)} n_j) dA \quad (5.45) \end{aligned}$$

Combining equations (5.44) and (5.45), using relation (5.32) between the averages, and representing the area integrals by Γ_s , one obtains an averaged equation of motion for fluid one of the form

$$\begin{aligned} \eta_1^0 \rho_1^0 \frac{\partial}{\partial t} \bar{v}_i^{(1)} = & \xi_1 \frac{\partial}{\partial x_k} \left[\eta_1^0 \frac{\partial \bar{v}_j^{(1)}}{\partial x_j} \delta_{ik} + I_{1s}^A + I_{12}^A \right] - \eta_1^0 \frac{\partial}{\partial x_i} \bar{p}_1 - f_{1s}^C - f_{12}^C \\ & + \mu_1 \frac{\partial}{\partial x_k} \left[\eta_1^0 \left(\frac{\partial \bar{v}_i^{(1)}}{\partial x_k} + \frac{\partial \bar{v}_k^{(1)}}{\partial x_i} - \frac{2}{3} \frac{\partial \bar{v}_j^{(1)}}{\partial x_j} \delta_{ik} \right) + I_{1s}^B + I_{12}^B \right]. \end{aligned} \quad (5.46)$$

Similarly, the averaged equation of motion for fluid two is

$$\begin{aligned} \eta_2^0 \rho_2^0 \frac{\partial}{\partial t} \bar{v}_i^{(2)} = & \xi_2 \frac{\partial}{\partial x_k} \left[\eta_2^0 \frac{\partial \bar{v}_j^{(2)}}{\partial x_j} \delta_{ik} + I_{2s}^A + I_{21}^A \right] - \eta_2^0 \frac{\partial}{\partial x_i} \bar{p}_2 - f_{2s}^C - f_{21}^C \\ & + \mu_2 \frac{\partial}{\partial x_k} \left[\eta_2^0 \left(\frac{\partial \bar{v}_i^{(2)}}{\partial x_k} + \frac{\partial \bar{v}_k^{(2)}}{\partial x_i} - \frac{2}{3} \frac{\partial \bar{v}_j^{(2)}}{\partial x_j} \delta_{ik} \right) + I_{2s}^B + I_{21}^B \right]. \end{aligned} \quad (5.47)$$

The volume average of the equation of motion for the solid (after linearization) is

$$\begin{aligned} (1-\eta_0) \rho_s^0 \frac{\partial^2}{\partial t^2} \bar{u}_i^s = & K_s \frac{\partial}{\partial x_k} \left[(1-\eta_0) \frac{\partial \bar{u}_j^s}{\partial x_j} \delta_{ik} + I_{s1}^A + I_{s2}^A \right] - f_{s1}^C - f_{s2}^C \\ & + \mu_s \frac{\partial}{\partial x_k} \left[(1-\eta_0) \left(\frac{\partial \bar{u}_i^s}{\partial x_k} + \frac{\partial \bar{u}_k^s}{\partial x_i} - \frac{2}{3} \frac{\partial \bar{u}_j^s}{\partial x_j} \delta_{ik} \right) + I_{s1}^B + I_{s2}^B \right]. \end{aligned} \quad (5.48)$$

The above equations are obtained directly by applying the averaging procedure to the microscopic equations and linearizing. It should be noted that in decomposing the pressure terms in the fluid equations of motion (5.46) and (5.47) p_0 and not \bar{p} was used. For the case under consideration (fluid saturations are constant through space), the two decompositions should produce identical results to first order (Eastwood, 1991). The above equations are general in form but not very useful unless one can evaluate the area integrals. These area integrals represent the component interactions at the pore scale interfaces and therefore their evaluation will depend on the boundary conditions at the pore scale.

5.3.3 Evaluation of Area Integrals

The area integrals are subdivided into groups denoted by superscripts A, B, C. The surface integrals denoted by a superscript A, are scalar quantities and represent changes in relative volumetric proportions of the phase during deformation. In order to account for all the solid surface which is in contact with the fluid it is necessary to combine I_{s1}^A and I_{s2}^A . The integrand $u_j^i n_j \delta_{ik} dA$ is an element of volume of solid swept out by the displacement u_i over a surface element dA during deformation (de la Cruz & Spanos, 1989b). Hence, integrating over all solid surfaces the above surface integrals may be related to the change in porosity as

$$I_{s1}^A + I_{s2}^A = \frac{1}{V} \int_{A_s} u_j^i n_j \delta_{ik} dA = -(\eta - \eta_0) . \quad (5.49)$$

For fluid two, the combination of area integrals I_{s1}^A and I_{s2}^A covers all of the fluid two surface and $v_j^{(2)} n_j \delta_{ik} dA$ is the time rate of change of the volume of fluid two swept out over a surface element dA by the velocity $v^{(2)}$, therefore

$$I_{s1}^A + I_{s2}^A = \frac{1}{V} \int_{A_s} v_j^{(2)} n_j \delta_{ik} dA = \frac{\partial \eta_2}{\partial t} . \quad (5.50)$$

Similarly, in order to account for all the fluid one surface it is necessary to combine the surface area in contact with the solid, I_{s1}^A , and the surface area in contact with fluid two I_{s2}^A . Following the same argument as above, one obtains

$$I_{s1}^A + I_{s2}^A = \frac{1}{V} \int_{A_s} v_j^{(1)} n_j \delta_{ik} dA = \frac{\partial \eta_1}{\partial t} \quad (5.51)$$

Given the solution of the above area integrals and the volume fraction equation (5.2) it is obvious that these six area integrals are not all independent.

The "B" group of area integrals are second rank tensors that account for additional shear strains of the porous material due to pore structure and component interaction at pore

scale interfaces. Following the argument presented in section 4.4, for generalized macroscopic shear deformation in fully saturated porous media, the most general expansions would be

$$\begin{aligned} \Gamma_{10}^{\text{B}} = & \eta_1^{\text{B}} c_1^{(10)} \left[\frac{\partial v_i^{(1)}}{\partial x_k} + \frac{\partial v_k^{(1)}}{\partial x_i} - \frac{2}{3} \delta_{ik} \frac{\partial v_j^{(1)}}{\partial x_j} \right] - \eta_2^{\text{B}} c_2^{(10)} \left[\frac{\partial v_i^{(2)}}{\partial x_k} + \frac{\partial v_k^{(2)}}{\partial x_i} - \frac{2}{3} \delta_{ik} \frac{\partial v_j^{(2)}}{\partial x_j} \right] \\ & - (1-\eta_0) c_3^{(10)} \frac{\partial}{\partial x} \left[\frac{\partial u_i^{\text{A}}}{\partial x_k} + \frac{\partial u_k^{\text{A}}}{\partial x_i} - \frac{2}{3} \delta_{ik} \frac{\partial u_j^{\text{A}}}{\partial x_j} \right] \end{aligned} \quad (5.52a)$$

$$\begin{aligned} \Gamma_{12}^{\text{B}} = & \eta_1^{\text{B}} c_1^{(12)} \left[\frac{\partial v_i^{(1)}}{\partial x_k} + \frac{\partial v_k^{(1)}}{\partial x_i} - \frac{2}{3} \delta_{ik} \frac{\partial v_j^{(1)}}{\partial x_j} \right] - \eta_2^{\text{B}} c_2^{(12)} \left[\frac{\partial v_i^{(2)}}{\partial x_k} + \frac{\partial v_k^{(2)}}{\partial x_i} - \frac{2}{3} \delta_{ik} \frac{\partial v_j^{(2)}}{\partial x_j} \right] \\ & - (1-\eta_0) c_3^{(12)} \frac{\partial}{\partial x} \left[\frac{\partial u_i^{\text{A}}}{\partial x_k} + \frac{\partial u_k^{\text{A}}}{\partial x_i} - \frac{2}{3} \delta_{ik} \frac{\partial u_j^{\text{A}}}{\partial x_j} \right] \end{aligned} \quad (5.52b)$$

$$\begin{aligned} \Gamma_{20}^{\text{B}} = & -\eta_1^{\text{B}} c_1^{(20)} \left[\frac{\partial v_i^{(1)}}{\partial x_k} + \frac{\partial v_k^{(1)}}{\partial x_i} - \frac{2}{3} \delta_{ik} \frac{\partial v_j^{(1)}}{\partial x_j} \right] + \eta_2^{\text{B}} c_2^{(20)} \left[\frac{\partial v_i^{(2)}}{\partial x_k} + \frac{\partial v_k^{(2)}}{\partial x_i} - \frac{2}{3} \delta_{ik} \frac{\partial v_j^{(2)}}{\partial x_j} \right] \\ & - (1-\eta_0) c_3^{(20)} \frac{\partial}{\partial x} \left[\frac{\partial u_i^{\text{A}}}{\partial x_k} + \frac{\partial u_k^{\text{A}}}{\partial x_i} - \frac{2}{3} \delta_{ik} \frac{\partial u_j^{\text{A}}}{\partial x_j} \right] \end{aligned} \quad (5.52c)$$

$$\begin{aligned} \Gamma_{21}^{\text{B}} = & -\eta_1^{\text{B}} c_1^{(21)} \left[\frac{\partial v_i^{(1)}}{\partial x_k} + \frac{\partial v_k^{(1)}}{\partial x_i} - \frac{2}{3} \delta_{ik} \frac{\partial v_j^{(1)}}{\partial x_j} \right] + \eta_2^{\text{B}} c_2^{(21)} \left[\frac{\partial v_i^{(2)}}{\partial x_k} + \frac{\partial v_k^{(2)}}{\partial x_i} - \frac{2}{3} \delta_{ik} \frac{\partial v_j^{(2)}}{\partial x_j} \right] \\ & - (1-\eta_0) c_3^{(21)} \frac{\partial}{\partial x} \left[\frac{\partial u_i^{\text{A}}}{\partial x_k} + \frac{\partial u_k^{\text{A}}}{\partial x_i} - \frac{2}{3} \delta_{ik} \frac{\partial u_j^{\text{A}}}{\partial x_j} \right] \end{aligned} \quad (5.52d)$$

$$\begin{aligned} \Gamma_{31}^{\text{B}} = & -\eta_1^{\text{B}} c_1^{(31)} \left[\frac{\partial v_i^{(1)}}{\partial x_k} + \frac{\partial v_k^{(1)}}{\partial x_i} - \frac{2}{3} \delta_{ik} \frac{\partial v_j^{(1)}}{\partial x_j} \right] - \eta_2^{\text{B}} c_2^{(31)} \left[\frac{\partial v_i^{(2)}}{\partial x_k} + \frac{\partial v_k^{(2)}}{\partial x_i} - \frac{2}{3} \delta_{ik} \frac{\partial v_j^{(2)}}{\partial x_j} \right] \\ & + (1-\eta_0) c_3^{(31)} \left[\frac{\partial u_i^{\text{A}}}{\partial x_k} + \frac{\partial u_k^{\text{A}}}{\partial x_i} - \frac{2}{3} \delta_{ik} \frac{\partial u_j^{\text{A}}}{\partial x_j} \right] \end{aligned} \quad (5.52e)$$

and

$$\begin{aligned} \Gamma_{32}^{\text{B}} = & -\eta_1^{\text{B}} c_1^{(32)} \left[\frac{\partial v_i^{(1)}}{\partial x_k} + \frac{\partial v_k^{(1)}}{\partial x_i} - \frac{2}{3} \delta_{ik} \frac{\partial v_j^{(1)}}{\partial x_j} \right] - \eta_2^{\text{B}} c_2^{(32)} \left[\frac{\partial v_i^{(2)}}{\partial x_k} + \frac{\partial v_k^{(2)}}{\partial x_i} - \frac{2}{3} \delta_{ik} \frac{\partial v_j^{(2)}}{\partial x_j} \right] \\ & + (1-\eta_0) c_3^{(32)} \left[\frac{\partial u_i^{\text{A}}}{\partial x_k} + \frac{\partial u_k^{\text{A}}}{\partial x_i} - \frac{2}{3} \delta_{ik} \frac{\partial u_j^{\text{A}}}{\partial x_j} \right] \end{aligned} \quad (5.52f)$$

where the c 's are dimensionless constants. If one assumes the no-slip condition at the pore scale interfaces, these integrals are not all independent. The relationships between the various integrals as a consequence of such a condition are given in table 5.1.

Interface	Boundary Condition	Integral Relation	Constants
Fluid 1/ Solid	$v_1 = -\frac{\partial}{\partial x} u_1$	$I_{1s}^B = -\frac{\partial}{\partial x} I_{s1}^B$	$c_1^{(1s)} = c_1^{(s1)}, c_2^{(1s)} = -c_2^{(s1)},$ $c_3^{(1s)} = c_3^{(s1)}$
Fluid 2/ Solid	$v_2 = -\frac{\partial}{\partial x} u_2$	$I_{2s}^B = -\frac{\partial}{\partial x} I_{s2}^B$	$c_1^{(2s)} = -c_1^{(s2)}, c_2^{(2s)} = c_2^{(s2)},$ $c_3^{(2s)} = c_3^{(s2)}$
Fluid 1/ Fluid 2	$v_1 = -v_2$	$I_{12}^B = -I_{21}^B$	$c_1^{(12)} = c_1^{(21)}, c_2^{(12)} = c_2^{(21)},$ $c_3^{(12)} = -c_3^{(21)}$

Table 5.1 Relationships between area integrals as a consequence of the no-slip boundary condition at the pore scale interfaces.

The sum of the integral I_{s1}^B and I_{s2}^B should represent the alteration in shear deformation of the solid component, namely

$$\begin{aligned}
 I_{1s}^B + I_{2s}^B = & \\
 -\eta_{1s} \left[c_1^{(s1)} + c_1^{(s2)} \right] & \left[\frac{\partial u_1^{(1)}}{\partial x_k} + \frac{\partial u_1^{(1)}}{\partial x_l} - \frac{2}{3} \delta_{kl} \frac{\partial u_1^{(1)}}{\partial x_j} \right] - \eta_{2s} \left[c_2^{(s1)} - c_2^{(s2)} \right] \left[\frac{\partial u_1^{(2)}}{\partial x_k} + \frac{\partial u_1^{(2)}}{\partial x_l} - \frac{2}{3} \delta_{kl} \frac{\partial u_1^{(2)}}{\partial x_j} \right] \\
 & + (1 - \eta_{1s}) \left[c_3^{(s1)} + c_3^{(s2)} \right] \left[\frac{\partial u_1^{(1)}}{\partial x_k} + \frac{\partial u_1^{(1)}}{\partial x_l} - \frac{2}{3} \delta_{kl} \frac{\partial u_1^{(1)}}{\partial x_j} \right] \quad (5.53)
 \end{aligned}$$

The first two terms in equation (5.53) are proportional to fluid displacement and as argued in chapter 4 these terms must be zero, hence

$$c_1^{(s1)} = -c_1^{(s2)} \quad (5.54)$$

and

$$c_2^{(s1)} = -c_2^{(s2)} \quad (5.55)$$

with the resulting expansion

$$\Gamma_{1s}^0 + \Gamma_{2s}^0 = (1 - \eta_0)(c_2^{(s1)} + c_2^{(s2)}) \left[\frac{\partial \bar{u}_1^0}{\partial x_k} + \frac{\partial \bar{u}_k^0}{\partial x_1} - \frac{2}{3} \delta_{ik} \frac{\partial \bar{u}_j^0}{\partial x_j} \right] \quad (5.56)$$

Substituting expression (5.56) into the equation of motion for the solid (5.48) and combining shear terms one may define a macroscopic shear modulus, μ_M , as

$$\mu_M = (1 - \eta_0) \mu_d (1 + c_2^{(s1)} + c_2^{(s2)}) \quad (5.57)$$

as was performed in chapter 4. An estimate of this macroscopic shear modulus may be obtained through a quasi-static shear measurement or a Young's modulus type experiment.

Using the relationships between the constants given in table 5.1 and equations (5.54) and (5.55) the general expansion for fluid one is given by

$$\begin{aligned} \Gamma_{1s}^0 + \Gamma_{12}^0 = & \eta_0 (c_1^{(1s)} + c_1^{(12)}) \left[\frac{\partial \bar{v}_1^{(1)}}{\partial x_k} + \frac{\partial \bar{v}_k^{(1)}}{\partial x_1} - \frac{2}{3} \delta_{ik} \frac{\partial \bar{v}_j^{(1)}}{\partial x_j} \right] + \eta_0 (c_2^{(1s)} + c_2^{(12)}) \left[\frac{\partial \bar{v}_1^{(2)}}{\partial x_k} + \frac{\partial \bar{v}_k^{(2)}}{\partial x_1} - \frac{2}{3} \delta_{ik} \frac{\partial \bar{v}_j^{(2)}}{\partial x_j} \right] \\ & - (1 - \eta_0)(c_2^{(s1)} + c_2^{(s2)}) \frac{\partial}{\partial t} \left[\frac{\partial \bar{u}_1^0}{\partial x_k} + \frac{\partial \bar{u}_k^0}{\partial x_1} - \frac{2}{3} \delta_{ik} \frac{\partial \bar{u}_j^0}{\partial x_j} \right] \end{aligned} \quad (5.58)$$

and for fluid two the general expansion is given by,

$$\begin{aligned} \Gamma_{2s}^0 + \Gamma_{21}^0 = & -\eta_0 (c_1^{(1s)} + c_1^{(12)}) \left[\frac{\partial \bar{v}_1^{(1)}}{\partial x_k} + \frac{\partial \bar{v}_k^{(1)}}{\partial x_1} - \frac{2}{3} \delta_{ik} \frac{\partial \bar{v}_j^{(1)}}{\partial x_j} \right] + \eta_0 (c_2^{(1s)} + c_2^{(12)}) \left[\frac{\partial \bar{v}_1^{(2)}}{\partial x_k} + \frac{\partial \bar{v}_k^{(2)}}{\partial x_1} - \frac{2}{3} \delta_{ik} \frac{\partial \bar{v}_j^{(2)}}{\partial x_j} \right] \\ & - (1 - \eta_0)(c_2^{(s2)} - c_2^{(s1)}) \frac{\partial}{\partial t} \left[\frac{\partial \bar{u}_1^0}{\partial x_k} + \frac{\partial \bar{u}_k^0}{\partial x_1} - \frac{2}{3} \delta_{ik} \frac{\partial \bar{u}_j^0}{\partial x_j} \right] \end{aligned} \quad (5.59)$$

Substituting the expansion (5.58) into the equation of motion (5.46) for fluid one, the first term may be combined with the existing shear term so that an effective viscosity $\mu_{\text{eff}}^{(1)}$, (due to distribution) may be defined:

$$\mu_{\text{eff}}^{(1)} = \eta_1^0 \mu_1 (1 + c_1^{(1s)} + c_1^{(12)}). \quad (5.60)$$

The second term represents the shear stress induced into fluid one due to the rate of shearing of fluid two and the third term represents the shear stress induced in fluid one due to the rate of shearing of the solid.

Similarly for fluid two, an effective viscosity $\mu_{\text{eff}}^{(2)}$, (due to distribution) is defined:

$$\mu_{\text{eff}}^{(2)} = \eta_2^0 \mu_2 (1 + c_2^{(1s)} + c_2^{(12)}) . \quad (5.61)$$

To this point, the expansions for the "B" group of integrals may be written in a form such that there is a minimum of four independent parameters introduced. These are $\mu_{\text{eff}}^{(1)}$, $\mu_{\text{eff}}^{(2)}$, μ_M and $c_1^{(12)}$. The coefficient $c_1^{(12)}$ represents additional shear stresses, induced into the fluids due to deformation of the interface between the fluids as a consequence of solid shearing. For this reason, the coefficient appears with opposite sign in the fluid equations of motion. It will be shown that in the limit as the two fluids become identical, the above fluid integrals (5.58) and (5.59) may added together and the resulting shear generalization is the same as presented in chapter 4.

The "C" group of area integrals arise from the volume averaging of the equations of motion. These area integrals represent the force per unit volume exerted by one component on the other across the interfaces due to any motion. Following Eastwood (1991) these surface integrals are decomposed in a more general form than originally considered by de la Cruz & Spanos (1999b):

$$\mathbf{f}_{1i} = \left[Q_1^{(s1)} \overline{v_i^{(s)}} - Q_1^{(s1)} \overline{v_i^{(1)}} - Q_2^{(s1)} \overline{v_i^{(2)}} \right] + \left[\rho_1^{(s1)} \frac{\partial}{\partial x} \overline{v_i^{(s)}} - \rho_1^{(s1)} \frac{\partial}{\partial x} \overline{v_i^{(1)}} - \rho_2^{(s1)} \frac{\partial}{\partial x} \overline{v_i^{(2)}} \right] \quad (5.62a)$$

$$\mathbf{f}_{1r} = \left[Q_1^{(1s)} \overline{v_i^{(1)}} - Q_2^{(1s)} \overline{v_i^{(2)}} - Q_1^{(1s)} \overline{v_i^{(s)}} \right] + \left[\rho_1^{(1s)} \frac{\partial}{\partial x} \overline{v_i^{(1)}} - \rho_2^{(1s)} \frac{\partial}{\partial x} \overline{v_i^{(2)}} - \rho_1^{(1s)} \frac{\partial}{\partial x} \overline{v_i^{(s)}} \right] \quad (5.62b)$$

$$\Gamma_{12}^c = [Q_1^{(12)} \bar{v}_1^{(1)} - Q_2^{(12)} \bar{v}_1^{(2)} - Q_6^{(12)} \bar{v}_1^{(s)}] + \left[\rho_1^{(12)} \frac{\partial \bar{v}_1^{(1)}}{\partial t} - \rho_2^{(12)} \frac{\partial \bar{v}_1^{(2)}}{\partial t} - \rho_s^{(12)} \frac{\partial \bar{v}_1^{(s)}}{\partial t} \right] \quad (5.62c)$$

$$\Gamma_{21}^c = [Q_2^{(21)} \bar{v}_1^{(2)} - Q_1^{(21)} \bar{v}_1^{(1)} - Q_6^{(21)} \bar{v}_1^{(s)}] + \left[\rho_2^{(21)} \frac{\partial \bar{v}_1^{(2)}}{\partial t} - \rho_1^{(21)} \frac{\partial \bar{v}_1^{(1)}}{\partial t} - \rho_s^{(21)} \frac{\partial \bar{v}_1^{(s)}}{\partial t} \right] \quad (5.62d)$$

$$\Gamma_{s2}^c = [Q_6^{(s2)} \bar{v}_1^{(s)} - Q_1^{(s2)} \bar{v}_1^{(1)} - Q_2^{(s2)} \bar{v}_1^{(2)}] + \left[\rho_s^{(s2)} \frac{\partial \bar{v}_1^{(s)}}{\partial t} - \rho_1^{(s2)} \frac{\partial \bar{v}_1^{(1)}}{\partial t} - \rho_2^{(s2)} \frac{\partial \bar{v}_1^{(2)}}{\partial t} \right] \quad (5.62e)$$

$$\Gamma_{2s}^c = [Q_6^{(2s)} \bar{v}_1^{(2)} - Q_1^{(2s)} \bar{v}_1^{(1)} - Q_2^{(2s)} \bar{v}_1^{(s)}] + \left[\rho_s^{(2s)} \frac{\partial \bar{v}_1^{(2)}}{\partial t} - \rho_1^{(2s)} \frac{\partial \bar{v}_1^{(1)}}{\partial t} - \rho_2^{(2s)} \frac{\partial \bar{v}_1^{(s)}}{\partial t} \right] \quad (5.62f)$$

In order to obtain the total force per unit volume on the solid we must add the force exerted due to fluid one (5.62a) and the force due to fluid two (5.62e); thus we obtain

$$\begin{aligned} \Gamma_s^c &= \Gamma_{s1}^c + \Gamma_{s2}^c \\ &= Q_6^{(s)} \bar{v}_1^{(s)} - Q_1^{(s)} \bar{v}_1^{(1)} - Q_2^{(s)} \bar{v}_1^{(2)} + \rho_s^{(s)} \frac{\partial \bar{v}_1^{(s)}}{\partial t} - \rho_1^{(s)} \frac{\partial \bar{v}_1^{(1)}}{\partial t} - \rho_2^{(s)} \frac{\partial \bar{v}_1^{(2)}}{\partial t} \end{aligned} \quad (5.63)$$

and similarly, for fluid one, we have

$$\begin{aligned} \Gamma_1^c &= \Gamma_{1s}^c + \Gamma_{12}^c \\ &= Q_1^{(1)} \bar{v}_1^{(1)} - Q_2^{(1)} \bar{v}_1^{(2)} - Q_6^{(1)} \bar{v}_1^{(s)} + \rho_1^{(1)} \frac{\partial \bar{v}_1^{(1)}}{\partial t} - \rho_2^{(1)} \frac{\partial \bar{v}_1^{(2)}}{\partial t} - \rho_s^{(1)} \frac{\partial \bar{v}_1^{(s)}}{\partial t} \end{aligned} \quad (5.64)$$

and for fluid two

$$\begin{aligned} \Gamma_2^c &= \Gamma_{2s}^c + \Gamma_{21}^c \\ &= Q_2^{(2)} \bar{v}_1^{(2)} - Q_1^{(2)} \bar{v}_1^{(1)} - Q_6^{(2)} \bar{v}_1^{(s)} + \rho_2^{(2)} \frac{\partial \bar{v}_1^{(2)}}{\partial t} - \rho_1^{(2)} \frac{\partial \bar{v}_1^{(1)}}{\partial t} - \rho_s^{(2)} \frac{\partial \bar{v}_1^{(s)}}{\partial t} \end{aligned} \quad (5.65)$$

where

$$Q_j^{(k)} = \sum_l Q_j^{(kl)} \quad \begin{array}{l} ; j, k = s, 1, 2 \\ ; l = s, 1, 2 ; l \neq k \end{array} \quad (5.66)$$

and

$$\rho_j^{(k)} = \sum_l \rho_j^{(l)} \quad ; j, k = s, 1, 2 \quad ; l = s, 1, 2 ; l \neq k \quad (5.67)$$

These forces should be invariant in different reference frames (Galilean invariance). For example let us consider the body force represented by I_s^C . If the reference frame is chosen to move at say the solid velocity, $\bar{v}^{(s)}$, then I_s^C is

$$I_s^C = -Q_s^{(s)}(\bar{v}_i^{(1)} - \bar{v}_i^{(s)}) - Q_2^{(s)}(\bar{v}_i^{(2)} - \bar{v}_i^{(s)}) + \rho_s^{(s)} \frac{\partial \bar{v}_i^{(s)}}{\partial x} - \rho_1^{(s)} \frac{\partial \bar{v}_i^{(1)}}{\partial x} - \rho_2^{(s)} \frac{\partial \bar{v}_i^{(2)}}{\partial x} \quad (5.68)$$

If the frame is moving at the fluid one velocity, $\bar{v}^{(1)}$, then I_s^C is

$$I_s^C = -Q_s^{(s)}(\bar{v}_i^{(s)} - \bar{v}_i^{(1)}) - Q_2^{(s)}(\bar{v}_i^{(2)} - \bar{v}_i^{(1)}) + \rho_s^{(s)} \frac{\partial \bar{v}_i^{(s)}}{\partial x} - \rho_1^{(s)} \frac{\partial \bar{v}_i^{(1)}}{\partial x} - \rho_2^{(s)} \frac{\partial \bar{v}_i^{(2)}}{\partial x} \quad (5.69)$$

The two expressions (5.68) and (5.69) however must be equal and the conditions imposed on the coefficients are

$$Q_s^{(s)} = Q_s^{(s)} + Q_s^{(s)} \quad (5.70a)$$

Using the same reasoning for the forces represented by I_1^C and I_2^C results in the following equalities:

$$Q_1^{(1)} = Q_1^{(1)} + Q_1^{(1)} \quad (5.70b)$$

and

$$Q_2^{(2)} = Q_2^{(2)} + Q_2^{(2)} \quad (5.70c)$$

Assuming a similar invariance for accelerated frames yields

$$\rho_s^{(s)} = \rho_1^{(s)} + \rho_2^{(s)} \quad (5.71a)$$

$$\rho_1^{(1)} = \rho_s^{(1)} + \rho_2^{(1)} \quad (5.71b)$$

and

$$\rho_2^{(2)} = \rho_i^{(2)} + \rho_1^{(2)} . \quad (5.71c)$$

In the most general situation, as discussed above, the interaction represented by the "C" group of integrals will introduce six Q's and six ρ 's.

The conditions imposed between the various "C" integrals due to continuity of stress at the pore scale interfaces are summarized in table 5.2. The boundary condition between fluid one and fluid two is for the case where the two fluids are miscible. For immiscible fluids, this boundary condition is dependent on surface tension. The surface tension term must be decomposed in terms of the macroscopic vectors present in the macroscopic description. Unfortunately this decomposition in the most general sense precludes further simplification at this time. Therefore, if surface tension is important we have one less relation between area integrals.

The relationships presented in table 5.2 can be combined to obtain two additional relationships between macroscopic parameters

$$-Q_2^{(1)} - Q_i^{(1)} + Q_1^{(2)} + Q_1^{(s)} = 0 \quad (5.72)$$

and

$$-Q_1^{(2)} - Q_i^{(2)} + Q_2^{(1)} + Q_2^{(s)} = 0 \quad (5.73)$$

Assuming that surface tension is negligible does not alter the form of the equations but does reduce the number of independent Q's to four through the use of relations (5.72) and (5.73). Similar relations exist for the ρ 's. For the remainder of this chapter we will assume that the fluids are immiscible and therefore relations (5.72) and (5.73) will not be used.

Interface	Boundary Condition	Integral Relation	Constants
Fluid 1/ Solid	$\sigma_{ik}^s n_k = (\sigma_{ik}^{(1)} - p_1 \delta_{ik}) n_k$	$\Gamma_{s1}^C = -\Gamma_{1s}^C$	$Q_s^{(s1)} = -Q_s^{(1s)}, Q_1^{(s1)} = -Q_1^{(1s)}$ $Q_2^{(s1)} = -Q_2^{(1s)}, \rho_s^{(s1)} = \rho_s^{(1s)}$ $\rho_1^{(s1)} = \rho_1^{(1s)}, \rho_2^{(s1)} = -\rho_2^{(1s)}$
Fluid 2/ Solid	$\sigma_{ik}^s n_k = (\sigma_{ik}^{(2)} - p_2 \delta_{ik}) n_k$	$\Gamma_{s2}^C = -\Gamma_{2s}^C$	$Q_s^{(s2)} = -Q_s^{(2s)}, Q_1^{(s2)} = -Q_1^{(2s)}$ $Q_2^{(s2)} = -Q_2^{(2s)}, \rho_s^{(s2)} = \rho_s^{(2s)}$ $\rho_1^{(s2)} = -\rho_1^{(2s)}, \rho_2^{(s2)} = \rho_2^{(2s)}$
Fluid 1/ Fluid 2*	$\begin{aligned} &(\sigma_{ik}^{(1)} - p_1 \delta_{ik}) n_k = \\ &(\sigma_{ik}^{(2)} - p_2 \delta_{ik}) n_k \end{aligned}$	$\Gamma_{12}^C = -\Gamma_{21}^C$	$Q_s^{(12)} = -Q_s^{(21)}, Q_1^{(12)} = -Q_1^{(21)}$ $Q_2^{(12)} = -Q_2^{(21)}, \rho_s^{(12)} = -\rho_s^{(21)}$ $\rho_1^{(12)} = \rho_1^{(21)}, \rho_2^{(12)} = \rho_2^{(21)}$

Table 5.2 Relationships between area integrals as a consequence of the continuity of stress boundary condition at the pore scale interfaces. The conditions at the fluid 1 - fluid 2 interface are valid only if the fluids are miscible.

Selective adhesion between solid and one of the fluids is a fairly common observation. It is of interest to examine if such wettability of the solid can reduce the number of independent parameters in the above expansions. The assumption that the solid is in contact with only fluid one requires that all I_{s2} and I_{2s} integrals vanish. This does not alter the expansions for the "A" group of integrals. For the "B" group of integrals we obtain

$$\Gamma_{2s}^B = -\frac{\partial}{\partial t} \Gamma_{s2}^B = 0 \quad (5.74)$$

which in turn requires

$$c_1^{(2s)} = -c_1^{(s2)} = c_2^{(2s)} = c_2^{(s2)} = c_3^{(2s)} = c_3^{(s2)} = 0 \quad (5.75)$$

Condition (5.54) leads to

$$-c_1^{(s2)} = c_1^{(s1)} = c_1^{(1s)} = 0 \quad (5.76)$$

while condition (5.55) gives

$$-c_2^{(s2)} = c_2^{(s1)} = -c_2^{(1s)} = 0 \quad (5.77)$$

The assumption that fluid one wets the solid alters the expressions for the effective coefficients to be

$$\mu_M = (1 - \eta_o)\mu_s(1 + c_1^{(s1)}) \quad (5.78a)$$

$$\mu_{\text{eff}}^{(1)} = \eta_1^o \mu_1(1 + c_1^{(12)}) \quad (5.78b)$$

and

$$\mu_{\text{eff}}^{(2)} = \eta_2^o \mu_2(1 + c_2^{(12)}) \quad (5.78c)$$

but does not reduce the number of independent coefficients.

The wettability assumption also imposes

$$\Gamma_{s2}^C = \Gamma_{2s}^C = 0 \quad (5.79)$$

which produces the following constraints on the coefficients:

$$Q_s^{(s2)} = Q_1^{(s2)} = Q_2^{(s2)} = 0 \quad (5.80a)$$

$$Q_s^{(2s)} = Q_1^{(2s)} = Q_2^{(2s)} = 0 \quad (5.80b)$$

$$\rho_s^{(s2)} = \rho_1^{(s2)} = \rho_2^{(s2)} = 0 \quad (5.80c)$$

and

$$\rho_s^{(2s)} = \rho_1^{(2s)} = \rho_2^{(2s)} = 0 . \quad (5.80d)$$

The constraints given by (5.80) do not reduce the number of independent coefficients and we still have six Q 's and six ρ 's .

5.3.4 Conclusions

Volume averaging is used to construct a system of equations to describe low frequency wave propagation through a porous medium saturated by two fluids. The continuity equations are reproduced exactly. Volume averaging the equations of motion and the constitutive equations introduce area integrals which must be evaluated.

The area integrals produced as a consequence of volum. averaging represent the interaction between the phases. Relationships between these various integrals are dependent on the pore scale boundary conditions. The integrals have been divided into three groups denoted by A, B, and C. The first group of area integrals are scalar and introduce the porosity and volume fraction of the porous system as dynamic variables which warrant further discussion. The second group of area integrals are second order tensors, and represent additional shear deformations due to the interactions and distribution of the phases. The most general expansion of these integrals introduces four independent macroscopic parameters. The assumption of having a solid matrix only contacted by one of the fluids does not reduce the number of independent parameters. The third group of area integrals discussed are vector quantities and represent the force per unit volume exerted by one component on the other across the interfaces due to any motion. The most general expansion introduces six independent parameters, Q 's, proportional to relative velocity of the components and six independent parameters, ρ 's, proportional to relative accelerations of the components. If it is assumed that surface tension is negligible then the number of independent Q 's can be reduced to four as well as the number of independent ρ 's.

5.4 General Equations for Wave Propagation in a Porous Medium Saturated by Two Fluids

The system of equations, governing low frequency wave propagation in a porous medium saturated by two fluids, as described in the previous sections of this chapter are as follows:

Volume Fraction Equation

$$\eta = \eta_1 + \eta_2 \quad (5.81)$$

Equations of Motion

$$\begin{aligned} (1-\eta_0)\rho_f \frac{\partial^2 \bar{u}_i^s}{\partial t^2} &= K_s \frac{\partial}{\partial x_k} \left[(1-\eta_0) \frac{\partial \bar{u}_j^s}{\partial x_j} \delta_{ik} - (\eta-\eta_0) \right] \delta_{ik} + Q_1^{(s)} (\bar{v}_i^{(1)} - \bar{v}_i^{(s)}) \\ &+ \mu_{sf} \frac{\partial}{\partial x_k} \left[\left(\frac{\partial \bar{u}_i^s}{\partial x_k} + \frac{\partial \bar{u}_k^s}{\partial x_i} - \frac{2}{3} \frac{\partial \bar{u}_j^s}{\partial x_j} \delta_{ik} \right) \right] + Q_2^{(s)} (\bar{v}_i^{(2)} - \bar{v}_i^{(s)}) \\ &+ \rho_1^{(s)} \frac{\partial}{\partial t} (\bar{v}_i^{(1)} - \bar{v}_i^{(s)}) + \rho_2^{(s)} \frac{\partial}{\partial t} (\bar{v}_i^{(2)} - \bar{v}_i^{(s)}) \end{aligned} \quad (5.82)$$

$$\begin{aligned} \eta_1 \rho_1 \frac{\partial}{\partial t} \bar{v}_i^{(1)} &= \zeta_1 \frac{\partial}{\partial x_k} \left[\eta_1 \frac{\partial \bar{v}_j^{(1)}}{\partial x_j} \delta_{ik} + \frac{\partial \eta_1}{\partial t} \right] + \mu_{sf}^{(1)} \frac{\partial}{\partial x_k} \left[\left(\frac{\partial \bar{v}_i^{(1)}}{\partial x_k} + \frac{\partial \bar{v}_k^{(1)}}{\partial x_i} - \frac{2}{3} \frac{\partial \bar{v}_j^{(1)}}{\partial x_j} \delta_{ik} \right) \right] \\ &- \eta_1 \frac{\partial}{\partial x_i} \bar{p}_1 - \eta_1 \mu_1 \left(\frac{\mu_{sf}^{(2)}}{\eta_2 \mu_2} - 1 \right) \frac{\partial}{\partial x_k} \left[\frac{\partial \bar{v}_i^{(2)}}{\partial x_k} + \frac{\partial \bar{v}_k^{(2)}}{\partial x_i} - \frac{2}{3} \delta_{ik} \frac{\partial \bar{v}_j^{(2)}}{\partial x_j} \right] \\ &- (1-\eta_0) \mu_1 (c_3^{(s1)} + c_3^{(s2)}) \frac{\partial}{\partial x_k} \frac{\partial}{\partial t} \left[\frac{\partial \bar{u}_i^s}{\partial x_k} + \frac{\partial \bar{u}_k^s}{\partial x_i} - \frac{2}{3} \delta_{ik} \frac{\partial \bar{u}_j^s}{\partial x_j} \right] + Q_1^{(1)} (\bar{v}_i^{(s)} - \bar{v}_i^{(1)}) \\ &+ Q_2^{(1)} (\bar{v}_i^{(2)} - \bar{v}_i^{(1)}) + \rho_1^{(1)} \frac{\partial}{\partial t} (\bar{v}_i^{(s)} - \bar{v}_i^{(1)}) + \rho_2^{(1)} \frac{\partial}{\partial t} (\bar{v}_i^{(2)} - \bar{v}_i^{(1)}) \end{aligned} \quad (5.83)$$

$$\begin{aligned}
\eta_2^0 \rho_2^0 \frac{\partial}{\partial t} \bar{v}_i^{(2)} &= \xi_2 \frac{\partial}{\partial x_k} \left[\eta_2^0 \frac{\partial \bar{v}_j^{(2)}}{\partial x_j} \delta_{ik} + \frac{\partial \eta_2}{\partial t} \right] + \mu_{eff}^{(2)} \frac{\partial}{\partial x_k} \left[\left(\frac{\partial \bar{v}_i^{(2)}}{\partial x_k} + \frac{\partial \bar{v}_k^{(2)}}{\partial x_i} - \frac{2}{3} \frac{\partial \bar{v}_j^{(2)}}{\partial x_j} \delta_{ik} \right) \right] \\
&\quad - \eta_2^0 \frac{\partial}{\partial x_i} \bar{p}_2 - \eta_1^0 \mu_2 \left(\frac{\mu_{eff}^{(1)}}{\eta_1^0 \mu_1} - 1 \right) \frac{\partial}{\partial x_k} \left[\frac{\partial \bar{v}_i^{(1)}}{\partial x_k} + \frac{\partial \bar{v}_k^{(1)}}{\partial x_i} - \frac{2}{3} \delta_{ik} \frac{\partial \bar{v}_j^{(1)}}{\partial x_j} \right] \\
&\quad - (1 - \eta_0) \mu_2 (c_i^{(2)} - c_i^{(12)}) \frac{\partial}{\partial x_k} \frac{\partial}{\partial t} \left[\frac{\partial \bar{u}_i^s}{\partial x_k} + \frac{\partial \bar{u}_k^s}{\partial x_i} - \frac{2}{3} \delta_{ik} \frac{\partial \bar{u}_j^s}{\partial x_j} \right] + Q_i^{(2)} (\bar{v}_i^{(1)} - \bar{v}_i^{(2)}) \\
&\quad + Q_i^{(2)} (\bar{v}_i^{(1)} - \bar{v}_i^{(2)}) + \rho_s^{(2)} \frac{\partial}{\partial t} (\bar{v}_i^{(1)} - \bar{v}_i^{(2)}) + \rho_1^{(2)} \frac{\partial}{\partial t} (\bar{v}_i^{(1)} - \bar{v}_i^{(2)})
\end{aligned} \tag{5.84}$$

Equations of continuity

$$\frac{(\bar{\rho}_s - \rho_s^0)}{\rho_s^0} - \frac{(\eta - \eta_0)}{(1 - \eta_0)} + \frac{\partial \bar{u}_i^s}{\partial x_i} = 0 \tag{5.85}$$

$$\frac{1}{\rho_1^0} \frac{\partial \bar{\rho}_1}{\partial t} + \frac{1}{\eta_1^0} \frac{\partial}{\partial t} \eta_1 + \frac{\partial \bar{v}_i^{(1)}}{\partial x_i} = 0 \tag{5.86}$$

$$\frac{1}{\rho_2^0} \frac{\partial \bar{\rho}_2}{\partial t} + \frac{1}{\eta_2^0} \frac{\partial}{\partial t} \eta_2 + \frac{\partial \bar{v}_i^{(2)}}{\partial x_i} = 0 \tag{5.87}$$

Pressure Equations

$$\frac{1}{K_s} (\bar{p}_s - p_f) = -\nabla \cdot \bar{u}_s + \frac{(\eta - \eta_0)}{(1 - \eta_0)} \tag{5.88}$$

$$\frac{1}{K_1} \frac{\partial \bar{p}_1}{\partial t} = -\nabla \cdot \bar{v}_1 - \frac{1}{\eta_1^0} \frac{\partial}{\partial t} \eta_1 \tag{5.89}$$

$$\frac{1}{K_2} \frac{\partial \bar{p}_2}{\partial t} = -\nabla \cdot \bar{v}_2 - \frac{1}{\eta_2^0} \frac{\partial}{\partial t} \eta_2 \tag{5.90}$$

Porosity equation

$$\frac{\partial \eta}{\partial t} = \delta_0 \nabla \cdot \bar{v}_s - \delta_1 \nabla \cdot \bar{v}_1 - \delta_2 \nabla \cdot \bar{v}_2 \tag{5.91}$$

Saturation (volume fraction) equation

$$\frac{\partial \eta_1}{\partial t} = \delta_s \nabla \cdot \bar{v}_s + \delta_2 \nabla \cdot \bar{v}_2 - \delta_1 \nabla \cdot \bar{v}_1 \quad (5.92)$$

In order to obtain a complete set of equations describing the propagation of a dilatational wave a porosity equation (5.91) and a saturation equation (5.92) must be introduced. The porosity equation (5.91) for a porous medium saturated by two fluids contains three macroscopic parameters in its most general form. Similar to the case considered in chapter 4, this equation should be regarded as a process dependent statement rather than an actual equation of state for the porous medium. Suitable values of δ_s , δ_1 , and δ_2 will depend on the process considered. The saturation equation is also required because the relative proportion of fluids may change during deformation. Again this equation should be regarded as a process dependent statement. The use of such a statement in the description of capillary pressure (Spanos *et al.*, 1993) for incompressible flow of two fluids illustrates that the actual values for δ_s , δ_1 , and δ_2 will depend on the process.

5.5 Special Limiting Cases of General Equations

Given the complexity of the general system of equations it is necessary to check the validity in various limiting cases. The first case to consider is when the volume fraction of one of the fluids, say fluid two, goes to zero, i.e.

$$\eta_2 \rightarrow 0 \quad (5.93)$$

and from equation (5.79) it is required that

$$\eta_1 \rightarrow \eta. \quad (5.94)$$

In this limit, the system of equations (5.81) to (5.92) should reduce to the system of equations (4.63) to (4.68) governing wave propagation in a porous medium saturated by

one fluid. As the volume fraction of fluid two goes to zero the interfaces in contact with fluid two must also vanish, which requires that all area integrals over such interfaces be zero, i.e.

$$I_{12}^k, I_{21}^k, I_{12}^k, I_{21}^k = 0 \quad ; k = A, B, C . \quad (5.95)$$

The material shear modulus is modified to be

$$\mu_M = (1-\eta_0)\mu_s(1+c_s^{(s1)}) , \quad (5.96)$$

the effective viscosity of fluid one becomes

$$\mu_{\text{eff}}^{(1)} = \eta_1^0 \mu_1 , \quad (5.97)$$

and the effective fluid viscosity of fluid two (5.61) tends to zero. All equations for fluid two can be shown to vanish. In this limiting case, the macroscopic continuity equation and pressure equation for the solid remain unchanged and are the same as derived in chapter 4. The solid equation of motion (5.82) may be written as

$$\begin{aligned} (1-\eta_0)\rho_2^s \frac{\partial^2 \bar{u}_i^s}{\partial t^2} = & K_s \frac{\partial}{\partial x_k} \left[(1-\eta_0) \frac{\partial \bar{u}_j^s}{\partial x_j} \delta_{ik} - (\eta-\eta_0) \right] \delta_{ik} + Q_1^{(s)} (\bar{v}_i^{(1)} - \bar{v}_i^{(s)}) \\ & + \mu_M \frac{\partial}{\partial x_k} \left[\left(\frac{\partial \bar{u}_i^s}{\partial x_k} + \frac{\partial \bar{u}_k^s}{\partial x_i} - \frac{2}{3} \frac{\partial \bar{u}_j^s}{\partial x_j} \delta_{ik} \right) \right] + \rho_1^{(s)} \frac{\partial}{\partial t} (\bar{v}_i^{(1)} - \bar{v}_i^{(s)}) \end{aligned} \quad (5.98)$$

but requires that $Q_2^{(s)} = 0$ and $\rho_2^{(s)} = 0$. This simply means that these parameters must have a saturation dependence. The macroscopic continuity equation and pressure equation for fluid one become the same as equations (4.66) and (4.68) for the single fluid case considered in chapter 4. The equation of motion (5.81) may be written in a form like that of equation (4.64), i.e.

$$\begin{aligned}
\eta_o \rho_1^o \frac{\partial \bar{v}_i^{(1)}}{\partial t} = & \xi_1 \frac{\partial}{\partial x_k} \left[\eta_o \frac{\partial \bar{v}_j^{(1)}}{\partial x_j} \delta_{ik} + \frac{\partial \eta_o}{\partial t} \right] + Q_2^{(1)} (\bar{v}_i^{(2)} \cdot \bar{v}_i^{(1)}) + \rho_2^{(1)} \frac{\partial}{\partial t} (\bar{v}_i^{(2)} \cdot \bar{v}_i^{(1)}) \\
& - \eta_o \frac{\partial \bar{p}_1}{\partial x_i} + \eta_o \mu_1 \frac{\partial}{\partial x_k} \left[\left(\frac{\partial \bar{v}_i^{(1)}}{\partial x_k} + \frac{\partial \bar{v}_k^{(1)}}{\partial x_i} - \frac{2}{3} \frac{\partial \bar{v}_j^{(1)}}{\partial x_j} \delta_{ik} \right) \right] \\
& - \frac{\mu_1}{\mu_2} (\mu_{21} - (1-\eta_o)\mu_o) \frac{\partial}{\partial x_k} \frac{\partial}{\partial t} \left[\frac{\partial \bar{u}_i^2}{\partial x_k} + \frac{\partial \bar{u}_k^2}{\partial x_i} - \frac{2}{3} \delta_{ik} \frac{\partial \bar{u}_j^2}{\partial x_j} \right]
\end{aligned} \tag{5.99}$$

by using equation (5.96) and requiring that $Q_2^{(1)} = 0$ and $\rho_2^{(1)} = 0$. Again, this simply implies that these two parameters must depend on the volume fraction of fluid two.

The porosity equation (5.91) and the saturation equation (5.92) should be identical statements and be equivalent to equation (4.71), i.e.

$$\frac{\partial \eta}{\partial t} = \delta_o \nabla \cdot \mathbf{v}_o - \delta_f \nabla \cdot \mathbf{v}_f \quad . \tag{5.100}$$

which simply requires that

$$\delta_o = \delta_s \quad , \tag{5.101a}$$

$$\delta_1 = \delta_1 = \delta_f \quad , \tag{5.101b}$$

and

$$\delta_2 = \delta_2 = 0 \tag{5.101c}$$

in the limit as $\eta_2 \rightarrow 0$.

The second limit which is considered is when the properties of the two fluids approach each other. Again, in this limit, the system of equations (5.82 to 5.92) should reduce to the system of equations (4.63 to 4.68) governing wave propagation in a porous medium saturated by one fluid. In this case the continuity equation (5.85) and the pressure equation (5.88) for the solid is unaltered. Combining the continuity equations for fluid one (5.86) and fluid two (5.87) and letting $\bar{\rho}_1 \rightarrow \bar{\rho}_f$, $\bar{\rho}_2 \rightarrow \bar{\rho}_f$, we have

$$\eta_0 \frac{\partial \bar{p}}{\partial t} + \rho_1^0 \frac{\partial \eta}{\partial t} + \rho_1^0 \left(\eta_1^0 \frac{\partial \bar{v}_1^{(1)}}{\partial x_1} + \eta_2^0 \frac{\partial \bar{v}_1^{(2)}}{\partial x_1} \right) = 0 \quad (5.102)$$

which, when compared to the continuity equation for one fluid, requires the velocities to be related as

$$\eta \bar{v}_1 = \eta_1 \bar{v}_1^{(1)} + \eta_2 \bar{v}_1^{(2)} . \quad (5.103)$$

Combining the pressure equations for the two fluids in a similar fashion requires that the pressures be related as

$$\eta p_1 = \eta_1 p_1 + \eta_2 p_2 . \quad (5.104)$$

The equation of motion for the solid (5.82) can be written as

$$\begin{aligned} (1-\eta_0) \rho_1^0 \frac{\partial^2 \bar{u}_i^s}{\partial t^2} = & K_0 \frac{\partial}{\partial x_k} \left[(1-\eta_0) \frac{\partial \bar{u}_j^s}{\partial x_j} \delta_{ik} - (\eta_1 - \eta_0) \right] \delta_{ik} + (Q_1^{(s)} + Q_2^{(s)}) (\bar{v}_1^{(1)} - \bar{v}_1^{(2)}) \\ & + \mu_M \frac{\partial}{\partial x_k} \left[\left(\frac{\partial \bar{u}_i^s}{\partial x_k} + \frac{\partial \bar{u}_k^s}{\partial x_i} - \frac{2}{3} \frac{\partial \bar{u}_j^s}{\partial x_j} \delta_{ik} \right) \right] + (\rho_1^{(s)} + \rho_2^{(s)}) \frac{\partial}{\partial t} (\bar{v}_1^{(1)} - \bar{v}_1^{(2)}) \end{aligned} \quad (5.105)$$

with the additional constraints

$$\frac{Q_1^{(s)}}{\eta_1} = \frac{Q_2^{(s)}}{\eta_2} \quad (5.106a)$$

and

$$\frac{\rho_1^{(s)}}{\eta_1} = \frac{\rho_2^{(s)}}{\eta_2} . \quad (5.106b)$$

The sum of the equation of motion for fluid one and fluid two may be written as

$$\begin{aligned}
\eta_o \rho_f \frac{\partial}{\partial t} \bar{v}_i^{(n)} = & \xi_r \frac{\partial}{\partial x_k} \left[\eta_o \frac{\partial \bar{v}_j^{(n)}}{\partial x_j} \delta_{ik} + \frac{\partial \eta_o}{\partial t} \right] + \eta_o \mu_r \frac{\partial}{\partial x_k} \left[\left(\frac{\partial \bar{v}_i^{(n)}}{\partial x_k} + \frac{\partial \bar{v}_k^{(n)}}{\partial x_i} - \frac{2}{3} \frac{\partial \bar{v}_j^{(n)}}{\partial x_j} \delta_{ik} \right) \right] \\
& - \eta_o \frac{\partial}{\partial x_i} \bar{p}_r + (Q_s^{(1)} + Q_s^{(2)}) (\bar{v}_i^{(s)} - \bar{v}_i^{(n)}) + (\rho_s^{(1)} + \rho_s^{(2)}) \frac{\partial}{\partial t} (\bar{v}_i^{(s)} - \bar{v}_i^{(n)}) \\
& - \frac{\mu_r}{\mu_s} (\mu_M - (1 - \eta_o) \mu_s) \frac{\partial}{\partial x_k} \frac{\partial}{\partial t} \left[\frac{\partial \bar{u}_i^r}{\partial x_k} + \frac{\partial \bar{u}_k^r}{\partial x_i} - \frac{2}{3} \delta_{ik} \frac{\partial \bar{u}_j^r}{\partial x_j} \right]
\end{aligned} \tag{5.107}$$

using the above velocity (5.103) and pressure (5.104) relations. In this limit the effective viscosities are related as

$$\frac{\mu_{\text{eff}}^{(1)}}{\eta_1} + \frac{\mu_{\text{eff}}^{(2)}}{\eta_2} = \mu_r \tag{5.108}$$

and the mobility coefficients, Q 's, must be related by

$$Q_s^{(1)} + Q_s^{(1)} = \frac{\eta_o}{\eta_1} (Q_s^{(1)} + Q_2^{(1)} - Q_1^{(2)}) = \frac{\eta_o}{\eta_2} (Q_s^{(2)} + Q_1^{(2)} - Q_2^{(1)}) \tag{5.109}$$

which can be reduced to

$$Q_1^{(2)} - Q_2^{(1)} = \frac{\eta_2}{\eta_o} Q_s^{(1)} - \frac{\eta_1}{\eta_o} Q_s^{(2)} \tag{5.110}$$

and, also for the ρ 's,

$$\begin{aligned}
Q_s^{(1)} + Q_s^{(1)} = \frac{\eta_o}{\eta_1} (Q_s^{(1)} + Q_2^{(1)} - Q_1^{(2)}) = \frac{\eta_o}{\eta_2} (Q_s^{(2)} + Q_1^{(2)} - Q_2^{(1)}) \\
\rho_1^{(2)} - \rho_2^{(1)} = \frac{\eta_2}{\eta_o} \rho_s^{(1)} - \frac{\eta_1}{\eta_o} \rho_s^{(2)}
\end{aligned} \tag{5.111}$$

The porosity equation (5.99) can be in the same form as in chapter 4, i.e.,

$$\frac{\partial \eta}{\partial t} = \delta_s \nabla \cdot \bar{v}_s - \delta_f \nabla \cdot \bar{v}_f \tag{5.112}$$

$$\frac{\delta_1}{\eta_1} = \frac{\delta_2}{\eta_2} = \frac{\delta}{\eta_0} . \quad (5.113)$$

Two separate limits have been studied. In both cases, the general system of equations reduces to the case where only one fluid saturates the porous medium. Several relationships between the parameters has been deduced which appear to be valid only in the limits. Given the amount of independent parameters, other limiting cases will have to be addressed in order to obtain a clearer understanding of their relationships. At that time an attempt at describing experimental procedures for their measurement should be carried out.

5.6 Conclusions

Experimental measurements surveyed in the literature indicate that the presence of an additional fluid or incomplete saturation greatly modifies the character of seismic waves propagating through a porous medium. The seismic properties vary with saturation through the entire range; however, the greatest variation in phase velocity and attenuation occur at very low saturation (nearly empty) or near complete saturation. In the very low saturation range, rapid decreases in V_p and V_s and associated increases in Q_p^{-1} and Q_s^{-1} are observed with the addition of a small amount of water. At near complete saturation, the phase velocity and Q^{-1} for the waves depend upon the method by which the sample was saturated. The P-wave appears to exhibit this process dependence more strongly than do the S-waves.

An approximation of the dynamics of porous media saturated by two fluids has been obtained by utilizing a composite fluid model and the equations derived in chapter 4. This involves replacing the the fluid parameters of the single fluid model, the equations presented in chapter 4, with "effective" fluid parameters. The effects on the macroscopic parameters can only be postulated. This composite fluid model contains assumptions such as, surface tension is not important, and the solid matrix is in contact with only one of the fluids. This model should be used to obtain an approximate description of the gross processes and it should not be expected that it be able to describe, for example, the differences in phase velocity due to the method of sample saturation by a simple alteration of the parameters.

A general system of equations was derived for a porous medium consisting of a homogeneous isotropic elastic solid and the pore space filled with two immiscible viscous fluids. The most general expansions were carried out and relationships between parameters were constructed from very general physical requirements. It was assumed however, that the porous matrix has a uniform porosity and that the fluid phases be uniformly distributed in order to avoid the additional macroscopic parameters which are required when porosity gradients or saturation gradients are present.

In order to obtain a complete set of equations describing the propagation of a dilatational wave, a porosity equation (5.91) and a saturation equation (5.92) must be introduced. Similar to the case considered in chapter 4, this equation should be regarded as a process dependent statement. A saturation equation is also required because the relative proportion of fluids may change during deformation. Again this equation should be regarded as a process dependent statement. The use of such a statement in the description of capillary pressure (Spanos, 1993) for incompressible flow of two fluids illustrates that the actual values for ϕ_s , ϕ_1 , and ϕ_2 will depend on the process.

The selective adhesion between solid and one of the fluids is a fairly common observation. An interesting result is that such an assumption (or requirement in some cases) does not reduce the number of independent parameters in the above expansions.

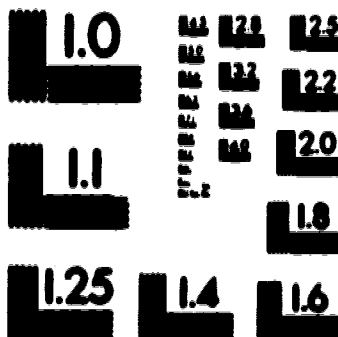
Two separate limits have been studied. In both cases, the general system of equations reduces to the case where only one fluid saturates the porous medium. Given the amount of independent parameters in the general system of equations, other limiting cases will have to be addressed in order to obtain a clearer understanding of their interrelationships. At that time an attempt at describing experimental procedures for their measurement should be carried out.

3

of/de

3

PM-1 3 1/2" x 4" PHOTOGRAPHIC MICROCOPY TARGET
NBS 1910a ANSI/ISO #2 EQUIVALENT



PRECISION™ RESOLUTION TARGETS

CHAPTER 6 CONCLUSIONS

The simplest model utilized for the earth is an elastic solid model. As mentioned previously, for wave propagation, this model predicts the existence of one P wave and one S wave, does not allow for attenuation, and the waves are nondispersive. In the past, attenuation has been added into the single continuum model by allowing the bulk and shear moduli of the medium to be described by complex numbers (simplified viscoelastic approximation). However, it is very difficult to make an association between the measured attenuation and the actual physical mechanism responsible. Furthermore, most physical systems of interest in exploration geophysics and seismically monitored oil recovery processes involve a single fluid phase or multiple fluid phases in a porous medium and the extra degrees of freedom introduced in a multicomponent system can not be duplicated by any single continuum model.

The first models for seismic wave propagation in porous media which involved two coupled and interacting continua were proposed by Gassmann (1951a) and Biot (1956b, 1956c). More recently, macroscopic models have been obtained by applying various homogenization schemes to the governing equations at the small scale. However, the Biot (1956b, 1956c) theory is still the most widely used.

The Biot model is semi-phenomenological in nature and is characterized by two coupled differential vector equations. The model predicts the existence of two P-waves and one S-wave. The stress-strain relations were previously obtained by Biot (1941a, 1955). In the development of the stress-strain relations Biot (1941) introduced the assumption of the existence of a potential energy of the soil in order to obtain a relation between phenomenological parameters and thereby reducing the number of macroscopic parameters by one. The majority of his later works (Biot, 1956b, 1956c, 1962a, 1962b) commence with use of the energy potential for the porous media.

Although there has been many studies conducted using this theory none of these examine the consequence of the assumption of an energy potential as put forth by Biot. Using recently developed (de la Cruz *et al.*, 1993) macroscopic relations for equilibrium

thermodynamics of porous media, the internal energy for a porous medium is discussed in the context of a system consisting of two superposed continua with implications to Biot's use of an energy potential.

If the internal energy of a porous medium is identified as sum of the internal energies of each phase, $W = U_f + U_s$, and Biot's (1956b) average solid and fluid displacements are simply the phase averages, \bar{u}_s and \bar{u}_f , then $\delta_s = \delta_f = 0$ is required for Biot's relations (2.81) and (2.82) to be valid. Hence the use of an energy potential in the context of Biot (1956b) would require that no change in porosity occur during deformation. The other alternative is to associate Biot's $\nabla \cdot \bar{u}_f$ and \bar{u}_{ik}^f with $\nabla \cdot \bar{u}_f + \frac{\eta - \eta_0}{\eta_0}$ and $\bar{u}_{ik}^f - \frac{1}{3} \delta_{ik} \frac{(\eta - \eta_0)}{(1 - \eta_0)}$ derived here. This would imply that Biot's macroscopic displacements are not simply average displacements of the components. Although Biot's (1956b) final equations are of the correct form, his use of the energy potential appears to introduce inconsistencies.

The description of quasi-static deformations of a porous material presented in chapter 3 is based on the quasi-static limit of the low-frequency wave propagation work of *de la Cruz & Spanos (1985;1989b)*. The deformation of the porous material involves the deformation of solid and fluid components as well as the interaction between these components. Such interactions require additional material parameters for an adequate description. Because of the pore fluids' ability to flow, compressibility experiments are conducted so that the pore fluid is allowed to flow freely out of the sample, these are called "drained" experiments. If the fluid is restricted to remain within the sample then the experiments are classified as "undrained".

The description of macroscopic shearing shows that the volume of a sample of porous material is unchanged (to first order). Therefore it makes no difference if this deformation is induced with the sample in a drained or undrained configuration. Consequently, the drained shear modulus must equal the undrained shear modulus.

Four different drained compressibilities are defined (see table 3.1) and calculated using the quasi-static form of the system of equations. The results obtained have many points of contact with those found in the literature. In particular, all identities (see table 3.2) among drained compressibilities given in e.g. *Zimmerman (1991)* are verified, thus providing an

alternative route towards them. It is shown that, for a porous medium under drained conditions, the stress tensor is of the same form as for elastic theory and therefore similar relationships between "Young's" modulus, "Poisson's" ratio, drained bulk modulus and shear modulus exist.

The undrained compressibility is also described in this work and its relation to the various drained compressibilities verified. The undrained bulk modulus can be uniquely related to one drained bulk modulus subject to an assumption about the behavior of the sample in the hydrostatic limit ($K_{unj} = K(1) = K_s$). The description of "undrained Young's modulus" and "undrained Poissons ratio" leads to relationships with the undrained bulk modulus which are analogous to those of elasticity.

For greater experimental flexibility, a one parameter family of compressibilities is introduced which includes the drained and the undrained compressibilities as members. The family of compressibilities is used to obtain expressions for the induced pore pressure coefficient and the coefficient of effective stress. These expressions reduce to the common expressions in the literature with the use of the assumption in the hydrostatic limit.

The use of the assumption, $K_{unj} = K(1) = K_s$ in the hydrostatic limit allows the construction of more simplified relations between poroelastic parameters. The validity of such an assumption is still under debate and the error associated with this assumption when describing a porous medium subject to a quasi-static process requires further experimental investigation.

Several generalizations to the de la Cruz & Spanos (1989b) model for seismic wave propagation are carried out in chapter 4. In the work of de la Cruz & Spanos (1985, 1989b), the macroscopic continuum equations which describe wave propagation in a fluid filled porous medium have been constructed by using volume averaging (see section 2.1) in conjunction with physical arguments. The description includes thermomechanical coupling. Thermomechanical coupling refers to the first order heating of the phases from compression and the expansion/contraction of the phases due to heating and cooling.

The first generalization is to include bulk viscosity, ξ_f . Numerical simulations illustrate that the bulk viscosity, ξ_f , increases the attenuation of the 1st P wave and its effect becomes

more significant when the saturating fluid has a large viscosity. Furthermore, effects of bulk viscosity are larger in samples with small values of drained bulk modulus or small permeabilities.

The second generalization is to introduce a macroscopic shear modulus μ_M as a phenomenological parameter (but is none the less well-defined in terms of pore-scale quantities). The macroscopic shear modulus, μ_M , alters the values of phase velocity and attenuation of both rotational and dilatational waves. The phase velocity of the 1st P wave and 1st S wave increases dramatically with increasing material shear modulus. The attenuation of the 1st S wave increases with decreasing material shear modulus. In the low material shear modulus regime the attenuation increases very rapidly, which is not surprising since this mode must vanish as the shear strength of the material vanishes. For a water filled sample, the attenuation of the 1st P wave exhibits a minimum in the low material shear modulus regime and then increases continually afterwards. The change in attenuation of the 1st P wave with respect to changes in material shear modulus differ substantially, depending on the viscosity of the saturating fluid.

The third generalization introduces macroscopic heat conductivities κ_M^f , κ_M^s into the heat equations. These appear only when thermomechanical coupling is considered and will therefore only affect the dilatational waves. For the cases considered in the numerical simulations, these two parameters are unimportant with respect to altering the phase velocity and attenuation of the dilatational waves.

Utilizing quasi-static experiments, the solid compliance factor, δ_s and fluid compliance factor, δ_f may be determined from values of a drained bulk modulus, K_{bc} , and an unjacketed bulk modulus, K_{unj} . Using this approach assumes that the processes governing the compression of the samples during quasi-static loading and wave propagation are sufficiently similar. Numerical simulations show that significant changes in dilatational phase velocity and attenuation occur when the drained bulk modulus deviates from the quasi-static value. Changes in attenuation of the 1st P wave due to changes in drained bulk modulus are dependent on the viscosity of the saturating fluid. Another assumption commonly used in the literature is that the unjacketed bulk modulus, K_{unj} , is simply equal to the bulk modulus of the solid component. Such an assumption greatly simplifies the problem because now one only requires a measurement of drained bulk modulus.

Numerical calculations show that the phase velocity and attenuation of the P waves are very sensitive to changes in the value ofunjacketed bulk modulus. As in the case of the drained bulk modulus, changes in attenuation with respect to changes inunjacketed bulk modulus are dramatically different for saturating fluids of different viscosities.

There are three other macroscopic parameters in the system of equations governing low frequency wave propagation. Numerical studies show that the permeability, K , has significant effects on the attenuation of both 1st S and 1st P waves within the seismic frequency range but requires large permeabilities for the cases studied. Changes in phase velocities can be neglected for the cases studied. The induced mass coefficient, ρ_{12} , only becomes important at frequencies in excess of 10^4 hz and therefore can be considered unimportant for seismic waves. In laboratory experiments, especially if the 2nd P wave is of interest, a value for the induced mass coefficient will be required. The intercomponent conduction coefficient is only present when thermomechanical coupling is included. The empirical thermal parameter, γ , can change the attenuation of the P waves but has little effect on the phase velocity for the models considered. The frequency at which component temperatures are equal is dependent on this parameter.

Experimental measurements surveyed in the literature indicate that the presence of an additional fluid or partial saturation greatly modifies the character of seismic waves propagating through a porous medium. The seismic properties vary with saturation through the entire range; however, the greatest variation in phase velocity and attenuation occurs at very low saturation (nearly empty) or near complete saturation. In chapter 5, an approximation is obtained by using the equations presented in chapter 4 and the assumption that the two fluids form a composite or effective fluid. This analysis is based solely on descriptions obtained from volume averaging. The composite fluid model contains assumptions such as negligible surface tension and the solid matrix is in contact with only one of the fluids. This model should only be used to obtain approximate descriptions of the gross features of the wave propagation process.

A general system of equations is derived for a porous medium consisting of a homogeneous isotropic elastic solid with the pore space filled with two immiscible viscous fluids. Volume averaging is used to construct the basic equations. The most general expansions are carried out and relationships between the parameters are constructed from

very general physical requirements. In order to obtain a complete set of equations describing the propagation of a dilatational wave, a porosity equation (5.89) and a saturation equation (5.90) must be introduced. Similar to the case considered in chapter 4, these equations should be regarded as process dependent statements. Two limiting cases are considered. Given the amount of independent parameters in the general system of equations, other limiting cases will have to be addressed in order to obtain a clearer understanding of their inter relationships. At that time an attempt at describing experimental procedures for their measurement should be carried out.

The volume averaging technique can be used to provide the framework for macroscopic theories of interacting continua. The primary advantage of such an approach is that there is a connection with the well established continuum descriptions at the pore scale (e.g. elasticity, single continuum thermodynamics). The laws which hold for each component at the pore scale cannot be violated in the macroscopic description. Such a requirement places restrictions on the form of the macroscopic equations as well as the values for the macroscopic parameters. Interacting continua are characterized by separate vector fields. The greatest difficulties arise in formulating the interaction between these fields. Furthermore, because of their interaction, additional degrees of freedom are introduced. These fields can only be combined into one vector field under very restrictive assumptions.

REFERENCES

- Aki, K. and Richards, P.G., 1980, *Quantitative Seismology: Theory and Methods* Volume 1, W.H. Freeman and Company, New York
- Bacri, J.-C. and Salin, D., 1986, Sound Velocity in Sandstone Saturated with Oil and Brine at Different Concentrations, *Geophys. Res. Lett.*, 13(4), 326-328.
- Bacri, J.-C. and Salin, D., 1990, Ultrasonic Diagnosis in Multiphase Flows. *Colloque de Physique*, C2, 51(2), 13-16.
- Bear, J. and Corapcioglu., 1989, Wave Propagation in Saturated Porous Media - Governing Equations, *Inter. Symp. on Wave Propagation in Granular Media*, ASME Winter Annual Meeting, San Francisco, CA.
- Bedford, A., Costley, R.D. and Stern, M., 1984, On the Drag and Virtual Mass Coefficient in Biot's Equations, *J. Acoust. Soc. Am.*, 76(6), 1804-1809.
- Bedford, A. and Drumheller, D.S., 1983, Recent Advances: Theories of Immiscible and Structured Mixtures, *Int. J. Engng Sci.*, 21(8), 863-960.
- Bell, M.L. and Nur, A., 1978 Strength Changes Due to Reservoir-Induced Pore-Pressure and Application to Lake Oroville, *J. Geophys. Res.*, 83, 4469-4483.
- Berryman, J.G., 1979, Theory of Elastic Properties of Composite Materials, *Appl. Phys. Lett.*, 35(11), 856-858.
- Berryman, J.G., 1980 Confirmation of Biot's Theory, *Appl. Phys. Lett.*, 37(4), 382-384.
- Berryman, J.G. and Thigpen, L., 1985, Effective Constants for Wave Propagation Through Partially Saturated Porous Media, *Appl. Phys. Lett.*, 46(8), 722-724.
- Berryman, J.G., 1992, Effective Stress for Transport Properties of Inhomogeneous Porous Rock, *J. Geophys. Res.*, 97(B12), 17409-17424
- Berryman, J.G. and Milton, G.W., 1991, Exact Results for Generalized Gassmann's Equations in Composite Porous Media with two Constituents, *Geophysics*, 56(12), 1930-1960.
- Berryman, J.G., Thigpen, L. Chin, R.C.Y., 1988, Bulk Elastic Wave Propagation in Partially Saturated Porous Solids, *J. Acoust. Soc. Am.*, 84(1), 360-373.
- Biot, M.A., 1941, General Theory of Three Dimensional Consolidation, *J. Appl. Phys.*, 12, 155-164.
- Biot, M.A., 1955, Theory of Elasticity and Consolidation for a Porous Anisotropic Solid, *J. Appl. Phys.*, 26(2), 182-185.

- Biot, M.A., 1956a, General Solutions of the Equations of Elasticity and Consolidation for a Porous Material, *J. Appl. Mech.*, 78, 91-96.
- Biot, M.A., 1956b, Theory of Propagation of Elastic Waves in a Fluid-Saturated Porous Solid. I. Low Frequency Range, *J. Acoust. Soc. Am.*, 28(2), 168-178.
- Biot, M.A., 1956c, Theory of Propagation of Elastic Waves in a Fluid-Saturated Porous Solid. II. Higher Frequency Range, *J. Acoust. Soc. Am.*, 28(2), 179-191.
- Biot, M.A., 1962a, Mechanics of Deformation and Acoustic Propagation in Porous Media, *J. Appl. Phys.*, 33(4), 1482-1498.
- Biot, M.A., 1962b, Generalized Theory of Acoustic Propagation in Porous Dissipative Media, *J. Acoust. Soc. Am.*, 34(9), 1254-1264.
- Biot, M.A. and Willis, D.G., 1957 The Elastic Coefficients of the Theory of Consolidation *J. Appl. Mech.*, 24, 594-601.
- Bishop, A.W., 1973, The Influence of an Undrained Change in Stress on the Pore Pressure in Porous Media of Low Compressibility, *Geotech.*, 23, 435-442.
- Bishop, A.W., 1976, The Influence of System Compressibility on the Observed Pore-Pressure Response to an Undrained Change in Stress in Saturated Rock, *Geotech.*, 26, 371-375.
- Borchardt, R.D., 1973, Energy and Plane Waves in Linear Viscoelastic Media, *J. Geophys. Res.*, 78, 2442-2453.
- Borchardt, R.D., Glassmoyer, G. and Wennerberg, L., 1986, Influence of Welded Boundaries in Anelastic Media on Energy Flow, and Characteristics of P, S-I, and S-II Waves: Observational Evidence for Inhomogeneous Body Waves in Low Loss Solids, *J. Geophys. Res.*, 91(B11), 11,503-11,518.
- Brace, W.F. and Martin R.J. III, 1968, A Test of Effective Stress Law for Crystalline Rocks of Low Porosity, *Int. J. Rock Mech. Min. Sci.*, 5, 415-426.
- Brandt, H., 1955, A Study of the Speed of Sound in Porous Granular Media. *J. Appl. Mech.*, 22, 479-486.
- Brown, R.J.S., 1980, Connection Between Formation Factor for Electrical Resistivity and Fluid-Solid Coupling Factor in Biot's Equations for Acoustic Waves in Fluid-Filled Porous Media, *Geophysics*, 45(8), 1269-1275.
- Brown, R.J.S. and Korrings, J., 1975, On the Dependence of the Elastic Properties of a Porous Rock on the Compressibility of the Pore Fluid, *Geophysics*, 40(4), 608-616.
- Budiansky, B., O'Connell, R.J., 1976, Elastic Moduli of a Cracked Solid, *Int. J. Solids Struct.*, 12, 81-97.
- Budiansky, B., Sumner, E.E. Jr. and O'Connell, R.J., 1983, Bulk Thermoelastic Attenuation of Composite Materials, *J. Geophys. Res.*, 88(B12), 10343-10348.

- Bulau, J.R., Tittmann, B.R., Abdel-Gawad, M., and Salvado, C., 1984, The Role of Aqueous Fluids in the Internal Friction of Rock, *J. Geophys. Res.*, **89**(B6), 4207-4212.
- Burridge, R. and Keller, J.B., 1981, Poroelasticity Equations Derived from Microstructure, *J. Acoust. Soc.*, **70**(4), 1140-1146.
- Campbell, H.G., 1977, *An Introduction to Matrices, Vectors, and Linear Programming*, Prentice-Hall, New Jersey
- Carroll, M.M., 1979, An Effective Stress Law for Anisotropic Elastic Deformation, *J. Geophys. Res.*, **84**(B13), 7510-7512.
- Carroll, M.M. and Katsube, N., 1983, The Role of Terzaghi Effective Stress in Linearly Elastic Deformations. *ASME J. of Energy Resources Tech.*, **105**(4), 509-511.
- Caviglia, G., Morro, A. and Straughan, B., 1992, Reflection and Refraction at a Fluid-Porous Medium Interface, *J. Acoust. Soc. Am.*, **92**(2), 1113-1119.
- Champoux, Y. and Stinson, M.R., 1992, On Acoustical Models for Sound Propagation in Rigid Frame Porous Materials and the Influence of Shape Factors, *J. Acoust. Soc. Am.*, **92**(2), 1120-1131.
- Chatterjee, A.K., Mal, A.K. and Knopoff, L., 1978, Elastic Moduli of Two Component Systems. *J. Geophys. Res.*, **83**(B4), 1785-1792.
- Christensen, R.M., 1982, *Theory of Viscoelasticity: An Introduction*, 2nd ed., Academic Press, New York.
- Christensen, N.I. and Wang, H.F., 1985, The Influence of Pore Pressure and Confining Pressure on the Dynamic Elastic Properties of Berea Sandstone, *Geophysics*, **50**(2), 207-213.
- Clark, V.A., 1992, The Effect of Oil Under In-situ Conditions on the Seismic Properties of Rocks, *Geophysics*, **57**(7), 894-901.
- Clark, V.A., Spencer, T.W. and Tittmann, B.R., 1981, The Effect of Thermal Cycling on the Seismic Quality Factor Q of Some Sedimentary Rocks, *J. Geophys. Res.*, **86**(B8), 7087-7094.
- Clark, V.A., Tittmann, B.R. and Spencer, T.W., 1980, Effect of Volatiles on Attenuation (Q-1) and Velocity in Sedimentary Rocks, *J. Geophys. Res.*, **85**(B10), 5190-5198.
- Costley, R.D. and Bedford, A., 1968, An Experimental Study of Acoustic Waves in Saturated Glass Beads, *J. Acoust. Soc. Am.*, **53**(6), 2165-2174.
- Coyner, K.B., 1977, *Effects of Stress, Pore Pressure, and Pore Fluids on Bulk Strain, Velocity, and Permeability in Rocks*, Ph. D Thesis, Massachusetts Institute of Technology, 361 pp.

- Crochet, M.J. and Naghdi, P.M., 1966, On Constitutive Equations for Flow of Fluid Through an Elastic Solid, *Int. J. Engng Sci.*, 4, 383-401.
- de la Cruz, V., Sahay, P.N., and Spanos, T.J.T., 1993, Thermodynamics of Porous Media, *Proc. Roy. Soc. Lond., Ser. A*, 443, 247-255.
- de la Cruz, V. and Spanos, T.J.T., 1989a, Seismic Boundary Conditions for Porous Media, *J. Geophys. Res.*, 94 (B3), 3025-3029.
- de la Cruz, V. and Spanos, T.J.T., 1989b, Thermomechanical Coupling During Seismic Wave Propagation in a Porous Medium, *J. Geophys. Res.*, 94(B1), 637-642.
- de la Cruz, V. and Spanos, T.J.T., 1985, Seismic Wave Propagation in a Porous Medium. *Geophysics*, 50(10), 1556-1565.
- de la Cruz. and Spanos, T.J.T., 1983, Mobilization of Oil Ganglia, *AIChE*, 29(7), 854-858.
- Deresiewicz, H. and Levy, A., 1967, The Effect of boundaries on wave propagation in a liquid-filled porous solid-II: Transmission through a stratified medium, *Bull seism. Soc. Am.*, 57, 381-392.
- Detournay, E., 1993, Constitutive Equations: Overview and Theoretical Background, in *A Short Course in Poroelasticity in Rock Mechanics*, the 34th U.S. Symposium on Rock Mechanics, June 27-30, 1993, University of Wisconsin-Madison.
- Dobrynin, V.M., 1985, Effect of Overburden Pressure on Some Properties of Sandstones, *Soc. Petrol. Eng. J.*, 2, 360-366.
- Domenico, S.N., 1974, Effect of Water Saturation on Seismic Reflectivity of Sand Reservoirs Encased in Shale, *Geophysics*, 39(6), 759-769.
- Domenico, S.N., 1976, Effect of Brine-Gas Mixture on Velocity in an Unconsolidated Sand Reservoir, *Geophysics*, 41(5), 882-894.
- Drusik, R.K., Johnson, J.N. and Walsh, J.B., 1978, The Influence of Pore-Pressure on the Mechanical Properties of Kayenta Sandstone, *J. Geophys. Res.*, 83(B6), 2817-2824.
- Duffy, J. And Mindlin, R.D., 1957, Stress-Strain Relations of a Granular Medium, *J. Appl. Mech.*, 24, 585-593.
- Dullien, F.A.L., 1992, *Porous Media: Fluid Transport and Pore Structure*, Academic Press, San Diego.
- Dunlop, K.N.B., King, G.A. and Breitenbach, E.A., 1991, Monitoring Oil/Water Fronts by Direct Measurements, *Soc. Petrol. Eng. J.*, May, 596-602.
- Dunlop, K.N.B., King, G.A. and Breitenbach, E.A., 1991, Author's Reply to Discussion of Monitoring Oil/Water Fronts by Direct Measurements, *Soc. Petrol. Eng. J.*, Dec., 1525.

- Dutta, N.C., 1980, Theoretical Analysis of Observed Second Bulk Compressibility Wave in a Fluid-Saturated Porous Solid At Ultrasonic Frequencies, *Appl. Phys. Lett.*, **37(10)**, 898-900.
- Dutta, N.C., 1979, Seismic Loss Mechanisms. Research Workshop Report.
- Dutta, N.C. and Odé, H., 1979a, Attenuation and Dispersion of Compressional Waves in Fluid-Filled Porous Rocks with Partial Gas Saturation (White Model)- Part I: Biot Theory, *Geophysics*, **44(11)**, 1777-1788.
- Dutta, N.C. and Odé, H., 1979b, Attenuation and Dispersion of Compressional Waves in Fluid-Filled Porous Rocks with Partial Gas Saturation (White Model)- Part II: Results, *Geophysics*, **44(11)**, 1789-1805.
- Dutta, N.C. and Seriff, A.J., 1979, On White's Model Of Attenuation in Rocks with Partial Gas Saturation, *Geophysics*, **44(11)**, 1806-1812.
- Dvorkin, J., Mavko, G. and Nur, A., 1992, The Dynamics of Viscous Compressible Fluid in a Fracture, *Geophysics*, **57(5)**, 720-726.
- Dvorkin, J. and Nur, A., 1993, Dynamic Poroelasticity: A Unified Model with the Squirt and the Biot Mechanisms, *Geophysics*, **58(4)**, 524-533.
- Eastwood, J.E., 1991, *Thermodynamics of Porous Media*, Ph.D. Thesis, University of Alberta, 183 pp.
- Eshelby, J.D., 1957, The Determination of the Elastic Field of an Ellipsoidal Inclusion and Related Problems, *Proc. Roy. Soc. Lond., Ser. A.*, **241**, 376-396.
- Fang, W.W., Langsath, M.G., and Schultheiss, P.J., 1993, Analysis and Application of In Situ Pore Pressure Measurements in Marine Sediments, *J. Geophys. Res.*, **98(B5)**, 7921-7938.
- Fatt, I., 1959, The Biot-Willis Elastic Coefficients for a Sandstone, *ASME J. Appl. Mech.*, June, 296-297
- Forsythe, W.E., 1959, *Smithsonian Physical Tables*, The Smithsonian Institute, Baltimore.
- Friend, D., 1992, Ultrasonic Compressional and Shear Velocities in Dry Clastic Rocks as a Function of Porosity, Clay Content, and Confining Pressure, *Geophys. J. Int.*, **108**, 125-135.
- García-Coalla, L.S. and Uribe, F.J., 1991, Extended Irreversible Thermodynamics Beyond the Linear Regime: A Critical Overview, *J. Non Equilib. Thermodyn.*, **16**, 89-128.
- Garg, S.K. and Nayfeh, A.H., 1986, Compressional Wave Propagation in Liquid and/or Gas Saturated Elastic Porous Media, *J. Appl. Phys.*, **60(1)**, 3045-3055.

- Garg, S.K. and Nur, A., 1973, Effective Stress Laws for Fluid Saturated Porous Rocks, *J. Geophys. Res.*, **78**(26), 5911-5921
- Gassmann, F., 1951a, Über die Elastizität poröser Medien, *Vierteljahresschrift d. Naturf. Ges. zurich*, **96**, 1-24.
- Gassmann, F., 1951b, Elastic Waves Through a Packing of Spheres, *Geophysics*, **16**(4), 673-68.
- Geertsma, J., 1957, The Effect of Fluid Pressure Decline on Volumetric Changes of Porous Rocks, *Petrol Trans of the AIME*, **210**, 331-340.
- Goldberg, D. and Zinszner, B., 1989, P-wave Attenuation Measurements From Laboratory Resonance and Sonic Waveform Data, *Geophysics*, **54**(1), 76-81.
- Gordon, R.B. and Davis, L.A., 1968, Velocity and Attenuation of Seismic Waves in Imperfectly Elastic Rock, *J. Geophys. Res.*, **73**, 3917-3935.
- Green, A.E. and Naghdi, P.M., 1965, A Dynamical Theory of Interacting Continua, *Int. J. Engng Sci.*, **3**, 231-241.
- Green, D.H. and Wang, H.F., 1986, Fluid Pressure Response to Undrained Compression in Saturated Sedimentary Rock, *Geophysics*, **51**(4), 948-956.
- Gurtin, M.E., 1988, Multiphase Thermodynamics with Interfacial Structure 1. Heat Conduction and the Capillary Balance Law, *Arch. for Rat. Mech. Anal.*, **104**, 185-221.
- Gurtin, M.E. and Struthers, A., 1990, Multiphase Thermodynamics with Interfacial Structure 3. Evolving Phase Boundaries in the Presence of Bulk Deformation, *Arch. for Rat. Mech. Anal.*, **112**, 97-160.
- Han, D.-H., Nur, A. and Morgan, D., 1986, Effects of Porosity and Clay Content on Wave Velocities in Sandstones, *Geophysics*, **51**(11), 2093-2107.
- Handin, J., Hager, Jr., R.V., Friedman, M., and Feather, J.N., 1963, Experimental Deformation of Sedimentary Rocks Under Confining Pressure: Pore Pressure Tests, *Bull. Am. Assoc. Petrol. Geol.*, **47**(5), 717-755.
- Hashin, Z., 1963, Analysis of Composite Materials- A Survey, *J. Appl. Mech.*, **30**, 481-505.
- Hashin, Z. and Shtrikman, S., 1961a, Note on the Variational Approach to the Theory of Composite Elastic Materials, *J. Franklin Inst.*, **271**, 336-341.
- Hashin, Z. and Shtrikman, S., 1961b, Note on the Effective Constants of Composite Materials, *J. Franklin Inst.*, **271**, 423 - 426.
- Hashin, Z. and Shtrikman, S., 1962a, A Variational Approach to the Theory of the Elastic Behavior of Polycrystals, *J. Mech. Phys. Solids*, **10**, 343-352.

- Hashin, Z. and Shtrikman, S., 1962b, On Some Variational Principles in Anisotropic and Nonhomogeneous Elasticity, *J. Mech. Phys. Solids*, **10**, 335-342.
- Hashin, Z. and Shtrikman, S., 1963, A Variational Approach to the Theory of the Elastic Behavior of Multiphase Materials, *J. Mech. Phys. Solids*, **11**, 127-140.
- Hawkins, J.A. and Bedford, A., 1992, Variational Theory of Bubbly Media with a Distribution of Bubble Sizes II. Porous Solid, *Int. J. Engng Sci.*, **30(9)**, 1177-1186.
- Healy, J. H., W. W. Rubey, D.T. Griggs, and C.B. Raleigh, 1968, The Denver earthquakes, *Science*, **161**, 1301-1310.
- Hickey, C.J., 1990, Numerical Studies of Seismic Wave Propagation in Porous Media. M.Sc. Thesis, University of Alberta, 135 pp.
- Hickey, C.J., Eastwood, J.E., and Spanos, T.J.T., 1991, Seismic Wave Propagation in Oil Sands, *AOSTRA J. Res.*, **7**, 67-81.
- Hickey, C.J., Spanos, T.J.T. and de la Cruz, V., 1993, Deformation Parameters of Permeable Media, submitted to *Geophys. J. Int.*
- Hill, R., 1952, The Elastic Behaviour of a Crystalline Aggregate, *Proc. Phys. Soc.*, **A65**, 349-354.
- Hill, R., 1963, Elastic Properties of Reinforced Solids: Some Theoretical Principles, *J. Mech. Phys. Solids*, **11**, 357-372.
- Huang, J.H., 1971, Effective Thermal Conductivity of Porous Rocks, *J. Geophys. Res.*, **76(26)**, 6420-6427.
- Hubbard, M.K., 1956, Darcy's Law and Field Equations of Flow of Underground Fluids, *Am. Inst. Min. Metall. and Petrol. Eng.*, **207**, 222-239.
- Hudson, J.A., 1980, Overall Properties of a Cracked Solid, *Math. Proc. Camb. Phil. Soc.*, **88**, 371-384.
- Hudson, J.A., 1990a, Overall Elastic Properties of Isotropic Materials with Arbitrary Distribution of Circular Cracks, *Geophys. J. Int.*, **102**, 465-469.
- Hudson, J.A., 1990b, Attenuation due to Second-Order Scattering in Material Containing Cracks, *Geophys. J. Int.*, **102**, 485-490.
- Hudson, J.A. and Knopoff, L., 1989, Predicting the Overall Properties of Composite-Materials with Small Scale Inclusions or Cracks, *Pageoph.*, **131**, 551-576.
- Hughes, D.S. and Cooke, C.E., Jr., 1953, The Effect of Pressure on the Reduction of Pore Volume of Consolidated Sandstones, *Geophysics*, **18**, pp. 298-309.
- Hsu, C.T. and Cheng, P., 1990, Thermal Dispersion in a Porous Medium, *Int. J. Heat Mass Transfer*, **33(8)**, 1967-1997.

- Hwang, L.F. and Lellis, P.J., 1988, Bright Spots Related to High GOR Oil Reservoir in Green Canyon, *58th Ann. Int. Mtg., Soc. Expl. Geophys.*, Expanded Abstr., 761 - 763.
- Jackson, I., Paterson, M.S., Niesler, H. and Waterford, R.M., 1984, Rock Anelasticity Measurements at High Pressure, Low Strain Amplitude and Seismic Frequency, *Geophys. Res. Lett.*, 11(12), 1235-1238.
- Johnson, D.L., 1980, Equivalence Between Fourth Sound in Helium at Low Temperatures and the Biot Slow Wave in Consolidated Porous Media, *Appl. Phys. Lett.*, 37(12), 1065-1067.
- Johnson, D.L., Koplik, J. and Dashen, R., 1987, Theory of Dynamic Permeability and Tortuosity in Fluid Saturated Porous Media, *J. Fluid Mech.*, 176, 379-402.
- Johnson, D.L. and Piona, T.J., 1982, Acoustic Slow Waves and the Consolidation Transition, *J. Acoust. Soc. Am.*, 72(2), 556-565.
- Johnson, D.L., Piona, T.J., Scala, C., Pasierb, F., and Kojima, H., 1982, Tortuosity and acoustic slow waves, *Phys. Rev. Lett.*, 49, 1840-1844.
- Johnston, D.H., Toksöz, M.N. and Timur, A., 1979, Attenuation of Seismic Waves in Dry and Saturated Rocks: II. Mechanisms, *Geophysics*, 44(4), 691-711.
- Johnston, D.H. and Toksöz, M.N., 1980, Ultrasonic P and S Wave Attenuation in Dry and Saturated Rocks Under Pressure, *J. Geophys. Res.*, 85, 925-936.
- Jones, T.D. and Nur, A., 1983, Velocity and Attenuation in Sandstones at Elevated Temperatures and Pressures, *Geophys. Res. Lett.*, 10(2), 140-143.
- Karstberg, E.A., 1975, Elastic-Wave Velocity Measurements in Rocks and Other Methods by Phase-Delay Methods, *Geophysics*, 40(6), 955-960.
- Kampfmann, W. and Berckhomer, H., 1985, High Temperature Experiments on the Elastic and Anelastic Behaviour of Magmatic Rocks, *Phys. Earth. Planet. Int.*, 40, 223-247.
- Katsube, N., 1985, The Constitutive Theory for Fluid Filled Porous Materials, *J. Appl. Mech.*, 52, 185-189.
- Katsube, N. and Carroll, M.M., 1987a, The Modified Mixture Theory for Fluid Filled Porous Materials: Theory, *J. Appl. Mech.*, 54, 35-40.
- Katsube, N. and Carroll, M.M., 1987a, The Modified Mixture Theory for Fluid Filled Porous Materials: Applications, *J. Appl. Mech.*, 54, 41-46.
- Kaul, R.K., 1993, Poro-Elastic Seismics for Shaly Sandstone Reservoir Parameter Characterization. Preprint.
- Keller, K.B., 1964, Stochastic Equations and Wave Propagation in Random Media, *Proc. Symp. Appl. Math.*, 16, 145-170.

- Keller, J.B., 1977, *Statistical Mechanics and Statistical Methods in Theory and Application*, Plenum, New York.
- Kerr, F.H., 1992, An Effective Medium Approach to the Study of Plane Wave Propagation in an Elastic Matrix with Spherical Inclusions, *Int. J. Engng Sci.*, 30(2), 187-198.
- Khalatbari, A., Vo-Thanh, D. and Poirier, J-P., 1991, Effect of Fluid Viscosity and Saturation on the Ultrasonic Velocities in a Fontainebleau Sandstone. *Geophys. Res. Lett.*, 18(5), 885-888
- King, M.S., 1969, Static and Dynamic Moduli of Rocks Under Pressure, *Proc. U.S. 11th Symp. Rock Mech.*, 329-351.
- Klimentos, K., 1991a, Geometrical Corrections in Attenuation Measurements, *Geophys. Prospecting*, 39, 193-218.
- Klimentos, T., 1991b, The Effects of Porosity -Permeability-Clay Content on the Velocity of Compressional Waves, *Geophysics*, 56(12), 1930-1939.
- Knight, R. and Dvorkin, J., 1992, Seismic and Electrical Properties of Sandstones at Low Saturations, *J. Geophys. Res.*, 97(B12), 17425-17432.
- Knight, R. and Nolen-Hoeksema, R., 1990, A Laboratory Study of The Dependence of Elastic Wave Velocities on Pore Scale Fluid Distribution, *Geophys. Res. Lett.*, 17(10), 1529-1532.
- Knopoff, L., and Macdonald, G.J.F., 1958, Attenuation of small amplitude stress waves in solids, *Rev of Mod. Phys.*, 30, 1178-1192.
- Kowalski, S.J., 1992, On the Motion of a Fluid-Saturated Porous Solid, *Transport in Porous Media*, 9, 39-47.
- Kämpel, H.-J., 1991, Poroeasticity: Parameters Reviewed, *Geophys. J. Int.*, 106, 783-799.
- Kundu, P.K., 1990, *Fluid Mechanics*, Academic Press, Inc., San Diego.
- Kuster, G.T. and Toksöz, M.N., 1974a, Velocity and Attenuation of Seismic Waves in Two-Phase Media: Part I. Theoretical Formulations, *Geophysics*, 39(5), 587-606.
- Kuster, G.T. and Toksöz, M.N., 1974b, Velocity and Attenuation of Seismic Waves in Two-Phase Media: Part II. Experimental Results, *Geophysics*, 39(5), 607-618.
- Landau, L.D. and Lifshitz, E.M., 1975a, *Theory of Elasticity*, Pergamon. New York.
- Landau, L.D. and Lifshitz, E.M., 1975b, *Fluid Mechanics*, Pergamon, New York.
- Liu, Q-R. and Kanube, N., 1990, The Discovery of a Second Kind of Rotational Wave in a Fluid-Filled Porous Material, *J. Acoust. Soc. Am.*, 88(2), 1045-1053.

- Lockett, F.J., 1962, The Reflection and Refraction of Waves at an Interface Between Viscoelastic Media, *J. Mech. Phys. Solids*, 10, 53-64.
- Marie, C.M., 1982, On Macroscopic Equations Governing Multiphase Flow with Diffusion and Chemical Reactions in Porous Media, *Int. Journ. Eng. Sci.*, 20, 643-662.
- Mason, K.P. and Kuo, J.T., 1971, Internal Friction in Pennsylvania Slate, *J. Geophys. Res.*, 76, 2084-2089.
- Mavko, G., 1979, Frictional Attenuation: An Inherent Amplitude Dependence, *J. Geophys. Res.*, 84, 4769-4775.
- Mavko, G. and Nur, A., 1979, Wave Attenuation in Partially Saturated Rocks, *Geophysics*, 44, 161-178.
- Mazzotti, A., 1990, Prestack Amplitude Analysis Methodology and Application to Seismic Bright Spots in the Po Valley, Italy, *Geophysics*, 55, 157-166.
- Mei, C.C. and Auriault, J.-L., 1989 Mechanics of Heterogeneous Porous Media With Several Spatial Scales, *Proc. R. Soc. Lond., Ser. A.*, 426, 391-423.
- Meeri, G., Adachi, K. and Ullrich, C.R., 1976, Pore-pressure response in Rock to Undrained Change in All Round Stress, *Geotech.*, 26, 317-330.
- Milton, G.W. and Phan-Thien, N., 1982, New Bounds on Effective Elastic Moduli of Two-Component Materials, *Proc. R. Soc. Lond., Ser. A.*, 389, 305-331.
- Mindlin, R.D., and Deresiewicz, H., 1953 Elastic spheres in contact under varying oblique forces, *J. appl. mech.* 20, 327-344.
- Mochizuki, S., 1982, Attenuation in Partially Saturated Rocks, *J. Geophys. Res.*, 87(B10), 8598-8604.
- Morland, L.W., 1972, A Simple Constitutive Theory for a Fluid Saturated Porous Solid, *J. Geophys. Res.*, 77(F), 890-900.
- Murphy III, W.F., 1982, Effects of Partial Water Saturation on Attenuation in Massilon Sandstone and Vycor Porous Glass, *J. Acoust. Soc. Am.*, 71(6), 1458-1468.
- Murphy III, W.F., Winkler, K.W. and Kleinberg, R.L., 1984, Frame Modulus Reduction in Sedimentary Rocks: The Effect of Adsorption on Grain Contacts. *Geophys. Res. Lett.*, 1(9), 805-808.
- Murphy III, W.F., Winkler, K.W. and Kleinberg, R.L., 1986, Acoustic Relaxation in Sedimentary Rocks: Dependence on Grain Contacts and Fluid Saturation, *Geophysics*, 51(3), 757-766.
- Nagy, P.B., Adler, L. and Benner, B.P., 1990, Slow Wave Propagation in Air Filled Porous Materials And Natural Rocks, *Appl. Phys. Lett.*, 56(25), 2504-2506.

- Nagy, P.B. and Adler, L., 1992, Nondestructive Evaluation of Porous Materials by Airborne Ultrasonic Waves, in *Quantitative Nondestructive Evaluation*, Vol. 11B, 2163-2170.
- Niblett, D.H., and Wilks, J., 1960, Dislocation damping in metals, *Advances in Phys.*, 9, 1-8.
- Nigmatulin, R.I. and Gubaidullin, A.A., 1992, Linear Waves in Saturated Porous Media, *Transport in Porous Media*, 9, 135-142.
- Nozad, I., Carbonell, R.G. and Whitaker, S., 1985, Heat Conduction in Multiphase Systems - I, *Chem. Eng. Sci.*, 40(5), 843-855.
- Nur, A., 1972, Dilatancy, pore fluids and Premonitory variations of t_s/t_p travel times, *Bull. Seismo. Soc. Am.*, 62, 1217-1222.
- Nur, A., and J.R. Booker, 1972, Aftershocks caused by fluid flow, *Science*, 175, 885.
- Nur, A. and Byerlee, J.D., 1971, An Exact Effective Stress Law for Elastic Deformation of Rocks With Fluids, *J. Geophys. Res.*, 76(26), 6414-6419.
- O'Connell, R.J. and Budiansky, B., 1974, Seismic Velocities in Dry and Saturated Cracked Solids, *J. Geophys. Res.*, 79(36), 5412-5426.
- O'Connell, R.J. and Budiansky, B., 1977, Viscoelastic Properties of Fluid Saturated Cracked Solids, *J. Geophys. Res.*, 82(36), 5719-5735.
- Ogushwitz, P.R., 1985a, Applicability of the Biot Theory. I. Low-Porosity Materials, *J. Acoust. Soc. Am.*, 77(2), 429-440.
- Ogushwitz, P.R., 1985b, Applicability of the Biot Theory. II. Suspensions, *J. Acoust. Soc. Am.*, 77(2), 441-452.
- Ogushwitz, P.R., 1985c, Applicability of the Biot Theory. I. Wave Speeds Versus Depth in Marine Sediments, *J. Acoust. Soc. Am.*, 77(2), pp. 453-464.
- O'Hara, S.G., 1985, Influence of Pressure, Temperature, and Pore Fluid on the Frequency-Dependent Attenuation of Elastic Waves in Berea Sandstone, *Phys. Rev. A*, 32(1), 472-488.
- Ostrander, W.J., 1984, Plane-wave Reflection Coefficients for Gas Sands at Non-Normal angles of Incidence, *Geophysics*, 49, 1637-1648.
- Paffenholz, J. and Burkhardt, H., 1989 Absorption and Modulus Measurements in the Seismic Frequency and Strain Range on Partially Saturated Sedimentary Rocks, *J. Geophys. Res.*, 94(B7), 9493-9507
- Paloczka, V.V., 1992, Compressional to Shear Wave Velocity Ratio of Granular Rocks: Role of Rough Grain Contacts, *Geophys. Res. Lett.*, 19(16), 1683-1686.

- Palmer, I.D. and Traviolia, M.L., 1980, Attenuation by Squirt Flow in Undersaturated Gas Sands, *Geophysics*, **45**, 1780-1792.
- Pandit, B.I. and King, M.S., 1979, The Variation of Elastic Wave Velocities and Quality Factor Q of a Sandstone with Moisture Content, *Can. J. Earth Sci.*, **16**(12), 2187-2195.
- Paul, B., 1962, The Elastic Moduli of Heterogeneous Materials, *J. Appl. Mech. Trans. ASME*, **29**, 765-766.
- Peacock, S. and Hudson, J.A., 1990, Seismic Properties of Rocks with Distributions of Small Cracks, *Geophys. J. Int.*, **102**, 471-484.
- Piona, T.J., 1980, Observation of a Second Bulk Compressional Wave in a Porous Medium at Ultrasonic Frequencies, *Appl. Phys. Lett.*, **36**(4), 259-261.
- Piona, T.J., D'Angelo, R., and Johnson, D.L., 1990, Velocity and Attenuation of Fast, Shear, and Slow Waves in Porous Media, *IEEE 1990 Ultrasonics Symposium*, 1233-1239.
- Prasad, M. and Meissner, R., 1992, Attenuation Mechanisms in Sand: Laboratory Versus Theoretical (Biot) Data, *Geophysics*, **57**(5), 710-719.
- Pride, S.R., Gangi, A.F. and Morgan, D., 1992, Deriving the Equations of Motion for Porous Isotropic Media, *J. Acoust. Soc. Am.*, **92**(6), 3278-3290.
- Rajendran, K. and Talwani, P., 1992, The Role of Elastic Undrained and Drained Responses in Triggering Earthquakes at Monticello Reservoir, South Carolina, *Bull. Seismo. Soc. Am.*, **82**, 1867-1888.
- Roux, A., 1929, Berechnung der Fließgrenze von Mischkristallen auf Grund des Fließbedingung für Einkristalle, *Zeitschrift für Angewandte Mathematik und Mechanik*, **9**, 49-58.
- Rice, J.R. and Cleary, M.P., 1976 Some Basic Stress Diffusion Solutions for Fluid Saturated Elastic Porous Media With Compressible Constituents, *Rev. Geophys. and Space Phys.*, **14**(2), 227-241.
- Robin, P.-Y. F., 1973, Note on Effective Pressure, *J. Geophys. Res.*, **78**(14), 2434-2437.
- Rosa, A.L.R., Arso, L.R. and Jaeger, R., 1985, Mapping Oil-Water Contact with Seismic Data in Campos Basin, Offshore Brazil. *35th Ann. Int. Mtg., Soc. Expl. Geophys.*, Expanded Abstr., 441-442.
- Sabatier, J.M., Bass, H.E., Bolin, L.N., Annenborough, K. and Sastry, V.V.S.S., 1986, The Interaction of Airborne Sound with the Porous Ground: The Theoretical Formulation, *J. Acoust. Soc. Am.*, **79**(5), 1345-1352.
- Sanchez-Palencia, E., 1980, *Non-Homogeneous Media and Vibration Theory*, Lecture Notes in Physics 127, Springer-Verlag, New York.

- Santos, J.E., Corbero, J.M. and Douglas, J., Jr., 1990a, Static and Dynamic Behavior of a Porous Solid Saturated by a Two-Phase Fluid, *J. Acoust. Soc. Am.*, **87**(4), 1428-1438.
- Santos, J.E., Douglas, J., Jr., Corbero, J.M. and Lovera, O.M., 1990b, A Model for Wave Propagation in a Porous Medium Saturated by a Two Phase Fluid, *J. Acoust. Soc. Am.*, **87**(4), 1439-1448.
- Sayers, C.M., 1993, Elastic Wave Anisotropy of Damaged Rocks: A Comment on "Crack Models for a Transversely Isotropic Medium", *Geophys. Abstr.*, May.
- Scheidegger, A.E., 1974, *The Physics of Flow Through Porous Media*, University of Toronto Press, Toronto.
- Schmitt, D.R. and Zoback, M.D., 1992, Diminished Pore Pressure in Low-Porosity Crystalline Rock under Tensional Failure: Apparent Strengthening by Dilatancy, *J. Geophys. Res.*, **97**(B1), 273-288.
- Schwarzschild, B., 1993, Earthquake Yields First Real Evidence of Remote Triggering, *Physics Today*, **46** (9), 17-19.
- Sears, F. M. and Bonner, B.P., 1981, Ultrasonic Attenuation Measurements by Spectral Ratios Utilizing Signal Processing Techniques, *IEEE Trans. Geosci. Remote Sens.*, **GE-19**, p. 95.
- Shankland, T.J., Johnson, P.A. and Hopson, T.M., 1993, Elastic Wave Attenuation and Velocity of Berea Sandstone Measured in the Frequency Domain, *Geophys. Res. Lett.*, **20**(5), 391-394.
- Sharma, M.D. and Vashisth, A., 1993, Comment on "Reflection and Refraction of Seismic Waves Incident Obliquely at the Boundary of Liquid-Saturated Porous Solid, *Bull. Seismo. Soc. Am.*, **83**(1), 291-294.
- Shuey, R.T., 1985, A Simplification of the Zoeppritz Equations, *Geophysics*, **50**, 609-614.
- Skempton, A.W., 1954, The Pore-Pressure Coefficients A and B, *Geotechnique*, **4**, 143-147.
- Slattery, J.C., 1969 Single Phase flow Through Porous Media, *AIChE.*, **15**, 866-872.
- Smolders, D.M.J., de la Rosette, J.P.M. and Van Dongen, M.E.H., 1992, Waves in Partially Saturated Porous Media, *Transport in Porous Media*, **9**, 25-37.
- Spanos, T.J.T., de la Cruz, V., and Yang, D., 1993, Macroscopic Capillary Pressure, Preprint.
- Stoll, R.D., 1979, *Sediment Acoustics*, Lecture Notes in Earth Sciences, **26**, Springer-Verlag, New York, 153 pp.

- Stoll, R.D., 1979, Experimental Studies of Attenuation in Sediments, *J. Acoust. Soc. Am.*, **66**, 1152-1160.
- Taber, D., 1991, *Gases, Liquids and Solids and Other States of Matter*, Cambridge University Press, Cambridge.
- Terzaghi, K., 1923, Die Berechnung der Durchlässigkeitsziffer des Tonen aus dem Verlauf der hydrodynamischen Spannungserscheinungen, *Sitzungsber. Akad. Wiss. Wien Math. Naturwiss. Kl., Abt. 2A*, **132**, p. 105.
- Thomsen, L., 1972, Elasticity of Polycrystals and Rocks, *J. Geophys. Res.*, **77**(2), 315-327.
- Thomsen, L., 1985, Biot-Consistent Elastic Moduli of Porous Rocks: Low Frequency Limit, *Geophysics*, **50**(12), 2797-2807.
- Thigpen, L. and Berryman, J.G., 1985, Mechanics of Porous Elastic Materials Containing Multiphase Fluids, *Int. J. Engng Sci.*, **23**(11), 1203-1214.
- Tokatz, M.N., Johnston, D.H. and Timur, A., 1979, Attenuation of Seismic Waves in Dry and Saturated Rocks: I. Laboratory Measurements, *Geophysics*, **44**(4), 681-690.
- Tokatz, M.N., Mandel, B., and Dainty, A.M., 1990, Frequency Dependent Attenuation in the Crust, *Geophys. Res. Lett.*, **17**(7), 973-976.
- Uday, N. and Spanos, T.J.T., 1993, The Equations of Miscible Flow with Negligible Molecular Diffusion, *Transport in Porous Media*, **10**, 1-41
- Vaisnys, J.R., 1968, Propagation of Acoustic Waves Through a System Undergoing Phase Transformation, *J. Geophys. Res.*, **73** (24), 7675 - 7683.
- van der Grieten, J.G.M. and van Dongen, M.E.H., 1985, A Shock-Tube Technique for Studying Pore-Pressure Propagation in a Dry and Water-Saturated Porous Medium, *J. Appl. Phys.*, **58**(8), 2937-2942.
- van der Grieten, J.G.M. and van Dongen, M.E.H., 1987, Strain and Pore-Pressure Propagation in a Water-Saturated Porous Medium, *J. Appl. Phys.*, **62**(12), 4682-4687.
- van der Knaap, W., 1959, Non-Linear Behavior of Elastic Porous Media, *Petrol. Trans. AIME*, **216**, 179-186.
- Verma, L.S., Shrotriya, A.K., Singh, R. and Chaudhary, D.R., 1991, Prediction and Measurement of Effective Thermal Conductivity of Three-Phase System, *J. Phys. D: Appl. Phys.*, **24**, 1515-1526.
- Vernik, L. and Nur, A., 1992, Ultrasonic Velocity and Anisotropy of Hydrocarbon Source Rocks, *Geophysics*, **57**(5), 727-735.
- Voigt, W., 1910, *Lehrbuch der Kristallphysik*, Teubner, Berlin.

- Vo-Thanh, D., 1990, Effects of Fluid Viscosity on Shear-Wave Attenuation in Saturated Sandstones, *Geophysics*, 55(6), 712-722.
- Vo-Thanh, D., 1991 Effects of Fluid Viscosity on Shear-Wave Attenuation in Partially Saturated Sandstone, *Geophysics*, 56(8), 1252-1258.
- Vo-Thanh, D., 1992, Effect of Temperature and Fluid Viscosity on the Ultrasonic Velocities in Lavoux Calcite Rock, *Geophys. J. Int.*, 110, 614-618.
- Walpole, L.J., 1966, On Bounds for the Overall Elastic Moduli of Inhomogeneous Systems 1, *J. Mech. Phys. Solids*, 14, 151-162.
- Walsh, J.B., 1965a, The Effects of Cracks on the Compressibility of Rocks, *J. Geophys. Res.*, 70, 381-389.
- Walsh, J.B., 1965b, The Effects of Cracks on the Uniaxial Compression of Rocks, *J. Geophys. Res.*, 70, 399-411.
- Walsh, J.B., 1966, Seismic Wave Attenuation in Rock Due to Friction, *J. Geophys. Res.*, 71, 2591-2599.
- Walsh, J.B., 1968, Attenuation in Partially Melted Material, *J. Geophys. Res.*, 73(6), 2209-2216.
- Walsh, J.B., 1969, New Analysis of Attenuation in Partially Melted Rock, *J. Geophys. Res.*, 74, 4333-4337.
- Walton, K. and Digby, P.J., 1987, Wave Propagation Through Fluid Saturated Porous Rock, *J. Appl. Mech.*, 54, 788-793.
- Wang, H., 1993, Constitutive Equations: Laboratory Measurements in *A Short Course in Poroelasticity in Rock Mechanics*, the 34th U.S. Symposium on Rock Mechanics, June 27-30, 1993, University of Wisconsin-Madison.
- Wang, Z. and Nur, A., 1990, Dispersion Analysis of Acoustic Velocities in Rocks, *J. Acoust. Soc. Am.*, 70(6), 2384-2395.
- Wang, Z. and Nur, A., 1988, Effects of Temperature on Wave Velocities in Sands and Sandstones with Heavy Hydrocarbons, *SPE Res. Eng.*, Feb., 158-164.
- Warner, K.L., 1990, An Ultrasonic Study of Liquid Helium Filled Porous Ceramics. Ph.D. Thesis, University of Delaware, 161 pp.
- Warner, K.L., 1986, Sound Velocity and Attenuation Measurements at Low Temperatures in Fluid Filled Porous Media, M.Sc. Thesis, University of Delaware, 81 pp.
- Waterman, P.C. and Truell, R., 1961, Multiple Scattering of Waves, *J. Math. Phys.*, 2, 512-537.
- Watt, P.J., Davies, G.F. and O'Connell, R.J., 1976, The Elastic Properties of Composite Materials, *Rev. Geophys. and Space Phys.*, 14 (4), 541-563.

- Watt, P.J. and O'Connell, R.J., 1980, An Experimental Investigation of the Hashin-Shtrikman Bounds on Two-Phase Aggregate Elastic Properties, *Phys. Earth Planetary Int.*, 21, 359-370.
- Weast, R.C., 1969, *C.R.C. Handbook of Chemistry and Physics*, The Chemical Rubber Co., Ohio.
- Whitaker, S., 1969, Advances in Theory of Fluid Motion in Porous Media, *Ind. and Eng. Chem.*, 61(12), 14-28.
- Whitaker, S., 1966 The Equations of Motion in Porous Media, *Chem. Eng. Sci.*, 21, 291-300.
- White, J.E., 1975, Computed Seismic Speeds and Attenuation in Rocks With Partial Gas Saturation, *Geophysics*, 40(2), 224-232.
- Willis, J.R., 1981, Variational and Related Methods for the Overall Properties of Composites, in *Advances in Applied Mechanics*, 21, Academic Press, New York, 1-78.
- Winkler, K.W., 1983, Contact Stiffness in Granular Porous Materials: Comparison Between Theory and Experiment, *Geophys. Res. Lett.*, 10(11), 1073-1076.
- Winkler, K.W. and Nur, A., 1982, Seismic Attenuation: Effects of Pore Fluids and Frictional Sliding, *Geophysics*, 44, 1-15.
- Winkler, K.W., Nur, A. and Gladwin, M., 1979, Friction and Seismic Attenuation in Rocks, *Nature*, 227, 528-531.
- Winkler, K.W. and Pione, T.J., 1982, Techniques for Measuring Ultrasonic Velocity and Attenuation Spectra in Rocks Under Pressure, *J. Geophys. Res.*, 87 (B13), 10776-10780.
- Winkler, K.W., 1985, Dispersion Analysis of Velocity and Attenuation in Berea Sandstone, *J. Geophys. Res.*, 90(B6), 6793-6800.
- Winkler, K.W., 1986, Estimates of Velocity Dispersion Between Seismic and Ultrasonic Frequencies, *Geophysics*, 51(1), 183-189.
- Woodside, W. and Meesmer, J.H., 1961a, Thermal Conductivity of Porous Media. I. Unconsolidated Sands, *J. Appl. Phys.*, 32(9), 1688-1699.
- Woodside, W. and Meesmer, J.H., 1961b, Thermal Conductivity of Porous Media. II. Consolidated Rocks, *J. Appl. Phys.*, 32(9), 1699-1706.
- Wu, K., Xue, Q. and Adler, L., 1990, Reflection and Transmission of Elastic Waves From a Fluid Saturated Porous Boundary, *J. Acoust. Soc. Am.*, 87(6), 2349-2358.
- Wyllie, M.R.J., Gardner, L.W. and Gregory, A.R., 1962, Studies of Elastic Wave Attenuation in Porous Media, *Geophysics*, 27(5), 569-589.

- Wyllie, M.R.J., Gregory, A.R. and Gardner, L.W., 1956, Elastic Wave Velocities in Heterogeneous and Porous Media, *Geophysics*, 21(1), 41-70.
- Xu, S. and King, M.S., 1990, Attenuation of Elastic Waves in a Cracked Solid, *Geophys. J. Int.*, 101, 169-180.
- Yew, C.H. and Jogi, P.N., 1976, Study of Wave motions in Fluid-Saturated Porous Rock, *J. Acoust. Soc. Am.*, 60(1), 2-8.
- Yew, C.H. and Yogi, P.N., 1978, The Determination of Biot's Parameters of Sandstones Part 1: Static Tests, *Exp. Mech.*, May, 167-172.
- Yih, C.S., 1969, *Fluid Mechanics*, McGraw-Hill, New York.
- Yin, C.-S., Batzle, M.L. and Smith, B.J., 1992 Effects of Partial Liquid/Gas Saturation on Extensional Wave Attenuation in Berea Sandstone, *Geophys. Res. Lett.*, 19(13), 1399-1402
- Yoshida, H., Yun, J.H., Echigo, R. and Tomimura, T., 1990, Transient Characteristics of Combined Conduction, Convection, and Radiation Heat Transfer in Porous Media, *Int. J. Heat Mass Transfer*, 33(5), 847-857.
- Zarotti, F. and Carbonell, R.G., 1984, Development of Transport Equations For Multiphase Systems II, *Chem. Engng Sci.*, 39, 263-278.
- Zemansky, M.W., 1957, *Heat and Thermodynamics*, McGraw-Hill, New York.
- Zimmerman, R.W., 1989, Thermal Conductivity of Fluid-Saturated Rocks, *J. Petrol. Sci. Eng.*, 3, 219-227.
- Zimmerman, R.W., 1991, *Compressibility of Sandstones*. Developments in Petroleum Science 29. Ed. G.V. Chilingarian, Elsevier, Amsterdam.
- Zimmerman, R.W., Somerton, W.H. and King, M.S., 1986, Compressibility of Porous Rocks, *J. Geophys. Res.*, 91 (B12), 12,765-12,777.

END

2 8 1 0 8 1 9 6

FIN